An Evaluation of the Effects of Marine Oil-spills, Remediation Strategies, and Shipwrecks on Microbial Community Structure and Succession

Gareth Edward Thomas

A thesis submitted for the degree of
Doctor of Philosophy in Environmental Biology

School of Life Sciences
University of Essex
October 2020

“The great heroes and heroines of our society are of course the teachers,
and in particular the teachers of kids in their first years.
Once a child has been shown what the natural world is, it will live with them forever.”
Sir David Attenborough

I dedicate this work to my daughter *Liliana Ray Thomas*, born in the second year of my PhD research, may the natural world inspire her every day.

Summary

The evaluation of how *Bacteria* respond to oil-contamination, and the application of dispersants and biosurfactants, in North Sea seawater microcosms is the focus of Chapter Two. Analysis revealed that dispersants and biosurfactants, which significantly reduced the interfacial tension between oil and water, significantly increased growth of obligate hydrocarbonoclastic bacteria (OHCB) in 24 hours, translating into significantly enhanced alkane-biodegradation. Early sampling of microcosms revealed how the OHCB *Oleispira*, hitherto considered a psychrophile, can dominate bacterial communities at the relatively high temperature of 16ºC. Bacterial response to oil-pollution is examined further in Chapter Three, where an *in situ* oil-slick is compared to a chemically dispersed oil-slick in the North Sea. Results suggest a lack of hydrocarbon-degrading bacteria (HCB) growth, even in samples with measurable hydrocarbons, could potentially be attributed to phosphorous limitation. Whilst the Ecological Index of Hydrocarbon Exposure, which quantifies the proportion of a bacterial community with hydrocarbon-biodegradation potential, revealed an extremely low score, highlighting a limited capacity for the environment, at the time of sampling, to naturally attenuate oil. Analysis of sediments contaminated by the Agia Zoni II oil-spill (Greece, 2017), in Chapter Four, demonstrated significant growth of HCB five-days post-oil-spill. Whilst the relative abundance of HCB declined as oil was removed, a legacy effect was observed, with the OHCB *Alcanivorax* and *Cycloclasticus* persisting for several months after the oil-spill. Finally, analysis of sediments around a North Sea shipwreck (HMS *Royal Oak*), in Chapter Five, revealed low levels of pyrogenic polycyclic aromatic hydrocarbons and little evidence of HCB, indicating sediments showed no long-term impact by previous oil-pollution from the shipwreck. This thesis not only advances our understanding of microbial response to oil-spills, remediation strategies, and shipwrecks, in a range of marine environments, but also highlights the importance of harnessing such knowledge and data to advance post-incident monitoring guidelines and models.

Acknowledgments

First and foremost, I would like to thank my PhD supervisors (Dr Boyd McKew, Professor Terry McGenity, and Jan Brant) for their unwavering support, guidance, and friendship over the last three years. I cannot overstate how grateful and fortunate I feel to have been under their tutelage and for them allowing me the autonomy to develop both my research and personal growth. In addition to thanking all co-authors, there are others I would specifically like to thank relating to each individual chapter:

- **Chapter Two**: thank you to Ben Gregson, Dave Clark, John Green, and Tania Cresswell-Maynard for their support and guidance not only in this chapter but in all my work. Thank you to Fred Coulon and Pablo Moreno, from Cranfield University, for their technical support and training.
- **Chapter Three**: thank you to Rijkswaterstaat for primary funding of the project, including use of ARCA, HEBO-CAT-7, and Rotterdam research vessels. Specifically, thank you to Marieke Zeinstra (formerly NHL Stenden University) and Michiel Visser, from Rijkswaterstaat, for their unwavering determination in ensuring this experiment went ahead (despite the weather!).
- **Chapter Four**: thank you to Anastasia Miliou, and the staff and volunteers at Archipelagos Institute of Marine Conservation, for logistical support in Greece.
- **Chapter Five**: thank you to Freya Goodsir, and all the staff involved at Cefas, for allowing me the opportunity to be involved in this fascinating project.

Additionally, I would like to thank the National Environmental Research Council (NERC; NE/R016569/1, NE/L002582/1), the Centre for Environment, Fisheries, and Aquaculture Science (Cefas), Rijkswaterstaat, ITOPF (R&D Award 2018, ExpOS'D), and the Ministry of Defence Salvage and Marine Operations Wreck Management Programme for their financial support which allowed these projects to be completed. Additionally, I would like to thank EnvEast Doctoral Training Partnership for the opportunity to complete this thesis, financial support (NE/L002582/1), training, support, and guidance.

Lastly, and on a personal level, thank you to all my colleagues and friends from labs 3.25, 3.07, and 5.28 for their technical and motivational support! I would like to thank my parents (Colin and Wendy), family, and friends for their support and guidance. Specifically, thank you to my wife, Laura, for her kindness, support, and love, and to my daughter, Liliana, for always making me laugh. You are my motivation.

Declarations

I declare that this thesis is the result of my own work and was written entirely by myself. Any specific chapter declarations, where any specific work was undertaken by others, is as follows:

- **Chapter Two**: Pablo Moreno and Fred Coulon, from Cranfield University, assisted with the preparation and running of GC-MS samples. Pablo Moreno quantified GC-MS sample data for days 7, 14, and 21. Dave Clark wrote the R script which performed the second layer of formatting on the phylogenetic tree. The analysis which created the tree, in MEGA, and the first and final layers of formatting was undertaken by me. Dave Clark wrote the R script, which was used for analysis and figure creation, for the co-occurrence network analysis, and assisted in the results/experimental procedures write-up sections (specifically for the co-occurrence network analysis).
- **Chapter Four**: Staff and volunteers, from Archipelagos Institute of Marine Conservation, assisted with the sampling campaign in Greece (collecting samples in September, October, January, and March). Pablo Moreno and Fred Coulon, from Cranfield University, assisted with the preparation and running of GC-MS samples.
- **Chapter Five**: The collection of samples, as well as GC-MS preparation, running, and quantification, was conducted by staff at Cefas.

Publications

The following publications occured during the course of my PhD:

- **Chapter Three, Technical Report** (Appendix 1): Zeinstra, M., Brussaard, C., McGenity, T.J., McKew, B.A., **Thomas, G.E.**, Murk, T., et al. (2020) ExpOS'D: Experimental Oil Spill Data-sharing.
- **Chapter Four, Paper** (Appendix 2): **Thomas, G.E.**, Cameron, T.C., Campo, P., Clark, D.R., Coulon, F., Gregson, B.H., et al. (2020) Bacterial Community Legacy Effects Following the Agia Zoni II Oil-Spill, Greece. *Front Microbiol* **11**: 1–15.

Table of Contents

Chapter One

Introduction

Marine Oil Pollution

The extraction, processing, and transportation of oil continues to increase, and new oil fields are regularly being discovered (Rystad Energy, 2020). In 2019 global crude oil production was 82 million barrels a day. Comparatively, ten years prior, in 2009, global crude oil production was 73 million barrels a day and ten years prior to that, 1999, it was 69 million barrels a day. Despite the COVID-19 pandemic, recent forecasts predict that global production and consumption of oil will return to pre-COVID19 levels of ~100 million barrels per day by mid-2021 (U.S. Energy Information Administration, 2020).

Increasing exploration, transportation, and production of oil results in a large quantity of oil and petroleum products entering the marine environment. It is estimated that 1.3 million tonnes (best estimate) of oil enters the marine environment per annum; with estimates ranging from a minimum 430,000 to a maximum 8.3 million tonnes. A large proportion of this oil comes from natural oil seeps (best estimate 600,000 tonnes), with the remaining 54% coming from anthropogenic sources, which includes extraction (best estimate 38,000 tonnes), transportation (best estimate 150,000 tonnes), and consumption (best estimate 480,000 tonnes) (Table 1.1) (National Research Council, 2003). These wide-ranging, and potentially outdated, estimations demonstrate the difficulty in quantifying the true nature of marine oil pollution but still represent the best current approximations.

Tanker and exploration oil-spills are actively researched by scientists and funded by governments, industry, and NGOs. This is due to the potential impacts tanker and exploration oil-spills may have, with a large quantity of oil entering the marine environment at an increased rate compared to natural oil seeps. The most infamous oil-spill in recent history (2010) is the Macondo oil-spill (Macondo being the well/prospect name), also known as the Deep-Water Horizon (DWH; name of the oil-rig) spill. Occurring in the Gulf of Mexico, 700,000 tonnes of oil were released at a depth of 1,500 meters due to a well-head blowout. The DWH oil-spill is the largest peace-time oil-spill since the Atlantic Empress tanker-oil-spill of 1979 (287,000 tonnes; Table 1.2; ITOPF, 2019).

Vessel oil-spills represent a global issue, although many of the 20 largest oil spills were around the European coastline (Fig. 1.1). However, table 1.2 does not account for the thousands of minor oil-spills that also occur. For example, the Mediterranean has been subject to 989 recorded oil-pollution incidents (REMPEC,

2018). Globally, in the 1970's there were a total of 543 medium oil-spills (7-700 tonnes) and 245 large oil-spills (>700 tonnes). In the 2010's there were 44 medium oil-spills and 18 large oil-spills, representing ~13% of the oil-spills that occurred in the 1970s (ITOPF, 2019). Evidently, advances are being made to prevent oil-spills, but due to the increase demand on oil, they remain a major threat. In 2017, there were six oil-spills greater than 7 tonnes, including a tanker oil-spill (Agia Zoni II, September) in the Saronic Gulf, Greece. This tanker oil-spill is the subject of research in Chapter Four.

Table 1.1: worldwide best, minimum, and maximum estimates (000's of tonnes) for annual release of crude oil and petroleum products into the marine environment (National Research Council, 2003).

Sources	Best Est.	Min. Est	Max. Est
Natural Seeps	600	200	2000
Extraction of Petroleum	38	20	62
Platforms	0.86	0.29	1.4
Atmospheric deposition	1.3	0.38	2.6
Produced waters	36	19	58
Transportation of Petroleum	150	120	260
Pipeline spills	12	6.1	37
Tank vessel spills	100	93	130
Operational discharges (cargo washings)	36	18	72
Coastal Facility Spills	4.9	2.4	15
Atmospheric deposition	0.4	0.2	1
Consumption of Petroleum	480	130	6000
Land-based (river and runoff)	140	6.8	5000
Spills (non-tank vessels)	7.1	6.5	8.8
Operational discharges	270	90	810
Atmospheric deposition	52	23	200
Jettisoned aircraft fuel	7.5	5	22
Total	**1300**	**470**	**8300**

NB: totals may not equal sum of components due to independent rounding.

Table 1.2: the 20 largest vessel oil-spills since 1967 (ITOPF, 2019)

Position	Ship	Year	Location	Spill size in tonnes
1	Atlantic Empress	1979	Off Tobago, West Indies	287,000
2	Abt Summer	1991	700 nautical miles off Angola	260,000
3	Castillo de Bellver	1983	Off Saldanha Bay, South Africa	252,000
4	Amoco Cadiz	1978	Off Brittany, France	223,000
5	Haven	1991	Genoa, Italy	144,000
6	Odyssey	1988	700 nautical miles off Nova Scotia, Canada	132,000
7	Torrey Canyon	1967	Scilly Isles, UK	119,000
8	Sea Star	1972	Gulf of Oman	115,000
9	Sanchi	2018	Off Shanghai, China	113,000
10	Irenes Serenade	1980	Navarino Bay, Greece	100,000
11	Urquiola	1976	La Coruna, Spain	100,000
12	Hawaiian Patriot	1977	300 nautical miles off Honolulu	95,000
13	Independenta	1979	Bosphorus, Turkey	95,000
14	Jakob Maersk	1975	Oporto, Portugal	88,000
15	Braer	1993	Shetland Islands, UK	85,000
16	Aegean Sea	1992	La Coruna, Spain	74,000
17	Sea Empress	1996	Milford Haven, UK	72,000
18	Khark 5	1989	120 miles off Atlantic coast of Morocco	70,000
19	Nova	1985	Off Kharg Island, Gulf of Iran	70,000
20	Katina P	1992	Off Maputo, Mozambique	67,000

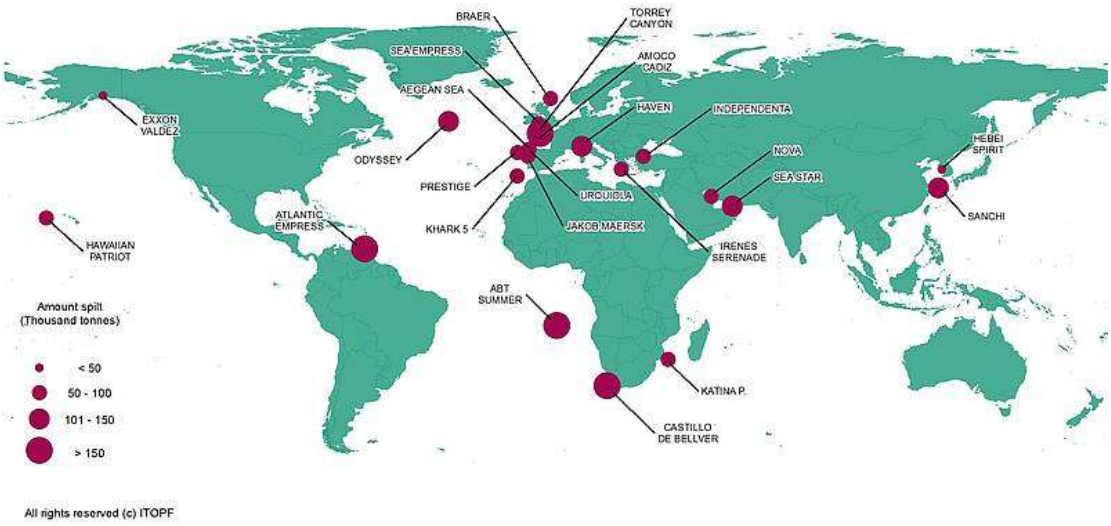

Fig. 1.1: global locations of the top 20 vessel spills from 1967; also included are Prestige (21st), Exxon Valdez (35th), and Hebei Spirit (131st) (taken from ITOPF, 2019).

Biological and Ecological Impacts of Marine Oil Pollution

Effects of marine oil pollution are widespread and both direct and indirect. Oil pollution directly damages the natural aesthetics of marine environments by coating sediment and plant life, as well as killing animal and vegetation of varying kinds. Crude oil and its petroleum derivatives can have toxic effects, especially oils with higher proportions of volatile compounds (VOCs) and polycyclic aromatic hydrocarbons (PAHs) (IARC, 1987; National Toxicology Program, 2011; Manzetti, 2013). Even at sub-lethal levels, these toxic effects can damage physiological and neurological processes, for example, oil-contamination was reported to cause abnormal protein expression in gill tissues of larval and adult killifish (Whitehead *et al.*, 2012). Oil pollution is known to have severe consequences on fish eggs and larvae even in small concentrations (Xu *et al.*, 2016). However, large death rates of adult fish, in oil-contaminated environments, is rare as they can avoid contamination by swimming away. This is also observed for non-furred marine mammals and reptiles, with one model predicting <1% probability of cetaceans, pinnipeds, manatees, and sea turtles encountering and dying from an oil-slick (French-McCay, 2004). Turtles are however affected during nesting season, when oil washes up on the coast where eggs are buried (Milton *et al.*, 2010). Marine mammals that spend more time in shore, such as seals and otters, are more susceptible to oil-contamination, as they are at risk when the water repellent and insulation properties of their fur become damaged by oil, which they rely on to regulate body temperature (Geraci and St Aubin, 1991). Seabirds are the most vulnerable animals and are known to perish in substantial numbers in major oil-spills. This is due to primarily two reasons: 1) oil contamination of feathers results in the loss of water repealing properties, and thus thermal regulation, and 2) birds will begin to preen excessively, and in doing so, they ingest oil particles leading to internal organ malfunctions and failures (Hall, 1994). During the Exxon Valdez tanker-oil-spill in 1989, an estimated 100,000 – 300,000 birds died, primarily (~74%) consisting of the species *Uria aalge* (common murre) (Piatt *et al.*, 1990). Henkel *et al.* in 2014 estimated that over one million birds could have been contaminated by the DWH spill.

Oil pollution does not only affect individual species but can cause drastic alterations to animal communities. A reduction of 66% of total species richness (which included polychaetes, molluscs, crustaceans, and other invertebrates) was observed in affected coastal beaches after the Prestige oil-spill, in Galicia, Spain (De La Huz *et al.*, 2005). It is worth noting that species richness is not only affected by acute oil-spills. A relationship has been observed between closer proximity to oil platforms (and thus contaminants/drill cuttings) and lower benthic fauna diversity (Kingston, 1992). The severity of these effects often depends on the environment that has been affected by

the oil-spill, due to their resilience (Table 1.3; ITOPF, 2013). Mangroves are severely affected by oil-spills due to the enduring perseverance of oil trapped in the anoxic sediments and ensuing release into the water column (Burns *et al.*, 1993). This has indirect effects on coral reefs due to their connectivity with mangroves.

Table 1.3: various habitats and their expected recovery time from an oil-spill (ITOPF, 2013).

Environment	Recovery Time
Plankton	Weeks / Months
Sandy Beaches	1 – 2 Years
Exposed Rocky Shores	1 – 3 Years
Sheltered Rocky Shores	1 – 5 Years
Saltmarshes	3 – 5 Years
Mangroves	>10 Years

NB: recovery periods are indicative after oiling and rely on many factors inc. the amount/type of oil spilled.

Socioeconomic Impacts of Marine Oil Pollution

Oil pollution can lead to large socioeconomic effects, including revenue and job losses from tourism, especially in coastal/recreational diving areas and fishing communities. For example, the 80,000-tonne crude oil-spill in Shetland waters, by the oil-tanker Braer (1993), caused fisheries to be immediately shut down due to fear of contamination, affecting fisherman for more than six years. The impacted waters included salmon farms, many of which became contaminated and the fish had to be destroyed. In total the financial compensation to the Shetland Seafood Industry was over £29 million (Goodlad, 1996).

Financial effects of oil-spills are vast and impact many stake holders, including local communities, individuals, industry, and governments. Prior to the DWH spill, the Exxon Valdez oil-spill was historically the costliest peace-time recorded oil spill. Occurring in 1989 the Exxon Valdez vessel crashed into the coast of Prince William Sound in Alaska, contaminating over 1,300 miles of coastline. Tourism and fisheries were severely affected, with commercial fishermen losing $136.5 million in 1989 and subsequently an estimated $580.4 million (Dorsett, 2010). Moreover, clean up (including penalties and settlements) was predicted to cost $3.8 billion with another $507 million in punitive damages. Whilst this is recorded as the most expensive oil-tanker spill, it is overshadowed by DWH's exploration spill 21 years later. In settlements, court fees, and penalties BP have paid out >$65 billion (Bousso, 2018). Additionally, containment and clean-up costs were predicted at $37 billion.

Financial effects are not only observed from exploration or tanker oil-spills but can be occurred also from marine wrecks, which leak oil products contained within them. Often it is advisable to remove oil from wrecks which contain large quantities.

Overall, the cost to clean-up oil from the marine environment is dependent upon a number of factors, including location, proximity to shoreline, oil type, quantity spilled, and response strategies. However, an average cost to clean an oil-spill in North America is $19,814 per tonne of oil (Etkin, 2000). The T/B Cleveco barge wreck, which sunk in 1942, had 1,095 tonnes of oil removed at an operational cost of $5.62 million, however, had that oil spilled into the environment it could have cost up to $21.7 million to clean-up (at $19,814 per tonne of oil).

Increasing exploration, transportation, and production of oil means oil pollution will continue to be a major marine threat and one that requires continued investigation. Therefore, it is important researchers, oil-spill responders, and industry have comprehensive understanding of the composition and classifications of crude oil and its petroleum derivatives (see "*Chemical Composition of Crude Oil and Petroleum Products*", page 7). Additionally, the physical, chemical, and biological processes involved in the natural attenuation of crude oil in the marine environment (see "*Natural Attenuation of Marine Oil Pollution*", page 9), as well as the suite of remediation strategies available to oil-spill responders (see "*The Application of Dispersants*", page 17). Moreover, understanding how oil-spills, remediation strategies, and shipwrecks (which can hold and potentially leak oil) effect microbial community structure and succession, will allow oil-spill response guidelines and models to be refined and made more effective (see "*Oil-degrading Microbial Communities*", page 28).

Crude Oil

Petroleum products (such as petroleum naphtha, gasoline, and diesel fuel) are the refined products of the "unprocessed" form, crude oil. This naturally occurring oil is a mix of many distinct organic compounds, primarily hydrocarbons (organic compounds that consist of only hydrogen and carbon). The research field of petroleomics involves the identification of the totality of constituents of naturally occurring crude oil (Marshall and Rodgers, 2008). Crude oil forms geochemically via the processes of diagenesis and catagenesis under high pressures and temperatures in marine sediment (Philp, 1985). Diagenesis is a chemical, physical, or biological transformation of sedimentary rock, thus occurring after the process of lithification, in the top few hundred meters. Proteins, carbohydrates, and lipids breakdown under increasing pressure and temperature (although relatively low compared to catagenesis) and result in the creation of two primary products, kerogens and bitumens (Smith and March, 2006). Biogenic theory states that via the process of thermal alteration of the kerogens, which are temperature-dependent, kerogens break down to form hydrocarbons; this process (under much higher pressures and

temperatures) is known as catagenesis. Hydrocarbons, whilst principally produced via geochemical processes, are also produced biologically (Heider *et al.*, 1998); through such processes as archaeal and bacterial methanogenesis. Additionally, some species of cyanobacteria can produce medium chained alkanes (Han and Calvin, 1969; Lea-Smith *et al.*, 2015). Hydrocarbons are, comparatively, chemically unreactive, however, it's their combustion into CO_2 and H_2O in the presence of O_2 that provides the means to be used as fuels.

Chemical Composition of Crude Oil and Petroleum Products

The two major hydrocarbon components of crude oil are saturated hydrocarbons (including aliphatic and alicyclic alkanes) and aromatic hydrocarbons. Saturated hydrocarbons contain only singled bonded carbon compounds (C–C) and have the general formula C_2H_{2n} (Norcorss, 1988). Aliphatic structured hydrocarbons are comprised of straight chains (termed "*n*-alkanes") and are generally the largest fraction of most crude oils (for example, *n*-hexadecane; Fig. 1.2). Additionally, there are branched alkanes (termed "isoalkanes" with the general formula $C_nH_{2n}+_2$), such as phytane (2,6,10,14-Tetramethylhexadecane) and pristane (2,6,10,14-Tetramethylpentadecane; Fig 1.2), which are the most abundant branched alkanes in most crude oils. The cycloalkanes (or alicyclic) structured hydrocarbons within crude oil are comprised primarily of five- or six-carbon rings (cyclopentanes and cyclohexanes (Fig. 1.2)), with the majority having one or more alkyl substituent (missing one hydrogen). There are also unsaturated aliphatic hydrocarbons (double bonded alkenes and triple bonded alkynes) and, although they are absent in crude oil, they can appear in refined products such as gasoline. This occurs when there is insufficient hydrogen to saturate a molecule and thus double/triple bonds are formed during the cracking process. Cracking occurs when complex molecules such as kerogens are broken down into simpler molecules such a short-chained alkanes (Potter and Simmons, 1998).

Aromatic hydrocarbons are present in all crude oils as well as many petroleum products. Aromatic hydrocarbons are a separate class of unsaturated hydrocarbons, often highly toxic, mutagenic, and/or carcinogenic, and are based around a 6-carbon benzene ring structure (Weisman, 1998). These include the monoaromatic hydrocarbons referred to as "BTEX" (benzene (Fig. 1.3), toluene, ethylbenzene, and xylene). Additionally, there are polycyclic aromatic hydrocarbons (PAHs), which form two or more fused aromatic rings; these characterise a sizeable proportion of petroleum products. Whilst the exact composition of crude oil and petroleum products vary widely, significant PAHs include naphthalene (2-ring), phenanthrenes (3-ring),

pyrene (4-ring), and 1,2-benzopyrene (5-ring) as well as methylated PAHs (Figure 1.3).

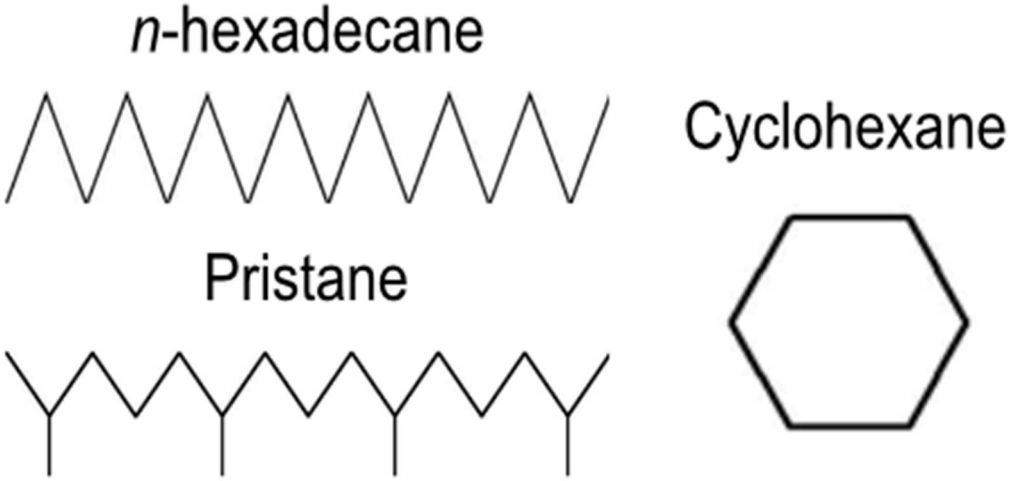

Fig. 1.2: chemical structures of representative alkanes: *n*-hexadecane (*n*-alkane), pristane (branched alkane), and cyclohexane.

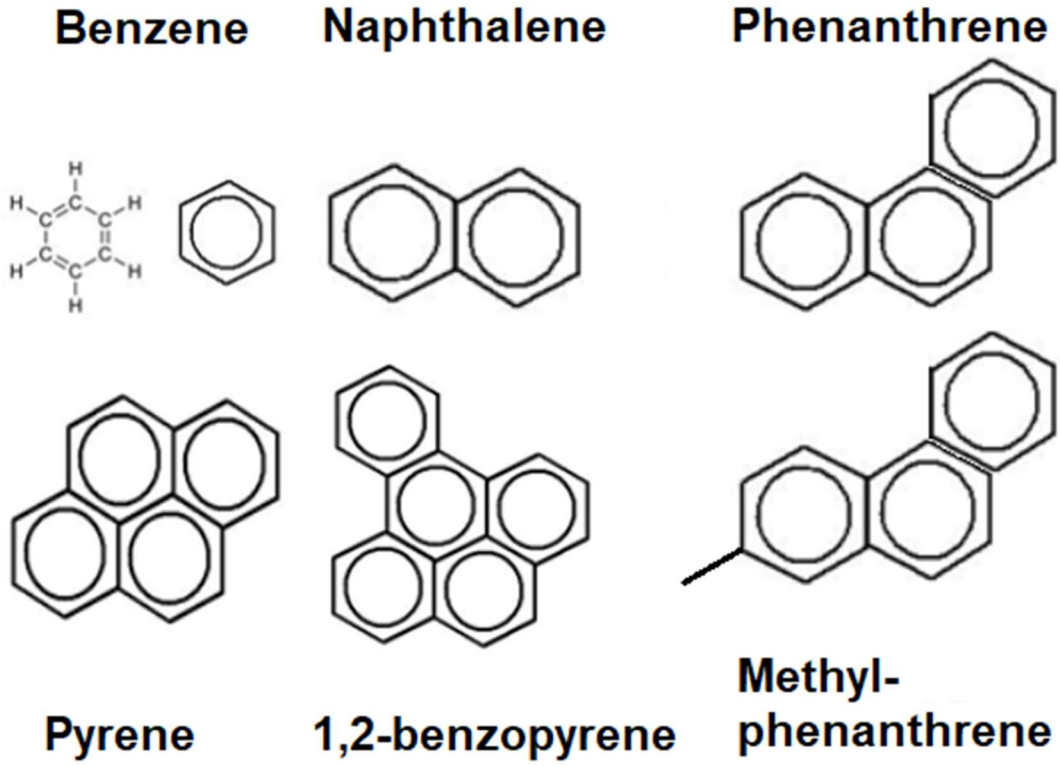

Fig. 1.3: chemical structures of representative of aromatics: monocyclic aromatic benzene and polycyclic aromatic (PAHs) naphthalene (2-ring), phenanthrene (3-ring), pyrene (4-ring), 1,2-benzopyrene (5-ring), and methyl-phenanthrene (methylated PAH).

Two further classes of crude oil contain polar non-hydrocarbons and are termed the asphaltenes and the resins. These polar molecules consist primarily of carbon and hydrogen but also include nitrogen (0.6 – 3.3% asphaltenes, 0.5% ± 0.15

resins), oxygen (0.3 – 4.9% asphaltenes, 1% ± 0.20 resins), and sulfur (0.3 – 10.3% asphaltenes, 0.4 – 5.1% resins). Primarily in crude oil the asphaltenes are defined operationally as *n*-heptane (C_7H_{16})-insoluble and the resins as soluble (Speight, 2004).

Classification of Crude Oil

Crude oil can be further classified by their molecular weight and sulfur content. Sweet oil has a sulfur content of <0.5% and is easier to refine, extract, and transport. In comparison, sour oil has a sulfur content of >0.5%, some forming hydrogen sulphide, and is therefore considerably more toxic, foul, and corrosive. Classification of crude oil's weight is either light, medium, heavy, or extra heavy. Weight is classified by API (American Petroleum Institute) gravity, an inverse measure of the petroleum's liquid density relative to that of water. In full salinity sweater at <10° API the oil will sink, this is also referred to extra heavy, between 10.1° and 22.2° API it is heavy, between 22.3 and 31.1° it is medium, and the product is referred to as light when API is >31.1°. Light oils are typically higher in aromatic and saturated hydrocarbons, whereas in comparison, heavy oils have an increased proportion of asphaltene and resin (Head *et al.*, 2003).

Natural Attenuation of Marine Oil Pollution

As previously mentioned in "*Marine Oil Pollution*" (page 1), crude oil and petroleum products enter the marine environment from several natural and anthropogenic sources. Natural attenuation of crude oil in marine environments is affected by many different chemical, physical, and biological processes.

Chemical and Physical Processes

Chemical and physical processes that affect the movement and degradation of oil pollution are time dependent. During the early phase on an oil-spill, the first hours and days, the oil will create a slick and begin to spread. Spreading is affected by the wind, waves, and turbulence and will often form narrow bands parallel to the wind. During this time such processes as evaporation, dispersion, emulsification, dissolution, and biodegradation occur. In the latter phase, weeks into months and years, processes such as oxidation, sedimentation, and further biodegradation occur (Fig. 1.4; ITOPF, 2014). Collectively these processes are known as weathering, and weathering of oil is dependent upon several factors, including oil type, weather, and environmental conditions (e.g. nutrients, wind, waves, temperature, salinity, temperature, and sunlight) (Brandvik *et al.*, 2010).

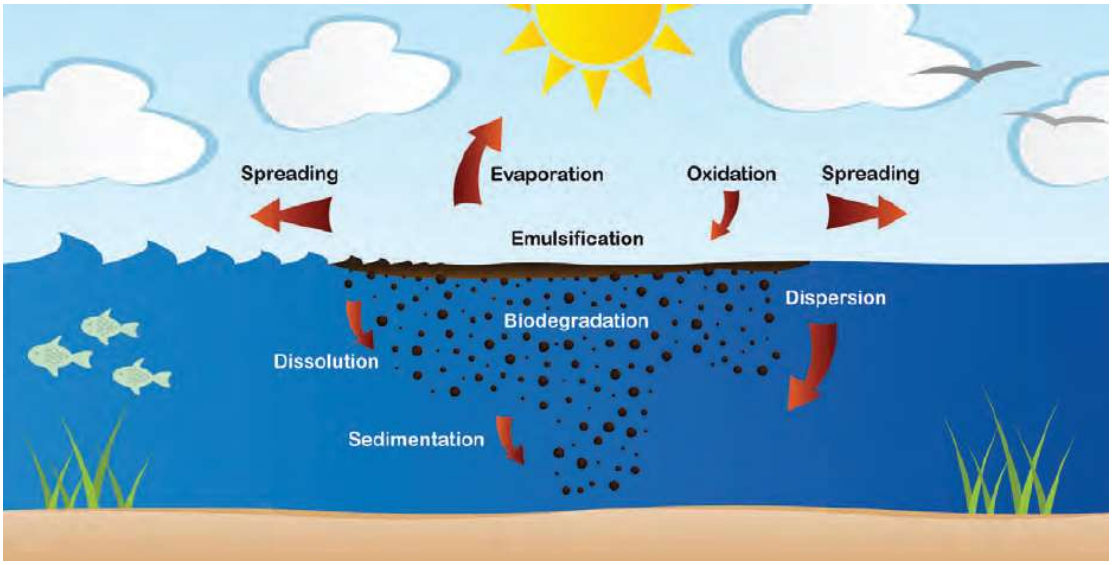

Fig. 1.4: schematic displaying chemical, physical, and biological processes that affect the natural attenuation of crude oil and petroleum products after an oil-spill. Figure credit (ITOPF, 2011a).

During the early phase, evaporation occurs first and is one of the most crucial processes as it removes a significant proportion of lighter (up to 75%) and medium (up to 40%) oils (Fingas, 1995). Volatile compounds are removed first as lighter hydrocarbons (*n*-alkanes $<C_{10\text{-}14}$) are evaporated, proportionally increasing the amount of higher molecular weight compounds (Reijnhart and Rose, 1982). Dissolution is a relatively less significant process, due to the fact most crude oils and petroleum products contain a relatively low proportion of light monoaromatic compounds (BTEX compounds), that are the most soluble in sea water. Dissolution is enhanced by increased dispersion of oil droplets within the water column, a consideration when evaluating the use of dispersant remediation strategies, especially as BTEX compounds are acutely toxic (Stevens and Wardrop, 2005). Spreading ensues as oil is less dense than the water it is floating upon, wind and current energy cause oil to spread faster. Emulsification occurs when waves and turbulence cause oil droplets to break up into smaller droplets and become mixed in the water column. Larger oil droplets often rise to the sea surface, whilst small droplets remain in the water column.

Dispersed oil droplets have a greater surface area to volume ratio than floating surface oil, encouraging other processes such as dissolution, sedimentation, and biodegradation. The process of dispersion and mixing causes oil to become trapped within the water (oil-in-water emulsification), increasing surface area to volume ratio and thus rates of biodegradation, as oil droplets are more likely to come into contact with hydrocarbon-degrading microbes (Wang and Wang, 2018). However, in high turbulence conditions a water-in-oil emulsion occurs (often termed “chocolate mousse” due to its appearance). This occurrence can increase the volume of oil by three to five

times due to the proportion of water (65-80%) in the mousse (National Research Council, 2003), lowering the surface area to volume ratio (see "*The Application of Dispersants*", page 17).

In the long-term the process of photooxidation occurs, although, crude oil is generally unreactive to oxidation, it is heightened in the presence of water. In the most basic form, the oxidative reaction formula is $C_nH_{2n+2} + O_2 \leftrightarrow CO_2 + H_2O$ (whereby C_nH_{2n+2} represents the organic compound alkane). Photooxidation causes the oil to be degraded into more soluble compounds such as the lighter alcohols and organic acids (National Research Council, 2003; D'Auria *et al.*, 2008). Sensitivity to photooxidation increases with greater size and increasing alkyl substitutions (Garrett *et al.*, 1998) and thus photooxidation affects aromatic compounds first. The photooxidation reaction includes direct photoreactions, whereby the reactant forms a less stable intermediate due to the absorption of light energy, and indirect photoreactions, whereby species absorb the light energy. Either way, both produce an intermediary (e.g. hydroxyl radicals) that attack the hydrocarbon molecule; most reactions occur indirectly due to the low efficiency of sunlight absorption by hydrocarbons (National Research Council, 2003). When photooxidation breaks down oil the produced by-products are often more toxic than the original substance (Lacaze and Villedon de Naïde, 1976; Lee, 2003). Petroleum products can also be degraded by photooxidation, being broken down into polar ketones, aldehydes, carboxylic acids, and esters. These reactions can lead to a build-up of higher molecular weight products that can eventually create tar and gum residues (National Research Council, 2003). Cai *et al*. (2017) documented how certain surfactants (Span 80, Tween 85) can increase the rate of photodegradation of PAHs, by boosting absorbance of solar radiation without altering degradation pathways. Moreover, the widespread and swift changes to the physical and chemical properties of oil by photooxidation may influence oil fate, transport, and the selection of response tools (Ward and Overton, 2020).

The last of the non-biological processes to be discussed is sedimentation. Sinking of oil occurs when API gravity is <10º and can be from a naturally heavy oil, via the loss of smaller hydrocarbons, or via the aggregation of oil/sediment (sedimentation), eventually settling onto the benthos. Sedimentation can occur via marine oil snow (MOS), whereby dispersed oil droplets interact with minerals and organic matter (e.g. microbes, faecal matter, dead cells), and depending on the type of aggregate can sink to the sediment (Quigg *et al.*, 2020). There is ongoing debate into whether the application of dispersants on oil-spills increases (Doyle *et al.*, 2018; Wirth *et al.*, 2018; Bretherton *et al.*, 2019) or inhibits (Passow, 2016; Passow *et al.*, 2017) the formation of MOS. As well as sedimentation in open waters, oil can be

washed onto the shoreline, although naturally buoyant oil can detach from sediment and transfer back into the water column (National Research Council, 2003).

Biological Processes

Oil-degrading microorganisms are able to degrade specific hydrocarbons, utilising carbon as an energy source, dependent upon which metabolic processes the microbe possess. For example, oxidative phosphorylation, the oxidation of hydrocarbons via the use of oxygenase enzymes. A secondary biological pathway, detoxification, occurs when an organism metabolises the hydrocarbons to more water-soluble products for excretion through the body (National Research Council, 2003). Exact enzymes used along the pathways can vary widely depending on the hydrocarbon being degraded (Ji *et al.*, 2013). It has been observed that these processes can be conducted not only aerobically but also anaerobically (Heider *et al.*, 1998). See "*Biodegradation Pathways"* (page 33) for more information.

Individual microorganisms are often only capable of biodegrading a relatively small proportion of different hydrocarbons. Therefore, a heterogeneous hydrocarbon-degrading microbial community, with broad enzymatic capabilities, are capable of degrading a complex suite of hydrocarbons in oil-spills (Bossert and Bartha, 1984). Some microorganisms, such as *Alcanivorax*, can degrade *n*-alkanes and branched alkanes, whilst others, such as *Cycloclasticus*, are able to degrade PAHs (Dyksterhouse *et al.*, 1995; Yakimov *et al.*, 1998, 2007; Head *et al.*, 2006; Niepceron *et al.*, 2010; Gao *et al.*, 2015) (see "*Diversity and Roles of Hydrocarbon-degrading Microbes*", page 29). It is often observed that less complex components of oil will be degraded first, alkanes and smaller aromatics are degraded faster than branched and cyclic compounds (Leahy & Colwell, 1990). Most hydrocarbon-degrading microorganisms are known to produce biosurfactants (e.g. *Alcanivorax* produces a glycolipid biosurfactant) (Banat, 1995; Vijayakumar and Saravanan, 2015), these surface-active substances increase the emulsification of hydrocarbons (see "*Biosurfactants*", page 21).

Oil exposure in marine environments can lead to a long-lasting adaptation within the microbial community. Prior exposure can be important in determining the rate at which any subsequent hydrocarbon inputs may be biodegraded (Leahy and Colwell, 1990). In pristine marine environments there is an increased biodegradation lag-time due to the fact hydrocarbon-degrading bacteria must produce the necessary enzymes to initiate biodegradation and creation of biosurfactant. For further details regarding oil-degrading microbial ecology and degradation pathways see "*Oil-degrading Microbial Communities*", page 28.

Limiting Factors

There are a variety of environmental factors, in addition to the composition of crude oil and its derivatives, that impact the rate of biodegradation. These factors include dissolved oxygen, nutrients, temperature, and pressure.

Oxygen concentration has a significant impact on hydrocarbon-biodegradation, as low concentrations limit aerobic microbial growth. The primary step in the aerobic hydrocarbon-degradation pathway is oxidation, via mono- and dioxygenases, which require one or two molecules of oxygen (van Beilen *et al.*, 2001; Madigan *et al.*, 2008). Anaerobic degradation can occur, but often at decreased rates. For example, studies of sediments from the Amoco Cadiz oil-spill found that anaerobic degradation was several orders of magnitudes slower than aerobic degradation (Hassanshahian and Cappello, 2013). Shoreline beaches with low wave activity will have depleted oxygen concentration and thus low biodegradation rates. When oxygen depleted sediments become contaminated with oil, physical removal techniques (e.g. absorption and skimming) should be sought prior to bioremediation (Caruso *et al.*, 2004).

Nitrogen (N) and phosphorous (P) are macronutrients vital for microbial growth, especially during hydrocarbon-biodegradation of an oil-slick (Atlas, 1981), and therefore, the availability of N and P in the presence of hydrocarbons is crucial (Ron and Rosenberg, 2014). This limiting factor is often due to competition between hydrocarbon-degrading bacteria and other microorganisms that require the nutrients. Nitrogen is required by bacteria for the synthesis of proteins and nitrogenous bases and comes in the forms of NH_4^+ and NO_3^- whilst phosphorous is required for nucleic acid and phospholipid synthesis and comes in the form of PO_4^{3-} (Bristow *et al.*, 2017). These nutrients are typically limiting in marine environments, and thus when a sudden abundance of carbon enters a marine system, as occurs with an oil-spill, nutrients quickly become a limiting factor and represent an even more important role than that of oxygen (Pruthi and Cameotra, 1997). Due to the fact both N and P are highly limiting factors in the process of hydrocarbon-biodegradation, external interventions are often sought; this comes in the form of biostimulation, whereby nutrients are applied to oil-contaminated environments to expedite the natural growth of microorganisms (Lebaron *et al.*, 1999). See section "*Oil-Spill Bioremediation Strategies*" (page 16) for more information.

Oil pollution is a global issue, occurring in a variety of habitats and conditions, however, hydrocarbon-biodegradation has been observed across a variety of marine environments (McFarlin *et al.*, 2014; Hazen *et al.*, 2016). Hydrocarbon-biodegradation has been observed across a wide-ranging temperature gradient in the marine

environment (from 0-35°C, with optimal growth at 15-30°C for aerobic hydrocarbon-biodegradation, Rawe *et al.*, 1993), the rate at which hydrocarbon-biodegradation occurs decreases with lower temperatures. Edwards & Grbic-Galic (1994) observed that a decrease from 35ºC to 20ºC resulted in a 25% reduction in toluene degradation. Additionally, biodegradation of total petroleum hydrocarbons (TPH) was significantly increased at 20ºC in comparison to 4ºC, and the rate of TPH-biodegradation peaked in microcosms at 20ºC with additional N and P (Coulon *et al.*, 2007). This is because at lower temperatures crude oil and its derivatives become more viscous, thus requiring increased wave energy to mix the oil and decrease surface area to volume ratio (Clayton Jr *et al.*, 1993; Chandrasekar *et al.*, 2005). Additionally, some alkanes can form crystals at temperatures <5ºC, further reducing bioavailability (Whyte *et al.*, 1998). An environments temperature selects for certain microorganisms, for example, at temperatures of 20ºC both the psychrophilic *Rhodococcus* spp. strain Q15 and mesophile *Pseudomonas oleovorans* will degrade dodecane. However, at temperatures of 10ºC the biodegradation rate of the mesophile *P. oleovorans* substantially reduces, whilst the psychrophilic *Rhodococcus* spp. strain Q15 will continue at its previous rate (Whyte *et al.*, 1998). The oil-degrading bacteria *Oleispira antarctica* dominates in colder (<4°C) oil-polluted environments (Yakimov *et al.*, 2003; Coulon *et al.*, 2007). *Oleispira*, considered a psychrophile, has been observed to grow well in pure cultures at 16ºC (Kube *et al.*, 2013; Gregson *et al.*, 2020), though are often outcompeted by other oil-degrading bacterial at warmer temperatures (King *et al.*, 2015; Brakstad *et al.*, 2018). Understanding how hydrocarbon-degrading bacteria respond in cold environments is especially important in polar regions where oil exploration is ongoing (Delille *et al.*, 1998; Brakstad *et al.*, 2008; McFarlin *et al.*, 2014).

Pressure is also known to alter biodegradation rates and has become of increasing interest since the DWH spill which occurred at a depth of 1,500 meters. Research by Prince *et al*. (2016) has observed that biodegradation of oil at higher pressures is decreased by approximately a third compared to surface conditions, with the biodegradation of higher molecular weight hydrocarbons being considerably slower.

Oil-Spill Remediation and Bioremediation Strategies

There are a variety of remediation tools available to the oil-spill response industry, with technologies and practices frequently under review for their efficiency and safety. The strategy oil-spill response companies adopt is based on analysis of a wide set of variables, for example, in the USA this includes: personnel health and safety, oil type/thickness/quantity, window-of-opportunity, oceanographic and

environmental conditions, proximity to shorelines and sensitive areas, geographical location, and cultural and political restrictions (National Oceanic and Atmospheric Administration (NOAA), 2010). The overall goal during oil-spill response is to minimise impact to natural and economic resources and drive the main considerations in Spill Impact Mitigation Assessment (SIMA, API *et al.*, 2017). A balance must be made between potential environmental/economic impacts and "natural recovery" or "recovery through intervention". NOAA state that "*The method, or combination of methods, that most reduces consequences effectively, should be the preferred response strategy. A method that increases impacts in the short term can be the preferred alternative if it speeds up recovery.*" (National Oceanic and Atmospheric Administration (NOAA), 2010). Here, a general overview of oil-spill remediation strategies is discussed prior to a detailed review into the application of dispersants or biosurfactants.

Oil-Spill Remediation Strategies

Often the first remediation strategy in open waters is to contain the oil. Booms are barriers which float on the water, often with a sizeable proportion under the surface, with the aim to contain, divert, deflect, or exclude oil in a particular location. Booming also concentrates oil, forming a thicker surface layer, which can then be skimmed, absorbed, or ignited. A skimmer is a mechanical device that can be used autonomously or in combination with booming. Skimming collects oil and separates it from the water prior to transferring it to a container for subsequent disposal. Skimmers either work by vacuum (suction skimmer), absorbents (oleophilic skimmers), or natural flow collection (weir skimmers) (ITOPF, 2013b). A consideration with both booming, absorbing, and skimming is wave height and flow speed, both booming and skimmers perform poorly if waves are more than 1 – 1.5 meters high or water flow is faster than one knot per hour (Cormack, 2013).

In situ burning, often in tangent with fire-resistant booming, occurs more often in ice-affected waters (Arctic) and is seen as a last-resort in emergencies or remote waters (National Research Council, 2014). Booming concentrates and thickens the surface oil, as ignition requires the oil to be at least 1-3 mm thick (National Oceanic and Atmospheric Administration, 2010). Fingas (2011a) gives an overview of *in situ* oil-spill burning. If the spilled oil has been significantly weathered, losing the lighter hydrocarbon fractions of the oil, it is significantly more difficult to ignite. Once ignited the oil burns on average at a rate of 0.5 to 4 mm per minute. Generally, the burning of oil ceases at a thickness of 1 mm, this is due to heat being conducted to the water below the oil surface. Many considerations must be evaluated before adopting *in situ*

burning, a balance between stopping the spread of oil and the large amount of air pollution it creates (Fisheries and Oceans Canada, 2001).

Booming, skimming, and burning (and the application on dispersants, discussed later) represent the major oil-spill strategies in open waters, however, terrestrial and shoreline oil-spill response may require additional tools. These can include high-pressure washing, containment beams, trenches, sorbent barriers, slurry walls, viscous liquid barriers, and the physical removal of sediment/land. However, these physical processes can have negative effects, for example, high-pressure washing on rocky shores reduces the abundance and diversity of vegetation and macrofauna (Broman *et al.*, 1983). Additionally, when contaminated sediment, for example from a shoreline, is physically removed it is processed or disposed of, this can include compositing, landfill, incineration, and washing and replacement. Though effective in the removal of oil (Dave and Ghaly, 2011), the bulk removal of coastal sediment can be environmentally damaging (Owens, 1972; Gundlach and Hayes, 1978; Petersen *et al.*, 2002), and, has economic and environmental costs associated with disposal, often to landfill sites. The efficiency of sediment removal, during its application during clean-up operations of the Agia Zoni II oil-spill, is evaluated in Chapter Four.

Oil-Spill Bioremediation Strategies

Biostimulation

Bioremediation is the anthropogenic intervention, often by the addition of microbes or plants or altering environmental conditions, to remove contaminants from an environment. Biostimulation is the process of altering the environment to stimulate indigenous microbes capable of bioremediation, often when applied to oil-spill remediation this involves the application of nutrients (National Oceanic and Atmospheric Administration, 2010). The effects of biostimulation and nutrient limitation on oil-degradation and microbial response has been thoroughly researched (Bragg *et al.*, 1994; Röling *et al.*, 2002; Yergeau *et al.*, 2015; Meng *et al.*, 2016). One bioremediation strategy that occurred during clean-up operations of the Exxon Valdez oil-spill included the application of 50,000 kg of nitrogen and 5,000 kg of phosphorous over consecutive summers, resulting in significantly enhanced hydrocarbon-degradation (Bragg *et al.*, 1994). In November 2002, the oil tanker Prestige sank off the coast of North-West Spain, releasing 60,000 tonnes of heavy crude oil. An *in situ* biostimulation assay was completed 12 months after the event (a beach on the Cantabrian coast in north Spain), with the application of S200, an oleophilic fertiliser containing nitrogen and phosphorous (Jiménez *et al.*, 2007). The addition of the

fertiliser significantly increased biodegradation of PAHs, alkanes of a high-molecular weight, and alkylated derivatives, concluding the fertiliser increased the bioavailability of these high-weight molecules to hydrocarbon-degrading bacteria. It has, however, been observed that nutrients are not always the most limiting factor. Coulon *et al.* (2007) observed that temperature had a more profound impact on microbial community diversity and hydrocarbon-biodegradation.

Bioaugmentation

Bioaugmentation, or "natural microbe seeding", is the application of high numbers of oil-degrading microbes to an environment with the purpose of expediting natural microbial hydrocarbon-degradation processes (El Fantroussi and Agathos, 2005). The efficacy of such an intervention is decidedly dependant on the environmental conditions of the contaminated site they're being applied too and the microbes being added (Vogel, 1996). Studies have shown coastlines, contaminated with thin and broadly dispersed oil, can be remediated using bioaugmentation (Hosokawa *et al.*, 2011). Where possible, bioaugmentation using autochthonous microbes (the addition of an exclusive microbial consortium indigenous to the environment) is considered to be a more promising bioremediation tool (McKew *et al.*, 2007; Hosokawa *et al.*, 2009; Nikolopoulou *et al.*, 2013). Increased hydrocarbon-biodegradation has also been observed when bioaugmentation was combined with biostimulation plus a washing agent (Crisafi *et al.*, 2016). Research has however demonstrated that bioaugmentation alone can be a better option when compared to bioaugmentation combined with biostimulation, perhaps due to increased microbial competition (Hassanshahian *et al.*, 2016).

The Application of Dispersants

In 2014 it was estimated the surfactant market was worth $33 billion (Ceresana Research, 2015) and it estimated to grow to $40 billion by 2021 (Markets and Markets, 2017). It is estimated that over 15 million tonnes of synthetic surfactants are produced annually; approximately half of which are soaps (Nakama, 2017). Their basic processes and role in the natural world mean they have many applications, for example, laundry products, biofilm prevention, biocidal wound healing, and the remediation of marine oil pollution (Marchant and Banat, 2012). Bioremediation using dispersants occurs via the application of a surfactant, often a commercial "dispersant" (e.g. Slickgone NS, a "Type 3" dispersant by Dasic International Ltd), to oil-contaminated environments. Dispersants transform oil on the surface of the water into micron-size droplets (10 – 300 μm, North *et al.*, 2015) in the water column. This dispersion of oil provides an increased surface area for microbial attachment, and

biodegradation can occur at lower nutrient concentrations as oil is dispersed over a wider area and thus decreasing in concentration (Prince *et al.*, 2013). Additionally, increased oil surface area to volume ratio allows hydrocarbon-degrading microbes to expend more energy on growth and less energy producing biosurfactants, thereby accelerating biodegradation (Prince *et al.*, 2016; Brakstad *et al.*, 2018). Here the composition, classification, toxicity, and efficiency of dispersants and biosurfactants is reviewed, whilst their effects on microbial communities is evaluated in the section "*Oil-degrading Microbial Communities*" (Page 28).

Surfactants (the word deriving from a blend of "surface-active agent") are compounds that lower the surface tension between two immiscible liquids, a liquid and a solid, or a liquid and a gas (Rosen and Kunjappu, 2012). Surfactants are amphiphilic, that is they have both hydrophilic and hydrophobic parts, allowing surfactants to dissolve in both polar- and non-polar solvents (Perfumo *et al.*, 2009). Surfactants adsorb preferably at interfaces; in a water solution they form first at the surface, their hydrophilic heads in the water and their hydrophobic tails towards the gaseous stage (air). Surfactants form strong interactions with both the aqueous and gaseous phases, reducing the interfacial tension between them. Once the surface is saturated the surfactant molecules sink, linking together to form micelles (Fig. 1.5A-C). The CMC (critical micelle concentration, the concentration of surfactants above which micelles form, McNaught and Wilkinson, 1997) can be determined by measuring the surface tension at different surfactant concentrations. Once the CMC has been reached the interfacial tension remains constant, at which point any reduction in interfacial tension ceases (McNaught and Wilkinson, 1997). Micelle structures form nanocontainers (Fig. 1.5D), establishing a suitable environment to hold oil, thus allowing the oil to become homogenised within the aqueous phase. Weak bonds in the nanocontainers mean it is not a rigid structure, allowing the nanocontainers to expand and adapt to oil molecules of varied size.

The tail of most surfactant molecules is similar, a hydrocarbon chain that can be branched, linear, or aromatic (Kronberg *et al.*, 2014). Flurosurfactants have a fluorocarbon chain, siloxane surfactants have siloxane chains. Several surfactants include a polyether chain, terminating in a highly polar anionic group. The tails can be singular or double. Classification occurs on the polarity of the surfactant head, anionic, cationic, zwitterionic, and non-ionic (Fig. 1.6). An anionic surfactant has a negatively charged head; often sulphate, phosphate, or carboxylate, the latter being the most common of all. A cationic surfactant possesses a positively charged head that is a pH dependant primary, secondary, or tertiary amine. Zwitterionic surfactants have both an anionic and cationic head; often found in biosurfactants and contain a phosphate

anion with an amine or ammonium (e.g. phospholipids). Lastly, the non-ionic surfactants contain no charge. They are covalently bonded, oxygen-containing, hydrophilic groups that are water soluble because of hydrogen bonding.

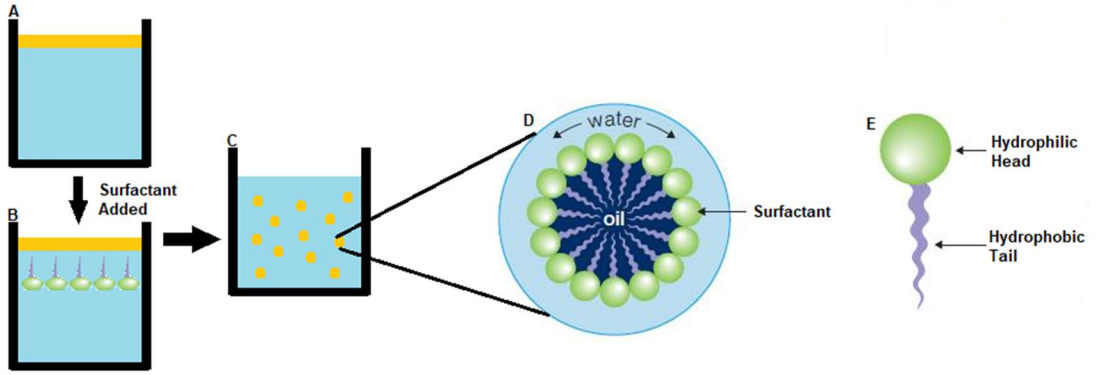

Fig. 1.5: schematic of oil on the surface of water (**A**), a surfactant is added to the surface and the surface becomes saturated (**B**), at this point the surfactant molecules sink and for micelles (**C**). Micelles form nanocontainers which hold the oil (**D**), they are formed of surfactant molecules (**E**) which have a hydrophilic head and hydrophobic tail.

Whilst the polar heads classify surfactants into main categories, they can further be divided based on the HLB system (hydrophilic-lipophilic balance) (Sperandio, 1965). The HLB scale runs from 0 to 20 and is based on the solubility characteristics of the surfactant in water and oil. Those surfactants with a lower HLB are more soluble in the oil phase, and those with a higher HLB are more soluble in the water phase. By testing the HLB system and blending surfactants, more efficient dispersant products can be achieved.

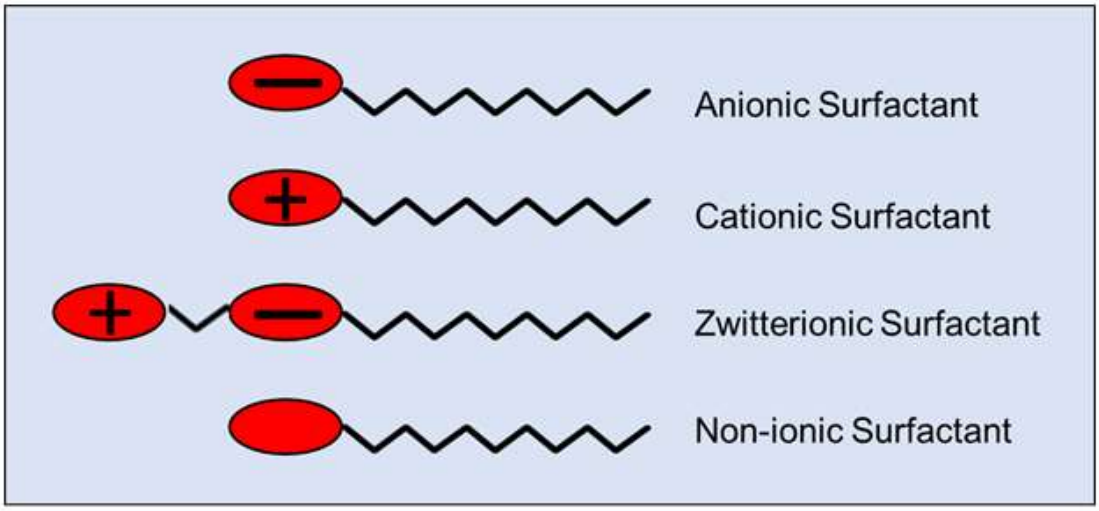

Fig. 1.6: classification of surfactants; including the anionic, cationic, zwitterionic, and non-ionic.

Dispersants

The composition of commercial dispersants has evolved over time. In the 1960's the first generation of dispersants were similar in composition to industrial cleaners and displayed elevated levels of toxicity and are no longer used in oil-spill

response. The second generation of dispersants (Type I) were often applied neat or at ratios at 1:1 to 3:1 (oil to dispersant) and are rarely used in oil-spill response. The third generation of dispersants are divided into Type II (generally mixed with sea water) and Type III (applied neat) and allow for a much higher surfactant content and thus require a lower oil to dispersant (20:1) ratio (ITOPF, 2011). Dispersants are generally comprised of a mixture of surface-active surfactants (non-ionic (e.g. Tween 80) and anionic (e.g. dioctyl sodium sulfosuccinate) ranging from 1-50%) and solvents (e.g. kerosene or glycol ether >50%) (Fiocco and Lewis, 1999; Kirby *et al.*, 2011), though exact compositions are proprietary information. The Type III dispersant Corexit is the most widely used oil-spill response dispersant in the United States, making up a large proportion of stockpiles. Two major constituents of Corexit 9500 are the anionic surfactant sodium dioctyl sulfosuccinate (sodium 1,4-bis(2-ethylhexoxy)-1,4-dioxobutane-2-sulfonate), and the solvent dipropylene glycol *n*-butyl ether (1-(2-butoxy-1-methylethoxy)-propan-2-ol) (Fig. 1.7) (Nalco Environmental Solutions, 2014). Corexit 9527 consisted of the solvent 2-butoxyethanol (2-Butoxyethan-1-ol) (Fig. 1.7) but due to concerns around adverse health effects by some application workers it was switched for dipropylene glycol *n*-butyl ether in Corexit 9500, which has also been shown to be slightly more effective with high-viscosity oils (National Research Council, 2005).

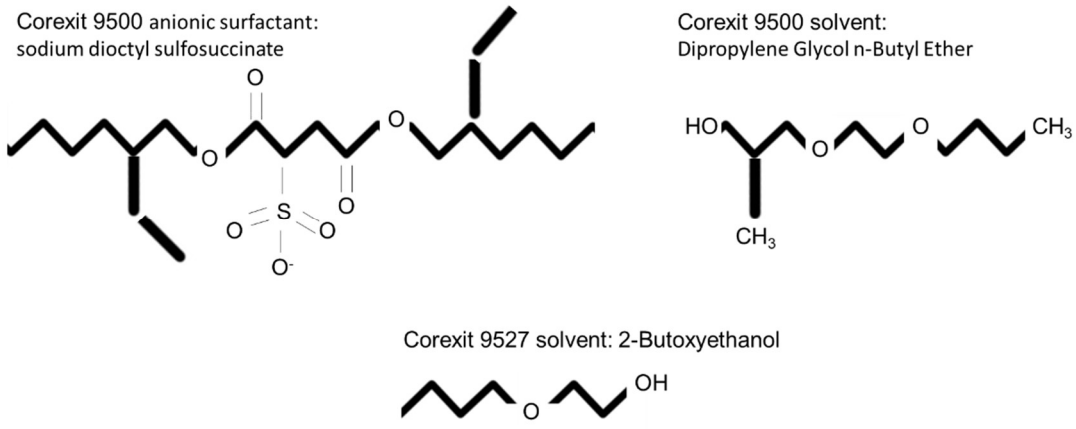

Fig. 1.7: chemical compositions of Corexit 9500's primary anionic surfactant sodium dioctyl sulfosuccinate (sodium 1,4-bis(2-ethylhexoxy)-1,4-dioxobutane-2-sulfonate), and solvent dipropylene glycol *n*-butyl ether (1-(2-butoxy-1-methylethoxy)-propan-2-ol). Previous used solvent 2-butoxyethanol (2-butoxyethan-1-ol) in Corexit 9527.

In the UK, eight dispersants make up the majority stored for oil-spill response. As of 2020, the UK has 1,170 tonnes of dispersants stockpiled. The three highest stockpiled brands are 1) Superdispersant 25 (522 tonnes), 2) Slickgone NS (211 tonnes), and 3) Finasol OSR 52 (70 tonnes) (Maritime and Coastguard Agency, 2020). Superdispersant 25 (supplied by Oil Slick Dispersants and stockpiled in the Shetlands)

is primarily used as a Type III dispersant and applied neat (although can be diluted with sea water at 10%). The dispersant's composition is a 2-butoxyethanol solvent 10-30% (as used in Corexit 9527) and an anionic surfactant 1-10% (sodium dioctyl sulfosuccinate, as used in Corexit 9500) (Oil Slick Dispersants, 2015). Slickgone NS (supplied by DASIC International Ltd and stockpiled round the UK) is also a Type III dispersant and can be used neat or diluted with seawater (10%). Slickgone NS's composition is an odourless kerosene (>50%) and an anionic surfactant 1-10% (sodium dioctyl sulfosuccinate) (DASIC International, 2002). Finasol OSR 52 (supplied by Total Fluides and stockpiled around the UK) is a Type III dispersant and in similarity to Superdispersant 25 and Slickgone NS can be applied neat or diluted with seawater (10%). Finasol OSR 52's composition includes 15-30% non-ionic surfactants, 0.2-5% anionic surfactants (including sodium dioctyl sulfosuccinate), and 60-70% hydrocarbons (C_{11}-C_{14} <2%) (Total-Fluides, 2012). The exact composition of the different synthetic dispersants are commercial secrets. However, in addition to the above, it is known that most commercial dispersants contain Tween 80 (2-[2-[3,4-bis(2-hydroxyethoxy)oxolan-2-yl]-2-(2-hydroxyethoxy)ethoxy]ethyl octadec-9-enoate)) and Span 80 (2-[2-[3,4-bis(2-hydroxyethoxy)oxolan-2-yl]-2-(2-hydroxyethoxy)ethoxy]ethyl octadec-9-enoate); both are non-ionic saccharide-based surfactants (John *et al.*, 2016).

Biosurfactants

Biosurfactants are surface-active substances produced by living cells (such as yeast, *Bacteria*, and *Fungi*). The biosurfactant market was worth $1.8 billion in 2016, and is expected to grow to between $2.6 and 5.2 billion by 2023 (Markets and Markets, 2017; Global Market Insights, 2018), with the market for the biosurfactant rhamnolipid expecting an 8% increase (Global Market Insights, 2018). Interest in biosurfactants comes from many different perspectives: diversity, selectivity, biodegradability (Zajic *et al.*, 1977), production via fermentation (Banat *et al.*, 2014), and potential applications including food industry (Vijayakumar and Saravanan, 2015), removal of heavy metals (Pacwa-Płociniczak *et al.*, 2011), enhanced oil recovery (Suwansukho *et al.*, 2008), and oil-spill bioremediation (Souza *et al.*, 2014). Production of biosurfactants is an area of research that is continuously increasing, with several cheaper and renewable substrates now being used, such as soybean (Lee *et al.*, 2008) and sunflower oil (White *et al.*, 2013). Cheaper and renewable substrates, along with innovations in fermentation and strain selection, are enhancing the production of biosurfactants. For example, renewable substrates include food and agriculture industrial residue, animal waste, and waste cooking oil (see references within Singh

et al., 2019). Studies have found that hydrolysis methods (acid hydrolysis, enzymatic hydrolysis) significantly increase total soluble sugar concentration in the fermentation process, increasing biosurfactant production (Konishi *et al.*, 2015; Moya Ramírez *et al.*, 2016). However, there is still an economic gap when scaling up to industrial production. Downstream processes account for 60-80% of the cost, and with the end-product being highly expensive it is not feasible for widespread application in oil-spill response. Continued research needs to occur into cheaper substrates as well as further innovation in the fermentation process (Banat *et al.*, 2014).

Biosurfactants have a polar (hydrophilic) moiety and non-polar (hydrophobic) group. Microbial production of biosurfactants occurs either extracellularly (to emulsify a substrate) or as part of the cell wall (to enable the passage of a substrate) (Mulligan and Gibbs, 1993). Biosurfactants are classified by their chemical composition and microbial origin. They can be classified into the following major groups: glycolipids (e.g. rhamnolipid, trehalolipid, sophorolipid, mannosylerythritol lipids), lipopeptides (e.g. surfactin (Fig. 1.8), lichenysin, fengycin) and phospholipids (the low molecular weight biosurfactants), and fatty acids, neutral lipids, and polymeric and particular compounds (high molecular weight biosurfactants) (Feldman, 1987; Rosenberg and Ron, 1999; Shekhar *et al.*, 2015). Most of these compounds are either anionic or non-ionic, with only a small fraction being cationic. The CMC of biosurfactants generally ranges from 1 to 200 mg l^{-1} (Mulligan, 2005). Regarding the potential of biosurfactant application in oil-spill remediation, most researched biosurfactants are glycolipids (carbohydrates with long-chain aliphatic or hydroxyaliphatic acids).

Rhamnolipids consist of either one or two sugar(s) glycosylated to a β-hydroxy(3-hydroxy) fatty acid (Lang and Wullbrandt, 1999). Rhamnolipid was first discovered being synthesised by the bacteria *Pseudomonas aeruginosa* (Jarvis and Johnson, 1949), which remains a model strain to understand the genes involved in the biosynthesis of rhamnolipids (Chong and Li, 2017). Rhamnolipid reduces surface tension of water from 72 to 29 mN m^{-1} and an interfacial tension of 0.25 mN m^{-1}. The CMC for rhamnolipid ranges from 0.1 to 10 mg l^{-1}. (Hisatsuka *et al.*, 1971). One example of a rhamnolipid (Type I) produced by *P. aeruginosa* is L-Rhamnosyl-L-rhamnosyl-β-hydroxydecanoate (Edwards and Hayashi, 1965) (Fig. 1.8). It has been demonstrated that both *rhlA* and *rhlB* genes are necessary to produce a mono-rhamnolipid, arranged in an operon, *rhlAB,* which code for the enzymes that catalyse the formation of haloacetic acids and mono-rhamnolipids respectively. For the biosynthesis of di-rhamnolipids the *rhlC* gene is also required, which codes for the RhlC enzyme that catalyses the addition of the second rhamnose moiety (Rahim *et al.*, 2001). The three key enzymes that encode for the production of rhamnolipid, RhlA,

RhlB, and RhlC, are also found in species from the genus *Burkholderia* (Chong and Li, 2017).

Trehalolipids are produced by the genera *Mycobacterium*, *Nocardia*, and *Rhodococcus*. Trehalolipid can reduce the surface tension of water from 72 mN m^{-1} to between 32 and 36 mN m^{-1}, an interfacial tension of 1 mN m^{-1}, and a CMC of approximately 4 mg l^{-1} (Rapp *et al.*, 1979). Trehalolipid structures are variable but generally consist of a non-ionic acylated derived trehalose sugar glycosylated to a mono-, di-, or tri-fatty acid (White *et al.*, 2013). An example of a trehalolipid is trehalose dimycolate (Fig. 1.8), produced by *Rhodococcus erythropolis* (Kretschmer *et al.*, 1982). White *et al.* (2013) observed that a purified trehalolipid produced by a strain of *Rhodococcus sp.* PML026 was able to maintain surface tension levels and the stability of emulsions in a range of conditions; pH from 2-12, temperature from 20-100°C, and NaCl concentration of 5-25% w/v.

Sophorolipids are primarily produced by yeasts, such as the *Torulopsis* and *Candida* genera. Sophorolipids generally consist of di-saccharide (2-O-β-o-glucopyranosyl-β-D-glucopyranose) derivatives, each linked to a hydroxy fatty acid (Davila *et al.*, 1994) (Fig. 1.8). An example of yeast that produces sophorolipids is *Torulopsis bombicola* and the sophorolipid is demonstrated to reduce the surface tension of water from 72 to 33 mN m^{-1}, and an interface tension of 1.8 mN m^{-1} (Göbbert *et al.*, 1984). It is worth noting that the production of biosurfactants from yeasts, such as *T. bombicola*, provide higher yields at reduced costs in comparison to the production of biosurfactants from bacteria (Cooper and Paddock, 1984). Minucelli *et al.* (2017) observed that the production of a sophorolipid by, and microbial growth of, *Candida bombicola* was optimal when it was grown on a medium containing both carbohydrate (e.g. glucose, sucrose, lactose), a lipidic carbon source (e.g. *n*-alkanes, corn oil, vegetable oil), and a nitrogen source such as yeast extract.

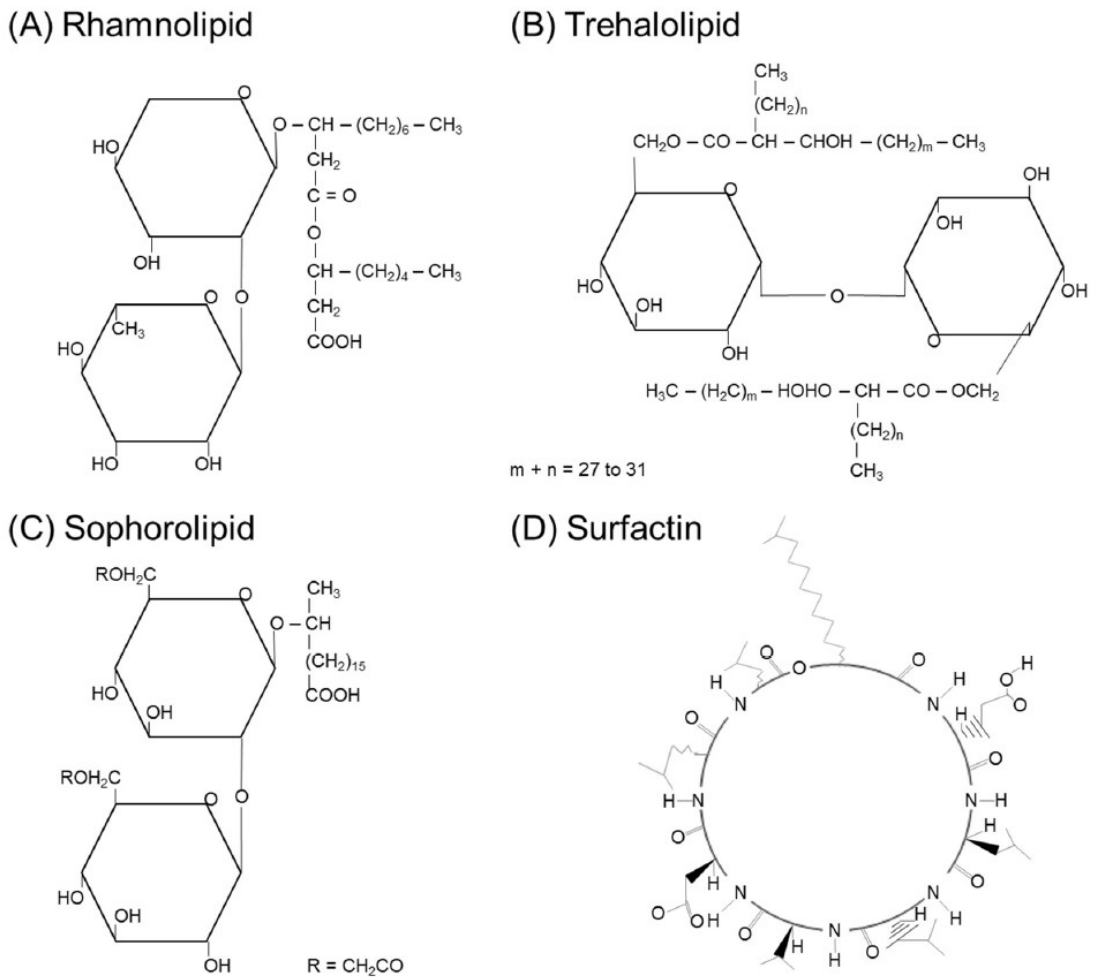

Fig. 1.8: representative biosurfactants chemical composition and structures. (**A**) Rhamnolipid Type I from Pseudomonas aeruginosa, (**B**) Trehalose dimycolate from Rhodococcus erythropolis, (**C**) Sophorolipid from Torulopsis bombicola, and (**D**) Surfactin cyclic lipopeptide from Bacillus subtilis.

Toxicity and Biological Impact

Understanding the toxicity of any substance applied to the environment is vital to protecting vulnerable ecosystems, their inhabitants, and ecosystem services. Additionally, it is important we protect those who apply a dispersant to an oil-slick, often by aeroplane or ship aerosols, and those in the immediate vicinity. Therefore, every country that uses dispersants will have their own tests prior to rules, guidelines, and regulations being drawn up that govern their use. The commercial dispersants Slickgone NS, Superdispersant 25, and Finasol OSR 52 are all approved for use in the UK. However, research into dispersant toxicity have raised concerns (Major *et al.*, 2012; Afshar-Mohajer *et al.*, 2019). The application of dispersants to crude oil, in studies of the Torrey Canyon oil-tanker spill, was demonstrated to increase toxicity significantly, causing increased mortality to organisms (especially littoral and sub-littoral species) and environmental damage (Bellamy *et al.*, 1967; LaRoche *et al.*, 1970; Southward and Southward, 1978). However, as previously discussed, first

generation dispersants were more toxic (Blumer, 1971). Since then, attention has been placed on the dispersants currently used, third generation Type II and Type III. Couillard *et al*. (2005) studied the effects of Corexit 9500 on killifish larvae (*Fundulus hetetroclitus*), finding that the dispersant caused a two- to five-fold increase in the concentration of total PAHs in the seawater, which in turn the larvae consumed. This caused a significant increase in larvae mortality and reduction in body size. Conversely, a study by Rial *et al*. (2014) found that four tested dispersants did not significantly decrease marine *Bacteria* biomass. Whilst an additional study found that Slickgone NS did not increase the toxicity of the hydrocarbon source they were testing (intermediate fuel oil IFO 180, BP) (Alexander *et al.*, 2017).

Whilst biosurfactants are produced naturally, they too should undergo vigorous toxicity testing prior to application. A study by Santos *et al*. (2017) evaluated the toxicity of a glycolipid produced by the yeast *Candida lipolytica*. The toxicity assay compared mortality rates of brine shrimp (*Artemia salina*) and bivalves (*Anomalocardia brasiliana*) in the presence of crude oil and/or biosurfactant. Santos observed that 100% of individuals survived when subjected to different dilutions of the crude biosurfactant. However, an isolated biosurfactant solution killed 100% of the shrimp larvae at a concentration of 0.08% but no mortality was observed from concentrations 0.02 to 0.06%. An additional study of glycolipids produced by *Candida sphaerica* UCP0995 demonstrated no toxicity towards microcrustaceans (*Artemia salina*) at 9 g l^{-1} (Luna *et al.*, 2013). A further study examined the toxicity of lipopeptides produced by a *Bacillus sp.* strain GY19. The research used post-larval Whiteleg shrimp (*Litopenaeus vannamei*) and adult copepods, exposing them to varying concentrations (0.5-3000 mg l^{-1}) of the biosurfactant. Mortality was calculated after 96 hours and then toxicity was compared to a commercial dispersant, Slickgone NS. The research concluded the toxicity of the lipopeptide was significantly lower than Slickgone NS, with the LC_{50} value for the Whiteleg shrimp at 1050 mg l^{-1} for the biosurfactant and 31 mg l^{-1} for Slickgone NS. Additionally, the copepod LC_{50} value was 1174 mg l^{-1} for the biosurfactant and 68 mg l^{-1} for Slickgone NS (Rongsayamanont *et al.*, 2017).

It is evident that the toxicity of biosurfactants is significantly less than that of commercial dispersants, likely due to the absence of additional solvents found in dispersants and the use of the anionic surfactant DOSS (Sodium 1,4-bis(2-ethylhexoxy)-1,4-dioxobutane-2-sulfonate). However, it should be noted that concerns have been raised over how toxicity testing is carried out, these concerns state that many toxicity studies are not truly reflective of environmental conditions and use inconsistent and unrealistic oil/dispersant concentrations and exposure durations (Bejarano *et al.*, 2014; Colvin *et al.*, 2020).

Hydrocarbon-biodegradation

There is a large amount of research into whether dispersants enhance hydrocarbon-biodegradation. Prince *et al*. (2013) evaluated Corexit 9500 and found that dispersed crude oil is rapidly and extensively biodegraded. Prince *et al*. (2015) also evaluated three commonly applied commercial dispersants: Corexit 9500, Slickgone NS, and Finasol OSR 52. Prince *et al*. (2015) found that all three dispersants significantly increased the biodegradation of hydrocarbons when compared to a floating slick with no added dispersants. On average the dispersants had increased biodegradation from 32% to 64% after 7 days and from 48% to 72% after 62 days, in comparison to a floating oil slick. This included a complete reduction of pristane and phytane, and >90% reduction of phenanthrene and methlyphenanthrenes, after 7 days. Prince *et al*. (2015) go onto state that the role of dispersants is not to stimulate biodegradation *per se* but to stop oil from reaching coastal areas. Once the oil is dispersed biodegradation occurs regardless of the presence of dispersants. There are many studies which also observe that dispersants increase hydrocarbon-biodegradation (Fiocco and Lewis, 1999; Brakstad *et al.*, 2014; Prince and Butler, 2014; Hazen *et al.*, 2016; Tremblay *et al.*, 2017). For example, Brakstad *et al*. (2015) compared hydrocarbon-biodegradation rates over varying oil droplet sizes, finding that biodegradation of *n*-alkanes and aromatic hydrocarbons was faster with oil droplets of 10 μm compared to 30 μm.

However, not all studies come to the same conclusion, with some stating that dispersants may actually inhibit the biodegradation of hydrocarbons. Foght and Westlake (1983) tested Corexit 9527 and found that the response was nutrient- and dispersant-concentration-dependant. Rahsepar *et al.* (2016) observed that the use of Corexit 9500, at a ratio of 20:1 (oil to dispersant), inhibited biodegradation. Inhibition was due to dispersants increasing the solubility of aromatic hydrocarbons and was demonstrated particularly when low or no presence of aromatic-degrading microbes were present. Kleindienst *et al*. (2015b), in contradiction to Prince *et al*. (2013), found that Corexit 9500 supressed the activity of hydrocarbon-degrading microbes. This was something Prince *et al*. (2016) rebutted, stating that water-accommodated-fraction (WAF) methodologies did not allow for the comparison of dispersed and floating oil. This is because WAF and CEWAF (chemically-enhanced water-accommodated-fraction, where a dispersant is applied to the WAF), methodologies are firstly physically dispersed by a mechanical vortex, and thus it is not comparing a floating oil-slick to one that has been chemically dispersed.

There are many factors which can limit the effectiveness of dispersants on hydrocarbon-biodegradation. Nitrogen and phosphorous play a vital role in microbial

growth as it is incorporated into their biomass (Jagadevan and Mukherji, 2004). The availability of these nutrients in the presence of hydrocarbons is vital (Ron and Rosenberg, 2014) (see "*Limiting Factors*", page 13). Kleindienst *et al*. (2015a) demonstrate that low levels of nutrients decrease the efficacy of dispersants on hydrocarbon-biodegradation. Other studies, however, state that hydrocarbon-degrading microbes do not need additional nutrients (biostimulation), as when the oil is dispersed there is a greater availability of nutrients (McFarlin *et al.*, 2014).

Environmental conditions, and the type of oil contaminating the environment, also affect how successful the application of dispersants on oil-spills are. Atlas and Hazen (2011) studied two of the worst oil-spills in US history: Deep-Water Horizon (DWH) and Exxon Valdez (EV). These two oil-spills occurred in vastly different environmental conditions and released different types of oil. The EV tanker discharged a medium oil (North Slope 29°API), on the water's surface, near the shore and in the near pristine sub-Arctic. A storm hit the EV location two days after the spill had occurred and caused much of the oil to be washed onto the coast. Given these conditions, the application of dispersants on the EV oil-spill was not undertaken, with water washing and the addition of nutrients (fertiliser) being the primary remediation strategies. In comparison, the Macondo oil-well, from the DWH oil-spill, discharged a light oil (Louisiana 35.2°API), at a depth of 1,500 m and 50 miles from coastlines in the sub-tropics, where oil seeps were present and oil spills had occurred previously. Approximately 1.84 million gallons of dispersant (Corexit 9500) were applied, both on the surface via aeroplane and boat application, and directly at the well-head-blowout (1,500 m depth) (White *et al.*, 2014). The DWH oil spill occurred in an environment where oil pollution had occurred previously, and thus microbial communities would have been primed to respond (Leahy and Colwell, 1990). This meant that when oil was dispersed, biodegradation occurred at a rapid rate, especially in the water column where large oil plumes were located (Yang *et al.*, 2016).

Temperature affects both the physical state of hydrocarbons (at low temperatures viscosity increases), the indigenous microbial community (at low temperatures enzymatic activity is decreased) (Wang and Wang, 2018), and the rate at which chemical reactions occur, with a double approximately every 10°C (Laidler, 1985). Ferguson *et al*. (2017) evaluated the effects of dispersant (Superdispersant 25) application on the biodegradation of oil in sub-Arctic deep-sea sediments (0°C and 5°C microcosms). Ferguson *et al*. (2017) observed that biodegradation was significantly decreased at the colder temperature (0°C), with some PAHs showing no signs of degradation at all. However, McFarlin *et al*. (2014) found that at -1°C crude

oil biodegradation was significantly increased at 10 and 28 days when the dispersant Corexit 9500 was applied in comparison to when it was not.

Biosurfactants display characteristics that allow them to function over a wide range of environmental factors, including temperature, pH, and salinity (Banat *et al.*, 2010); thus there is growing interest into oil-spill bioremediation potential. To this regard, rhamnolipids have received much attention, with increases in hydrocarbon-biodegradation being evidenced (Zhang *et al.*, 2005; Gonzini *et al.*, 2010; Kaczorek and Olszanowski, 2011; Gudiña *et al.*, 2015). McKew *et al*. (2007a) observed a significant reduction in *n*-alkanes in microcosms containing oil, nutrients, and rhamnolipids, in comparison to oil and nutrients alone. Additionally, trehalolipids produced by *Rhodococcus erythropolis* were demonstrated to increase the rate of phenanthrene-biodegradation in oil-contaminated soil-water slurry (Chang *et al.*, 2004). However, not all biosurfactants have been demonstrated to positively increase hydrocarbon-biodegradation. Saborimanesh & Mulligan (2015) observed that the biodegradation of biodiesel, diesel, and light crude oil, in seawater microcosms, was the same with or without the addition of sophorolipids. Surface tension measurements were not provided in the Saborimanesh & Mulligan (2015) study, however, it could be that no effect was observed due to the sophorolipid addition (80 mg L^{-1}) not reducing the interfacial surface tension between oil and water further than that would be achieved by the crude oil or petroleum products alone. The effects of sophorolipid addition to oil-slicks in microcosms is examined further in Chapter Two.

Balancing the trade-offs of different scenarios must be considered, for example, between the predicted effects of leaving oil on the water surface, versus dispersing oil into the water column and potentially to the seabed, which is often considered preferential to allowing oil to transfer to coastlines, particularly when these include environmentally sensitive areas. The effects of dispersants and biosurfactants, applied to oil-slicks, on the rate of hydrocarbon-biodegradation and microbial community composition and abundance, is evaluated in Chapter Two. Moreover, a comparison of two oil-slicks, one left to natural processes and the other chemically dispersed, is evaluated in Chapter Three.

Oil-degrading Microbial Communities

Certain genera and species of microbes are capable of hydrocarbon-biodegradation, providing a natural remediation resource in oil-contaminated environments. Understanding microbial community structure, succession, and roles of hydrocarbon-degrading microbes, and how they are affected by oil-spills, remediation

strategies, and shipwrecks, allows for the refinement and advancement of post-oil-spill monitoring models and oil-spill response guidelines (Kirby *et al.*, 2018).

Diversity and Roles of Hydrocarbon-degrading Microbes

Oil spills dramatically alter marine microbial community composition, resulting in a decrease in species richness and diversity, in conjunction with selection for hydrocarbon-degrading Bacteria (Head *et al.*, 2006; McGenity *et al.*, 2012). Certain microbes can degrade a range of hydrocarbons, these include the obligate hydrocarbonoclastic bacteria (OHCB; *Alcanivorax*, *Cycloclasticus*, *Oleispira*, *Oleibacter*, *Thalassolituus*), which use hydrocarbons as an almost exclusive source of carbon and energy (Yakimov *et al.*, 2007). Whilst OHCB have been demonstrated to degrade other compounds in pure culture (Zadjelovic *et al.*, 2020), there is still limited evidence that the OHCB are competitive for non-hydrocarbon substrates in the environment. This is evidenced by the fact OHCB are typically present in extremely low numbers in uncontaminated environments but rapidly increase in abundance following oil-spills (Kasai *et al.*, 2001; Yakimov *et al.*, 2004; Atlas and Hazen, 2011; Acosta-González *et al.*, 2015; Nogales and Bosch, 2019). Moreover, OHCB refers to the taxonomic grouping of these hydrocarbon-degrading bacteria, rather than their physiological features. Therefore, whilst it is evident that OHCB use a few other carbon and energy sources, for clarity they are referred to hereafter as “OHCB” to distinguish between these highly adapted and competitive hydrocarbon-degraders and those more metabolically diverse *Bacteria*, which can also degrade hydrocarbons.

How microbial communities respond to oil pollution is dependent on many different physical, chemical, and biological factors, including the type of oil-spilled and environmental conditions (e.g. currents, wind, UV, temperature, and nutrient concentrations). After an oil-spill perturbation, there is often an initial boom in the abundance of alkane-degrading microbes (e.g. *Alcanivorax*/*Oleispira*) followed by growth of PAH-degraders (e.g. *Colwellia*/*Cycloclasticus*) (Head *et al.*, 2006; McGenity *et al.*, 2012). Most individual hydrocarbon-degrading bacterium can only degrade a short range of hydrocarbons, typically either aliphatic or aromatic compounds. However, heterogeneous microbial communities provide the greatest opportunity to degrade the vast range of hydrocarbons within crude oil (Röling *et al.*, 2002). To understand hydrocarbon-degrading microbes, researchers define the catabolic capabilities of isolates, evaluate *in situ* observations, and conduct *ex situ* experiments. Here a focus on the OHCB is conducted, though many other hydrocarbon-degrading microbes play vital roles in oil-spill biodegradation, these are evaluated and discussed further in the following Chapters.

Alkane-degrading OHCB

The genus *Alcanivorax,* within the class *Gammaproteobacteria* and the order *Oceanospirillales*, currently contains 15 recorded species (LPSN)(NCBI Taxonomy Browser, 2020a). The type strain *Alcanivorax borkumensis* SK2, is a Gram-negative, rod shaped, aerobic OHCB, that grows on a spectrum of alkanes including branched-alkanes (Yakimov *et al.*, 1998). Typically in pristine environments *Alcanivorax* is in very low abundance, however, in the presence of crude oil it can rapidly dominate the bacterial communities (Topouzelis, 2008). Given its importance, the type strain *A. borkumensis* SK2 was the first OHCB to have its genome sequenced (Schneiker *et al.* 2006). *A. borkumensis* SK2 was demonstrated to be able to biodegrade a broad range of *n*-alkanes (C_{10} to C_{32}) and branched alkanes (pristane and phytane). This wide range of hydrocarbons as an energy source provides a competitive advantage in comparison to hydrocarbon-degrading bacteria that utilise a narrower range of hydrocarbons. *Alcanivorax* spp. produces key enzymes (alkane hydroxylases), AlkB1, AlkB2, AlmA, and P450-3. AlkB1 oxidises alkanes from C_5 to C_{12} and AlkB2 oxidises alkanes from C_8 to C_{16}, (Van Beilen *et al.*, 2004). AlmA, confirmed as a hydroxylase of long-chain alkanes (Wang and Shao, 2014), could also be involved in the hydroxylation of branched-alkanes (Gregson *et al.*, 2019); whilst branched alkanes strongly induce the expression of P450 cytochromes (Wang and Shao, 2012; Sevilla *et al.*, 2017; Gregson *et al.*, 2019). The strains *A. borkumensis* DSM11573^T and MM1 are observed to produce a glycolipid biosurfactant (18-(1-L-glucopyranosyl)-6,10,14-triheptyl4,8,12,16-tetroxy-3-aza-7,11,15-trioxa-pentaeicosanoic acid 1) (Passeri *et al.*, 1992; Abraham *et al.*, 1998), which can reduce the surface tension of water from 72 to 30 mN m^{-1} (Passeri *et al.*, 1992). *Alcanivorax spp.* can function in a broad range of salinities and temperatures (Yakimov *et al.*, 1998).

The genus *Oleibacter,* within the class *Gammaproteobacteria* from the order *Oceanospirillales*, currently contains just one species (LPSN), the type strain *Oleibacter marinus* 2O1. It is a Gram-negative, motile, mesophilic, aerobic, rod-shaped OHCB, that exhibits high *n*-alkane-degrading activity (Teramoto *et al.*, 2011). *O. marinus* was isolated from a tropical marine environment in Indonesia and grows from 10 to 40°C (optimum 25–30°C), at pH 6–10 (optimum pH 6-9), with 1–7 % (w/v) salinity. *Oleibacter* spp. have been observed in sediments at depths of >10,400 m in the Mariana Trench, where abundant *n*-alkanes were observed in sinking particles (23.5 µg/gdw) and in hadal surface sediments (2.3 µg/gdw) (Liu *et al.*, 2019).

The genus *Oleispira*, within the class *Gammaproteobacteria* from the order *Oceanospirillales*, contains two recorded species (LPSN. The type strain *Oleispira antarctica* RB-8 is a Gram-negative, rod shaped, aerobic OHCB, isolated from the

Ross Sea, Antarctica. *O. antarctica* RB-8 has an optimal growth range of temperatures from 1 – 15°C and salinity of 3 – 5% v/v, and is capable of nitrate reduction (Yakimov *et al.*, 2003). *O. antarctica* can aerobically utilise a range of *n*-alkanes as an energy source (C_{10} to C_{24}) but lacks the genes for enzymes necessary to grow on larger *n*-alkanes or branched alkanes (e.g. *almA*, *ladA*) (Gregson *et al.*, 2020). *Oleispira* spp. bloom in cold waters (5ºC), such as the polar seas or the deep sea (Mason *et al.*, 2012; Joye *et al.*, 2014), but are outcompeted by other OHCB at warmer temperatures (Coulon *et al.*, 2007; King *et al.*, 2015; Brakstad, *et al.*, 2018). Increased biosynthesis of proteins (e.g. FleQ, FliL, FlaB) that generate sufficient force for rotation of the flagellar, through seawater that becomes more viscous in colder temperatures, is observed in *O. antarctica* (Gregson *et al.*, 2020). Moreover, *Oleispira* has structural adaptation of hydrolytic enzymes to cold temperatures and cold-induced alteration in membrane lipid structures (Kube *et al.*, 2013).

The genus *Thalassolituus,* within the class *Gammaproteobacteria* from the order *Oceanospirillales* contains two recorded species: *T. marinus* and *T. oleivorans* (LPSN). The type strain *Thalassolituus oleivorans* MIL-1 is a halophilic, aerobic, Gram-negative, curved OHCB that is strictly aerobic and does not demonstrate the ability to grow via fermentation, denitrification, or phototrophically. *T. oleivorans* MIL-1 has a growth range of 0.5 – 5.7% v/v salinity (optimum 2.3%), 4 – 30°C temperature (optimum 20 – 25°C), and pH of 7.5 – 9 (optimum pH 8) (Yakimov *et al.*, 2004). *T. oleivorans* can utilise a range of *n*-alkanes (C_7 to C_{32}) (Yakimov, Giuliano, *et al.*, 2004; Gregson *et al.*, 2018), but not branched alkanes. The genes encoding for AlmA and ladA enzymes, involved in the degradation of *n*-alkanes longer than C_{30}, are not present in the *T. oleivorans* genome, however, *T. oleivorans* can grow on alkanes up to *n*-C_{32} due to the possession of genes that code for a subterminal Baeyer-Villiger monooxygenase (BVMO) (Gregson *et al.*, 2018).

PAH-degrading OHCB

The genus *Cycloclasticus,* within the class *Gammaproteobacteria* from the order *Thiotrichales*, contains five recorded species (one valid recorded species name; LPSN). The type strain *Cycloclasticus pugetti* PS-1 is an aerobic, Gram-negative, rod shaped OHCB that utilises aromatic compounds as a primary source of energy, including monoaromatics (e.g. toluene and xylenes) and PAHs (e.g. naphthalene and phenanthrene) (Dyksterhouse *et al.*, 1995). RHDs (ring-hydroxylating dioxygenase) are the key enzymes involved in PAH-degradation pathways and this is discussed further in "*Aerobic PAH-Degradation*". It has been demonstrated that the extent of C_{1-2}-alkyl aromatic hydrocarbon-degradation was significantly higher in *Cycloclasticus*

spp. in comparison to other known PAH-degraders; such as *Pseudomonas*, *Marinobacter*, and *Sphingomonas* (Kasai *et al.*, 2002). The genus *Cycloclasticus* includes *C. pugetti* (Dyksterhouse *et al.*, 1995), *C. oligotrophus* (Robertson and Button, 1999), *C. spirillensus* (Chung and King, 2001), and *C. zancles* (Messina *et al.*, 2016). The genus also includes one lineage that degrades very short-chained *n*-alkanes (symbiont of *Bathymodiolus*; Rubin-Blum *et al*., 2017). A study of deepwater-horizon observed an initial bloom of *Oceanospirillales* at the start of the spill (Apr 2010) but there was a shift in dominance to members of the genera *Cycloclasticus* and *Colwellia* in June 2010 (Hazen *et al.*, 2016).

Whilst the genus *Marinobacter* does not form part of the OHCB, one species is an obligate hydrocarbon-degrading bacterium, *Marinobacter hydrocarbonoclasticus*. *M. hydrocarbonclasticus* is a rod shaped bacterium that was first described in 1992 by Gauthier *et al*., and has a growth range of 10 - 45°C (optimum 32°C), with tolerance to 6-9.5 pH (optimum 7 – 7.5 pH) and salinity of 0.08 to 3.5% v/v (optimum 0.6% v/v). *M. hydrocarbonclasticus* is able to aerobically utilise both cyclic and non-cyclic hydrocarbons, including C_{14} to C_{21}, pristane, and phenanthrene (Al-Mallah *et al.*, 1990; Gauthier *et al.*, 1992). *M. hydrocarbonoclasticus* SP17 forms biofilms at the interface of oil and water, used as a strategy to overcome low bioavailability of hydrocarbons (Grimaud *et al.*, 2012).

It is worth noting, that in addition to hydrocarbon-degrading bacteria responding to oil-spills or seepages, hydrocarbon-degrading bacteria, for example certain *Alcanivorax* and *Marinobacter* species, are able to co-exist with microalgae and unicellular photosynthetic eukaryotes (Green *et al.*, 2004, 2006, 2015; Yakimov *et al.*, 2007; McGenity *et al.*, 2012). The study if microalgae-associated bacteria relationships have been central to new discoveries of PAH-degrading bacteria, such as *Porticoccus hydrocarbonoclasticus*, *Polycyclovorans algicola*, *Algiphilus aromaticivorans*, and *Arenibacter algicola* (Gutierrez, *et al.*, 2012a, 2013; Gutierrez, *et al.*, 2012b; Gutierrez *et al.*, 2014). The mechanisms associating hydrocarbon-degrading bacteria and phytoplankton in marine environments is still under evaluation, however, studies have demonstrated that some microalgae synthesise long-chain alkenones and accumulate/absorb PAHs (Andelman and Suess, 1970; Gunnison and Alexander, 1975; Marlowe *et al.*, 1984; Shaw *et al.*, 2003; Exton *et al.*, 2012).

The community structure and succession of OHCB, as well as more metabolically diverse oil-degrading bacteria, in varying environments are evaluated throughout the subsequent Chapters. This includes an *ex situ* oil/dispersant microcosm experiment (coastal water from the Thames Estuary, North Sea; Chapter Two), an *in situ* oil/dispersant experiment (open water, North Sea, Holland; Chapter

Three), an *in situ* real-world oil-spill (coastal sediments, Saronic Gulf, Greece; Chapter Four), and an *in situ* shipwreck (benthic sediments, Scapa Flow, North Sea; Chapter Five). Chapters 2 (Table S2.2) and 4 (Table S4.2) both contain supplementary tables which both provide comprehensive, though not exhaustive, literature references to the hydrocarbon-degradation capabilities of hydrocarbon-degrading bacteria.

Biodegradation Pathways

It is evident that hydrocarbon-degrading bacteria can utilise a wide range of hydrocarbons. These metabolic pathways have evolved over millions of years, as oil within marine environments (e.g. naturally formed hydrocarbon seeps) was present far before anthropogenic inputs.

Aerobic Alkane-degradation

Monooxygenase enzymes catalyse the transfer of molecular oxygen to a hydrocarbon molecule, with one of the two oxygen atoms formed as a hydroxyl group (OH) and the other being reduced to H_2O (van Beilen *et al.*, 2001; Madigan *et al.*, 2008). Oxidation of *n*-alkanes can occur via four pathways. Firstly, oxidation of *n*-alkane often occurs at the terminal carbon, via the enzyme alkane monooxygenase, yielding a primary alcohol. This alcohol is further oxidised to an aldehyde (catalysed by alcohol dehydrogenase) and then to a fatty acid (catalysed by aldehyde dehydrogenase). The fatty acids are subsequently metabolised to acetyl-CoA (via β-oxidation) and then move to the citric acid cycle, prior to the electron transport chain. Secondly, is bi-terminal oxidation, whereby oxidation of the *n*-alkane to the fatty acid occurs without rupturing the hydrocarbon chain, via ω-hydroxylation producing a ω-hydroxy fatty acid reduced to a dicarboxylic acid, which then enters β-oxidation. Thirdly, oxidation can occur at the second carbon, this involves oxidation via a sub-terminal pathway, producing a primary alcohol and a secondary alcohol or methyl acetone (Harayama *et al.*, 1999). Lastly, the Finnerty pathway, whereby dioxygenases transform *n*-alkanes first into *n*-alkyl hydroperoxides (catalysed by dioxygenase) and then to their corresponding alcohol or aldehyde, and finally fatty acids (Fig. 1.9) (Ji *et al.*, 2013; Abbasian *et al.*, 2015).

Proteins required to oxidise *n*-alkanes up to corresponding acyl-CoA derivative in *Alcanivorax borkumensis* SK2 are coded by the operon alkSB_1GJH. This gene cluster contains all the alkane hydroxylase genes required for alkane-degradation, including for example aklB1 (alkane hydroxylase). In addition to alkSB_1GJH operon being involved in alkane-degradation, *A. borkumensis* SK2 also contains the genes gntR (transcriptional negative regulator), alkB2 (alkane hydroxylase), rubA and rubB (rubredoxin reductase) and three cytochromes (P450(a), P450(b), P450(c)) the latter

of which clusters in an operon-like structure with genes encoding a ferredoxin (fdx), an alcohol dehydrogenase (*alkJ2*), a FAD-dependent oxidoreductase, and an araC transcriptional regulator gene (Schneiker *et al.*, 2006). P450 CYP153 genes, involved in the degradation of short- and medium-chain-length *n*-alkanes, are commonly found in alkane-degrading bacteria lacking *alkB* (Van Beilen *et al.*, 2006). The identification of two *alkB* paralogs (*alkMa* and *alkMb*), from the isolate *Acinetobacter venetianus* 6A2, were shown to be involved in the utilisation of *n*-alkanes (up to C_{20}) (Throne-Holst *et al.*, 2006). Screening of a library of transposon mutants of *Acinetobacter* strain DSM 17874, led to the identification of several genes possibly involved in long-chain *n*-alkane-degradation, including the gene *almA* (>C_{20}) (Throne-Holst *et al.*, 2007).

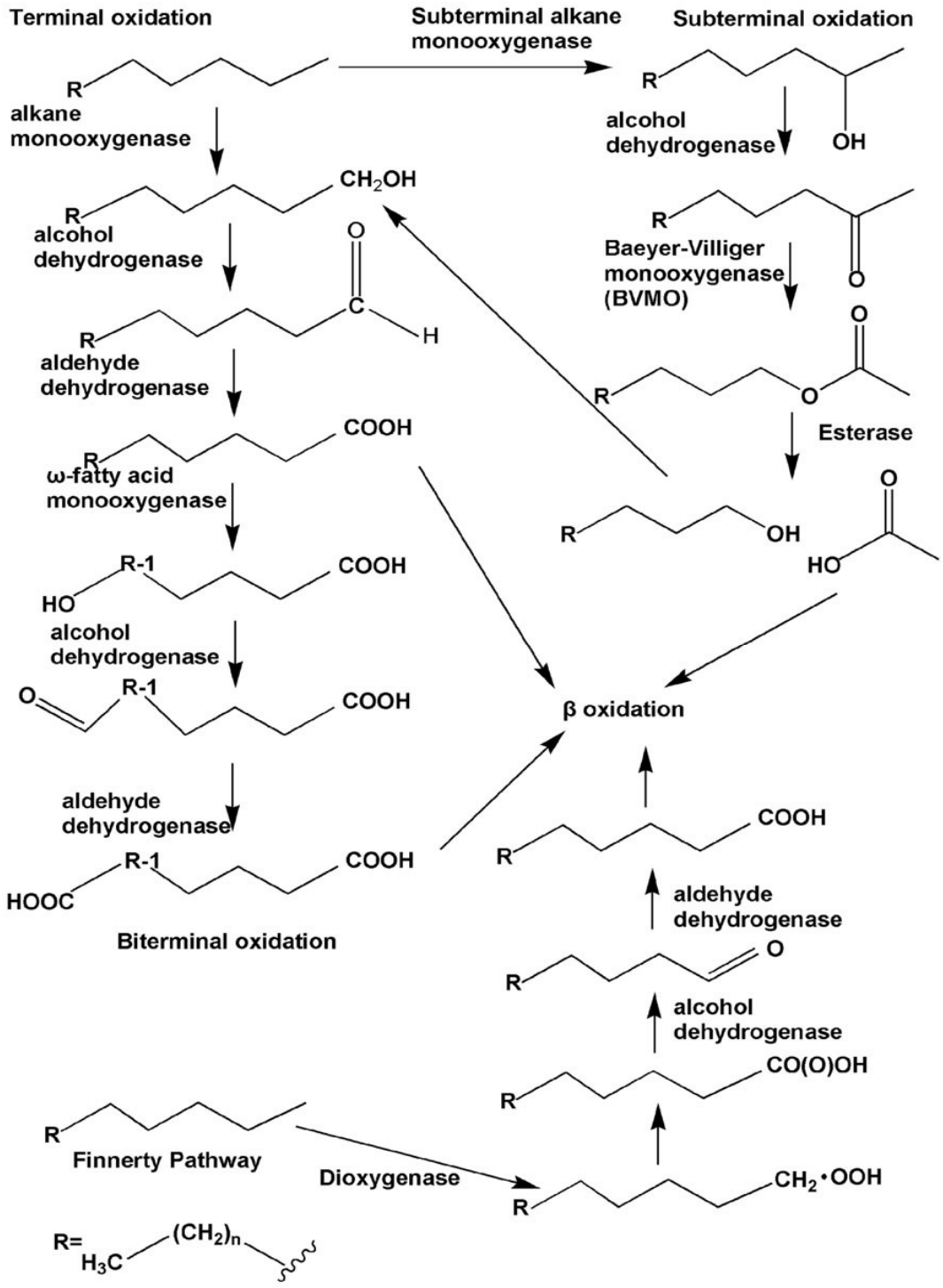

Fig. 1.9: the four types of aerobic alkane-degradation pathways; including terminal oxidation (top left), sub-terminal oxidation (top right), Finnerty pathway (bottom left), and bi-terminal oxidation (above Finnerty pathway). Image taken from *Ji et al., 2013*.

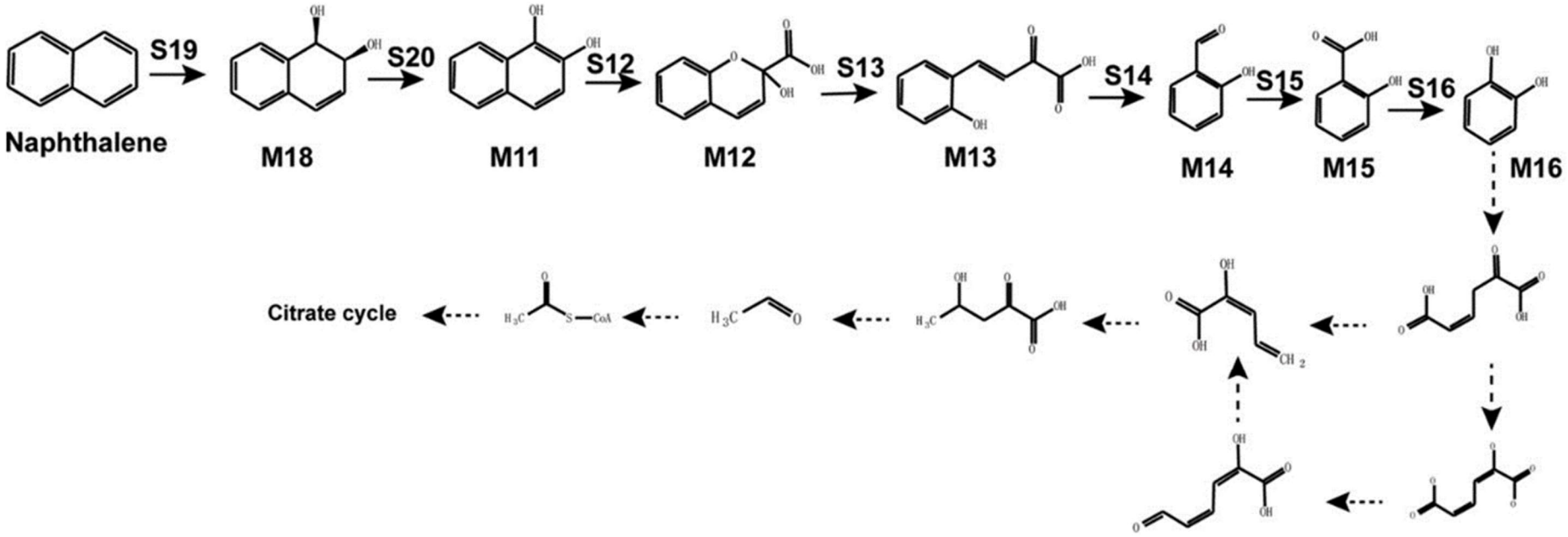

Fig. 1.10: complete naphthalene degradation pathway in Cycloclasticus sp. P1 based on genomic, transcriptomic, and other experimental analyses. Chemical designations: **M11**, 1,2-dihydroxynaphthalene; **M12**, 2-hydroxy-2H-chromene-2-carboxylic acid; **M13**, trans-o-hydroxybenzylidenepyruvic acid; **M14**, salicylaldehyde; **M15**, salicylic acid; **M16**, catechol; **M18**, (1R,2S)cis-l,2-naphthalenedihydrodiol. Enzyme designations: **S12**, cleavage dioxygenase (Q91_2224); **S13**, isomerase (Q91_2218); **S14**, hydratase-aldolase (Q91_0437); **S15**, salicylaldehyde dehydrogenase (Q91_0488); **S16**, salicylate 1-hydroxylase (Q91_1959); **S19**, naphthalene 1,2-dioxygenase (RHD-3); **S20**, NAD+-dependent cis-1,2-naphthalenedihydrodiol dehydrogenase (Q91_2228). Known metabolic pathways are represented by solid arrows. Predicted metabolic pathways are represented by dotted arrows. Taken from Wang et al., 2018.

Aerobic PAH-degradation

The first stages of aerobic PAH-degradation usually occur with the use of dioxygenases, whereby both atoms of the oxygen molecule are incorporated into the hydrocarbon molecule and the oxygen derived hydroxyl group incorporates into the aromatic ring (Kauppi *et al.*, 1998). Catechol and protocatechuatre are common products of this process and can be further reduced (via β-oxidation) to succinate, acetyl CoA, and pyruvate ready for entry into the citric acid cycle. The aerobic PAH-degradation pathway is often inhibited by the dihydroxylation of one aromatic ring by a dioxygenase, producing a dihydrodiol with a *cis*-configuration. The dihydrodiol is reduced to catechol following cleavage of the aromatic ring (via either *meta*-cleavage dioxygenase or *ortho*-cleavage oxygenase). There are many pathways for the metabolism of PAH compounds (dependant on how complex they are) and naphthalene is often used as a model (Fig. 1.10) (Wang *et al.*, 2018). RHDs (ring-hydroxylating dioxygenases) are the key enzymes involved in PAH-degradation pathways; *Cycloclasticus* sp. P1 has nine of these enzymes (RHD-1 to -9), each with a different purpose, for example, the first catabolic step in naphthalene-degradation (the formation of (1R,2S)naphthalene-cis-l,2-dihydrodiol) involves RHD-3 (naphthalene 1,2-dioxygenase). AromaDeg, a web-based resource, allows users to analyse protein sequences targeting aerobic degradation of aromatic hydrocarbons, based on a phylogenetic approach which reduces the quantity of protein misannotations (Duarte *et al.*, 2014).

Anaerobic Hydrocarbon-degradation

Anaerobic hydrocarbon-degradation occurs in the absence of oxygen and often the terminal electron acceptor is replaced with nitrate, sulphate, or iron. There are a variety of different anaerobic biodegradation pathways dependent on the type of hydrocarbon being degraded. For example these include, alkyl-/arylalkylsuccinate synthases, O_2-independent hydroxylation of ethylbenzene, and ATP-dependent and ATP-independent variants of reductive dearomatisation of the central intermediate benzoyl-CoA (Rabus *et al.*, 2016). Two further documented mechanisms, of *n*-alkane anaerobic degradation by sulphate-reducing bacteria, are the addition of fumarate and the carboxylation pathway. Fumarate addition occurs via the sub-terminal pathway on the second carbon, producing an alkylsuccinate. The alkylsuccinate is reduced further to a fatty acid, via β-oxidation and carbon skeleton rearrangement (Ji *et al.*, 2013). An example of fumarate addition is shown in figure 1.11, where fumarate is added to the methyl group of toluene (catalysed by benzylsuccinate synthase) and the hypothetical following steps are comparable to β-oxidation of an α-methyl-branched fatty acid

(CoA-transferase initiating the pathway) (Heider *et al.*, 1998). Strain Hxd3, an alkane-degrading sulphate reducer, was demonstrated to use carboxylation; occurring on the third carbon sub-terminal position whereby the *n*-alkane is reduced to a fatty acid. Carboxylation occurred with inorganic bicarbonate and the removal of two carbon atoms from the alkane chain terminus (So *et al.*, 2003).

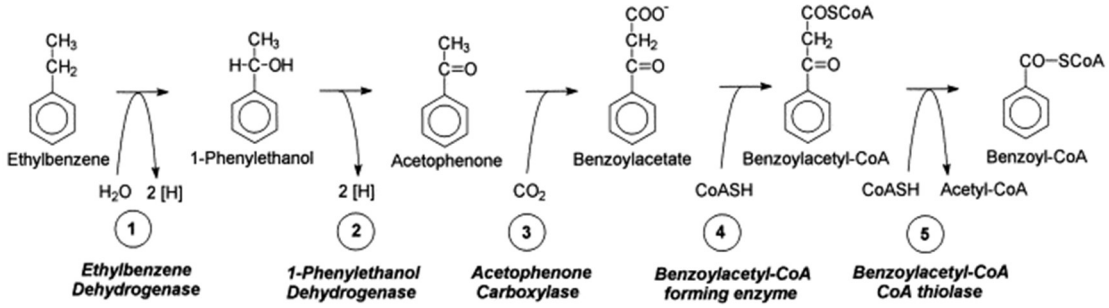

Fig. 1.11: proposed anaerobic degradation pathway of toluene via the process of fumarate addition. *Image taken from* Heider *et al.*, 1998.

Effects of Dispersant Application on Microbial Communities

It is evident that hydrocarbon-degrading microbes play a vital role in the removal of oil from the environment. Therefore, in the event of oil-spill response, it is central that remediation efforts do not inhibit the ability of hydrocarbon-degrading microbes. As discussed previously, active surfactants within dispersants transform oil into small, stable droplets (Gopalan and Katz, 2010) which are transported from the surface into the water column, creating an oil-in-water emulsion and increasing oil surface area (Fingas, 2011b). Subsequently, this increases bioavailability to hydrocarbon-degrading microbes and thus biodegradation (Prince *et al.*, 2013). Several studies suggest that dispersants enhance the growth of hydrocarbon-degrading bacteria (Hazen *et al.*, 2010; Dubinsky *et al.*, 2013; Brakstad *et al.*, 2018; Ribicic *et al.*, 2018) and increase hydrocarbon-biodegradation (Brakstad *et al.*, 2015; Prince *et al.*, 2016), other studies show that dispersants do not enhance hydrocarbon-biodegradation (Lindstrom and Braddock, 2002; Rahsepar *et al.*, 2016) or may even inhibit the growth of hydrocarbon-degrading bacteria (Hamdan and Fulmer, 2011; Kleindienst *et al.*, 2015).

Hamdan and Fulmer (2011) observed that, in comparison to samples with no additional dispersant, beached oil samples with the addition of the dispersant Corexit 9500 inhibited the production and viability of hydrocarbon-degrading bacteria assigned to the genera *Acineobacter* and *Marinobacter*. The latter of the two, *Marinobacter,* was the most sensitive, with a near 100% reduction in production and viability when Corexit 9500 was added (1,000 to 10,000 ppm). Similarly, Techtmann *et al.* (2017) demonstrated that at 5°C Corexit 9500 did not have any significant effect on microbial structure, however, at 25°C a decrease in *Marinobacter* was observed. Additionally,

Kleindienst *et al.* (2015) demonstrated that the use of dispersants allowed for the hydrocarbon- and dispersant-degrading genera *Colwellia* to outcompete certain hydrocarbon-degrading bacteria (*Marinobacter*), and thus provided no hydrocarbon-biodegradation advantage. In another study, whilst *Marinobacter* was not affected in oiled sediment microcosms, the OHCB *Cycloclasticus* was observed to be outcompeted when dispersant was applied in comparison to oil-only (Noirungsee *et al.*, 2020).

In contrast, Doyle *et al.* (2018), found dissimilar microbial community structures in oiled seawater mesocosms containing Corexit 9500 (CEWAF, ratio of 20:1 oil to dispersant), compared to those containing no oil or oil with no dispersant. Specific genera that thrived in the oil and dispersant mesocosms included members of the OHCB, *Alcanivorax* and *Oleibacter*, whereas oil-only mesocosms consisted more of *Glaceicola*, *Rhodobacteraceae*, and *Phaeodactylibacter*. Members of the OHCB genus *Thalassolituus* were not observed during the experiment but have been documented by Tremblay *et al.* (2017), who observed that oiled seawater microcosms with the addition of a dispersant (Corexit 9500) had increased levels of *Thalassolituus* and enhanced levels of hydrocarbon-biodegradation, in comparison to oil-only microcosms. This was also observed by Tremblay *et al.* in 2019 when they found that the addition of a dispersant (Corexit 9500), to oiled seawater microcosms, favoured the growth of *Thalassolituus* in the summer and the OHCB *Oleispira* in the winter.

In contrast to studies that either demonstrate dispersant application had positive or negative effects on microbial communities, Brakstad *et al.* (2017) observed the addition of dispersant (at increasing concentrations, Slickgone NS) had no significant effect on microbial communities. The composition of dispersants and biosurfactants varies widely, and their formulations are often proprietary information, so there is limited knowledge on how different dispersant and biosurfactant structures affect hydrocarbon-degrading bacteria and hydrocarbon-degradation rates. These topics are evaluated further in Chapters Two and Three.

Effects of Hydrocarbon Seepages from Shipwrecks on Microbial Communities

Globally an estimated 3 million shipwrecks lay on the seafloor (Croome, 1999), of which >8,600 are World War (WWI and WWII) shipwrecks (Monfils *et al.*, 2006). World War shipwrecks are estimated to contain 2.5 – 20.4 million tonnes of petroleum products and thus represent a significant threat to the marine environment. In the last two decades the focus on evaluating the environmental impact from shipwrecks has significantly increased (Landquist *et al.*, 2013) with a particular focus on oil-pollution (Michel *et al.*, 2005; Faksness *et al.*, 2015; Amir-Heidari *et al.*, 2019). In spite of recent research interest, there is a global paucity of studies investigating how shipwrecks

impact indigenous microbial communities or evaluating their actual or potential oil pollution. Most of the current literature focuses on archaeological wood (Liu *et al.*, 2018), artefacts (Li *et al.*, 2018), shipwrecks as artificial reefs (Church *et al.*, 2009; Mugge *et al.*, 2019), and microbial induced corrosion (Russell *et al.*, 2004). Studies which have researched microbial communities on shipwrecks (biofilms) have observed that microbes play a significant role in shipwreck degradation and preservation (Svane and Petersen, 2001), as well as the recruitment of macro-organisms to artificial reefs (Huggett *et al.*, 2006). Research into the effects of present and/or historic oil-spills on microbial communities are lacking.

A study by Hamdan *et al.* (2018), analysed microbiomes of sediments near shipwrecks in the Gulf of Mexico and observed that World War II and 19th century shipwrecks influenced microbial diversity in surface sediments 2 m from the shipwrecks. Observations included a significant increase in a Gammaproteobacteria phylotype associated to the family *Piscirickettsiaceae*, proximate to shipwrecks. However, two of the shipwrecks, which were impacted by the Macondo oil spill, had no significant effect on microbial diversity and composition. It was suggested either the greater depths of these shipwrecks, or the Macondo oil spill itself, obscured any potential impacts of the shipwrecks on microbial community composition. Analyses of *in-situ* microbial communities can provide data that are valuable in the design of post-incident monitoring guidelines and assist in determining whether fuel oil continues to leak from vessels (Kirby *et al.*, 2018).

Aims and Objectives of the Thesis

There is a wealth of literature surrounding marine oil-spills, and the application of remediation efforts such as dispersants, and their impacts on microbial ecology and the rate of hydrocarbon-degradation. However, the efficacy of dispersant application to marine oil-spills is still under scrutiny. Therefore, one of the primary aims of this thesis is to conduct both *in situ* and *ex situ* oil/dispersant experiments to provide clarification and guidance on the application of dispersants to marine oil-spills. Chapter Two evaluated how different dispersants and biosurfactants (with varying compositions), applied to *ex-situ* oiled-seawater microcosms, effected the structure and succession of hydrocarbon-degrading bacteria and hydrocarbon-degradation rates. Whilst, in Chapter Three the practice of dispersant application, in oil-spill response, was conducted in an *in-situ* experiment in the North Sea, off the coast of Holland. The primary aims of this project was to establish whether the application of a dispersant to an oil-slick would increase hydrocarbon-degradation over a 24-hour period and evaluate differences in microbial community composition between a natural

oil-slick and a chemically dispersed oil-slick. Additionally, sampling real-world oil-spills is exceptionally rare, with research often being conducted retrospectively or simulated in the laboratory, therefore Chapter Four permitted a rare insight into how bacterial and archaeal communities respond to a real-world in-situ oil spill (Agia Zoni II, off the coast of Athens, Greece) over a seven-month period. The primary aims of the project were to compare and assess microbial community response at oil-contaminated and uncontaminated sites and evaluate the efficiency of oil-spill response strategies adopted by oil-spill responders. Finally, there is a paucity of work conducted on the effects of hydrocarbon seepages from shipwrecks and thus the primary aim of Chapter Five was a technical evaluation into whether previous oil contamination by the World War II shipwreck HMS *Royal Oak*, located in the embayment Scapa Flow (Orkney Islands, Scotland, UK), caused long-term impact to surrounding benthic bacterial communities.

Evaluating the effects of such perturbations on microbial ecology will provide in-depth knowledge as to how microbes respond across a range of marine environments. Currently the only tool that utilises microbial data to provide guidance in oil-spill-response is the Ecological Index of Hydrocarbon Exposure (EIHE) and the evaluation of this index across a broad range of marine environments will highlight the strengths and weaknesses of such a tool. Additionally, an assessment of *in situ* and *ex situ* experimental sampling and methodologies will provide guidance on conducting future oil-spill research. The thesis' projects span a variety of marine environments (hypernutrified/oligotrophic, coastal/pelagic, seawater/sediment)_providing temporal and spatial scales, as well as distributions of environmental conditions, in which these aims can be applied.

Chapter Two

Effects of dispersants and biosurfactants on crude-oil biodegradation and bacterial community succession

Abstract

Given the widespread application of dispersants in oil-spill response, and in cleaning oil-storage containers, it is important to understand how they stimulate hydrocarbon-biodegradation and hydrocarbon-degrading bacterial communities. Dispersants (Finasol OSR 52, Slickgone NS, Superdispersant 25) and biosurfactants (rhamnolipid, trehalolipid, sophorolipid) were added to seawater microcosms at 16°C amended with crude oil. Dispersant and biosurfactant treatments (excluding sophorolipid) significantly increased bacterial 16S rRNA gene abundance at day one by an order of magnitude in comparison to the oil-only controls, driven primarily by growth of obligate hydrocarbonoclastic bacteria (OHCB). This growth translated into significant *n*-alkane-degradation (20-38%) at day one compared to oil-only controls (6%). Dispersant and biosurfactant treatments (excluding sophorolipid) reduced the lag-phase of OHCB growth, with the genus *Oleispira* dominating at day one, followed by increase abundance of *Thalassolituus* at day three and *Alcanivorax* and *Cycloclasticus* at day seven. Succession of OHCB began at day three in the oil-only controls and sophorolipid treatments, which also selected for the genus *Glaciecola*. Additionally, rhamnolipid selected for the genera *Arcobacter*, *Pseudomonas*, and *Zhongshania*, whilst trehalolipid and Superdispersant 25 selected for the genera *Alkalimarinus* and *Neptuniibacter*, respectively. Rapid bacterial growth and *n*-alkane biodegradation highlight positive benefits of the application of dispersants on oil slicks.

Introduction

Oil spills have been one of the primary inputs of pollution into the marine environment since the turn of the 20th century, when large oil-tankers became prominent (Burger, 1997). The extraction, processing, and transportation of oil continues to increase, and new oil fields are regularly being discovered (Rystad Energy, 2020). Despite the COVID-19 pandemic, recent forecasts predict that global production and consumption of oil will return to pre-COVID19 levels of ~100 million barrels per day by mid-2021 (U.S. Energy Information Administration, 2020). Thus, oil pollution remains a significant threat to marine ecosystems, tourism, and fisheries.

A key remediation tool in response to oil pollution is the application of dispersants (ITOPF, 2011b). The active surfactants within dispersants transform oil

into small, stable droplets (Gopalan and Katz, 2010). These oil droplets are transported from the surface into the water column, creating an oil-in-water emulsion, increasing oil surface area (Fingas, 2011b), and thus increasing bioavailability to hydrocarbon-degrading microbes (Prince *et al.*, 2013). The Deepwater Horizon oil spill in 2010 stimulated a new wave of research into dispersant use, when approximately 10 million litres of Corexit 9500A/9527 were applied during the incident (35% subsea at the wellhead and 65% on the surface; Kujawinski *et al.*, 2011). The objective during the Deepwater Horizon oil spill was to limit impact to surrounding coastlines, and evidence supports the general success of this strategy, with a delay in oil reaching the surface (Atlas and Hazen, 2011; Brandvik *et al.*, 2017). However, the use of dispersants as a form of oil-spill remediation remains a source of contention. While several studies suggest that dispersants enhance the growth of hydrocarbon-degrading bacteria (HCB) (Hazen *et al.*, 2010; Dubinsky *et al.*, 2013; Brakstad *et al.*, 2018; Ribicic *et al.*, 2018) and increase biodegradation (Brakstad *et al.*, 2015; Prince *et al.*, 2016), other studies show that dispersants do not enhance biodegradation (Lindstrom and Braddock, 2002; Rahsepar *et al.*, 2016) or may even inhibit the growth of HCB (Hamdan and Fulmer, 2011; Kleindienst *et al.*, 2015). Ultimately, the environmental impact and fate of an oil spill are among the main considerations of the Spill Impact Mitigation Assessment (SIMA, API *et al.*, 2017) process during decision-making for incident response. Balancing the trade-offs of different scenarios must be considered, for example, between the predicted effects of leaving oil on the water surface, versus dispersing oil into the water column and potentially to the seabed, which is often considered preferential to allowing oil to transfer to coastlines, particularly when these include environmentally sensitive areas.

Dispersants are generally comprised of a mixture of surface-active surfactants (non-ionic (e.g. Tween 80) and anionic (e.g. dioctyl sodium sulfosuccinate), constituting 1-50%) and solvents (e.g. kerosene or glycol ether, constituting >50%) (Kirby *et al.*, 2011), though exact compositions are proprietary information. Many dispersants are used globally, and countries have different products stockpiled in case of an oil spill. Dispersants are widely tested for effectiveness and toxicity, for example, the United Kingdom has approval schemes that authorise the stockpiling and application of dispersants such as Finasol OSR 52, Slickgone NS, and Superdispersant 25 (European Maritime Safety Agency, 2009).

Additionally, there are many biosurfactants, each with a variety of potential applications (Banat *et al.*, 2000; Chong and Li, 2017; Kapellos, 2017); though the cost of producing biosurfactants restricts their application to very specific clean-up operations. However, due to the fact that biosurfactants are one of the most in-demand

biotechnological compounds, promising strategies for lower cost production are emerging (Singh *et al.*, 2019). Oil-spill remediation potential of biosurfactants, as well as their effects on bacterial community composition, remains relatively understudied, and so also merits investigation alongside commonly used commercial dispersants. Biosurfactants are synthesised naturally by many microorganisms and consist of a polar (hydrophilic) moiety and non-polar (hydrophobic) group. Rhamnolipids have either 1 or 2 sugar(s) glycosylated to a β-hydroxy(3-hydroxy) fatty acid (Lang and Wullbrandt, 1999). Sophorolipids generally consist of di-saccharide (2-O-β-o-glucopyranosyl-β-D-glucopyranose) derivatives, each linked to a hydroxy fatty acid (Davila *et al.*, 1994). Trehalolipids structures are variable but generally consist of a non-ionic acylated derived trehalose sugar glycosylated to a mono-, di-, or tri-fatty acid (White *et al.*, 2013). The majority of hydrocarbon-degrading microorganisms are known to produce biosurfactants that assist in the emulsification of hydrocarbons (Banat, 1995; Vijayakuma and Saravanan, 2015).

It remains unclear how the different compositions of commercial dispersants and biosurfactants may affect bacterial community composition and abundance, and thus biodegradation rates. Therefore, we tested the effects and efficacy of three of the most widely stockpiled commercial dispersants (Finasol OSR 52 (TOTAL), Slickgone NS (Dasic International Ltd.), and Superdispersant 25 (Oil Technics) in seawater microcosms (Supplementary Materials Fig. S2.1). Whilst exact compositions are proprietary information, all three tested dispersants contain between 0.2% and 10% dioctyl sodium sulfosuccinate, varying proportions of non-ionic surfactants, and solvents (e.g. kerosene and 2-butoxyethanol) from <10% to >50% (DASIC-International, 2002; Total-Fluides, 2012; Oil-Slick-Dispersants, 2015). Additionally, we tested three biosurfactants, selected based on their range of structures and potential for commercial application: rhamnolipid isolated from *Pseudomonas aeruginosa* (15% active ingredient in 85% distilled water; JBR-215, Jeneil Biosurfactant Company), sophorolipid from *Candida* spp. (15% active ingredient in 85% distilled water; Sigma), and trehalolipid from *Rhodococcus* sp. strain PML026 (100% active ingredient; Sambles and White, 2015). Seawater was sampled from a fully saline, coastal region, at the mouth of the Thames estuary (see Supplementary Materials Fig. S2.1 and full site description in Experimental Procedures). The sampling site is therefore representative of similar coastal regions that are both typically rich in nutrients and often subject to oil contamination and occasional large spills (particularly in the UK and Europe, ITOPF, 2019). Dispersant use on estuaries has been readily applied in the past (Little and Little, 1991; Gilson, 2006) with continued research into their sustained use in coastal/estuary environments (Coolbaugh *et al.*, 2017), and after weighing up

both the advantages and risks of using dispersants in coastal areas, it may be considered that in some cases dispersants could provide a net environmental benefit (Floch Le *et al.*, 2014)."

We hypothesised significant positive effects, by those dispersants and biosurfactants that can efficiently decrease the interfacial surface tension between oil and water, on both bacterial growth and hydrocarbon-biodegradation. This effect would be seen in the early stages before microbes can synthesise their own surfactants and when macronutrients are not limiting. We additionally aimed to uncover whether different dispersant or biosurfactant formulations may select for different hydrocarbon-degrading communities.

Results

Effects of Dispersants and Biosurfactants Seawater Surface Tension

The addition of dispersants and biosurfactants significantly reduced the surface tension of the seawater (initial value, 69.66 ± 0.24 mN m^{-1}; Supplementary Materials, Fig. S2.2). There was a reduction in the surface tension of seawater to 60.33 ± 1.25 mN m^{-1} when sophorolipid was added (Supplementary Materials, Fig. S2.2), but a much greater effect (coef. = 35.66, t = 82.18, P<0.001) was observed with all other dispersants and biosurfactants that reduced the surface tension to between 28 and 34 mN m^{-1}.

Effects of Dispersants and Biosurfactants on Hydrocarbon Concentrations

Immediately after adding NSO-1 crude oil, the concentration of *n*-alkanes (C_{12} to C_{26}) plus branched alkanes (pristane and phytane) was 50.59 (± 3.41) µg ml^{-1} (Fig. 2.1) and PAHs (mainly naphthalene, anthracene, phenanthrene and their methylated derivatives) was 4.37 (± 1.09) µg ml^{-1} (see Supplementary Materials Fig. S2.3 for full oil composition). At day one, no significant biodegradation of either alkanes or PAHs was observed in the oil-only controls or in microcosms treated with sophorolipid. In contrast, the addition of dispersants and the other two biosurfactants significantly enhanced total alkane-degradation relative to both the time-zero controls (21-42% reduction; coef. = -0.75, t = -3.85, P<0.01) and the oil-only controls (20-38% reduction; coef. = -0.56, t = -3.13, P<0.05). There was no significant (P>0.05) reduction in the concentration of any PAHs in any treatments at day one.

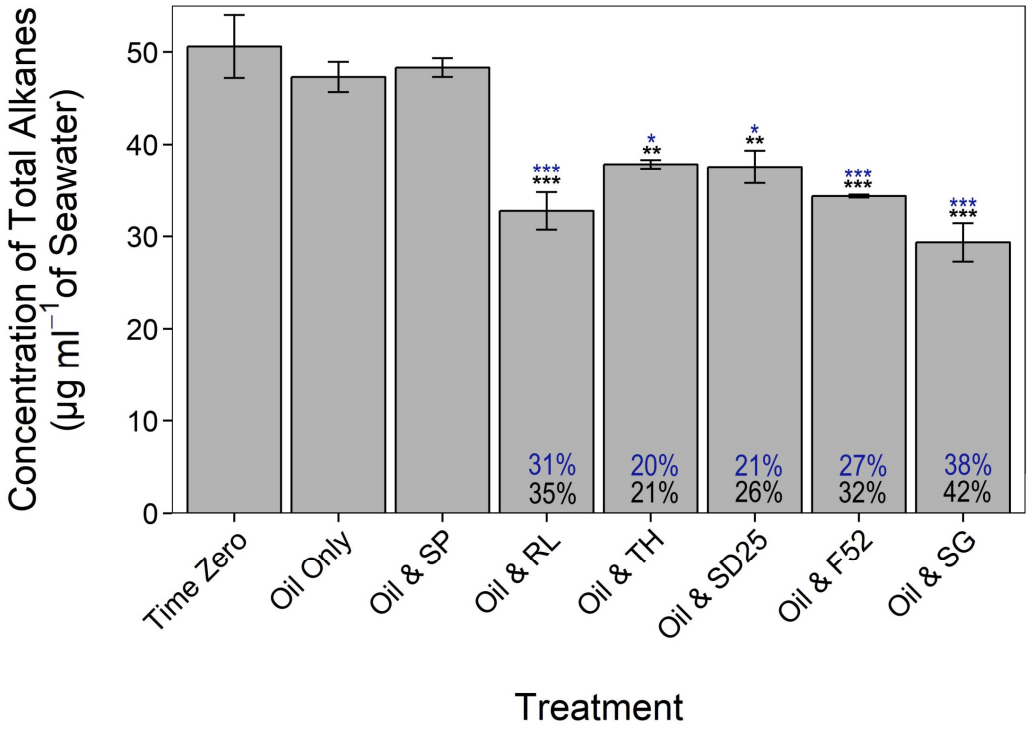

Fig. 2.1: Total alkane concentrations (mean ± SE, *n* = 2) at day one. Blue (upper) percentages (and asterixis) represent degradation in comparison to the oil-only control. Black (lower) percentages (and asterixis) represent degradation in comparison to starting concentration ("Time Zero"). Dispersant and biosurfactant codes are as follows; SP = Sophorolipid, RL = Rhamnolipid, TH = Trehalolipid, SD25 = Superdispersant 25, F52 = Finasol OSR 52, SG = Slickgone NS. *** P<0.001, ** P<0.01, * P<0.05.

By day three, the total concentration of alkanes had decreased further, however, there were no significant differences between any treatments, as biodegradation in the oil-only controls and sophorolipid treatments matched those in all other treatments. By day seven, the reduction in total alkane concentration was on average >80%, increasing further to 96-100% by day 14. PAH biodegradation did not differ significantly throughout the experiment in any treatments, but total concentration reduced on average by 88% by day seven and by 92% by day 14. All losses are attributed to biodegradation, as no abiotic losses were observed in the killed controls.

Effects of Oil and/or Dispersants/Biosurfactants on Bacterial Community Composition and Abundance

In order to quantify the effects of dispersants and biosurfactants, when applied to oil-contaminated microcosms, on bacterial abundance, diversity and community composition, bacterial 16S rRNA genes were analysed by qPCR and amplicon library sequencing. High-throughput 16S rRNA sequencing resulted in an average of 50,761 (range 3,905 – 698,800) sequence reads for *Bacteria*. At day one, the bacterial 16S rRNA gene abundance had significantly increased (coef. = 1.46, t = 4.83, P<0.001) in all treatments containing dispersants or biosurfactants (except sophorolipid) in

comparison to the oil-only controls (ranging from 4-fold (trehalolipid) to 17-fold (rhamnolipid); Fig. 2.2A,B). Additionally, all dispersants and biosurfactants (excluding sophorolipid) stimulated a significant increase of 6- to 23-fold in the numbers of obligate hydrocarbonoclastic bacteria (referred to hereafter as “OHCB” to distinguish between these highly competitive hydrocarbon-degraders and those more metabolically diverse Bacteria, which potentially can also degrade hydrocarbons) relative to the oil-only controls (Fig. 2.2B). This represented an increase in the relative abundance of 16S rRNA genes, assigned to OHCB, of 14-32%, compared to no increase in the oil-only controls and sophorolipid treatments (which remained in the region of 2-3%). The increase in OHCB by day one resulted in distinct bacterial communities in all dispersant and biosurfactant treatments in comparison to the oil-only controls and sophorolipid treatments (Supplementary Materials Fig. S2.4). From day three onwards, bacterial 16S rRNA gene abundance in the oil-only controls increased to levels comparable to those in dispersant and biosurfactant treatments (Fig. 2.2A). The plateau of bacterial growth at day three is strongly correlated (0.86 R^2 to 0.99 R^2, $P<0.001$) to the nearly complete reduction of ammonia (-88% by day one and -98% by day 21). Phosphorus was reduced across all treatments by -53% by day one and by -78% by day 21 (Supplementary Materials Fig. S2.5).

Increases in the absolute abundance of *Bacteria* were driven by increases in the relative abundance of particular OTUs. In addition to known OHCB, key OTUs were investigated based on increases in relative abundance across multiple treatments, or selection by specific dispersants or biosurfactants (Fig. 2.3).

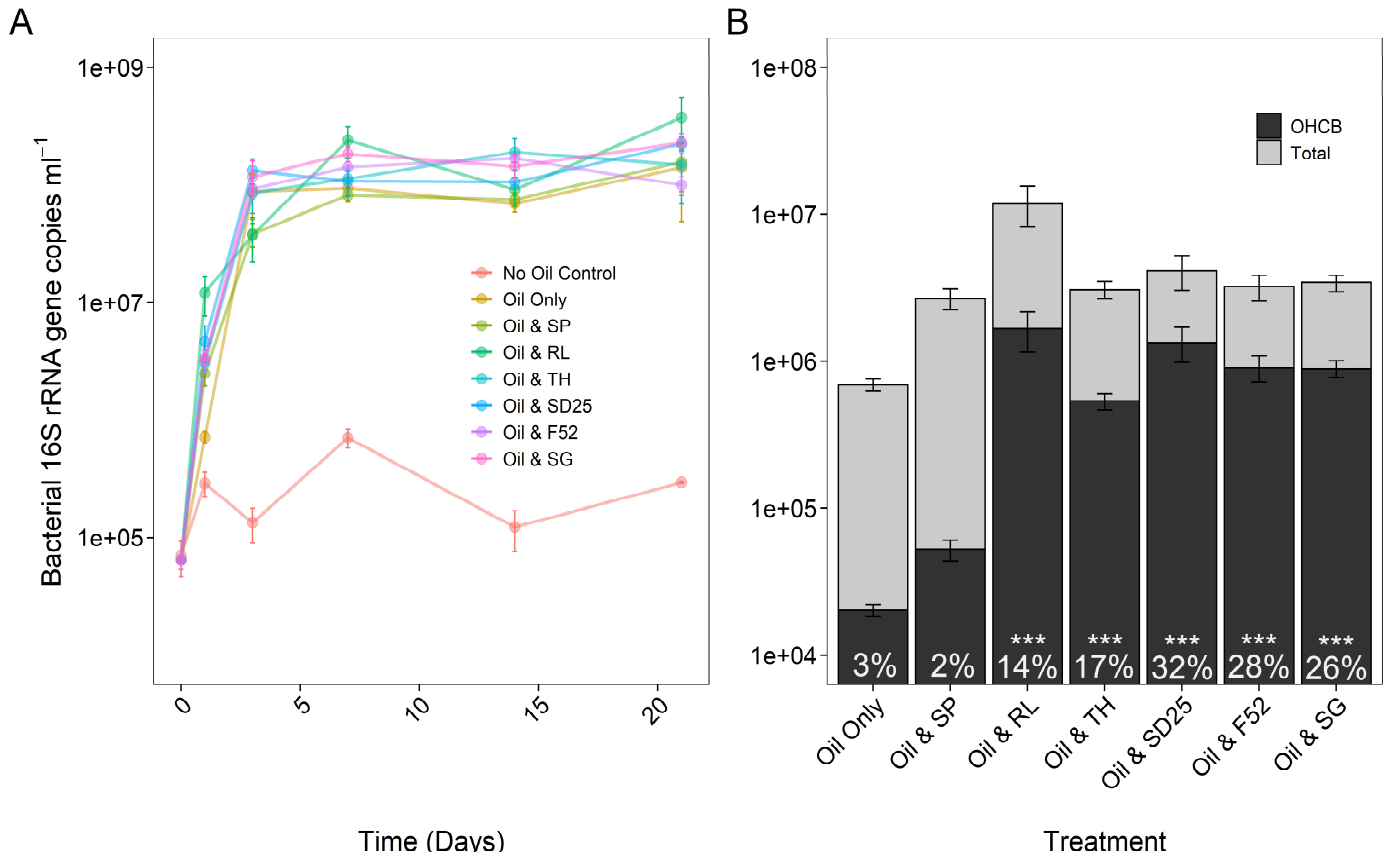

Fig. 2.2: Bacterial 16S rRNA gene abundance (mean ± SE, *n* = 3) over a 21-day period for total *Bacteria* (**A**) and at day one only, for total *Bacteria* and proportion (percentage figures) of obligate hydrocarbonoclastic bacteria (**B**) OHCB sequences are defined as from the genera: *Alcanivorax*, *Cycloclasticus*, *Oleibacter*, *Oleispira*, *Thalassolituus*. All microcosms contained seawater, nutrients, and oil (NSO-1 0.1% v/v), and some with additional dispersants or biosurfactants (0.005% v/v; 20:1 ratio of oil). Dispersant and biosurfactant codes are as follow: SP = Sophorolipid, RL = Rhamnolipid, TH = Trehalolipid, SD25 = Superdispersant 25, F52 = Finasol OSR 52, SG = Slickgone NS. Stars above percentage figures indicate significant differences in mean OHCB relative abundance compared to the oil-only control (*** P<0.001).

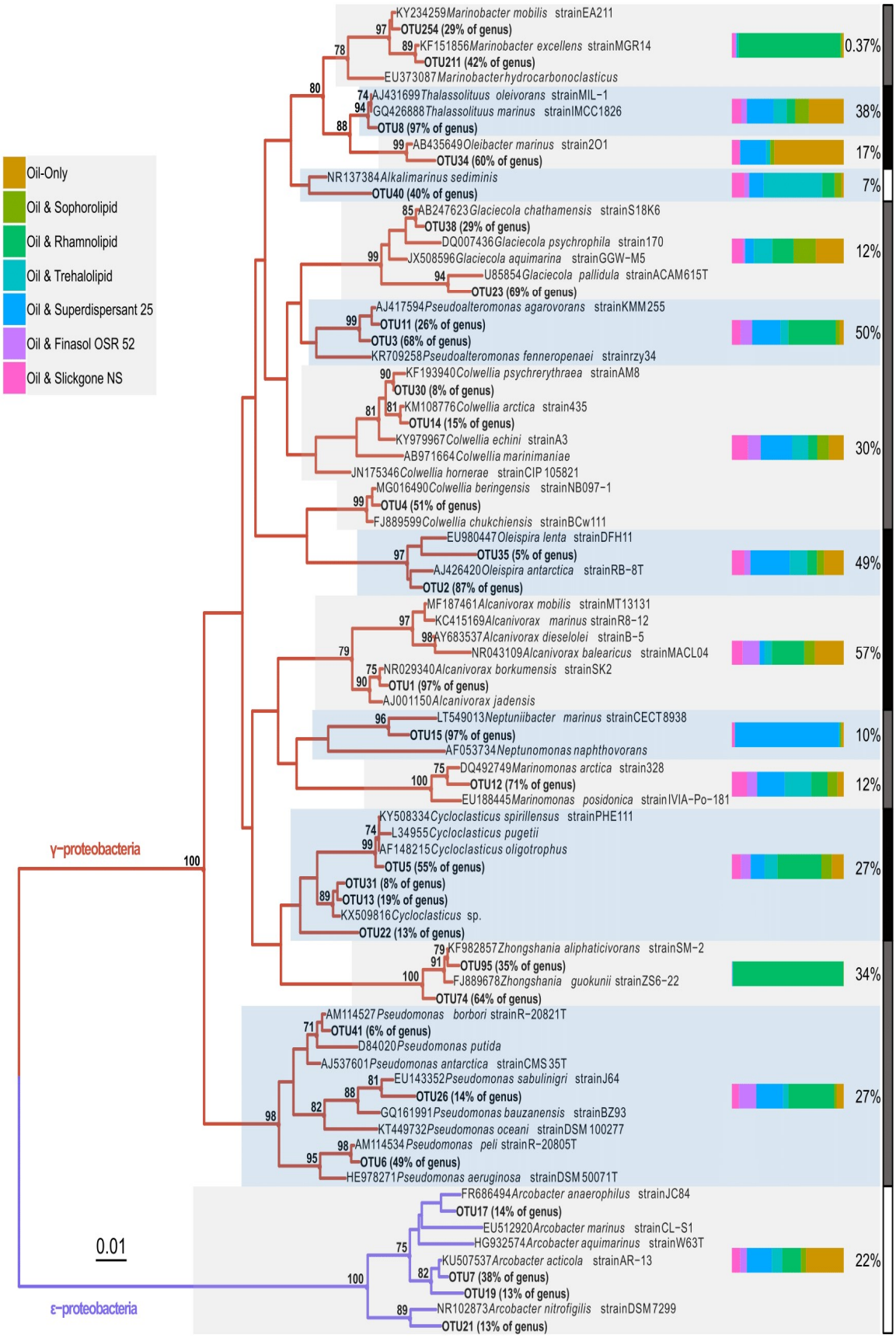
Oil-Only
Oil & Sophorolipid
Oil & Rhamnolipid
Oil & Trehalolipid
Oil & Superdispersant 25
Oil & Finasol OSR 52
Oil & Slickgone NS
KY234259 Marinobacter mobilis strainEA211
OTU254 (29% of genus)
KF151856 Marinobacter excellens strainMGR14
OTU211 (42% of genus)
EU373087 Marinobacter hydrocarbonoclasticus
0.37%
AJ431699 Thalassolituus oleivorans strainMIL-1
GQ426888 Thalassolituus marinus strainIMCC1826
OTU8 (97% of genus)
38%
AB435649 Oleibacter marinus strain2O1
OTU34 (60% of genus)
17%
NR137384 Alkalimarinus sediminis
OTU40 (40% of genus)
7%
AB247623 Glaciecola chathamensis strainS18K6
OTU38 (29% of genus)
DQ007436 Glaciecola psychrophila strain170
JX508596 Glaciecola aquimarina strainGGW-M5
U85854 Glaciecola pallidula strainACAM615T
OTU23 (69% of genus)
12%
AJ417594 Pseudoalteromonas agarovorans strainKMM255
OTU11 (26% of genus)
OTU3 (68% of genus)
KR709258 Pseudoalteromonas fenneropenaei strainrzy34
50%
KF193940 Colwellia psychrerythraea strainAM8
OTU30 (8% of genus)
KM108776 Colwellia arctica strain435
OTU14 (15% of genus)
KY979967 Colwellia echini strainA3
AB971664 Colwellia marinimaniae
JN175346 Colwellia hornerae strainCIP 105821
MG016490 Colwellia beringensis strainNB097-1
OTU4 (51% of genus)
FJ889599 Colwellia chukchiensis strainBCw111
30%
EU980447 Oleispira lenta strainDFH11
OTU35 (5% of genus)
AJ426420 Oleispira antarctica strainRB-8T
OTU2 (87% of genus)
49%
MF187461 Alcanivorax mobilis strainMT13131
KC415169 Alcanivorax marinus strainR8-12
AY683537 Alcanivorax dieselolei strainB-5
NR043109 Alcanivorax balearicus strainMACL04
NR029340 Alcanivorax borkumensis strainSK2
OTU1 (97% of genus)
AJ001150 Alcanivorax jadensis
57%
LT549013 Neptuniibacter marinus strainCECT8938
OTU15 (97% of genus)
AF053734 Neptunomonas naphthovorans
10%
DQ492749 Marinomonas arctica strain328
OTU12 (71% of genus)
EU188445 Marinomonas posidonica strainIVIA-Po-181
12%
KY508334 Cycloclasticus spirillensus strainPHE111
L34955 Cycloclasticus pugetii
AF148215 Cycloclasticus oligotrophus
OTU5 (55% of genus)
OTU31 (8% of genus)
OTU13 (19% of genus)
KX509816 Cycloclasticus sp.
OTU22 (13% of genus)
27%
KF982857 Zhongshania aliphaticivorans strainSM-2
OTU95 (35% of genus)
FJ889678 Zhongshania guokunii strainZS6-22
OTU74 (64% of genus)
34%
AM114527 Pseudomonas borbori strainR-20821T
OTU41 (6% of genus)
D84020 Pseudomonas putida
AJ537601 Pseudomonas antarctica strainCMS 35T
EU143352 Pseudomonas sabulinigri strainJ64
OTU26 (14% of genus)
GQ161991 Pseudomonas bauzanensis strainBZ93
KT449732 Pseudomonas oceani strainDSM 100277
AM114534 Pseudomonas peli strainR-20805T
OTU6 (49% of genus)
HE978271 Pseudomonas aeruginosa strainDSM 50071T
27%
FR686494 Arcobacter anaerophilus strainJC84
OTU17 (14% of genus)
EU512920 Arcobacter marinus strainCL-S1
HG932574 Arcobacter aquimarinus strainW63T
KU507537 Arcobacter acticola strainAR-13
OTU7 (38% of genus)
OTU19 (13% of genus)
NR102873 Arcobacter nitrofigilis strainDSM7299
OTU21 (13% of genus)
22%
γ-proteobacteria
ε-proteobacteria
0.01

Fig. 2.3: Unrooted Neighbour-Joining phylogeny based on 16S rRNA gene sequences from representative bacterial OTUs, which increased in relative abundance in microcosms containing seawater, nutrients, oil (NSO-1 0.1% v/v), and additional dispersants or biosurfactants (0.005% v/v; 20:1 ratio to oil) compared with oil-only. OTU sequences are aligned with known hydrocarbon-degrading Bacteria and closest relatives; bootstrap values >70 displayed (1,000 iterations). Evolutionary distances computed by Maximum Composite Likelihood protocol (using the Tamura-Nei model (Tamura and Nei, 1993)), sum of branch length = 1.52. Analysis involved 96 nucleotide sequences (including 30 OTUs in bold and 66 related strains), with a total of 276 positions in the final dataset. Evolutionary analyses were conducted in MEGA7. Horizontal bars (right of clades) represent the proportion of sequences assigned to OTUs within the clade in the different treatments (see colour key) over all time points (excluding day zero). Percentage figures show the maximum relative abundance reached for OTUs within that clade in any treatment at any time point (excluding day zero; see additional figures for treatment-specific bacterial succession). Vertical bars (right of percentage figures) represent OHCB (black), genera where some isolates have grown on hydrocarbons (grey), and genera that have increased in relative abundance in oil-contaminated environments, but no isolates have been shown to degrade hydrocarbons (white).

Oleispira and *Thalassolituus* increased in relative abundance at day one and three respectively, followed by growth of *Alcanivorax* and *Cycloclasticus* at day seven (Fig. 2.4A). This pattern of succession was consistent across all treatments, though OHCB growth developed later in the oil-only controls and sophorolipid treatments corresponding with delayed alkane-degradation. At day one, the alkane-degrading genus *Oleispira* (represented by OTU2 and OTU35, Fig. 2.3 and Fig. 2.4A) had significantly increased in relative abundance to 15 - 26%, from background levels (1-3%), in microcosms containing Finasol OSR 52, Slickgone NS, Superdispersant 25, and trehalolipid (coef. = 0.15, t = 4.28, $P<0.05$). By day three, *Oleispira* had also increased in the oil-only controls (to 38%) and sophorolipid treatment (to 31%) to levels found in all other treatments. The alkane-degrading genus *Thalassolituus* (represented by OTU8, Fig. 2.3 and Fig. 2.4A) increased in all treatments by day three, although the relative abundance was significantly higher in the oil-only controls (18%) and sophorolipid (15%) treatments (coef. = 13.09, t = 4.37, $P<0.05$). The alkane-degrading genus *Oleibacter* (represented by OTU34, Fig. 2.3 and Fig. 2.4A) grew in numerous treatments, and though its relative abundance remained comparatively low throughout (0-7%) larger increases were observed in the oil-only controls (5% and 7% at days three and seven respectively). By days seven or 14 (depending on the treatment) and through to day 21, both the alkane-degrading *Alcanivorax* (represented by OTU1, Fig. 2.3 and Fig. 2.4A) and the PAH-degrading *Cycloclasticus* (represented by OTUs 5, 13, 22, and 31, Fig. 2.3 and Fig. 2.4A) became the most dominant OHCB in all treatments (representing 15-43% and 6-18% at days seven and 14 respectively).

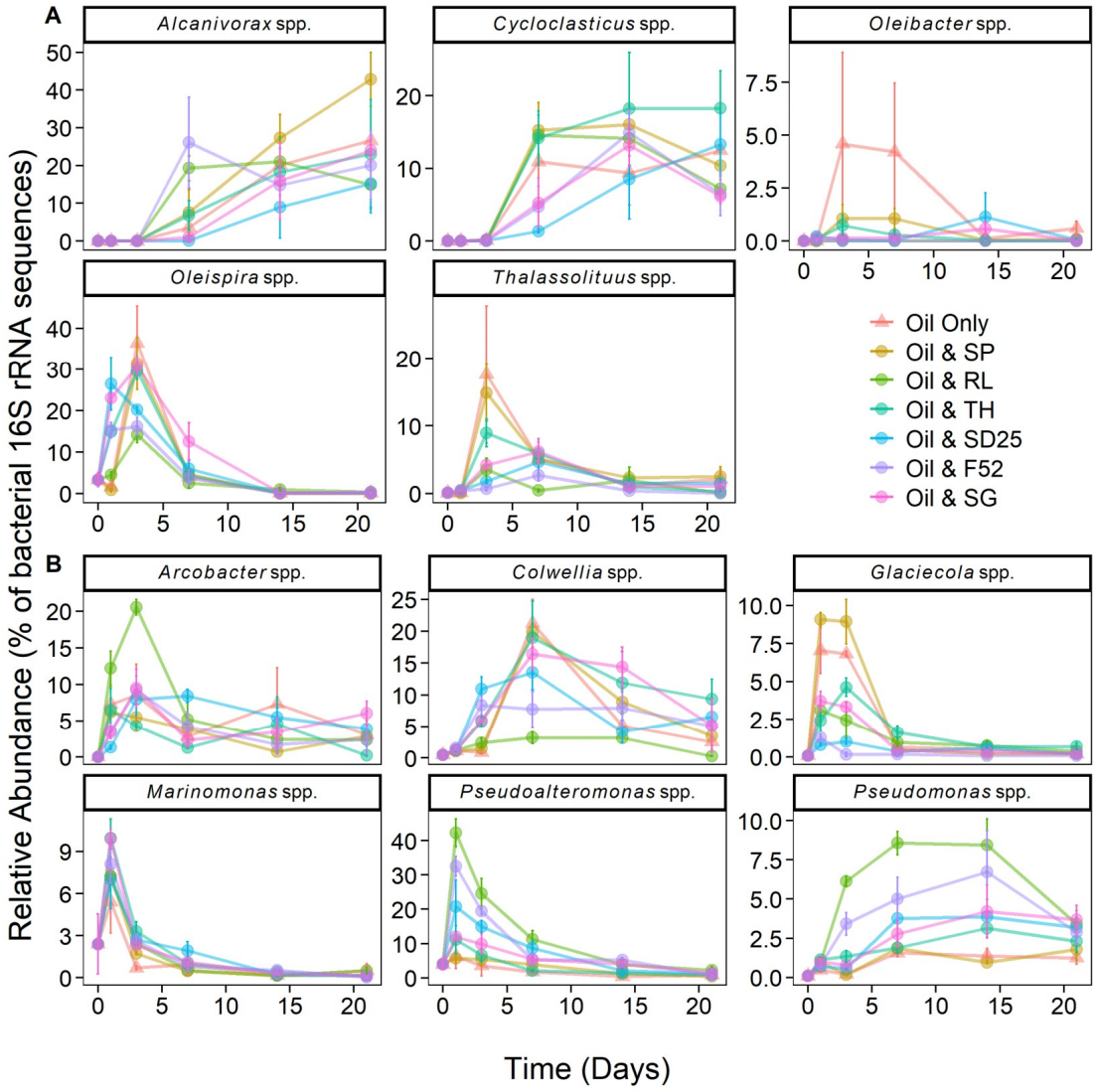

Fig. 2.4: Relative abundance (% of the bacterial community; mean ± SE, *n* = 3) of 16S rRNA gene sequences within OTUs assigned to obligate hydrocarbonoclastic bacteria (**A**), and Bacteria that were abundant (and are often associated with hydrocarbon-degradation; see Supplementary Materials Table S2.2) (**B**), over a 21-day period. All microcosms contained seawater, nutrients, and oil (NSO-1 0.1% v/v), and some with additional dispersants or biosurfactants (0.005% v/v; 20:1 ratio of oil). Dispersant and biosurfactant codes are as follow: SP = Sophorolipid, RL = Rhamnolipid, TH = Trehalolipid, SD25 = Superdispersant 25, F52 = Finasol OSR 52, SG = Slickgone NS.

OTUs assigned to more metabolically versatile Bacteria had more between-treatment variability compared to OTUs assigned to OHCB. These genera contain species that have been shown to degrade hydrocarbons, and/or that have been observed to increase in abundance in oil-contaminated marine environments (Supplementary Materials Table S2.2). However, like many prior studies (Supplementary Materials Table S2.2) it cannot always be assumed that such genera are degrading hydrocarbons, although large increases in relative abundance may often suggest that this is the case. *Pseudomonas* (represented by OTUs 6, 26, and 41, Fig. 2.3 and Fig. 2.4B) increased in relative abundance in most treatments by days one and three and remained above background levels (~0.09%) across all treatments (1 – 4%) by day 21. Additionally, there was a selection for *Pseudomonas* in Finasol OSR 52, and more so rhamnolipid, treatments, where significant increases in relative abundance (coef. = 0.12, t = 4.20, $P < 0.05$) were observed by days three (3 – 6%), seven (5 – 9%), and 14 (7 – 8%). In addition, the patterns of increase of genera *Arcobacter, Colwellia*, *Glaciecola*, *Marinomonas*, and *Pseudoalteromonas* are shown in Fig. 2.4B, their capacity for hydrocarbon-degradation referenced in Supplementary Materials Table S2.2, and their phylogenetic position of representative OTUs in Fig. 2.3. Furthermore, the genera *Alkalimarinus, Neptuniibacter* and *Zhongshania* significantly increased in relative abundance in trehalolipid, Superdispersant 25, and rhamnolipid treatments, respectively (Supplementary Materials Fig. S2.6).

The Ecological Index of Hydrocarbon Exposure (EIHE), which quantifies the proportion of the bacterial community with hydrocarbon-biodegradation potential (Lozada *et al.*, 2014), significantly increased (coef. = 0.41, t = 4.97, $P < 0.01$) at day one in oil microcosms containing Superdispersant 25 (0.59), rhamnolipid (0.61), and Finasol OSR 52 (0.63) in comparison to day zero (0.11) and to the oil-only controls, and sophorolipid treatments (0.18) (Supplementary Materials Fig. S2.7). By day three, the index measured in the oil-only controls and sophorolipid treatments had increased significantly (0.62 – 0.67; coef. = 0.49, t = 5.95, $P<0.001$) from day one. By day 21, the index ranges from 0.47 to 0.67 across all treatments remaining well above the index at day zero (0.11) prior to oil addition.

Effects of Oil and/or Dispersants/Biosurfactants on Bacterial Co-occurrence

After filtering the total bacterial OTU table to OTUs confidently identified as belonging to possible hydrocarbon-degrading genera (as defined by the EHIE index), 352 OTUs remained. Network construction revealed 1791 co-occurrences between taxa, which were largely dominated by positive, rather than negative, co-occurrences (Fig. S2.8A). OTUs in the network co-occurred with 10 others on average (median), as shown by the network node degree distribution (Fig. S2.8B). Clustering of the

network revealed 16 modules, with each module consisting of between 5 and 50 OTUs. The network had an overall modularity score 0.37, indicating that OTUs in the network formed sub-communities of co-occurring OTUs. One feature of many of the modules was the dominance of OTUs from specific genera (Fig. 2.5A). For example, module 16 was composed entirely of *Oleispira* OTUs that positively co-occurred with each other, whilst modules 2, 4, 7, and 8 had high proportions of *Marinomonas, Thalassolituus, Arcobacter,* and *Alcanivorax* OTUs, respectively. The propensity of OTUs within a genus to co-occur with others from the same genus is referred to as taxonomic assortativity. Our network had a taxonomic assortativity coefficient of 0.24, indicating positive assortativity. We further tested the association between an OTU's genus and its module using a Fisher test, revealing OTUs from different genera were not randomly distributed between modules, further supporting the role of taxonomic assortativity in our network. Examination of the total relative abundance (as a fraction of the hydrocarbon-degrading proportion of the bacterial community) revealed that many modules showed distinct treatment or successional peaks in abundance (Fig. 2.5B). Module 1 (composed of 67% *Arcobacter* OTUs), module 2 (29% *Marinomonas* OTUs), and module 16 (100% *Oleispira* OTUs) were more abundant early in the experiment, peaking in abundance during days one and three. In contrast, modules 8 (64% *Alcanivorax* OTUs) and 9 (36% *Colwellia* OTUs) peaked later in the experiment, further supporting the successional trends observed at the individual genus level. Module 5 represented a more diverse group of OTUs (21% *Pseudomonas* OTUs) that were clearly more abundant in the rhamnolipid treatment and increased in relative abundance towards the end of the experiment. Whilst OTUs within modules were predominantly connected by strong positive co-occurrences with each other, co-occurrences between OTUs from different modules were significantly weaker (Supplementary Materials Fig. S2.9; coef. = -0.08, t = -21.33, R^2 = 0.20, P<0.001). The weaker co-occurrences linking modules provides evidence against the concept of competitive exclusion in oil-degrading communities, where we might expect strongly negative co-occurrences to link species in different successional stages.

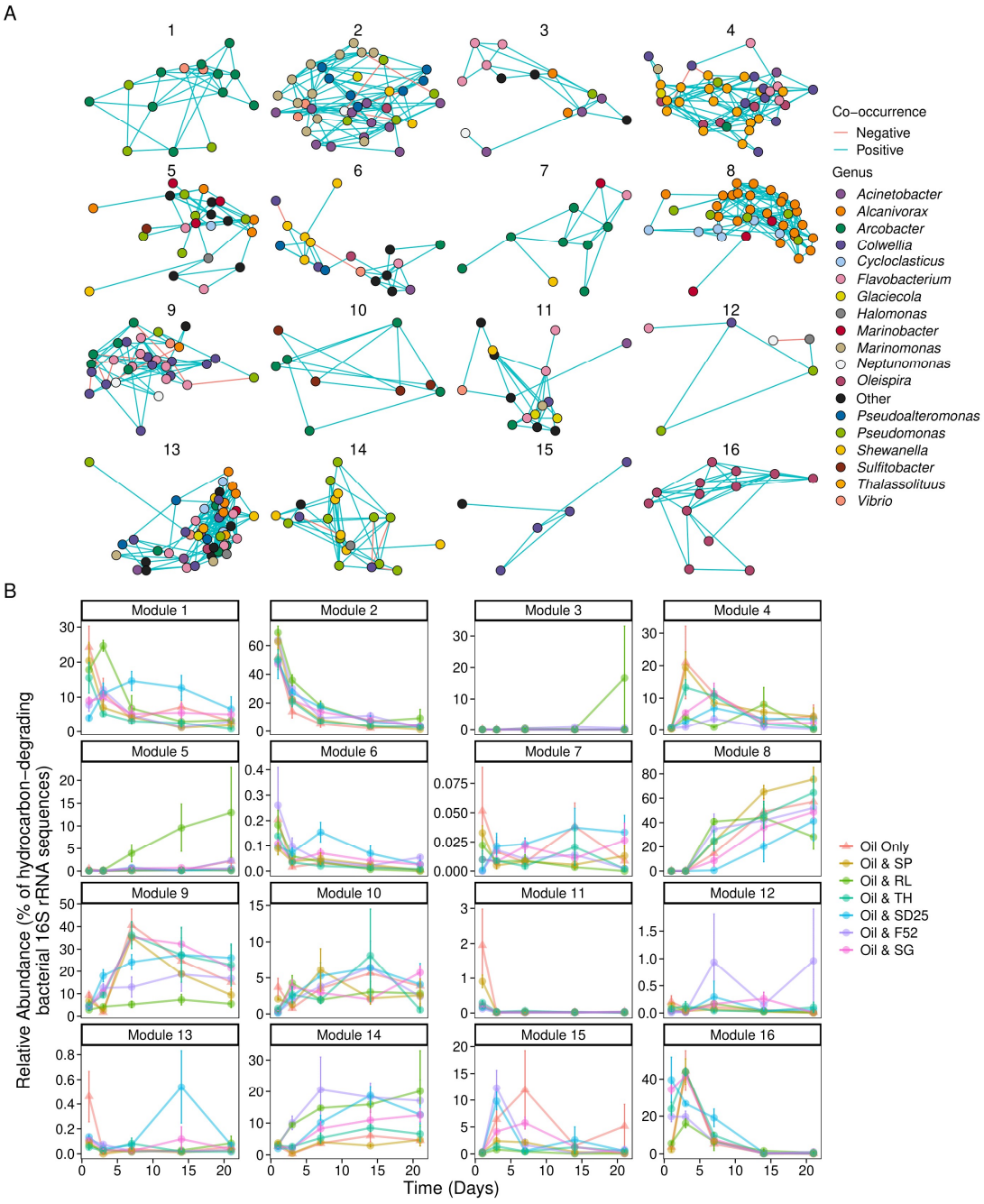

Fig. 2.5: (**A**) network modules based on clustering of a SPIEC-EASI co-occurrence network formed of OTUs from bacterial genera associated with hydrocarbon-degradation. Each point represents a single OTU, which are coloured according to their identity at the genus level (RDP classifier confidence >0.8). Blue edges represent positive co-occurrences between OTUs across the experiment, whereas red edges show negative co-occurrences. (**B**) The total relative abundance (as a proportion of bacterial genera associated with hydrocarbon-degradation) of OTUs in each module across the course of the experiment, based on counts of 16S rRNA sequences. All microcosms contained seawater, nutrients, and oil (NSO-1 0.1% v/v), and some with additional dispersants or biosurfactants (0.005% v/v; 20:1 ratio of oil). Dispersant and biosurfactant codes are as follow: SP = Sophorolipid, RL = Rhamnolipid, TH = Trehalolipid, SD25 = Superdispersant 25, F52 = Finasol OSR 52, SG = Slickgone NS.

Discussion

To what Extent do Different Dispersants/Biosurfactants Enhance the Growth of Hydrocarbon-degrading Bacteria and accelerate Hydrocarbon-degradation?

After only 24 hours, there was a clear selection for hydrocarbon-degrading Bacteria (HCB) in all treatments where dispersants or biosurfactants had significantly reduced the interfacial surface tension between oil and water, which was coupled with significant reductions in the concentration of alkanes (21 – 42%). Dispersants transform oil on the surface of the water into micron-size droplets (10 – 300 µm, Li *et al.*, 2008; Brakstad *et al.*, 2014; North *et al.*, 2015) in the water column. This dispersion of oil provides an increased surface area for microbial attachment, and biodegradation requires lower nutrient concentrations as oil is dispersed over a wider area (Prince *et al.*, 2013). Additionally, an increased oil surface area to volume ratio allows hydrocarbon-degrading microbes to expend more energy on growth and less energy producing biosurfactants, thereby accelerating biodegradation (Prince *et al.*, 2016; Brakstad *et al.*, 2018). However, contradictory evidence by Kleindienst *et al.* (2015) demonstrated that the use of dispersants allowed for the hydrocarbon- and dispersant-degrading genera *Colwellia* to outcompete certain HCB (*Marinobacter*), and thus provided no hydrocarbon-biodegradation advantage. Conclusions reached by Kleindienst et al. (2015) were likely due to differences in experimental procedure, as well as differences in indigenous bacterial communities between the Gulf of Mexico and the North Sea. Kleindienst et al. (2015) used water accommodated fractions (WAFs) (sampled seawater was stored for >1 month), whereby oil was mechanically and chemically dispersed with Corexit 9500. Additionally, sampling of WAFs first occurred after seven days. Whereas, in our study, dispersants and biosurfactants, which were different from Corexit, were added directly to the seawater surface, avoiding vigorous mechanical dispersion. Additionally, microcosms, which were set up immediately after seawater sampling, were sampled at day one, providing evidence of increased hydrocarbon-degradation with the application of dispersants and biosurfactants in the very early stages (except when sophorolipid was used).

By day three, alkane biodegradation and abundance of HCB in the oil-only controls and sophorolipid treatments had caught up with, and was equal to, all other treatments. This finding could be due partly to inorganic nitrogen becoming limited within the first few days and suggests that the later blooms of *Alcanivorax* and *Cycloclasticus* after seven days may rely on the turnover of organic nitrogen as cells die. As with the alkanes, PAHs were biodegraded, but there were no significant differences between any treatments. HCB able to degrade *n*-alkanes are known to

grow more rapidly than those degrading branched-alkanes and PAHs (Head *et al.*, 2006; Dubinsky *et al.*, 2013), during which time, in this study, nutrients had been depleted. Had there been a constant supply of inorganic nutrients, as expected during oil dispersed within the marine environment, microcosms containing dispersed oil may have maintained their enhanced biodegradation for longer, which could possibly also translate into significantly enhanced PAH-biodegradation.

Dispersal and dilution of oil within microcosms is limited due to their confined nature, in contrast to oil-spills in open waters, where oil can reduce rapidly to sub-ppm concentrations (Bejarano *et al.*, 2013). Dispersion over a wide area and lower concentration of oils may allow access to further inorganic nutrients and therefore lead to faster degradation of dispersed oil compared to undispersed oil on the sea surface. It has also been highlighted that *ex-situ* bottle experiments allow for higher oil concentrations which can in some cases inhibit hydrocarbon-degradation (Lee *et al.*, 2013; Prince *et al.*, 2016). Furthermore, Nedwed and Coolbaugh (2008) state that microcosm biodegradation experiments can be negatively biased due to the physical constraints of the container limiting the spread of oil. However, in spite of these previous findings, this study has demonstrated that even with a relatively high oil concentration, and the confined nature of microcosms, both dispersants and biosurfactants significantly increased the rate of hydrocarbon-biodegradation and the abundance of hydrocarbon-degrading bacteria.

This study has provided evidence that the biosurfactants rhamnolipid and trehalolipid, have the same ability to enhance hydrocarbon-degradation as commercial dispersants. However, their potential as a replacement for dispersants is currently limited due to the exceptionally high costs of large-scale production (Banat *et al.*, 2014; Varjani and Upasani, 2017). Sophorolipid reduced surface tension of the seawater to a much lesser extent than all other surfactants or dispersants, and thus did not increase hydrocarbon-biodegradation. In contrast, sophorolipid has previously been observed to increase hydrocarbon-degradation in oiled soil slurry reactors (Norman *et al.*, 2002; Kang *et al.*, 2010). Sophorolipid has been noted to decrease the surface tension of water from ~70 to ~36 mN m^{-1}, though this relies on a minimum sophorolipid concentration of 15-20 ppm (Ashby *et al.*, 2008; Daverey and Pakshirajan, 2010). In this study the final concentration of sophorolipid was 7.5 ppm and seawater surface tension (without oil) was only reduced from 70 to ~60 mN m^{-1}. All dispersants and biosurfactants were added at 0.005% v/v oil to dispersant, replicating industry standard (Fingas, 2000), highlighting that an increased initial sophorolipid concentration, or decreased ratio of oil to biosurfactant, would be required for sophorolipid to be effective.

The Psychrophilic OHCB Genus Oleispira Dominates in the First Few Days at the Relatively High Temperature of 16ºC

The initial relative abundance of OHCB in the seawater was very low, with only OTUs from the genus *Oleispira* detectable at approximately 3% (measured at "time-zero"). OTU35 had a 98.97% 16S rRNA sequence identity to the type strain isolated from Antarctica (closest match to *O. antarctica* strain RB-8T; Fig. 2.3), which in pure culture grows well at 16ºC, which is slightly beyond its broad growth optimum of 1-15ºC (Gregson *et al.*, 2020). *Oleispira* spp. bloom in cold waters (5ºC) but are outcompeted by other OHCB at warmer temperatures (Coulon *et al.*, 2007; King *et al.*, 2015; Brakstad, *et al.*, 2018).

The sampled seawater was measured at 13.8°C and therefore not the most suited environment for the psychrophilic *Oleispira*, which grows optimally in cold waters (5ºC), such as the polar seas or the deep sea (Mason *et al.*, 2012; Joye *et al.*, 2014). This may suggest why, despite *Oleispira* being the first OHCB to respond to the presence of oil, it was rapidly outcompeted. However, the relatively high abundance of *Oleispira in situ* would provide a competitive advantage (i.e. a priority effect), allowing it to become the dominant OHCB by day one, constituting 15-16% of sequence reads in four treatments (with lower abundance (1-4%) in oil-only, sophorolipid, and rhamnolipid microcosms). Thereafter, *Oleispira* is outcompeted by OHCB more competitive at 16°C. *O. antarctica* has previously been observed to grow rapidly within one day in microcosms with North Sea water and oil (0.01%) (Krolicka *et al.*, 2014), though these microcosms were incubated at 4°C. Alternatively, the dominance of the *Oleispira* OTUs in the warmer microcosms (16ºC) of this study, could potentially be due to OTU35 (which accounted for 96% of the relative abundance of sequences assigned to the *Oleispira* genus on days one and three) having a more mesophilic phenotype than currently cultivated *Oleispira* species. This would also help explain it's relatively high (1-3%) abundance within the *in situ* 13.8°C seawater and suggest a wider diversity within the genus than is currently known. Then again, many studies have evaluated HCB over a broader time series (Röling *et al.*, 2002; Kleindienst, Seidel, *et al.*, 2015; Garneau *et al.*, 2016), whereas in this study a finer timeline was adopted (one and three days). This finer timeline exposed the ability of *Oleispira* spp. to initially dominant in response to oil-contamination prior to being rapidly outcompeted, whereas this result may go undetected in studies of broader timelines.

Does Niche Partitioning Explain the Observed OHCB Succession?

Oleispira positively co-occurred only with other *Oleispira* OTUs (Module 16, Fig. 2.5), dominating OHCB communities during the early successional stages (1-3

days). By day three, OTUs from the genus *Oleispira* maintained a high level of relative abundance in the Finasol OSR 52, Slickgone NS, Superdispersant 25, and trehalolipid treatments. However, by day three, *Oleispira* also grew significantly in the oil-only controls, sophorolipid, and rhamnolipid treatments where it had initially been outcompeted by *Glaciecola* spp. or *Arcobacter* spp. Growth of *Oleispira* was also coupled with increased relative abundance of the alkane-degrading OHCB genus *Thalassolituus* (Yakimov et al., 2004; Fig. 2.3), potentially suggesting niche partitioning by the degradation of different alkanes. For example *Oleispira antarctica* has been shown to only grow on alkanes up to chain length of *n*-C_{24} (Gregson *et al.*, 2020), but *Thalassolituus oleivorans* can grow on alkanes up to *n*-C_{32} due to the possession of subterminal Baeyer-Villiger monooxygenase alkane oxidation pathways for longer-chained alkanes (Gregson *et al.*, 2018). By day seven, a significant increase is observed in relative abundance of OTU1 (alkane-degrading genus *Alcanivorax* (Yakimov *et al.*, 1998; Schneiker *et al.*, 2006); 99.67% 16S rRNA sequence identity match to *A. borkumensis* SK2; Fig. 2.3), prior to becoming dominant by days 14 and 21. The dominance of *Alcanivorax* occurs when shorter *n*-alkanes and inorganic nitrogen are mostly depleted. This is likely due to the ability of *Alcanivorax* to use both long-chained alkanes and branched alkanes (pristane and phytane) (Gregson *et al.*, 2019) as well as specific systems for scavenging nutrients in oligotrophic environments (Cappello and Yakimov, 2010). Four OTUs from the PAH-degrading genus *Cycloclasticus* (Dyksterhouse *et al.,* 1995; Fig. 2.3), which also has specific systems for scavenging nutrients in oligotrophic environments (Wang *et al.*, 1996), increased in relative abundance across all treatments by day seven, as alkanes are often degraded prior to more complex PAH molecules. Due to this, *Alcanivorax* spp. often flourish before *Cycloclasticus* spp. (McGenity *et al.*, 2012; Röling and Van Bodegom, 2014), though they can co-occur (Cappello *et al.*, 2007), including with the addition of the biosurfactant rhamnolipid (McKew *et al.*, 2007). This co-occurrence was observed in this study (Module 8, Fig. 2.5), from day seven onwards, and is likely due to the fact they do not compete for the same substrates. Additionally, it has been documented that *Alcanivorax* spp. may enhance PAH-degradation (McKew *et al*., 2007), potentially due to their biosurfactant enhancing PAH bioavailability. The six dispersants and biosurfactants, with their different compositions had no significant effect on OHCB succession, with similar patterns observed across all treatments.

Do Dispersants or Biosurfactants Select for Specific Bacterial Genera?

Specific biosurfactant or dispersant treatments resulted in selection for certain genera, which were either undetected or in significantly lower relative abundance in the other treatments. This occurred in treatments containing trehalolipid,

Superdispersant 25, and rhamnolipid. The biosurfactant trehalolipid triggered a significant increase in the relative abundance of OTU40, from the genus *Alkalimarinus* (97.29% 16S rRNA sequence identity to *A. sediminis*; Fig. 2.3) after three days. *Alkalimarinus* spp. are not known hydrocarbon-degraders, however, recently *A. sediminis* was found to significantly increase in relative abundance when PAHs bioaccumulated in bivalves (Noh *et al.*, 2018). Superdispersant 25 resulted in a significant increase in the relative abundance of OTU15 from the genus *Neptuniibacter* (97.34% 16S rRNA sequence identity to *N. marinus* strain CECT 8938; Fig. 2.3) after three days. The selection of *Neptuniibacter*, some strains of which contain the *soxA-D* gene cluster for the oxidisation of sulfur (Dombrowski *et al.*, 2016), could be due to Superdispersant 25 containing sulfur (Suja *et al.*, 2017). The biosurfactant rhamnolipid stimulated a significant increase in the relative abundance of two OTUs from the genus *Zhongshania* (98.34% and 96.35% 16S rRNA sequence identity to *Z. aliphaticivorans* strain SM-2; a known alkane-degrader (Naysim *et al.*, 2014)) by day 21. *Zhongshania* sp. has been observed as an abundant alkane-degrader in Norwegian seawater (Ribicic *et al.*, 2018).

Rhamnolipid Stimulates Pseudomonas *Dominance – a Case of Advantageous Compatibility with its Own Biosurfactant?*

During the first three days, rhamnolipid selected for four OTUs from the genus *Arcobacter* and two OTUs from the genus *Pseudoalteromonas* (Fig. 2.3). *Arcobacter* has been observed to increase in abundance in oiled environments (Supplementary Materials Table S2.2), especially oil sands (Hubert *et al.*, 2012), whilst some strains of *Pseudoalteromonas* spp. have been shown to grow on both *n*-alkanes and PAHs (Chronopoulou *et al.*, 2015). However, by day seven, OTUs from the genera *Arcobacter* and *Pseudoalteromonas* decrease in relative abundance as OTUs from the genus *Pseudomonas* (Fig. 2.3) were observed to significantly increase. This selection for *Pseudomonas* by rhamnolipid can be observed in Module 5 (Fig. 2.5) of the network analysis, where a bacterial consortium are selected by the rhamnolipid treatment, including *Pseudomonas* OTUs (OTUs 114, 187, 309, and 1155) which are observed to positively co-occur with others OTUs (e.g. *Alcanivorax* and *Marinobacter*). Additionally, whilst Module 14 (Fig. 2.5) demonstrates that other *Pseudomonas* OTUs, which positively co-occur with *Cycloclasticus* OTUs, appear to be distributed across all treatments, three of the *Pseudomonas* OTUs (OTUs 6, 26, and 41) within Module 14 (Fig. 2.5) are dominant in rhamnolipid treatments (Fig. 2.3).

Certain *Pseudomonas* spp. are known hydrocarbon-degraders, including the PAH naphthalene (Barnsley, 1976) and *n*-alkanes ranging from C_8-C_{36} (Varjani and Upasani, 2016). *P. aeruginosa* is known as a prominent producer of the biosurfactant

rhamnolipid in the presence of hydrocarbons (Ramya *et al.*, 2018), though some other species can also produce this class of glycolipid, including *P. chlororaphis, P. plantarii, P. putida,* and *P. fluorescens* (Geys *et al.*, 2014; Chong and Li, 2017). Moreover, specific *Pseudomonas* spp. are known to increase the rate of hydrocarbon-degradation in the presence of rhamnolipid addition (Zhang *et al.*, 2005). The significant increase in relative abundance of *Pseudomonas* spp. in microcosms containing rhamnolipid is potentially a form of advantageous compatibility. Rhamnolipids, whilst increasing hydrocarbon bioavailability, also modulate the swarming motility of *Pseudomonas* spp. (Caiazza *et al.*, 2005; Chrzanowski *et al.*, 2012). Hydrophobic compounds (i.e. hydrocarbons) are often surface-associated, and chemotaxis, via swarming, enhances their bioavailability/biodegradation (Marx and Aitken, 2000; Krell *et al.*, 2013; Ibrar and Zhang, 2020). Furthermore, rhamnolipid is a known antimicrobial (Haba *et al.*, 2003), therefore where the same biosurfactant is used to swarm over the hydrocarbon surface, this may prevent the establishment of competing microbes (Kearns, 2010), providing a competitive advantage over other hydrocarbon-degraders in rhamnolipid treatments.

Overall, this study has highlighted that dispersants and biosurfactants (excluding sophorolipid) not only reduce the interfacial surface tension of oil and water but also significantly increase the abundance of HCB, and thus the rate of hydrocarbon-biodegradation over the first 24 hours. Moreover, niche-partitioning drives a succession of obligate hydrocarbonoclastic bacteria (OHCB), which has shown how the OHCB *Oleispira*, hitherto considered to be a psychrophile, can dominate in the early stages of oil-spill response (the first three days), out-competing other OHCB. Additionally, some dispersants or biosurfactants can select for specific Bacteria, especially the biosurfactant rhamnolipid, which appears to provide an advantageous compatibility with the genus *Pseudomonas*.

Experimental Procedures

Sampling Site

“Seawater was sampled from the Thames estuary (Supplementary Materials Fig. S2.1), Earls Hope saltmarsh, Stanford le Hope, Essex, UK (51º30'N, 0º27'E). The hypernutrified Thames is one of the UK’s largest rivers and has over 50 tributaries that drain a diverse catchment, including agricultural and industrial land, and the most highly urbanised area of the UK. The sampling site is a fully saline, coastal region, at the mouth of the hypernutrified Thames estuary, which is subject to heavy shipping traffic from the DP World London Gateway (deep-sea container port, opened

November 2013) and oil/gas storage and transport facilities. Previously, the sampling site was near two oil-refineries (closed in 1999 and 2012). Due to heavy shipping traffic, and the transport and storage of oil, the sampling site is likely exposed to constant inputs of petroleum hydrocarbons." Samples were taken in November 2017 at high tide from the sea surface (13.8ºC, 35.1 PSU).

Microcosm Design and Sampling

Microcosms were created based on ten treatments (Supplementary Materials Table S2.1) using sterile 40 ml glass vials with PTFE-lined silicon septa. Treatments were destructively sampled in triplicate over a series of time points (1, 3, 7, 14, 21 days), ensuring samples were temporally independent. Each 40 ml microcosm (excluding seawater only) contained 20 ml of seawater (leaving equal proportion of air space; microcosms did not show signs of becoming anaerobic) which was supplemented with nutrients (final concentrations of 300 µM NH_4Cl and 20 µM K_2HPO_4); this allowed us to control for nutrient limitation and evaluate microbial response to oil/dispersants in the early phase. From time zero to day one, measurable hydrocarbons were reduced by 954.31 µM; it is worth noting this is only the hydrocarbons we were able to measure on the GC-MS and therefore the figure could be higher. Ammonium was reduced by 300 µM, a ratio of C:N of 3.18, whilst phosphate was reduced by 13.25 µM, a ratio of C:P of 72.02. Typically, C:N and C:P ratios supporting hydrocarbon-biodegradation are lower than the general bacterial requirement (6.625 and C:P 106:1) due to the low bioavailability of hydrocarbons and a different elemental cell composition of the produced biomass (Al Disi *et al.*, 2017). It is reported in the literature that the ratio of C:N and C:P for optimal hydrocarbon-biodegradation is dependent upon the environment, type of bacteria, and type of hydrocarbon (Simarro *et al.*, 2012). The sampling site is subjected to large annual inputs of DIN (dissolved inorganic nitrogen) and DIP (dissolved inorganic phosphorous) from the river Thames (Greenwood *et al.*, 2019) and the nutrient loadings are representative of background nitrogen and phosphorous concentrations recorded at the sampling site at other times (Coulon *et al.*, 2007). The oil (0.1% v/v final concentration) was a Norwegian Geochemical Standard, North Sea Oil (NSO-1) that had previously been weathered (distilled at 69°C). Oil was added to microcosms by reverse pipetting and time-zero samples were analysed to ensure consistent oil loadings, which consistently added 45.50 and 4.38 µg ml^{-1} ± 7% of resolvable alkanes and PAHS respectively". The dispersants were Slickgone NS, Superdispersant 25, and Finasol OSR 52 added to an industry standard (0.005% v/v), creating an industry standard ratio of 20:1 oil to dispersant (Fingas, 2000). The biosurfactants were rhamnolipid, sophorolipid, and trehalolipid, and were also added at a final

concentration of 0.005% v/v to create the same ratio; based on the percentage of active ingredient. Killed controls were also sampled at each time point to monitor abiotic hydrocarbon loss. All microcosms were incubated on a rotary shaker at 100 RPM at 16°C, replicating summer environmental conditions in the Thames estuary.

Surface Tension

Surface tension of seawater, and any changes due to the addition of dispersants or biosurfactants, was measured on a KRÜSS Force Tensiometer K6 using the Du Noüy ring method (Lecomte Du Noüy, 1919). Briefly, this involved lowering a platinum ring to just below the water's surface, applying tension until the water's surface breaks, at which point a measurement was recorded. To avoid contamination, surface tension was measured in independent seawater microcosms (20 ml), with dispersant or biosurfactants added at the same concentration used in the incubation microcosms.

Hydrocarbon-Degradation (GC-MS)

Hydrocarbons were extracted from the seawater microcosms (18 ml, after 2 ml was removed for DNA analysis) by vigorously shaking in 6 ml hexane:dichloromethane (1:1) followed by 30 minutes in an ultrasonic water bath. Deuterated alkanes (nonadecane $C_{19}d_{40}$ and triacontane $C_{30}d_{62}$ at 10 µg ml^{-1}) and PAH (naphthalene-d_8 and anthrancene-d_{10} at 10 µg ml^{-1}) internal standards were added to each sample and quantification was performed on an Agilent 7890A Gas Chromatography system coupled with a Turbomass Gold Mass Spectrometer with Triple-Axis detector, operating at 70 eV in positive ion mode, using conditions as previously described by Coulon *et al.* (2007). External multilevel calibrations were carried out using alkanes (Standard Solution (C_8-C_{40}); Sigma), methylated-PAHs (1-methylnapthalene, 2-methylanthracene, and 9,10-dimethylanthracene; Sigma), and PAH (QTM PAH Mix; Sigma) standards, the concentrations of which ranged from 1.125 to 18 µg ml^{-1}. For quality control, a 2.0 ng $µl^{-1}$ diesel standard solution (ASTM C12-C60 quantitative, Supelco) and a 1.0 ng $µl^{-1}$ PAH Mix Standard solution (Supelco) were analysed every 15 samples. The variation of the reproducibility of extraction and quantification of water samples were determined by successive extractions and injections (n = 6) of the same sample and estimated to be ± 8%. Extraction efficiency was measured at 89%. All alkanes between C_{10} and C_{36} including pristane and phytane and the following PAHs were quantified (naphthalene; all isomers of methyl-, dimethyl- and trimethyl-naphthalenes; acenaphthylene; acenaphthene; fluorine; phenanthrene; all isomers of methyl- and dimethyl-phenanthrenes/anthracenes; fluoranthene; pyrene; all isomers

of methyl- and dimethyl-pyrene; chrysene; all isomers of methyl- and dimethyl-chrysene). Only those hydrocarbons detected are shown in Fig. 2.2.

qPCR Analysis of Bacterial 16S rRNA Genes

At each time point, samples were vigorously shaken to allow dispersion of microcosm contents throughout, prior to 2 ml being sampled for DNA extraction. The 2 ml sample was centrifuged at 21,100 G for 20 minutes, leaving a cell pellet in the collection tube. The 2 ml supernatant was removed and stored for nutrient analysis (see Experimental Procedures subsection "*Nutrient Concentration*"). DNA was extracted from cell pellets using a DNeasy PowerSoil Kit (Qiagen), according to the manufacturer's instructions. DNA extracts were frozen at -20°C for downstream analysis, including qPCR (to monitor total bacterial biomass) and amplicon library sequencing (to evaluate bacterial community composition). The primers used for quantification of bacterial 16S rRNA gene were 341f - CCTACGGGNGGCWGCAG and 785r - GACTACHVGGGTATCTAATCC (Klindworth *et al.*, 2013). All qPCR reactions were performed using a CFX384™ Real-Time PCR Detection System (BioRad) with a PCR using reagents, cycle conditions, and standards as previously described (McKew and Smith, 2015; Tatti *et al.*, 2016). Inspection of standard curves showed that all assays produced satisfactory efficiency (91%) and R^2 values (>0.99). It should be noted that qPCR of the 16S rRNA gene, whilst providing a valuable comparison of bacterial growth between samples, does not reflect absolute bacterial biomass, as many species contain multiple copies of the 16S rRNA gene.

Nutrient Concentration

Nutrient analysis was conducted on all samples to determine concentrations of ammonium (NH_4^+) and phosphate (PO_4^{3-}) using a SEAL Analytical AA3 HR AutoAnalyzer tandem JASCO FP-2020 Plus fluorescence detector.

Amplicon Sequencing and Bioinformatics

Amplicon libraries were prepared, as per Illumina instructions, by a 25-cycle (*Bacteria*) PCR. PCR primers were the same as those used for qPCR but flanked with Illumina Nextera overhang sequences. A unique combination of Nextera XT Indices (Illumina) were added to PCR products from each sample, via an 8-cycle PCR. PCR products were quantified using a Quant-iT™ PicoGreen™ dsDNA Assay Kit (ThermoFisher Scientific) and pooled in equimolar concentrations. Quantification of the amplicon libraries was determined via NEBNext® Library Quant Kit for Illumina (New England BioLabs Inc.), prior to sequencing on the Illumina MiSeq® platform, using a MiSeq® 600 cycle v3 reagent kit and 20% PhiX sequencing control standard. Raw sequence data have been submitted to the European Nucleotide Archive

database under accession number PRJEB37243. Sequence output from the Illumina MiSeq platform were analysed within BioLinux (Field *et al.*, 2006), using a bioinformatics pipeline as described by Dumbrell *et al.* (2016). Forward sequence reads were quality trimmed using Sickle (Joshi and Fass, 2011) prior to error correction within SPades (Nurk *et al.*, 2013) using the BayesHammer algorithm (Nikolenko *et al.*, 2013). The quality filter and error corrected sequence reads were dereplicated, sorted by abundance, and clustered into OTUs (Operational Taxonomic Units) at the 97% sequencing identity via VSEARCH (Rognes *et al.*, 2016). Singleton OTUs were discarded, as well as chimeras using reference based chimera checking with UCHIME (Edgar *et al.*, 2011). Taxonomic assignment was conducted with the ribosomal database project (RDP) Classifier (Wang *et al.*, 2007). Non locus-specific, or artefactual, OTUs were discarded prior to statistical analyses, along with any OTUs that had <70% identity with any sequence in the RDP database.

Phylogenetic Analysis

The Neighbour-Joining protocol (Nei and Saitou, 1987) was used to infer the evolutionary history of partial 16S rRNA gene sequences Bacterial OTUs, aligned with known hydrocarbon-degrading Bacteria and closest neighbouring accessions using MUSCLE (Edgar, 2004). Bootstrapping analysis (1000 iterations) was conducted to determine the percentage of time associated taxa clustered together in replicate trees (Felsenstein, 1985); only bootstrap values >70% are shown. Evolutionary distances, units in the number of base substitutions per site, were calculated with the use of Maximum Composite Likelihood protocol (using the Tamura-Nei model (Tamura and Nei, 1993)). Phylogenetic analyses were conducted in MEGA7.

Statistical Analysis

Data were first tested for normality (Shapiro-Wilks test), those data which were normally distributed were tested for significance with ANOVAs or appropriate linear models. Non-normally distributed data were analysed using appropriate GLMs (Generalised Linear Models) as follows. The relative abundance of OTUs or genera in relation to oil exposure, dispersant/biosurfactant, and time were modelled using multivariate negative binomial GLMs (W. Wang *et al.*, 2010). Here, the number of sequences in each library was accounted for using an offset term, as described previously (Alzarhani *et al.*, 2019). The abundance of bacterial 16S rRNA gene copies was also modelled using negative binomial GLMs (Venables and Ripley, 2002). The significance of model terms was assessed via likelihood ratio tests. The Environmental Index of Hydrocarbon Exposure (Lozada *et al.*, 2014) was calculated using the script available at the ecolFudge GitHub page (https://github.com/Dave-Clark/ecolFudge,

Clark, 2019) and EIHE values modelled using poisson GLMs. Co-occurrence analysis was conducted by network analysis using the SPIEC-EASI algorithm (Kurtz *et al.*, 2015). To make this analysis computationally tractable and biologically interpretable, the total bacterial OTU table was filtered to OTUs confidently (RDP classifier confidence >0.8) assigned to putative hydrocarbon-degrading genera specified in the EIHE (Lozada *et al.*, 2014). OTUs assigned to several other genera (*Colwellia, Arcobacter, Glaciecola, Marinomonas, Zhongshania, Neptuniibacter,* and *Alkalimarinus*) that are not included in this index were also included, based on strong evidence for a direct or indirect role in hydrocarbon-degradation. For this analysis, unnormalised data were used, as the SPIEC-EASI algorithm applies its own internal log ratio transformation to normalise OTU counts. Network inference was conducted using the neighbourhood selection framework (50 permutations). The network was clustered, using a fast greedy clustering algorithm, to reveal any modules (smaller groups of OTUs with dense connections within the group, and few between groups). Additionally, the extent to which OTUs co-occurred with other OTUs in the same genus was evaluated by quantifying taxonomic assortativity. An assortativity coefficient quantifies whether nodes in a network tend to connect with other nodes that share properties (such as taxonomy), and ranges from -1 (disassortativity - OTUs never associate with others in the same genus) to 1 (assortativity - OTUs only ever associate with others in the same genus).

All statistical analyses were carried out in R3.6.1 (R Development Core Team, 2011) using a variety of packages available through the references (Venables and Ripley, 2002; Csardi and Nepusz, 2006; Hope, 2013; Wilke, 2015, 2020; Becker *et al.*, 2016; Auguie, 2017; Oksanen *et al.*, 2019; Hvitfeldt, 2020; Kassambara, 2020; Lenth, 2020; Pedersen, 2020). All plots were constructed using the “ggplot2” (Bodenhofer *et al.*, 2011) and “patchwork” (Pedersen, 2019) R packages.

Supplementary Materials

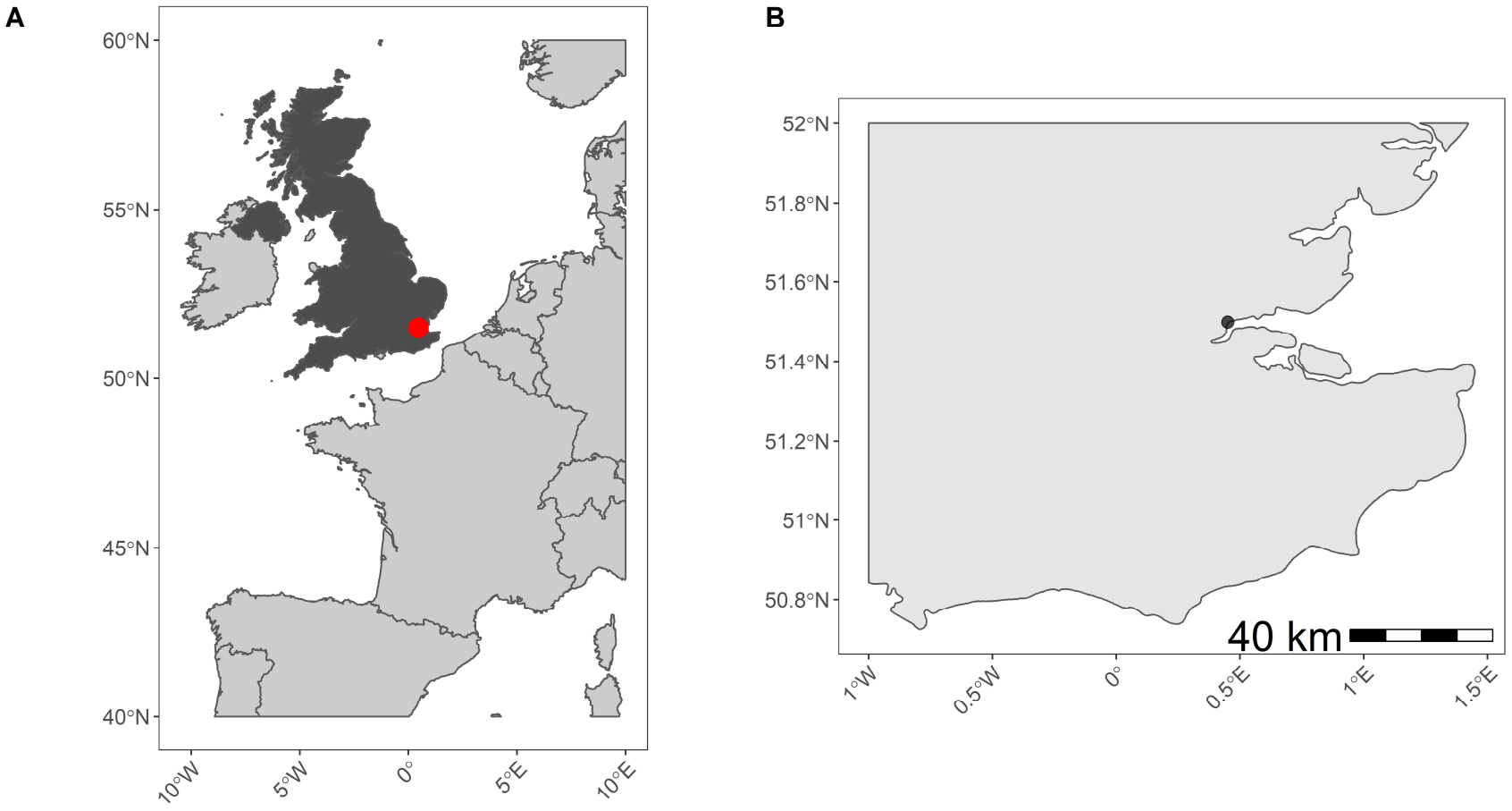

Fig. S2.1: Map of sampling site, United Kingdom (**A**) red circle indicates location for sampling site, which is located at Earls Hope salt marsh, Stanford le Hope, Thames estuary, Essex (**B**).

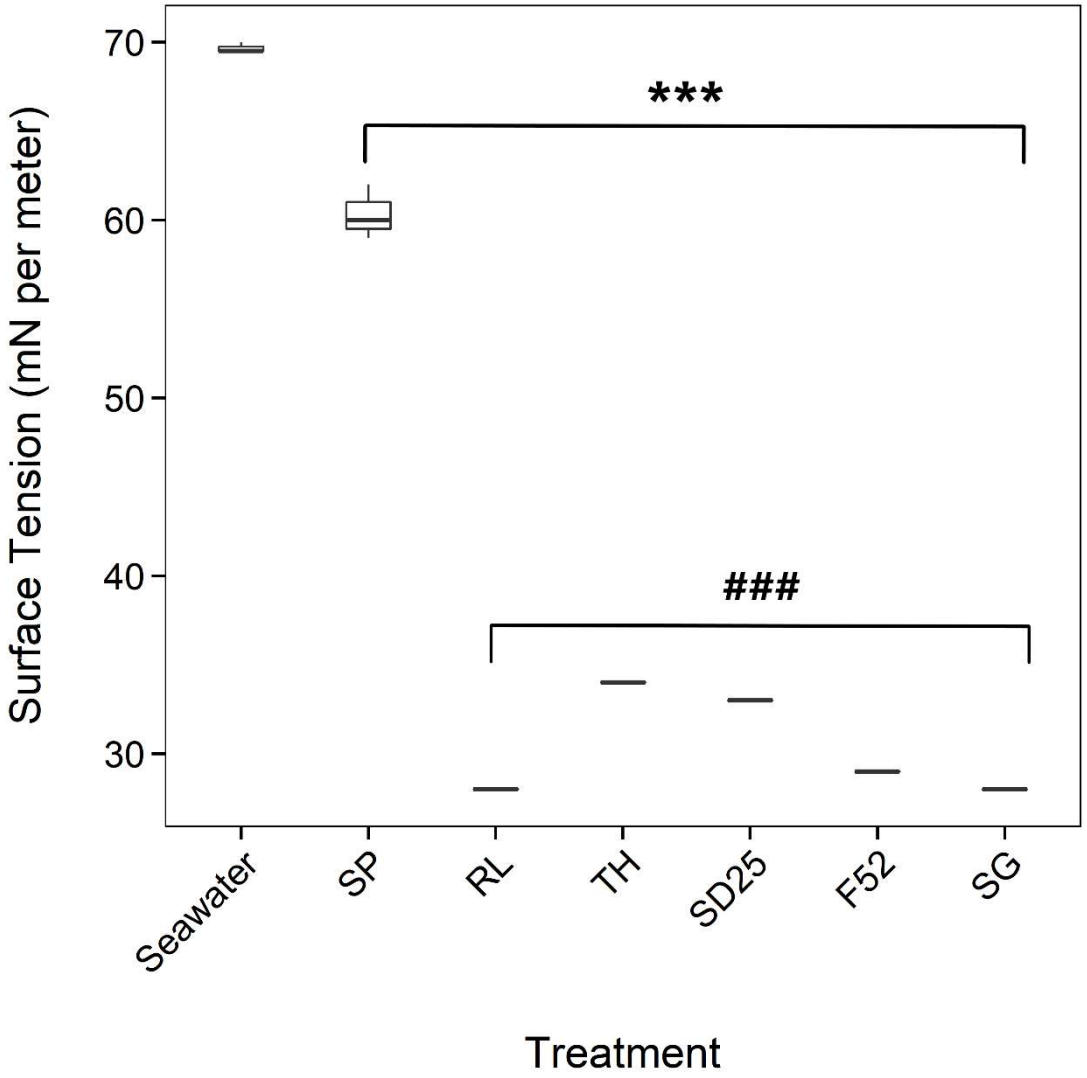

Fig. S2.2: Surface tension (mean ± SE, *n* = 3) measured in microcosms containing seawater or seawater with additional dispersants or biosurfactants (0.005% v/v). Dispersant and biosurfactant codes are as follow; SP = Sophorolipid, RL = Rhamnolipid, TH = Trehalolipid, SD25 = Superdispersant 25, F52 = Finasol OSR 52, SG = Slickgone NS. Stars (*** P<0.001) and octothorpes (### P<0.001) indicate significant changes in mean surface tension compared to seawater and sophorolipid respectively.

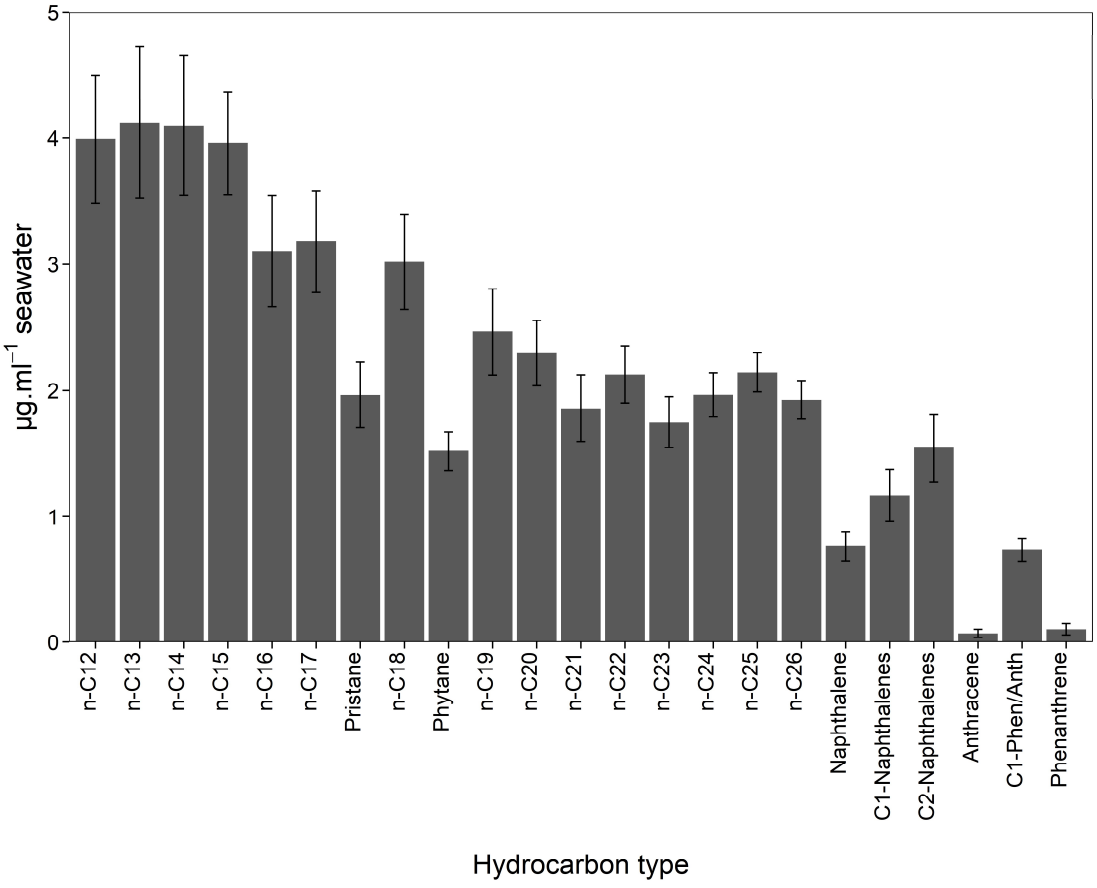

Fig. S2.3: Initial (time zero) measured hydrocarbon concentrations (mean ± SE, *n* = 3) within microcosms, including *n*-alkanes (C_{12} to C_{26}), branched alkanes pristane and phytane, and PAHs (naphthalene and phenanthrene/anthracene (Phen/Anth) and their methylated derivatives).

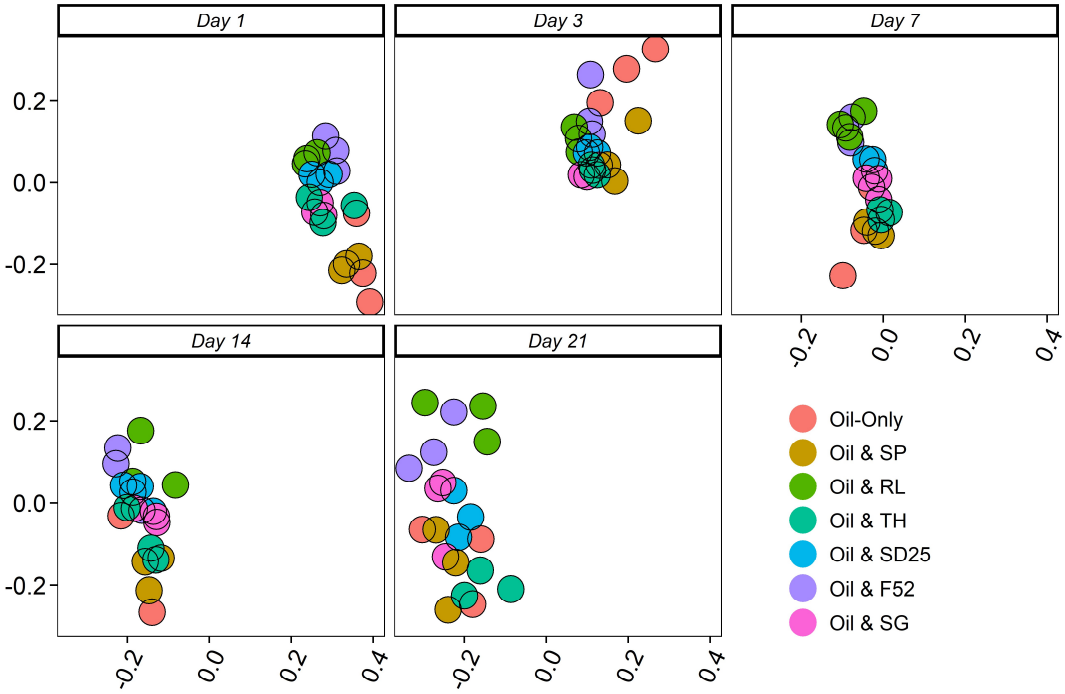

Fig. S2.4: NMDS (non-metric multidimensional scaling) ordination, based on clustered bacterial 16S rRNA OTUs at a 97% similarity threshold, displaying the effect of treatment, over time, on microbial community composition. Surfactant codes as follows; SP = Sophorolipid, RL = Rhamnolipid, TH = Trehalolipid, SD25 = Superdispersant 25, F52 = Finasol OSR 52, SG = Slickgone NS.

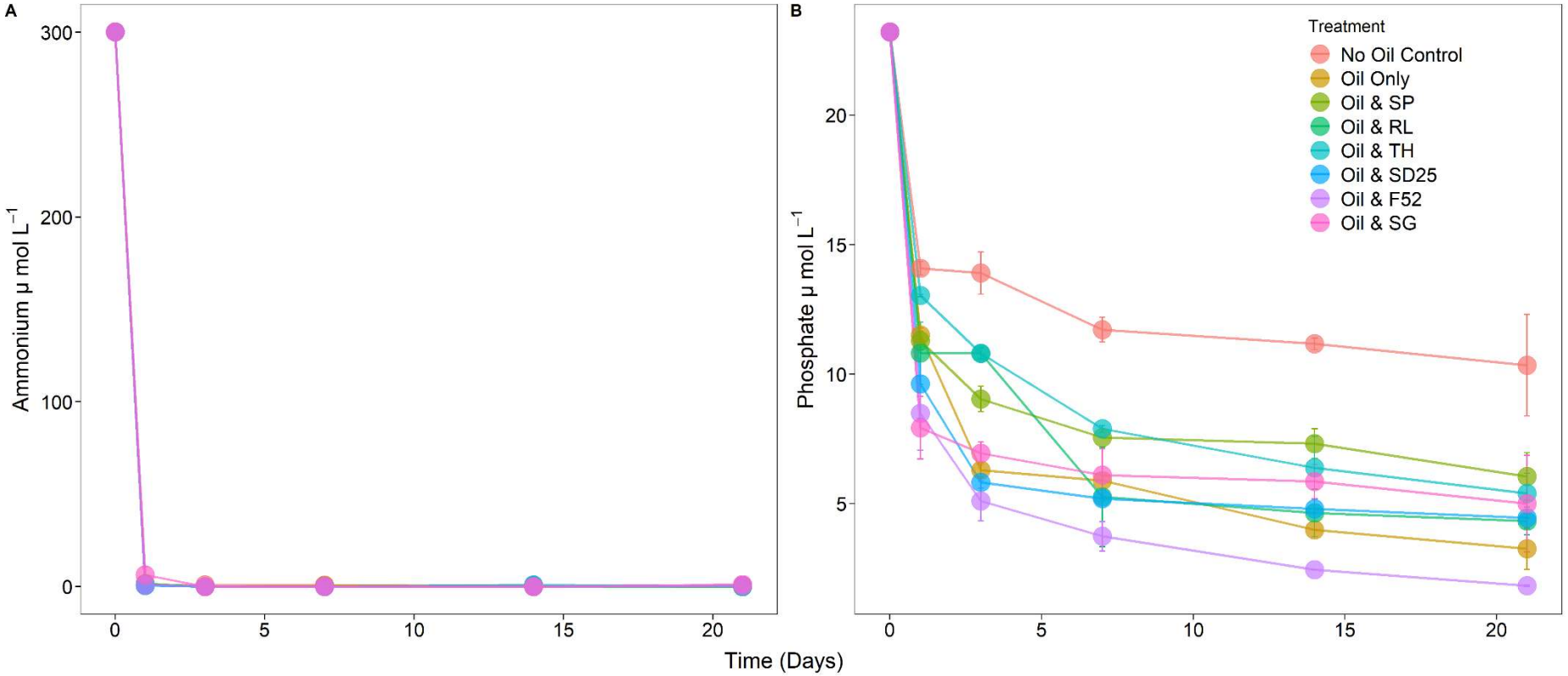

Fig. S2.5: Ammonium (**A**) and phosphate (**B**) (mean ± SE, *n* = 3) in microcosms containing seawater, nutrients, and oil (NSO-1 0.01% v/v), and those with additional dispersants or biosurfactants (0.005% v/v). Dispersant and biosurfactant codes are as follow; SP = Sophorolipid, RL = Rhamnolipid, TH = Trehalolipid, SD25 = Superdispersant 25, F52 = Finasol OSR 52, SG = Slickgone NS.

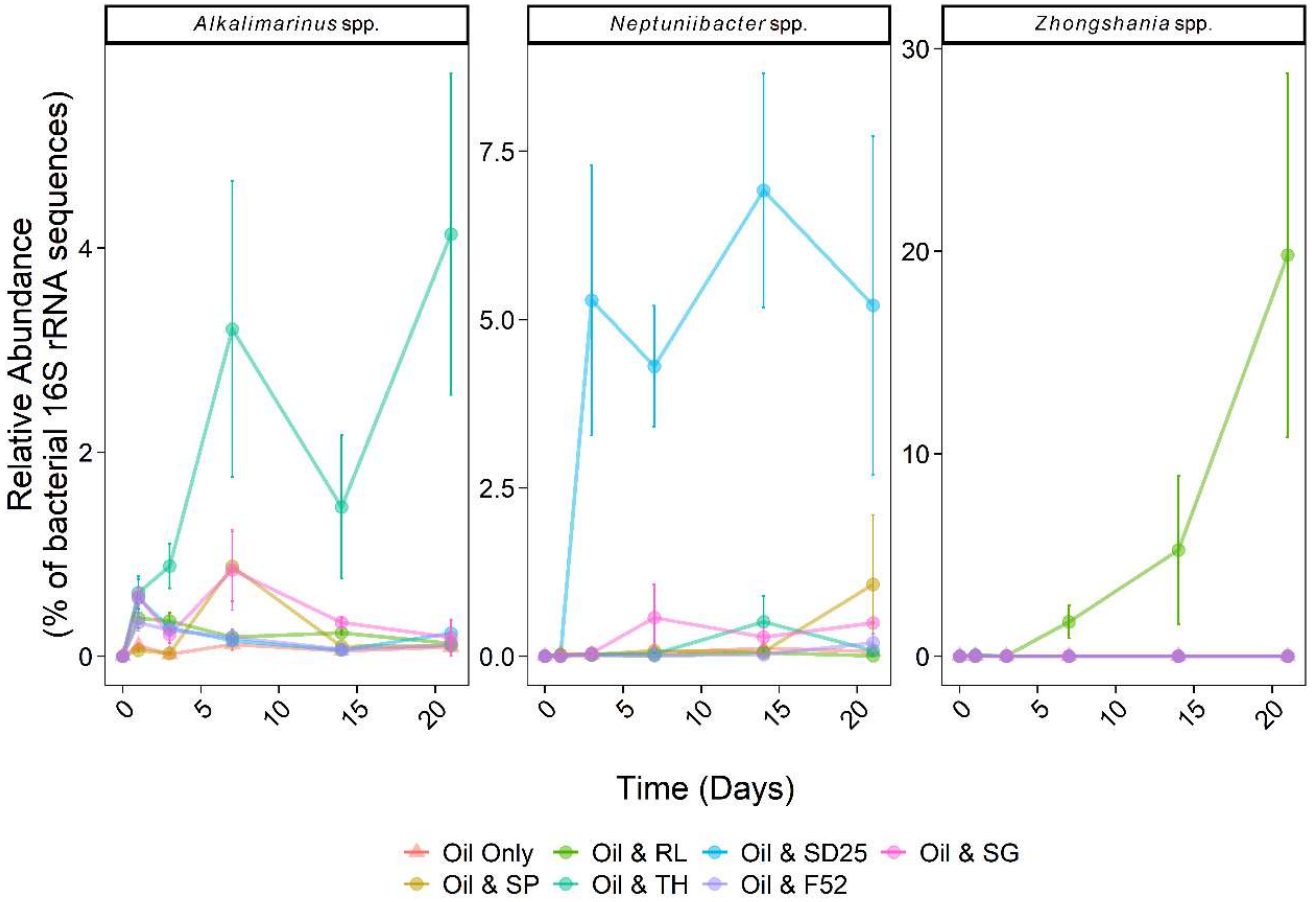

Fig. S2.6: Relative abundance (% of the bacterial community; mean ± SE, *n* = 3) of 16S rRNA gene sequences within OTUs assigned to Bacteria associated with oil-degradation (see Supplementary Materials Table S2.2) over a 21-day period. All microcosms contained seawater, nutrients, and oil (NSO-1 0.1% v/v), and some with additional dispersants or biosurfactants (0.005% v/v; 20:1 ratio of oil). Dispersant and biosurfactant codes are as follow: SP = Sophorolipid, RL = Rhamnolipid, TH = Trehalolipid, SD25 = Superdispersant 25, F52 = Finasol OSR 52, SG = Slickgone NS.

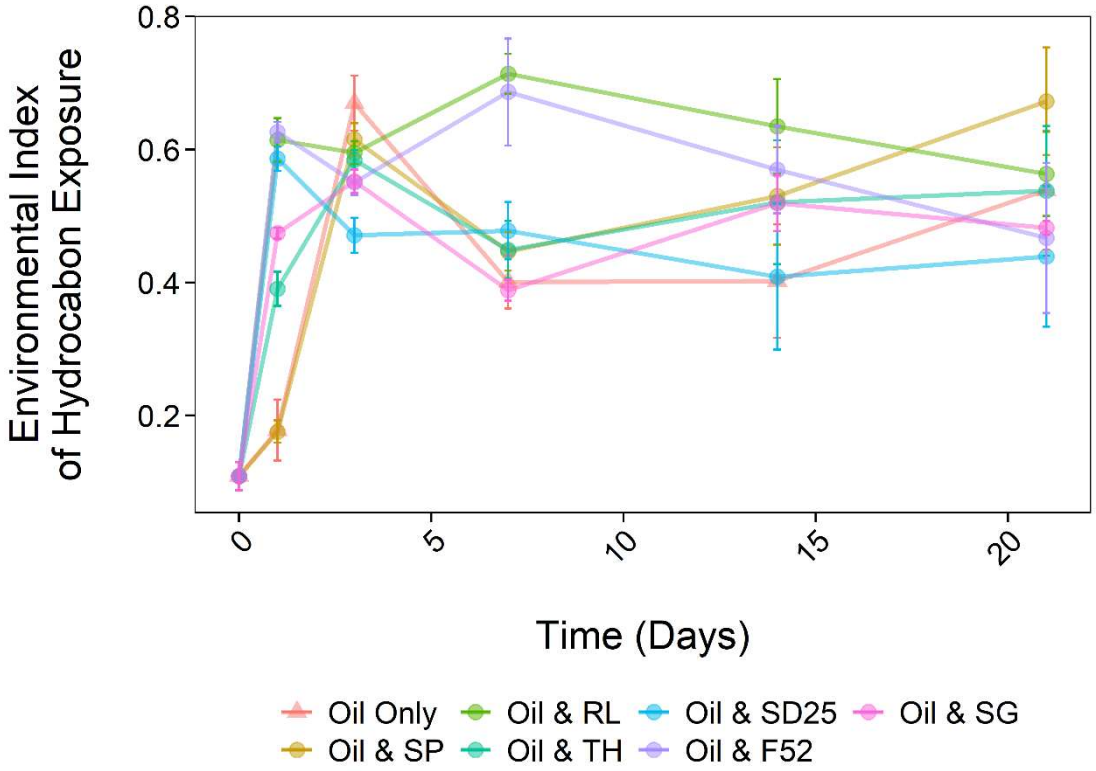

Fig. S2.7: Mean Ecological Index of Hydrocarbon Exposure (ratio %) representing relative abundance of oil-degrading/associated Bacteria, Lozada et al., 2014) measurements (± SE, *n* = 3) in microcosms containing seawater, nutrients, and oil (NSO-1 0. 1% v/v), and those with additional dispersants or biosurfactants (0.005% v/v). Dispersant and biosurfactant codes are as follow; SP = Sophorolipid, RL = Rhamnolipid, TH = Trehalolipid, SD25 = Superdispersant 25, F52 = Finasol OSR 52, SG = Slickgone NS.

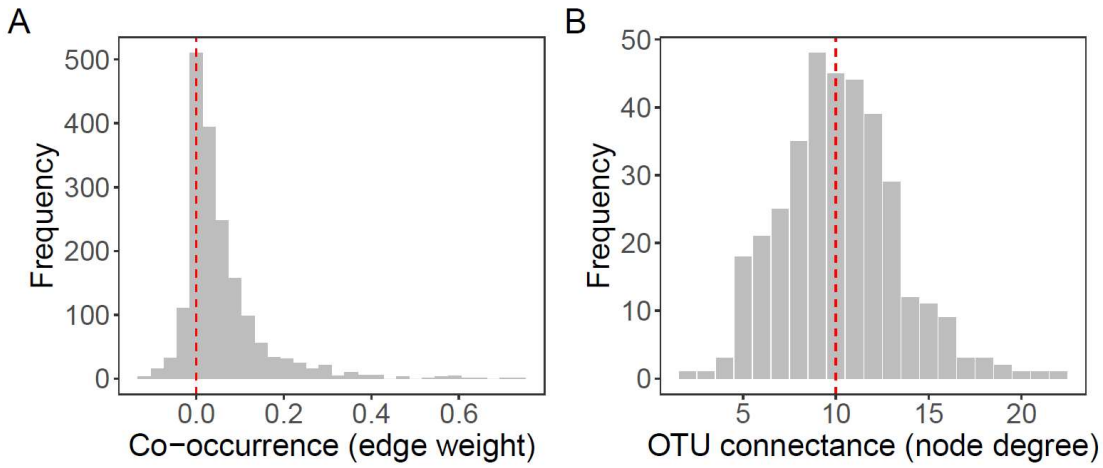

Fig. S2.8: (**A**) edge weight and (**B**) node degree distributions of the SPIEC-EASI co-occurrence network based on OTUs from bacterial genera associated with hydrocarbon-degradation. Edge weights indicate the direction and effect size of co-occurrences between OTUs, whilst node degree values indicate the number of OTUs each OTU co-occurs (positively or negatively) with. In (**A**), the dashed red line indicates 0 (no co-occurrence), whereas in (**B**) it indicates the median node degree (10) of OTUs in the network.

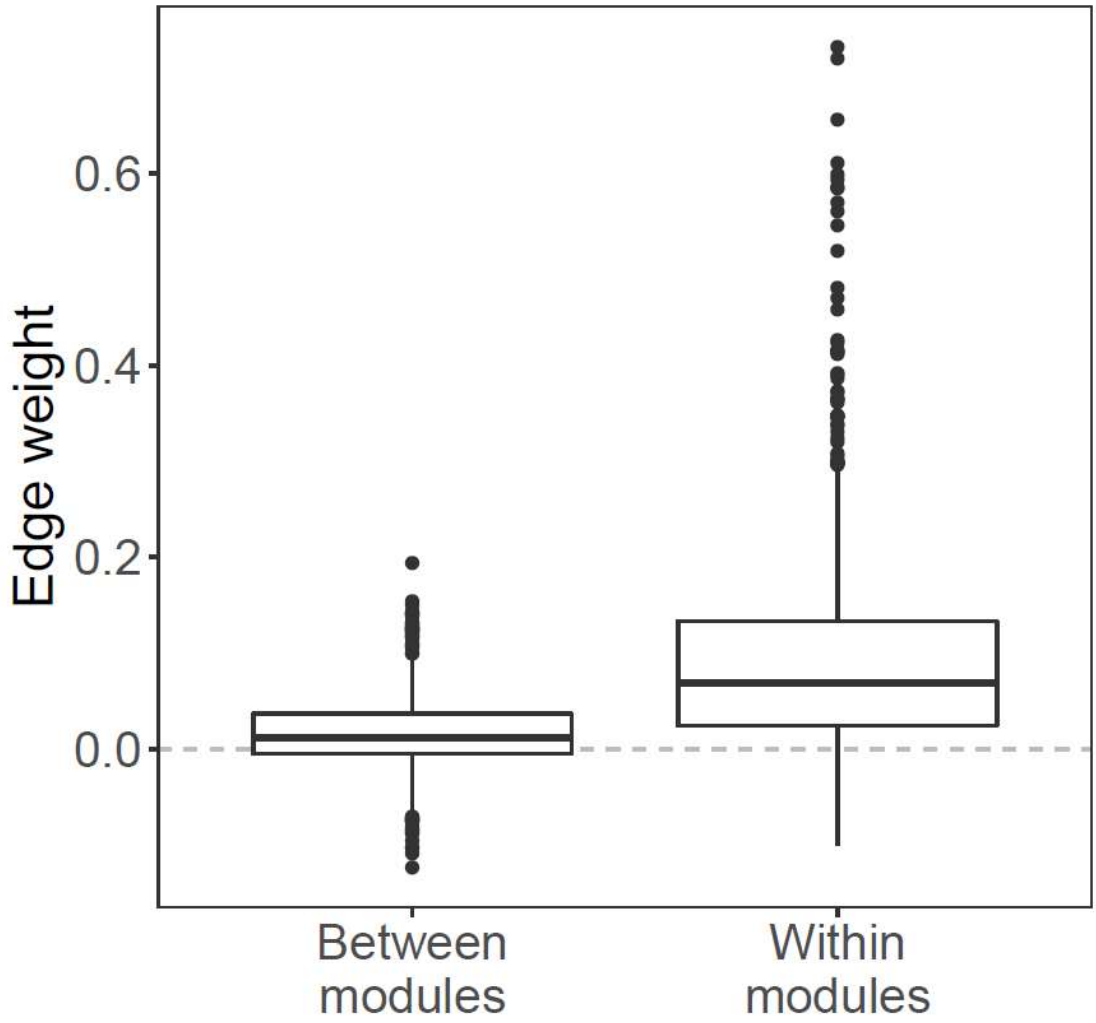

Fig. S2.9: comparison of edge weights connecting OTUs within and between modules. Positive values indicate positive co-occurrences and vice-versa, with values closer to 0 indicating weaker co-occurrences. Co-occurrences between OTUs within modules were significantly stronger and more positive than those between modules (coef. = 0.08, t = 21.33, P<0.001).

Table S2.1: Experimental design showing 10 treatments **(codes in parentheses)**; including concentrations and measurements of seawater, nutrients, crude oil (NSO-1), dispersant or surfactants, and, for the killed controls, mercuric chloride (HgCl2).

Treatment	Seawater	Nutrients	Oil (NSO-1)	Surfactant	$HgCl_2$
Seawater & Nutrients **(No-Oil Control)**	20 ml	300 µM NH_4Cl, 20 µM KH_2PO_4			
Seawater, Nutrients, & Oil **(Oil-Only)**	20 ml	300 µM NH_4Cl, 20 µM KH_2PO_4	0.1% v/v		
Slickgone NS **(Oil & SG)**	20 ml	300 µM NH_4Cl, 20 µM KH_2PO_4	0.1% v/v	0.005% v/v	
Superdispersant 25 **(Oil & SD25)**	20 ml	300 µM NH_4Cl, 20 µM KH_2PO_4	0.1% v/v	0.005% v/v	
Finasol OSR 52 **(Oil & F52)**	20 ml	300 µM NH_4Cl, 20 µM KH_2PO_4	0.1% v/v	0.005% v/v	
Rhamnolipid **(Oil & RL)**	20 ml	300 µM NH_4Cl, 20 µM KH_2PO_4	0.1% v/v	0.005% v/v	
Sophorolipid **(Oil & SP)**	20 ml	300 µM NH_4Cl, 20 µM KH_2PO_4	0.1% v/v	0.005% v/v	
Trehalolipid **(Oil & TH)**	20 ml	300 µM NH_4Cl, 20 µM KH_2PO_4	0.1% v/v	0.005% v/v	
Killed Control **(Kill)**	20 ml		0.1% v/v		1.1049 mM

Table. S2.2: Evidence demonstrating hydrocarbon-degradation (alkane of PAH) and growth in oil-polluted marine environments for certain genera of Bacteria (either so-called "obligate hydrocarbonoclastic bacteria" or more metabolically versatile).

Genus	**Hydrocarbon-Degradation Metabolic Capability**	**Isolated Alkane-Degraders**	**Isolated Polycyclic Aromatic Hydrocarbon-Degraders**	**Evidence for Increased Abundance in Oiled Marine Environments[×]**
Alcanivorax spp.	OHCB*	**Yes** Yakimov *et al.*, 1998	**No** Clear zone and colour change indicators of PAH-degradation (Yetti *et al.*, 2016) Also, may enhance PAH-degradation utilising alkyl sidechains on methylated PAHs (Yuan *et al.*, 2015; Noh *et al.*, 2018)	**Yes** Kasai *et al.*, 2001; Röling *et al.*, 2004; McKew *et al.*, 2007; Wang *et al.*, 2010; Teramoto *et al.*, 2013; Sanni *et al.*, 2015; Lee *et al.*, 2017; Liu *et al.*, 2019
Alkalimarinus spp.	Versatile[±]	**No**	**No**	**Yes** Noh *et al.*, 2018; Li *et al.*, 2019
Arcobacter spp.	Versatile[±]	**No**	**No** Potential for benzene degradation has been observed within *in-situ* microcosms in constructed wetlands (Nitz *et al.*, 2019)	**Yes** Coulon *et al.*, 2007; Hubert *et al.*, 2012; Isaac *et al.*, 2013; Wang *et al.*, 2014; Lormières and Oger, 2017
Colwellia spp.	Versatile[±]	**No**	**Yes** "Crude Oil" Bælum et al., 2012 Gutierrez *et al.*, 2013 Mason *et al.*, 2014	**Yes** Brakstad *et al.*, 2008; Redmond *et al.*, 2010; Dubinsky *et al.*, 2013; Bacosa *et al.*, 2018; Tremblay *et al.*, 2019
Cycloclasticus spp.	OHCB*	**No** Provision – *Cycloclasticus* sp. symbiont of *Bathymodiolus*	**Yes** Dyksterhouse *et al.*, 1995 Niepceron *et al.*, 2010	**Yes** Coulon *et al.*, 2007; Dubinsky *et al.*, 2013; Sanni *et al.*, 2015; Lee *et al.*, 2017;

		heckerae (Rubin-Blum *et al.*, 2017)		Liu *et al.*, 2017; Linda *et al.*, 2018; Tremblay *et al.*, 2019
Glaciecola spp.	Versatile±	**Yes** Chronopoulou *et al.*, 2015	**Yes** Chronopoulou *et al.*, 2015	**Yes** Brakstad *et al.*, 2008; Gontikaki *et al.*, 2018; Tremblay *et al.*, 2019
Marinomonas spp.	Versatile±	**No**	**Yes** Melcher *et al.*, 2002	**Yes** Brakstad *et al.*, 2008; Alonso-Gutiérrez *et al.*, 2008; Dong *et al.*, 2015; Gontikaki *et al.*, 2018
Neptuniibacter spp.	Versatile±	**No**	**Yes** Nagashima *et al.*, 2010	**Yes** Rivers *et al.*, 2013; Dombrowski *et al.*, 2016; Doyle *et al.*, 2018; Krolicka *et al.*, 2019
Oleibacter spp.	OHCB*	**Yes** Teramoto *et al.*, 2011	**No**	**Yes** Teramoto *et al.*, 2013; Sanni *et al.*, 2015; Liu *et al.*, 2017; Liu *et al.*, 2019
Oleispira spp.	OHCB*	**Yes** Yakimov *et al.*, 2003	**No**	**Yes** Coulon *et al.*, 2007; King *et al.*, 2015; Boccadoro *et al.*, 2018; Brakstad *et al.*, 2018; Tremblay *et al.*, 2019
Pseudoalteromonas spp.	Versatile±	**Yes** Chronopoulou *et al.*, 2015	**Yes** Chronopoulou *et al.*, 2015	**Yes** Kostka *et al.*, 2011; Dong *et al.*, 2015; Gontikaki *et al.*, 2018; Tremblay et al., 2019
Pseudomonas spp.	Versatile±	**Yes** van Beilen *et al.*, 2001 Zhang *et al.*, 2011	**Yes** Niepceron *et al.*, 2010 Zhang *et al.*, 2011	**Yes** Das and Mukherjee, 2007; Kostka *et al.*, 2011;

			Chebbi *et al.*, 2017	Dubinsky *et al.*, 2013; Dong *et al.*, 2015; Tremblay *et al.*, 2019
Thalassolituus spp.	OHCB*	**Yes** Yakimov *et al.*, 2004	**No**	**Yes** McKew *et al*., 2007; Sanni *et al.*, 2015; Lee *et al.*, 2017; Liu *et al.*, 2019
Zhongshania spp.	Versatile±	**Yes** Naysim *et al.*, 2014	**No**	**Yes** Ribicic *et al.*, 2018

* **OHCB** – refers to the so-called "obligate hydrocarbonoclastic bacteria" (Yakimov *et al.*, 2007)
± **Versatile** – has the metabolic capabilities to grow on a diverse range of substrates
× These lists are by no means exhaustive but are examples of the growth of these genera in either *in situ* or *ex situ* oil-based systems.

Chapter Three

A Comparison between Chemical and Natural Dispersion of a North Sea Oil-spill

Abstract

The application of dispersants to an oil-slick is a key remediation tool and thus understanding their effectiveness is vital. Two *in situ* oil-slicks were created in the North Sea (off the coast of The Netherlands), one left to natural processes whilst dispersant (Slickgone NS) was applied to the other. Analysis of seawater revealed only two samples with measurable hydrocarbons (221 ± 92 µg ml^{-1} seawater, from the surface of the "Slickgone Dispersed" oil-slick ~25.5 hours after oil-slick formation), this was likely due to environmental conditions hindering sampling. Additionally, 16S rRNA gene qPCR and amplicon analysis revealed extremely limited growth of obligate hydrocarbonoclastic bacteria (OHCB), detected at a relative abundance (%) of $<1\times10^{-6}$. Furthermore, the Ecological Index of Hydrocarbon Exposure (EIHE) score, which quantifies the proportion of the bacterial community with hydrocarbon-biodegradation potential, was extremely low at 0.012 (scale of 0 – 1). A lack of hydrocarbon-degrading bacteria growth at the time of sampling, even in samples with measurable hydrocarbons, could potentially be attributed to nutrient limitation (~25.5 hours after oil-slick creation total inorganic nitrogen was 3.33 µM and phosphorus was undetectable). The results of this study highlight a limited capacity for the environment, at the time of sampling, to naturally attenuate oil.

Introduction

Marine oil-contamination can cause a wide range of negative impacts (direct and indirect) to the environment and economy and can have social impacts on individuals and communities. The overall goal during oil-spill response is to minimise impact to biological life as well as natural and economic resources. A balance must be made between potential environmental/economic impacts and "natural recovery" or "recovery through intervention" (National Oceanic and Atmospheric Administration, 2010; IPIECA *et al.*, 2017). Oil spill response in the marine environment requires a comprehensive knowledge of immediate and surrounding environments, local stakeholders and political legislation, and available remediation tools. One such tool is the application of dispersants. Dispersants transform oil on the surface of the water into droplets (10 – 300 µm, North *et al.*, 2015) in the water column, which increases oil surface area for microbial attachment (Prince *et al.*, 2013), thus allowing hydrocarbon-degrading microbes to expend more energy on growth and less energy producing biosurfactants, thereby expediting hydrocarbon-biodegradation (Prince *et al.*, 2016; Brakstad *et al.*, 2018).

Slickgone NS, the dispersant used in this study, is comprised of a mixture of surface-active surfactants (non-ionic (e.g. Tween 80) and anionic (dioctyl sodium sulfosuccinate) constituting 1-50%) and solvents (kerosene, constituting >50%) (DASIC-International, 2002). The Deepwater Horizon oil-spill (2010), where 1.84 million gallons of dispersant (Corexit 9500) was applied both on the surface and at a depth of 1,500 m (White *et al.*, 2014), triggered a renaissance of research into the use of dispersants on oil spills. Prince *et al*. (2015) found that three commonly applied dispersants (Corexit 9500, Finasol OSR 52, and Slickgone NS) significantly increased the biodegradation of hydrocarbons when compared to a floating oil-slick, with no added dispersants. Several other studies also observe that dispersants increase biodegradation (Brakstad *et al.*, 2015; Prince *et al.*, 2016) and enhance the growth of hydrocarbon-degrading bacteria (HCB) (Hazen *et al.*, 2010; Dubinsky *et al.*, 2013; Ribicic *et al.*, 2018). Conflictingly, other studies show that dispersants may not enhance biodegradation (Lindstrom and Braddock, 2002; Rahsepar *et al.*, 2016) or may even inhibit the growth of HCB (Hamdan and Fulmer, 2011; Kleindienst *et al.*, 2015).

With contradictory results into the effects of dispersant application on oil spills it is evident that further research is required. Studies must replicate natural environmental conditions as best they can, the optimal way would be to collect samples during the application of a dispersant to a real-world oil-spill. However, due to logistical, financial, and safety issues this is often not possible. The next best option is to conduct a controlled experiment *in situ*, however, once again there are many legislative, economic, and technical barriers to such experiments being approved. Due to limitations sampling real-world, and experimental *in situ*, oil spills, most oil/dispersant research is conducted *ex situ*, either in microcosms (Techtmann *et al.*, 2017; Tremblay *et al.*, 2017), mesocosms (Meng *et al.*, 2016; Doyle *et al.*, 2018), or wave tanks (Li *et al.*, 2008; Buist *et al.*, 2011; O'Laughlin *et al.*, 2017). However, conducting *ex situ* oil spill experiments has potentially negative biases due to confinement, which would not necessarily occur *in situ*. Confinement does not allow dispersed oil to rapidly dilute to sub-ppm which would occur *in situ* (Bejarano *et al.*, 2013), and higher concentrations of oil can potentially inhibit hydrocarbon-degradation (Lee *et al.*, 2013; Prince *et al.*, 2016). Moreover, dispersion over a wider area, which would occur *in situ*, may allow access to further inorganic nutrients which in turn could lead to faster hydrocarbon-degradation. In addition, many *ex situ* oil/dispersant experiments compare water-accommodated fractions (WAF) to chemically-enhanced water-accommodated fractions (CEWAF) (Kleindienst *et al.*, 2015; DeLorenzo *et al.*, 2018; Bretherton *et al.*, 2019). This involves oil (and applied dispersant if CEWAF) being stirred into seawater for a set period of time, allowed to settle, and then the WAF (containing accommodated hydrocarbon fractions) is sampled from below the water's surface. Utilising this methodology however is not truly comparing an oil-slick to a chemically dispersed oil-slick, as both have been mechanically dispersed. Moreover, variations in mixing energy in WAF and

CEWAF, as well as increased oil surface area in CEWAF, mean the concentration of dissolved and particulate hydrocarbons in WAF and CEWAF can vary significantly (see review by Hodson *et al.*, 2019). Given the potential biases of conducting *ex situ* oil spill experiments, obtaining a permit to conduct a controlled oil release, with dispersant application, *in situ* is highly valuable.

The North Sea, in the north eastern area of the Atlantic Ocean, is located between the United Kingdom and borders continental west Europe (Belgium, Denmark, France, Germany, the Netherlands, and Norway). Socially and politically complex, the North Sea is home to Europe's largest fisheries (managed under the Common Fisheries Policy) and is the location of 24 active offshore oil-rigs (Sönnichsen, 2020). Approximately 13 miles off the coast of Scheveningen harbor, The Hague, Netherlands (Supplementary Materials Fig. S3.1) oil-slicks were created in the North Sea in April 2019 (Supplementary Materials Figures S3.2 and S3.3). One oil-slick was left to natural attenuation and dispersion whilst the other oil-slick was chemically dispersed using the widely applied commercial dispersant Slickgone NS. Samples were taken from both oil-slicks approximately 1, 5.5, and 25.5 hours after oil-slick creation, providing a rare and valuable opportunity to evaluate whether dispersant application on oil spills affects HCB growth and hydrocarbon-biodegradation *in situ*.

Results

Water Chemistry and other Environmental Variables

Seawater salinity was 30.9 (± 0.85) psu, pH 8.41 (± 0.02), and temperature 9.06 (± 0.11 °C), with no significant differences within "Uncontaminated Seawater", both oil-slicks, time points, or depths. During the first two sampling periods (~1.5 and ~5 hours after oil-slick creation) the average wind speed and wave height was 8.33 ± 0.71 m s^{-1} and 105.26 ± 17.32 cm (Supplementary Materials Fig. S3.4 and S3.5), respectively. Wind speed and wave height decreased by the third sampling period (~25.5 hours after oil-slick creation) to an average of 5.15 ± 0.66 m s^{-1} and 58.52 ± 7.63 cm (Supplementary Materials Fig. S3.4 and S3.5), respectively.

Aside from two surface seawater samples, no hydrocarbons were measured in all other samples either on the surface or at depths of 1.5 or 5 m. The two surface samples which did have measurable hydrocarbons were sampled from the "Slickgone Dispersed" oil-slick ~25.5 hours after oil-slick creation. Measurable hydrocarbons included *n*-alkanes (C_{14} – C_{31}), branched alkanes (pristane and phytane), and PAHs (phenanthrene and methyl-phenanthrene/anthracene) at average concentrations of 188.13 (± 76.91), 27.20 (± 11.91), and 5.84 (± 3.13) µg ml^{-1} seawater (Fig. 3.1), respectively. In comparison to a profile of the original crude oil (Supplementary Materials Fig. S3.6) *n*-alkanes C_{11} – C_{13} and PAHs naphthalene (and methyl- and dimethyl-naphthalene) and fluorene were not detected. In the

two samples with measurable hydrocarbons the ratio of *n*-C_{17}/pristane and *n*-C_{18}/phytane was 0.95 and 1.63, respectively, with no significant difference to the original oil (*n*-C_{17}/pristane (0.94) and *n*-C_{18}/phytane (1.47)), indicating no measurable biodegradation.

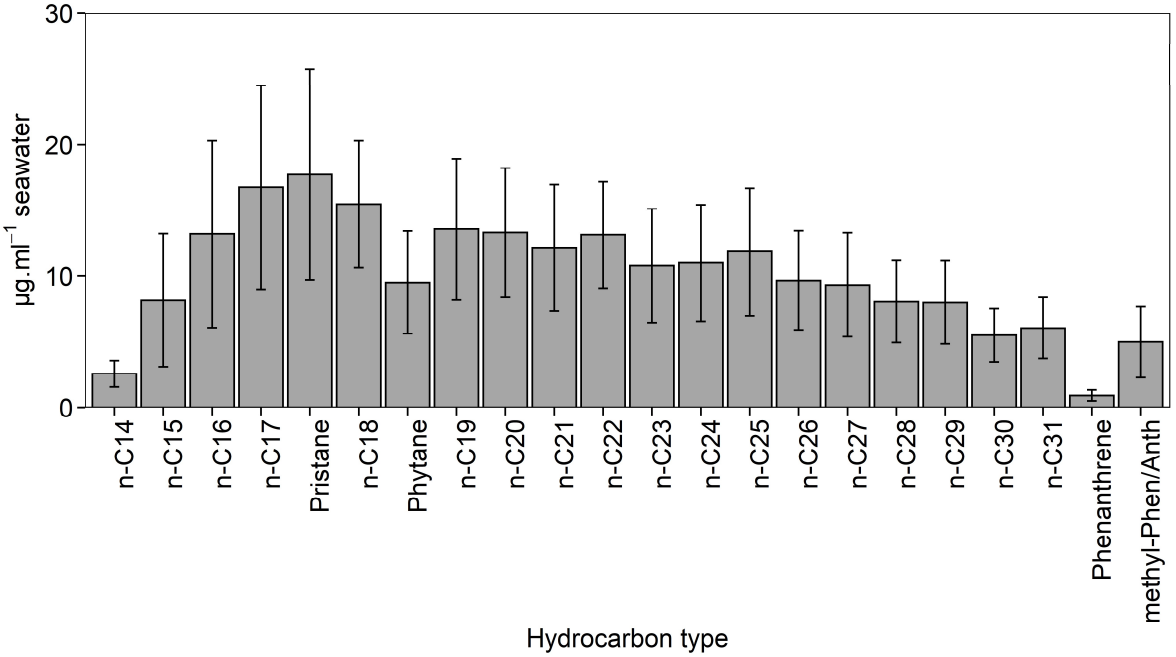

Fig. 3.1: Seawater samples taken from the "Slickgone Dispersed" oil-slick, ~25.5 hours after oil-slick creation. Measured hydrocarbon concentrations (mean ± SE, *n* = 2), including *n*-alkanes (C_{14} to C_{31}), branched alkanes pristane and phytane, and PAHs (phenanthrene and methyl-phenanthrene/anthracene (Phen/Anth)).

Across all samples, the average concentration of total inorganic nitrogen (TIN; sum of ammonia, nitrate, and nitrite; Fig. 3.2), approximately one hour after the oil-slick was created, was 26.67 (± 7.66) µM, with nitrate representing 93% of TIN. Approximately 5.5 hours after oil-slick creation the concentration of TIN remained relatively stable (23.74 ± 6.97 µM) before significantly decreasing (-86%; coef. -14.70, z -5.42, P<0.001) in both oil-slicks and the "Uncontaminated Seawater" after ~25.5 hours, in comparison to 1.5 and 5 hours, to an average of 3.33 (± 0.85) µM. Phosphate was undetected in all samples; the limit of detection was 0.02 µM.

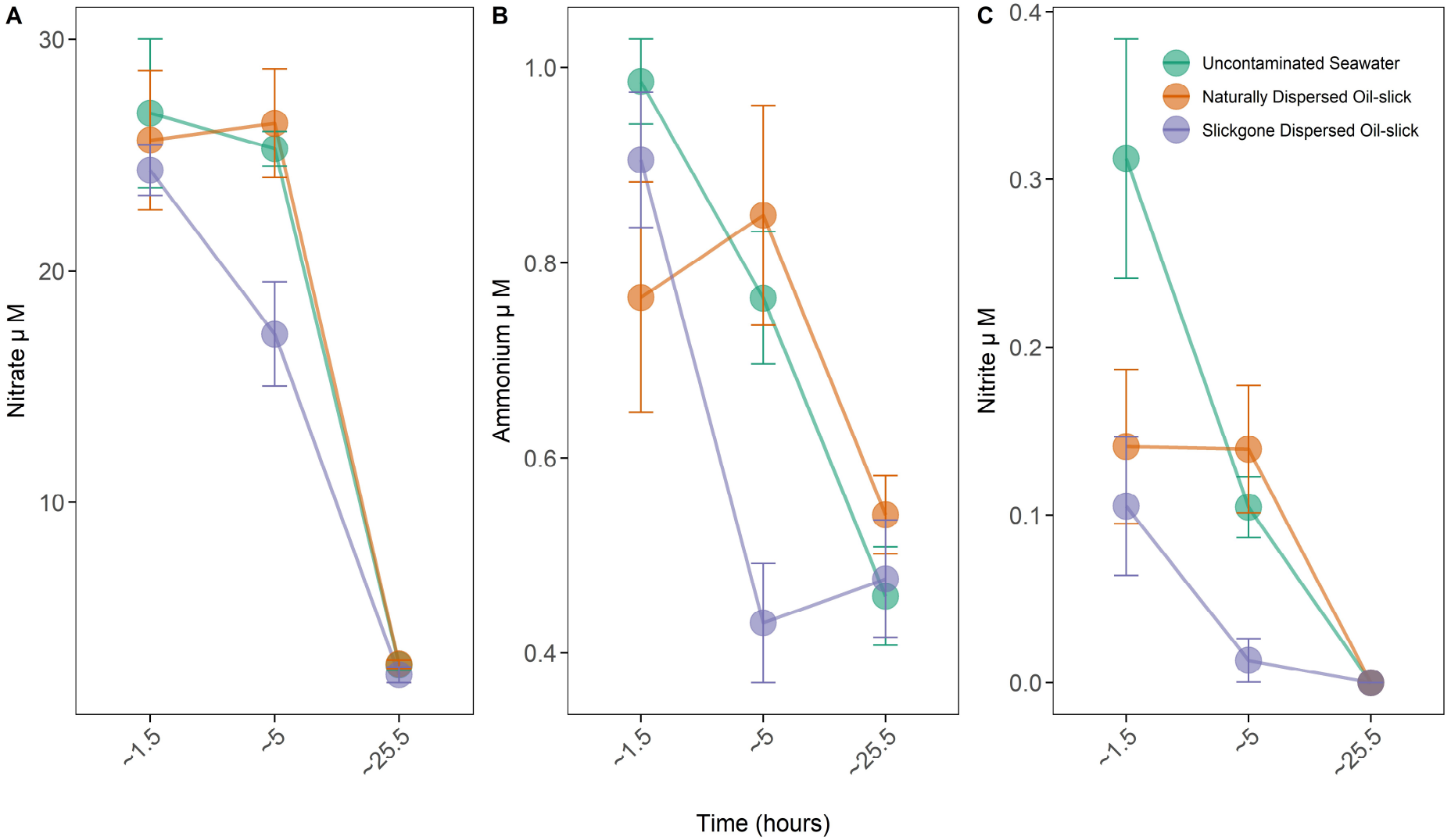

Fig. 3.2: Nitrate (**A**), ammonium (**B**), and nitrite (**C**) (mean ± SE, *n* = 3) from seawater samples taken from "Uncontaminated Seawater" as well as "Naturally Dispersed" and "Slickgone Dispersed" oil-slicks, ~1.5, ~5, and ~ 25.5 hours after oil-slicks were created. Phosphate was undetected in all samples; the limit of detection was 0.02 µM..

Effects of Oil and/or Dispersants on Bacterial Community Composition and Abundance

In order to quantify any effects of oil-slicks, depth, or time on bacterial abundance and community composition, 16S rRNA genes were analysed by qPCR and amplicon library sequencing. High-throughput 16S rRNA sequencing resulted in an average of 48,777 (range 5,747 – 201,395) sequence reads per sample. In the "Uncontaminated Seawater", at the surface, 1.5 m, and 5 m, bacterial 16S rRNA gene abundance was 86,293 (± 44,098), 98,438 (± 23,383) and 84,725 (± 25,164) copies ml^{-1} of seawater, respectively (Fig. 3.3A). The "Naturally Dispersed" and "Slickgone Dispersed" oil-slicks, over all timepoints and depths, had no significant effect on bacterial 16S rRNA gene abundance. However, there was a general temporal trend in both oil-slicks and the "Uncontaminated Seawater", whereby a reduction in bacterial 16S rRNA gene abundance was observed after 24 hours across all depths (55%, 82%, 21% reduction at surface, 1.5 m, and 5 m, respectively). The reduction in bacterial 16S rRNA gene abundance after 24 hours coincided with a change in bacterial community composition, in comparison to those communities observed at 1.5 and 5 hours (Fig. 3.3B; R^2 = 0.28, F = 15.90, $p<0.001$). However, the oil-slicks had no significant effect on bacterial community composition, and the composition was highly similar across all depths. The average Simpson index value across all depths was 0.97 (± 0.008), with no significant changes at any time.

Across all samples, twenty-five OTUs constituted 72% of the bacterial community (Supplementary Materials Table S3.1), with OTU1 and OTU20, both with a 100% identity match to *Candidatus* Pelagibacter spp., accounting for 17% of the entire bacterial community. The twenty-five OTUs, consisting of twelve genera, were also the primary drivers of the dissimilar bacterial community composition ~25.5 hours after oil-slick formation (Fig. 3.3B). Examples include increases, in "Uncontaminated Seawater" and both oil-slicks, ~25.5 hours after oil-slick formation, in relative abundance of OTUs assigned to *Halioglobus* (increased 109%), unclassified Bacteroidetes (297%), and unclassified *Flavobacteriaceae* (38%). Numerous OTUs also decreased in relative abundance including those assigned to *Planktomarina* (-55%), unclassified Actinobacteria (-79%), unclassified Betaproteobacteria (-61%), and unclassified *Cryomorphaceae* (-72%), in comparison to ~1.5 and ~5 hours (see Supplementary Materials Table S3.1 for full details).

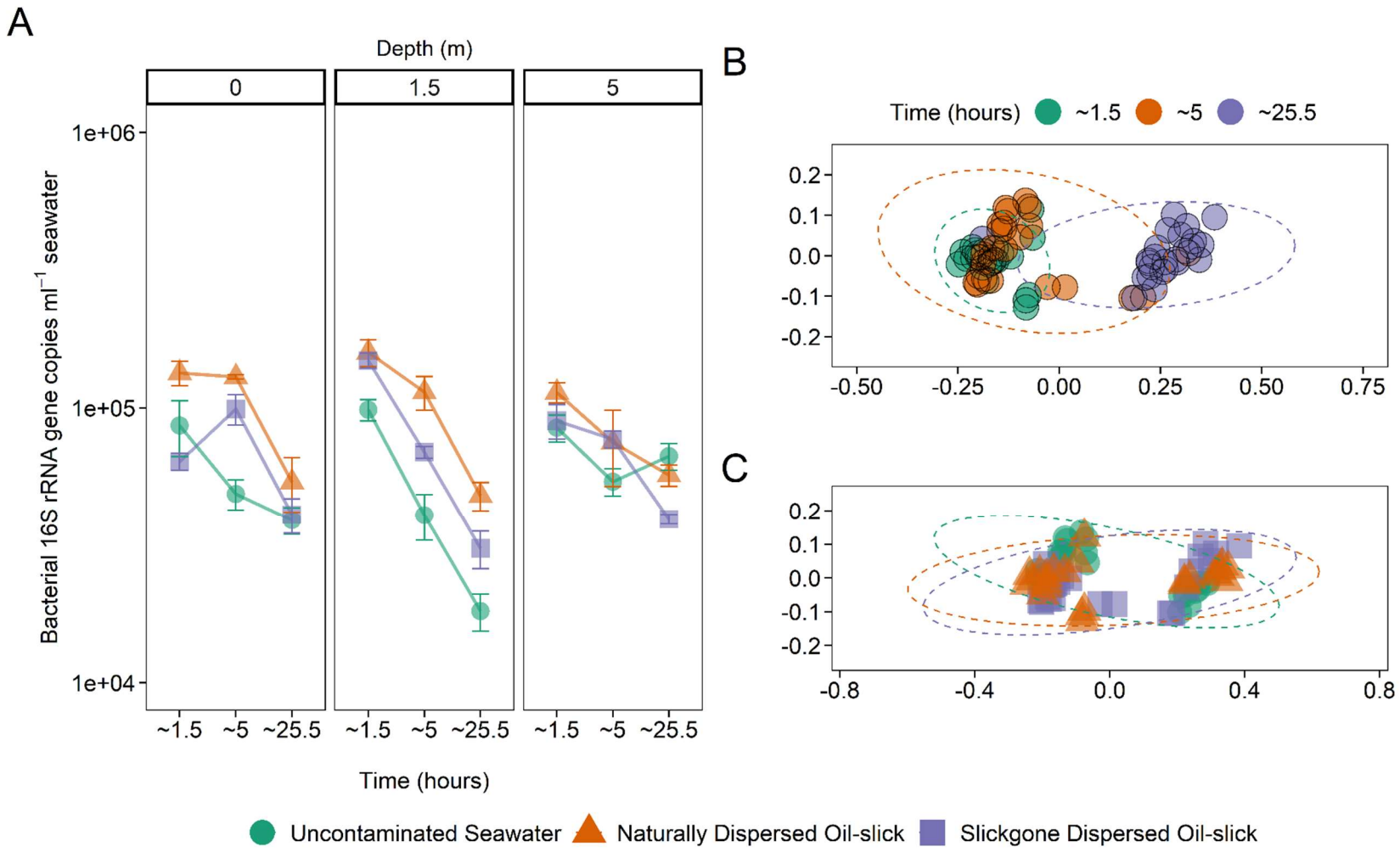

Fig 3.3: (A) Bacterial 16S rRNA gene abundance (mean ± SE, *n* = 3) from seawater samples taken from "Uncontaminated Seawater" as well as "Naturally Dispersed" and "Slickgone Dispersed" oil-slicks, ~1.5, ~5, and ~ 25.5 hours after oil-slicks were created. NMDS (non-metric multidimensional scaling) ordination, based on clustered bacterial 16S rRNA OTUs at a 97% confidence level, displaying the effect of time (hours) **(B)** and "Uncontaminated Seawater" or oil-slicks **(C)** on bacterial community composition.

The Ecological Index of Hydrocarbon Exposure (EIHE), which quantifies the proportion of the bacterial community with hydrocarbon-biodegradation potential (Lozada *et al.*, 2014), was extremely low, averaging 0.012 (± 0.003; scale of 0 – 1) over all seawater samples. There were no significant differences in the EIHE score between "Uncontaminated Seawater", both oil-slicks, time points, or depths (Fig. 3.4A-C). Compared to some other marine environments (Fig. 3.4D) it can be observed that the EIHE score of 0.012 is similar to that found in sediments around the WWII shipwreck HMS *Royal Oak*, where the EIHE score was 0.008 and PAH levels were 229.2 ± 126.5 μg kg^{-1} of dry sediment (Chapter Five). Furthermore, the EIHE score of 0.012 observed in this study is much lower than the EIHE scores observed in contaminated sediments (EIHE 0.52; TPH 1,093 – 3,773 μg g^{-1} dry sediment) sampled five-days after the Agia Zoni II oil-spill (Thomas *et al.*, 2020) and in oil-contaminated North Sea seawater samples (EIHE 0.58; TPH 54.95 μg ml^{-1}) from an *ex situ* oil/dispersant microcosm experiment (Chapter Two). The EIHE currently contains 63 genera (which contain species that have been shown to degrade hydrocarbons) and across all seawater samples from this study 22 of these genera were present, although often in low relative abundance (0.012%). The genera *Flavobacterium*, *Polaromonas*, *Sphingobium*, *Sphingomonas*, and *Sulfitobacter* (which contain many species that are unable to degrade-hydrocarbons) collectively made up a large proportion (87%) of sequences assigned to the EIHE. The relative abundance (%) of genera assigned to obligate hydrocarbonclastic bacteria (OHCB), a group of widely distributed marine bacteria with genomes that are geared towards using hydrocarbons as an almost exclusive source of carbon and energy (Yakimov *et al.*, 2007), was less than 1×10^{-6}. In the seawater, these trace levels of OHCB sequences were assigned to the genera *Alcanivorax*, *Cycloclasticus*, and *Oleispira*. The percentage of sequences assigned to OHCB and the EIHE indicate a distinct lack of growth of any known HCB in all samples, including the two samples which contained hydrocarbons.

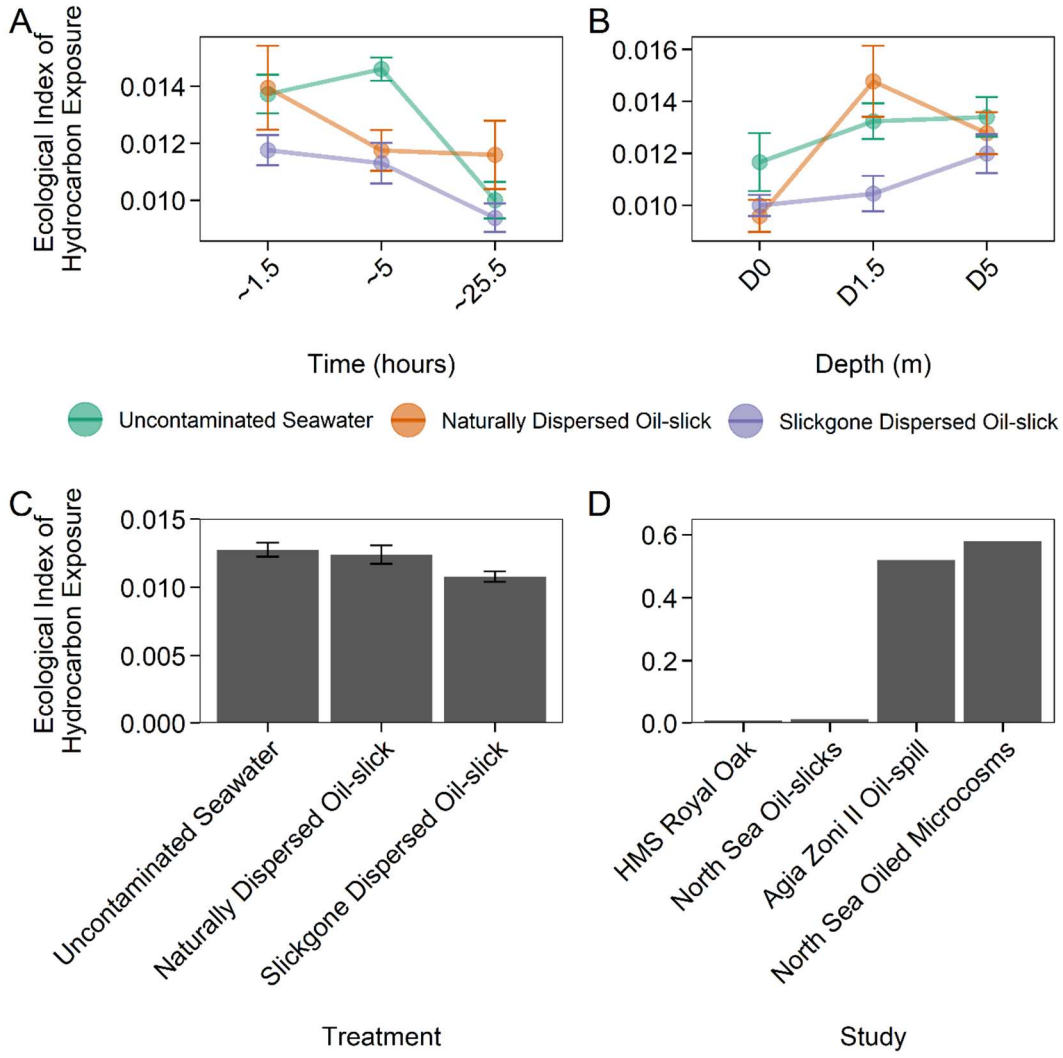

Fig. 3.4: Ecological Index of Hydrocarbon Exposure (EIHE) scores (± SE, *n* = 3, ratio % up to 1), representing relative abundance of bacteria with hydrocarbon-biodegradation potential (Lozada et al., 2014), from seawater sampled over ~25.5 hours (**A**), and over a 5 m depth profile (**B**), from "Uncontaminated Seawater" and "Naturally Dispersed" and "Slickgone Dispersed" oil-slicks (**C**). Additionally, a comparison between EIHE scores from seawater samples taken in this study ("North Sea Oil-slicks") and other marine environments (**D**): "HMS *Royal Oak*" (Chapter Five, average over all samples), "Agia Zoni II Oil-spill" (Thomas *et al.*, 2020, average at impacted sites in September 2017), and "North Sea Oiled Microcosms" (Chapter Two, average over all treatments at day 21).

Discussion

Hydrocarbon Analysis Reveals Difficulty in Conducting in situ Oil-spill Experiments

Analysis of hydrocarbons revealed that only two samples, from the "Slickgone Dispersed" oil-slick ~25.5 hours after oil-slick creation, contained any measurable hydrocarbons (221 ± 92 µg ml^{-1} seawater). These samples did not contain any measurable *n*-alkanes $<C_{14}$ or any naphthalene (or methylated-naphthalenes) or fluorene, in comparison to a profile of the oil, suggesting these hydrocarbons has

partitioned into the air and/or water. A similar *in situ* North Sea oil-spill by Gros *et al.* (2014) observed rapid mass transfer of >50% of $<C_{17}$ hydrocarbons, as well as no detectable naphthalene, from surface samples 25 hours after oil-slick creation. The lack of measurable hydrocarbons, in all other surface samples from this field trial, was despite the fact oil was clearly visible to the naked eye (see Supplementary Materials Fig. S3.7) and via radar, at all sampling time points. Samples were taken by reaching out of a rigid inflatable boat (RIB) and collecting surface oil/water in sterile vials. However, this proved difficult during the first day (16.04.2019) as increased wind speeds and wave heights, 8.33 ± 0.71 m s^{-1} and 105.26 ± 17.32 cm respectively, kept bouncing the RIB up and down, pushing the oily surface water beyond reach. On the second day, wind speed and wave height reduced to 5.15 ± 0.66 m s^{-1} and 58.52 ± 7.63 cm respectively, and samples were collected by means of a vial attached to a 2 m stick. Whilst the calmer environmental conditions, and the new sampling technique, meant sampling the oil/water interface was easier, movement of the RIB still made it difficult, resulting in only 2 of the 9 surface samples, collected ~25.5 hours after oil-slick creation, having any measurable hydrocarbons. These results reflect the difficulty in efficiently obtaining *in situ* oil-spill seawater samples from the surface oil/water interface. Samples collected at depths of 1.5 and 5 m would not have been affected as seawater was directly pumped from those depths into sterile vials.

The overarching criticism of *ex situ* oil-spill experiments is that the oil-spills are enclosed by some form of container, be it a microcosm, mesocosm, or wave tank. This containment is believed to create a number of biases, one of which is that containment decreases oil dispersal and dilution, which would otherwise dilute to sub-ppm *in situ* within 1 to 4 hours (Nedwed and Coolbaugh, 2008; Bejarano *et al.*, 2013). Therefore, adding oil at greater concentrations than sub-ppm, supposedly inhibits the growth of hydrocarbon-degrading bacteria (HCB), and thus the rate of hydrocarbon-biodegradation (Prince, *et al.*, 2016). The results of this study could suggest that the concentration of oil, from marine oil-slicks that have been sprayed with dispersant, does not always reduce to sub-ppm immediately, as the two samples with measurable oil (from the surface of the “Slickgone Dispersed” oil-slick ~25.5 hours after oil-slick creation) contained hydrocarbons at ~221 ppm. The application of dispersants to an oil-slick requires suitable environmental conditions, which include wind speeds of 4 – 12 m s^{-1} (ITOPF, 2011b) and full salinity seawater at 32-35 psu (Chandrasekar *et al.*, 2006). Additionally, dispersant efficacy is affected by the type of oil, as increasing oil viscosity decreases dispersant effectiveness, and therefore their application is more suited to light-to-medium oils (Trudel *et al.*, 2010). Weathering of oil increases viscosity, and thus the window of opportunity to apply dispersants to oil-slicks ranges

from a few hours to a few days (Chandrasekar *et al.*, 2005; ITOPF, 2011b). These criteria were met during this study, and therefore it is unlikely environmental conditions (wind speed, wave height, and salinity), oil type (light-medium Arabian Crude), or window of opportunity (one hour after oil-slick creation) inhibited dispersant efficiency. It should be noted, however, that the application of Slickgone NS on the oil-slick was below the recommended level to sufficiently coat the oil-slick. Approximately 200 litres of dispersant was applied to the oil-slick, however, the theoretical dosage was 700 litres to achieve the manufacturers recommendation of 40 – 50 L per 10,000 m^2 of oiled area (Zeinstra *et al.*, 2020). The fact that none of the samples pumped directly from 1.5 or 5 m depths contained any measurable hydrocarbons would suggest that, where the seawater was sampled, the dispersant had not been applied to that part of the oil-slick. Of course, it could be that the dispersant was applied, and the oil has been dispersed beyond 5 m, however, with visible oil on the surface this is unlikely.

Nutrient Limitation Potentially Inhibited the Growth of Hydrocarbon-degrading Bacteria

Certain microbes can degrade a range of hydrocarbons found in crude oil and its derivatives and thus oil-spills dramatically alter marine microbial community composition, resulting in a decrease in species richness and diversity, in conjunction with selection for HCB (Head *et al.*, 2006; McGenity *et al.*, 2012). However, during this study there was a clear lack of growth of OHCB or those genera with known hydrocarbon-degrading species. This lack of HCB growth is evidenced further by the absence of any hydrocarbon-biodegradation, as a comparison of ratios of *n*-C_{17}/pristane and *n*-C_{18}/phytane, commonly used to indicate the occurrence of alkane-biodegradation (Commendatore *et al.*, 2000; Commendatore and Esteves, 2004), between the samples with measurable hydrocarbons and the original oil profile, showed no significant difference. Notably, there was no significant difference in the relative abundance of HCB in the two samples that had measurable hydrocarbons (221 ppm), suggesting that growth of HCB was inhibited by some other limiting factor. The lack of HCB growth has been observed previously in a similar *in situ* oil-spill experiment (North Sea, off the coast of Holland) where no significant differences in bacterial community composition was observed between samples taken three meters below the surface of an oil-slick in comparison to uncontaminated seawater (Chronopoulou *et al.*, 2015).

Potentially, the growth of HCB in this study was inhibited by the absence of nutrients, specifically, ~25.5 hours after oil-slick creation the level of TIN significantly decreased in all samples (23.74 to 3.33 µM) as well as phosphorous being undetected. Both nitrogen (N) and phosphorous (P) are vital for microbial growth, for example, N is required for the synthesis of proteins and nitrogenous bases whilst P is required for

the synthesis of nucleic acid and phospholipids (Bristow *et al.*, 2017). N and P are especially important during hydrocarbon-degradation of an oil-slick (Atlas, 1981), and therefore, the availability of these nutrients in the presence of hydrocarbons is vital (Ron and Rosenberg, 2014). Certain HCB, such as the OHCB *Alcanivorax* and *Cycloclasticus*, have specific systems for scavenging nutrients in oligotrophic environments (Wang *et al.*, 1996; Cappello and Yakimov, 2010). However, given a lack of growth within the genera *Alcanivorax* and *Cycloclasticus*, either P concentration was too low, or growth was limited in some other way. The concentration of nutrients in the North Sea is primarily driven by a seasonal cycle, with higher levels of N and P in the winter months compared to the summer months (Tett and Walne, 1995). It is likely that the rapid decline of TIN, over ~1 day, was due to a decrease in vertical mixing, as wave energy declined. Phytoplankton blooms, which take place during times of increased sunlight and nutrients in the euphotic zone, often occur in the spring and last until summer when nutrients become depleted (Mann and Lazier, 2013). Satellite images captured by MODIS (Moderate Resolution Imaging Spectroradiometer) suggest a phytoplankton bloom in the North Sea began on March 29th, 2019 (NASA, 2019). Sampling of this study occurred on the 16th and 17th April 2019 and therefore the high abundance of phytoplankton could have depleted phosphorous. Typically concentrations of P in the marine seawater is much lower compared to N (Brion *et al.*, 2004) and P is considered the limiting factor in continental North Sea coastal waters (Brockmann *et al.*, 1990) especially within 20 miles of the coast (Peeters *et al.*, 1991); this study took place 13-miles from the coast.

Absence of Hydrocarbon-degrading Bacteria Growth Highlights the Environment's Limited Capacity, at the Time of Sampling, to Naturally Attenuate Oil

Government, oil-spill-responders, and industry must be able to evaluate the efficiency of oil-spill clean-up operations, to provide guidance on future risk-based scenarios, something that has been recognised in the UK cross-government initiative "PREMIAM" (Kirby *et al.*, 2018). One resource available to oil-spill-response monitoring is the analysis of bacterial community composition from environmental samples, as a proliferation of HCB, and thus a change in bacterial community composition, would suggest the environment in which the sample was taken was contaminated with oil. Moreover, analysis of bacterial communities would demonstrate the capabilities of an oil-contaminated environment to naturally attenuate oil and thus inform response operations. Such analysis can be incorporated into the Spill Impact Mitigation Assessment (IPIECA *et al.*, 2017).

One such tool to evaluate the microbial ecology, of an environment suspected to contain hydrocarbons, is the Ecological Index of Hydrocarbon Exposure (EIHE),

which aims to establish, on a scale of 0 to 1 (where 1 is equal to 100%), the relative abundance of bacteria in a given sample with the potential for hydrocarbon-degradation. The EIHE works by comparing the bacterial community composition of an environmental sample to a list of genera assigned to either OHCB or more metabolically diverse bacteria with known species able to degrade-hydrocarbons. In the samples obtained during this study the EIHE score was extremely low, averaging 0.012 (± 0.003), with no significant differences in the EIHE score between "Uncontaminated Seawater", both oil-slicks, time points, or depths (Fig. 3.4A-C). The EIHE score (0.012), in comparison to selected other marine environments (Fig. 3.4D), most closely matched the EIHE score calculated in sediments around HMS *Royal Oak* (Chapter Five), a shipwreck in Scapa Flow (Scotland), where analysis of hydrocarbons revealed only very low levels of pyrogenic PAHs (229.2 μg kg^{-1} of dry sediment). In contrast, oil-contaminated sediments (hydrocarbons at 1,093 – 3,773 μg g^{-1} dry sediment) following the Agia Zoni II oil-spill (Thomas *et al.*, 2020), as well as contaminated seawater samples (hydrocarbons at 54.96 μg ml^{-1}) from an *ex situ* North Sea oil-spill experiment (Chapter Two), had significantly higher (43- to 48-fold) EIHE scores, 0.52 and 0.58 respectively.

The EIHE tool does have its limitations, for example, key genera of bacteria known to contain species able to degrade-hydrocarbons (e.g. *Colwellia*; Mason *et al.*, 2014) are absent from the reference list. Another limitation is the over-estimation of hydrocarbon exposure in an environment, this is due to an inability to differentiate between those species able to degrade-hydrocarbons and those which cannot, in metabolically-diverse genera. For example, the relative abundance of all species of *Pseudomonas* is accounted for by the EIHE, when actually the genus contains 212 species (NCBI Taxonomy Browser, 2020b) of which only a limited amount are able to degrade-hydrocarbons. This limitation has been demonstrated previously, whereby analysis of sediment samples containing no hydrocarbons demonstrated an EIHE score of 0.30 (Thomas *et al.*, 2020); the study by Thomas *et al*. (2020) provides suggestions for future improvement of the EIHE tool. This study has however demonstrated a strength of the EIHE tool, the ability to detect whether an environment has the natural ability to attenuate oil. Ideally, surface samples would have been collected directly from the oil/water interface, but as discussed earlier environmental conditions hampered sampling. Nevertheless, an EIHE score of 0.012 in this study reveals an exceptionally low level of HCB within seawater samples, this includes the two samples which contained hydrocarbons. This demonstrates, at the time of sampling, the environment's ability to naturally attenuate oil was limited. It could be that ~25.5 hours were not enough sampling time to capture HCB growth, though

results in Chapter Two's microcosm experiment suggest that when nutrients are plentiful HCB growth is several orders of magnitude within 24 hours (though this might not be reflected in situ at 9°C). Therefore, potentially low levels of phosphorous limited HCB growth, but it cannot be said for certain that this was the limiting factor. Regardless of what is limiting the growth of HCB, such low levels can inform oil-spill response operations. In this study a limited ability for the environment to naturally attenuate oil would highlight a requirement for intervention measures, such as dispersal or physical removal of oil.

Developing in situ *Experimental Oil-spill Methodologies*

The results of this study have highlighted challenges in obtaining meaningful seawater surface samples that capture the oil/water interface, with only 2 of the 27 surface samples containing any measurable hydrocarbons. The primary challenge was the collection of surface samples from a RIB, which would bounce up and down on the waves pushing the oily surface water beyond reach, even in relatively calm waters (wind speed and wave height on day two was 5.15 ± 0.66 m s^{-1} and 58.52 ± 7.63 cm, respectively). One potential solution could be to use a ROSV (remotely operated surface vehicle), which could be remotely piloted (or autonomously via GPS way-points) into the oil-slick with minimal disturbance, collect a surface sample before returning to the crew for downstream processing. A ROSV for the purpose of oil-spill detection and sampling has previously been designed and built (Al Maawali *et al.*, 2019), and such designs could be adapted further. Of course, any ROSV project is subject to financial restraints but it could be designed to provide many more features than just surface seawater sampling. For example, logistical/safety additions could include a collision avoidance system and a volatile organic compounds sensor. Whilst sampling additions could include cameras/lighting, environmental sensors (e.g. temperature, conductivity, pH), GPS, which would all provide valuable real-time *in situ* metadata. Potentially, the ROSV could be tethered to a UAV (unmanned aerial vehicle) which could also provide infrared and aerial observations. Given a large enough capacity the ROSV could even be adapted to apply dispersant at a specific location, which could then immediately be sampled, avoiding any doubt as to the efficiency of dispersant application.

The efficacy of dispersant application was another limitation observed during this *in situ* oil-spill trial. This was primarily driven by time constraints, resulting in only 200 L, of the recommended 700 L, of dispersant actually being applied to the oil-slick. Technical recommendations advise more spraying passes through the oil-slick and that the dispersant spraying arms should be attached as far to the front of the ship as possible to ensure contact with oil, before it is pushed away by the ship's bow (Zeinstra

et al., 2020). The lack of time was due to strict regulations governing when the oil-slicks were allowed to be created and sampled. This also meant that three oil-slicks were created in one day, when the original plan was to create only two, and thus the sampling team were under immense pressure and effort which could have also affected sampling efficiency. Ideally more contingency time would be allocated in such trials, but due to high financial costs of operating numerous research vessels, and the availability of supporting services (i.e. airborne surveillance), this is not always possible. However, such considerations should be discussed when applying for the permit to conduct *in situ* oil-spill experiments. It is crucial any sampling limitations are overcome, as *in situ* oil-spill experiments can provide insightful results and observations into the processes that drive the fate and transport of oil in marine waters and thus guide oil-spill response management.

Experimental Procedures

Sampling Campaign

Sampling, dispersant application, and overall operational management took place from the Rijkswaterstaat's vessel "ARCA", whilst oil release was from the Rijkswaterstaat's vessel HEBO-CAT-7. Oil-slick creation took place on the 16th April 2019 approximately 13 miles off the coast of Scheveningen harbour, The Hague, Netherlands (Supplementary Materials Fig. S3.1). Full sampling and technical details can be found in the ITOPF ExpOS'D technical report (Zeinstra *et al.*, 2020) but in summary, the oil used was a light-medium Arabian Crude and was released as follows. Oil was continuously pumped directly out of tank containers, using an air membrane pump with a flow rate of 6.7 litres s^{-1}, via a 2-inch hose. This trailed 20 m behind the HEBO-CAT-7, on floatation bladders, travelling at 1.85 knots. Firstly, a test oil-slick ("Alpha") was created crosswind at 09:15, using ~1 m^3 of the crude oil. The natural dispersion oil-slick ("Naturally Dispersed") was created into the wind, approximately one hour after the test oil-slick, at 10:25, using ~2.5 m^3 of the crude oil. Finally, the oil-slick for chemical dispersion ("Slickgone Dispersed") was created into the wind at 11:40, using ~2.5 m^3 of the crude oil. The "Slickgone Dispersed" oil-slick was sprayed (by an onboard MARKLEEN Dispersant spray system) with Slickgone NS dispersant 30 minutes after release, this was applied for one hour at a ratio of 20:1 oil to dispersant. All oil-slicks were continuously monitored and recorded via radar, satellite imagery, and observations from Rijkswaterstaat's vessel "Rotterdam", plus the German, Belgium, and Netherland's air forces.

Sampling of the oil-slicks took place on a rigid inflatable boat (RIB, "Zodiac"". Triplicate 250 ml seawater samples were taken from the surface as well as at depths

of 1.5 m and 5 m, in sterile plastic containers. Surface samples were taken directly by reaching over the side of the RIB. Samples from 1.5 and 5 m depths were taken by means of a sterile hose, lowered to the required depth, and samples pumped into sterile plastic containers. 150 ml of this sample water was passed through Millipore® Sterivex™ filters (0.22 µm) and flash frozen at -150°C in a Cryogenic Vapour Shipper, to preserve DNA stability, prior to storage at -20°C. The filtrate from this process was also flash frozen prior to being stored at -20°C for nutrient analysis of ammonium (NH_4^+), phosphate (PO_4^{3-}), nitrate (NO_3^-), and nitrite (NO_2^-), using a SEAL Analytical AA3 HR AutoAnalyzer tandem JASCO FP-2020 Plus fluorescence detector. In addition, triplicate 40 ml seawater samples were collected from the surface as well as at depths of 1.5 m and 5 m (same method as above), in sterile brown-glass 50 ml vials capped with PTFE-lined silicon septa, and immediately frozen at -20°C, for hydrocarbon analysis. Sampling of oil-slicks occurred ~1.5 hours, ~5 hours (16th April 2019), and ~25.5 hours (17th April 2019) after oil-slick creation. Sampling took place in the locations detailed in Supplementary Materials Table S3.2; locations were recorded via the use on SENS2SEA radar detection.

Environmental Measurements

Temperature, salinity, and pH were all measured at the time of sampling (Supplementary Materials Table S3.2). Wave height measurements (Supplementary Materials Fig. S3.5) were collected by two stations: 'IJgeul 1' (4,264°E, 52,488°N, located 31 km of sampling site) and 'Q1 platform' (4,150°E, 52,925°N, located 75 km northeast of sampling site) (Zeinstra *et al.*, 2020). Wind speed/direction measurements (Supplementary Materials Fig. S3.6) were collected by two offshore stations: P11 (3,342°E, 52,359°N, 45 km northwest of sample site) and Europlatform (3,275°E, 51,998°N, 55 km southwest of sample site) (Zeinstra *et al.*, 2020).

Hydrocarbon-Degradation (GC-MS)

Hydrocarbons were extracted from 50 ml brown-glass vials (collected *in situ*) using a 20 ml solvent extraction of 1:1 hexane and dichloromethane, vigorously shaken for 30 seconds, and placed in an ultrasonic bath for 30 minutes. The 20 ml of solvent extract was then passed through reversed-phase solid phase extraction tubes (Supelclean™ ENVI™-18 SPE, Sigma), using an adapted method from Risdon *et al.* (2008), before being eluted to 6 ml and then concentrated to 1 ml using nitrogen gas. Deuterated alkane (nonadecane $C_{19}d_{40}$ and triacontane $C_{30}d_{62}$ at 10 µg ml^{-1}) and PAH (naphthalene-d_8 and anthrancene-d_{10} at 10 µg ml^{-1}) internal standards were added to each sample and quantification was performed on an Agilent 7890A Gas Chromatography system coupled with a Turbomass Gold Mass Spectrometer with

Triple-Axis detector, operating at 70 eV in positive ion mode, using conditions as previously described by Coulon *et al.* (2007). External multilevel calibrations were carried out using alkanes (Standard Solution (C_8-C_{40}); Sigma), methylated-PAHs (1-methylnapthalene, 2-methylanthracene, and 9,10-dimethylanthracene; Sigma), and PAH (QTM PAH Mix; Sigma) standards, the concentrations of which ranged from 1.125 to 18 μg ml^{-1}. For quality control, a 2.0 ng l^{-1} diesel standard solution (ASTM C12-C60 quantitative, Supelco) and a 1.0 ng l^{-1} PAH Mix Standard solution (Supelco) were analysed every 15 samples. The variation of the reproducibility of extraction and quantification of water samples were determined by successive extractions and injections (n = 6) of the same sample and estimated to be ± 8%. All alkanes between C_{10} and C_{36} including pristane and phytane and the following PAHs were quantified (naphthalene; all isomers of methyl-, dimethyl- and trimethyl-naphthalenes; acenaphthylene; acenaphthene; fluorine; phenanthrene; all isomers of methyl- and dimethyl-phenanthrenes/anthracenes; fluoranthene; pyrene; all isomers of methyl- and dimethyl-pyrene; chrysene; all isomers of methyl- and dimethyl-chrysene). Only those hydrocarbons detected are shown in Fig. 3.1.

qPCR Analysis of Bacterial 16S rRNA Genes

DNA was extracted from *in situ* seawater samples from thawed Millipore® Sterivex™ filters with a DNeasy PowerWater Sterivex Kit (Qiagen) according to the manufacturer's instructions. The primers used for quantification of bacterial 16S rRNA genes were 341f - CCTACGGGNGGCWGCAG and 785r – GACTACHVGGGTATCTAATCC (Klindworth *et al.*, 2013). qPCR was performed using a CFX384™ Real-Time PCR Detection System (BioRad) using reagents, cycle conditions, and standards as previously described (McKew and Smith, 2015; Tatti *et al.*, 2016). Inspection of standard curves showed that all assays produced satisfactory efficiency (85%) and R^2 values (>0.99). It should be noted that qPCR of the 16S rRNA gene, whilst providing a valuable comparison of bacterial growth between samples, does not reflect absolute bacterial biomass, as many species contain multiple copies of the 16S rRNA gene.

Amplicon Sequencing and Bioinformatics

Amplicon libraries were prepared, as per Illumina instructions, by a 25-cycle PCR. PCR primers were the same as those used for qPCR but flanked with Illumina overhang sequences. A unique combination of Nextera XT v2 Indices (Illumina) were added to PCR products from each sample, via an 8-cycle PCR. PCR products were quantified using Quant-iT PicoGreen dsDNA Assay Kit (TheromFisher Scientific) and pooled in equimolar concentrations. Quantification of the amplicon libraries was

determined via NEBNext® Library Quant Kit for Illumina (New England BioLabs Inc.), prior to sequencing on the Illumina MiSeq® platform, using a MiSeq® 600 cycle v3 reagent kit and 20% PhiX sequencing control standard. Sequence output from the Illumina MiSeq platform were analysed within BioLinux (Field *et al.*, 2006), using a bioinformatics pipeline as described by Dumbrell *et al.* (2016). Forward sequence reads were quality trimmed using Sickle (Davies and Evans, 1980) prior to error correction within SPades (Nurk *et al.*, 2013) using the BayesHammer algorithm (Nikolenko *et al.*, 2013). The quality filter and error corrected sequence reads were dereplicated, sorted by abundance, and clustered into OTUs (Operational Taxonomic Units) at the 97% level via VSEARCH (Rognes *et al.*, 2016). Singleton OTUs were discarded, as well as chimeras using reference based chimera checking with UCHIME (Edgar *et al.*, 2011). Taxonomic assignment was conducted with RDP Classifier (Wang *et al.*, 2007). Non locus-specific, or artefactual, OTUs were discarded prior to statistical analyses, along with any OTUs that had <70% identity with any sequence in the RDP database.

Statistical Analysis

Prior to community analysis, sequence data were rarefied to the lowest library sequence value (5,747). Data were first tested for normality (Shapiro-Wilks test), those data which were normally distributed were tested for significance with ANOVAs or appropriate linear models. Non-normally distributed data were analysed using appropriate GLMs (Generalised Linear Models) as follows. The relative abundance of OTUs or genera in relation “Uncontaminated Seawater”, both oil-slicks, depth, or time were modelled using multivariate negative binomial GLMs (W. Wang *et al.*, 2010). Here, the number of sequences in each library was accounted for using an offset term, as described previously (Alzarhani *et al.*, 2019). The abundance of bacterial 16S rRNA gene copies was also modelled using negative binomial GLMs (Venables and Ripley, 2002). The significance of model terms was assessed via likelihood ratio tests. The Environmental Index of Hydrocarbon Exposure (Lozada *et al.*, 2014) was calculated using the script available at the ecolFudge GitHub page (https://github.com/Dave-Clark/ecolFudge, Clark, 2019) and EIHE values modelled using poisson GLMs. All statistical analyses were carried out in R3.6.1 (R Development Core Team, 2011) using a variety of packages available through the references (Venables and Ripley, 2002; Csardi and Nepusz, 2006; Hope, 2013; Wilke, 2015, 2020; Becker *et al.*, 2016; Auguie, 2017; Oksanen *et al.*, 2019; Hvitfeldt, 2020; Kassambara, 2020; Lenth, 2020; Pedersen, 2020). All plots were constructed using the “ggplot2” (Bodenhofer *et al.*, 2011) and “patchwork” (Pedersen, 2019) R packages.

Supplementary Materials

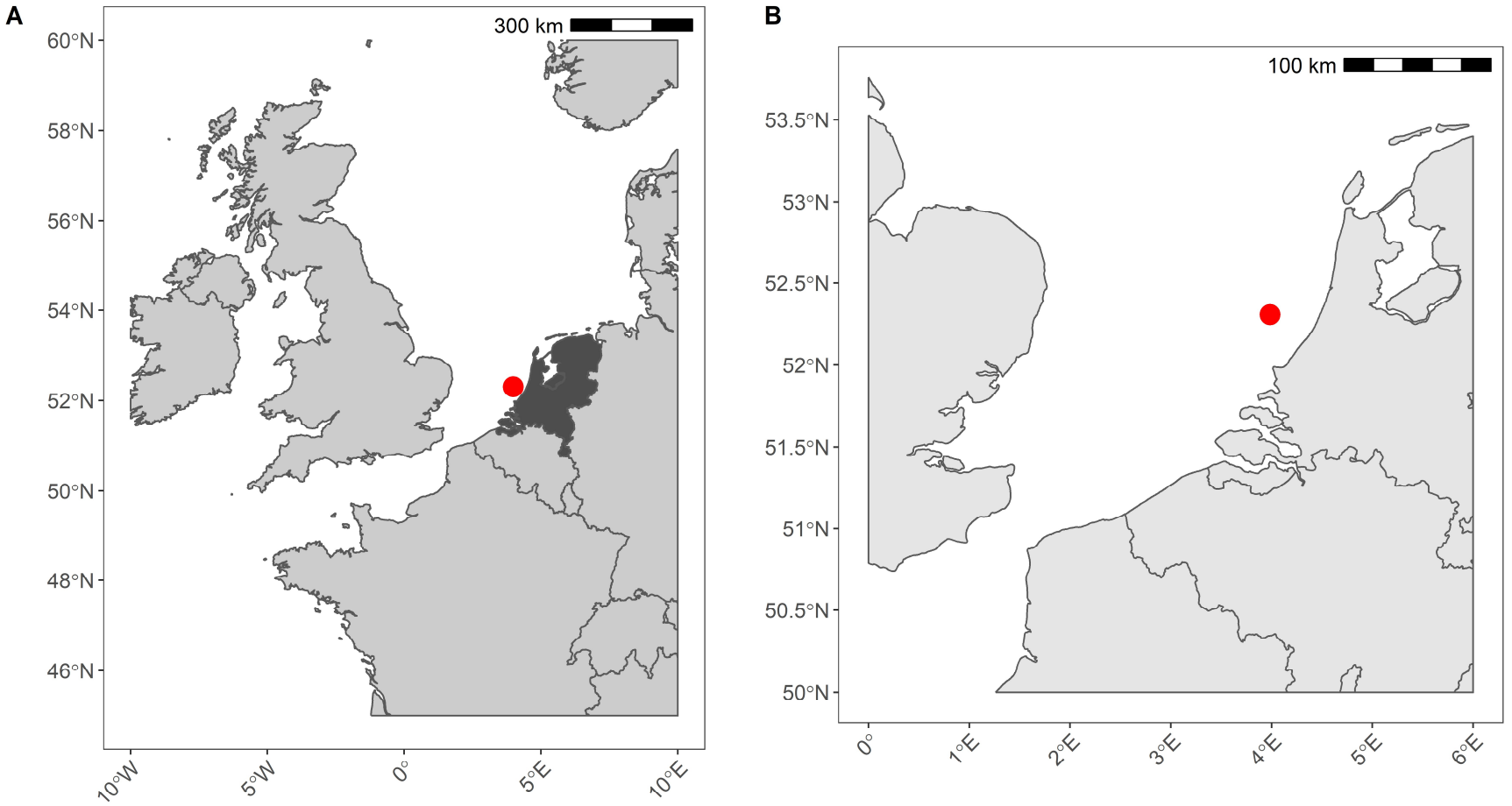

Figure S3.1: Map of sampling site (red circle), 13 nautical miles west off the coast of the Netherlands (A, dark grey), located at 52.30805556, 3.98388889 (B, zoomed in perspective)

Fig. S3.2: 16.04.2019 at 11:23 UTC. Test oil slick to the far left (“Alpha”), natural oil slick in the foreground (“Oil-only”), and chemically dispersed oil slick in the background (“Oil and Slickgone NS”) (Zeinstra *et al.*, 2020).

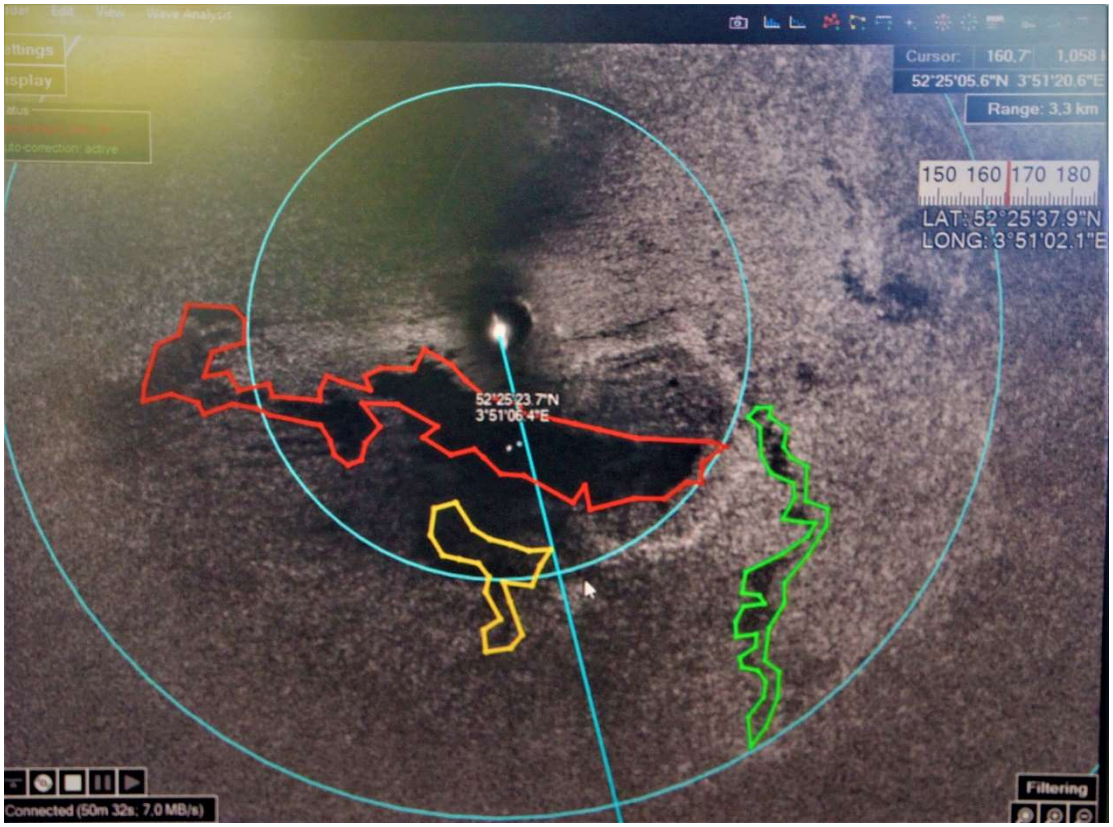

Fig. S3.3: 16.04.2019 at 11:54 UTC. Test oil slick coloured yellow ("Alpha"), natural oil slick coloured red ("Oil-Only"), and chemically dispersed oil slick coloured green ("Oil and Slickgone NS") (Zeinstra *et al.*, 2020).

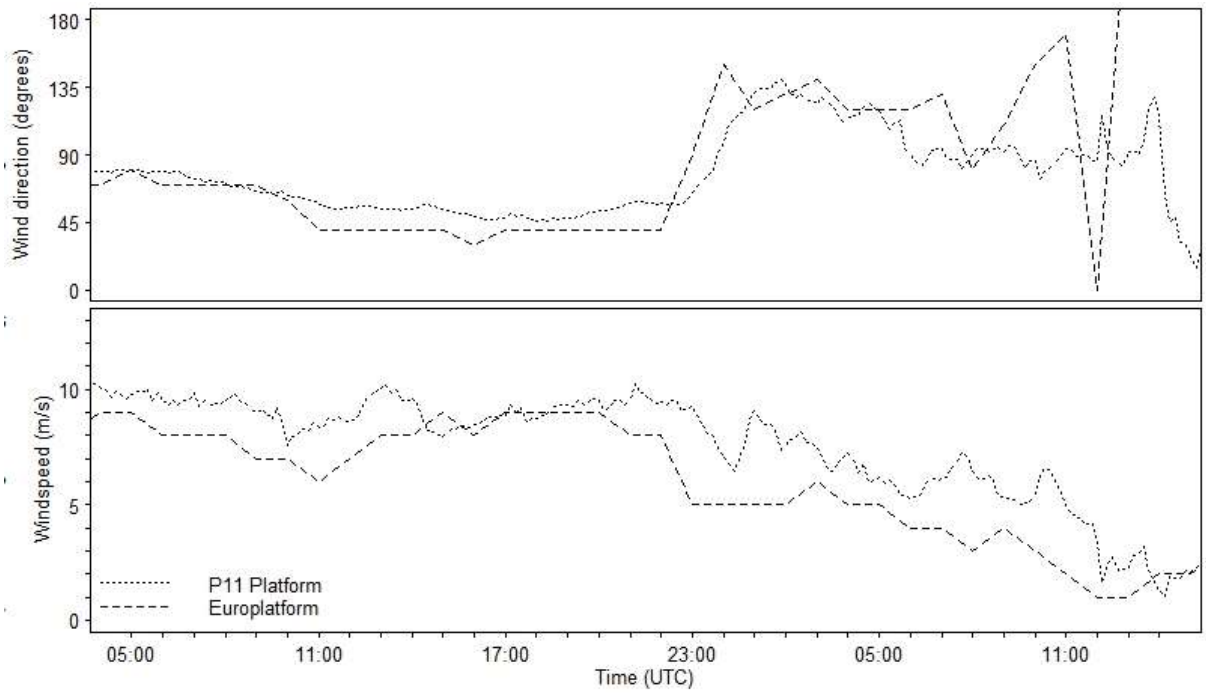

Fig. S3.4: Wind speed, and direction, on the first (16th April 2019, sampling between 11:00 and 17:00 UTC) and second (17th April 2019, sampling between 11:00 and 13:00 UTC) days of sampling. Data measured by two offshore stations P11 (3,342°E, 52,359°N, 45 km northwest of sample site) and Europlatform (3,275°E, 51,998°N, 55 km southwest of sample site). Data downloaded from https://waterinfo.rws.nl/#!/nav/index/ and https://www.knmi.nl/nederland-nu/klimatologie/uurgegevens_Noordzee (Zeinstra *et al.*, 2020).

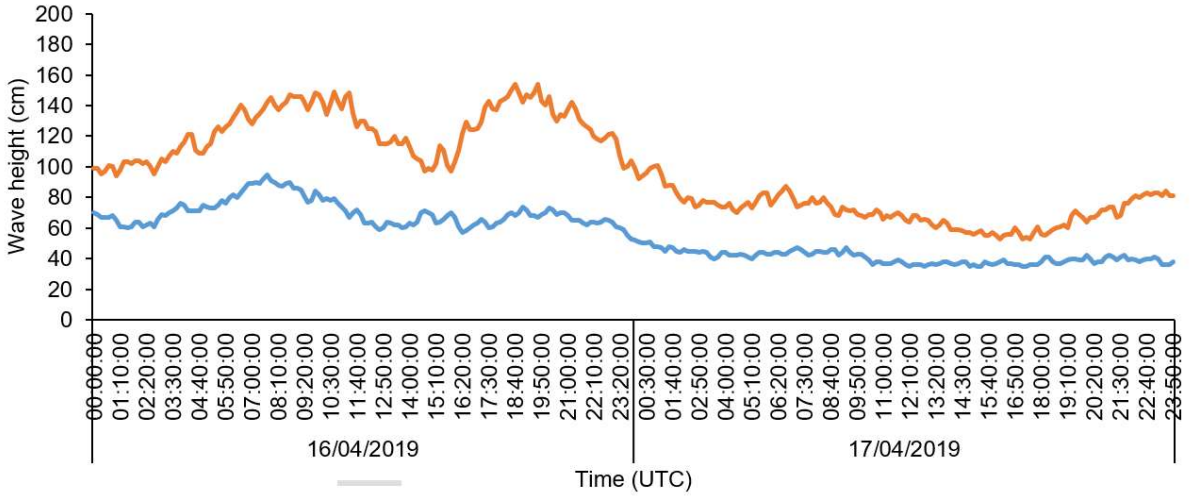

Fig. S3.5: Wave height (cm) on the first (16th April 2019, sampling between 11:00 and 17:00 UTC) and second (17th April 2019, sampling between 11:00 and 13:00 UTC) days of sampling. Data measured by two stations 'IJgeul 1' (blue line, 4,264°E, 52,488°N, located 31 km of sampling site) and 'Q1 platform' (orange line, 4,150°E, 52,925°N, located 75 km northeast of sampling site). Distances from the coast were: sampling site 24.1 km, IJgeul1 21.1 km, Q1 platform 55.2 km (Zeinstra *et al.*, 2020).

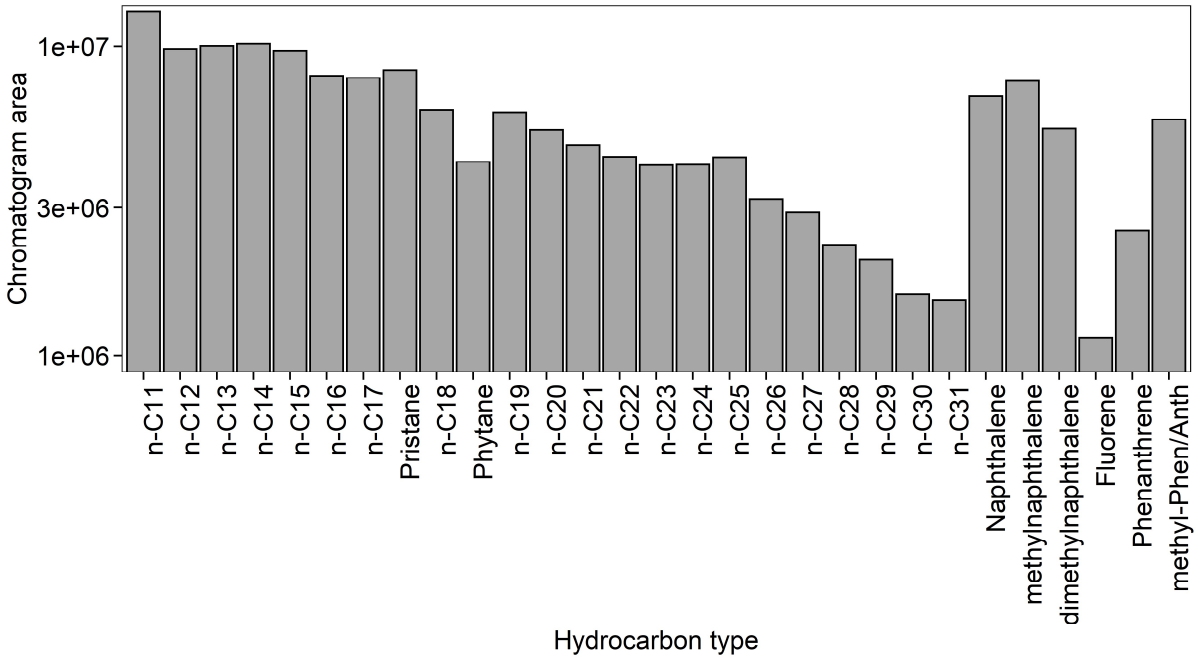

Fig. S3.6: light-medium Arabian Crude oil profile including *n*-alkanes (C_{11} to C_{31}), branched alkanes pristane and phytane, and PAHs (naphthalene, fluorene, phenanthrene, and any methylated derivatives (naphthalene and phenanthrene/anthracene (Phen/Anth)).

Fig. S3.7: 17.04.2019 at 12:34 UTC. Patch of oil-slick photograph (“Oil and Slickgone NS”), taken during sampling ~25.5 hours after the oil-slick was created (Zeinstra *et al.*, 2020).

Table S3.1: 25 OTUs grouped to their mostly closely matched bacterial taxonomy (plus BLAST identity matches to closest cultured Bacteria) with relative abundances, across all samples, of the total bacterial community and separated between time points ~1.5 and ~5 hours (averaged, **A**) and ~25.5 hours (**B**), after oil-slick creation.

Most closely matched bacterial taxonomy	Closest Cultured Identity Match (%)	Relative Abundance (%) of Community	Relative Abundance (%) at ~1.5 & ~5 hrs (A)	Relative Abundance (%) at ~25.5 hrs (B)	Difference between A and B
unclassified Actinobacteria	Actinobacterium SCGC AAA163-G08 (100%)	3.83	5.19	1.11	-78.61%
unclassified Alphaproteobacteria	Alpha proteobacterium SCGC AAA160-J14 (100%)	2.59	2.34	3.09	32.33%
unclassified Bacteroidetes	Bacteroidetes bacterium SCGC AAA160-A21 (98.95%)	8.70	4.37	17.4	297.25%
unclassified Betaproteobacteria	*Methylophilaceae* bacterium NB0070 (100%)	2.43	3.06	1.19	-61.05%
Candidatus *Pelagibacter*	*Candidatus* Pelagibacter sp. HIMB1321 (100%)	17.12	15.6	20.2	29.17%
unclassified *Cryomorphaceae*	Bacterium SCGC AAA074-P13 (100%)	3.53	4.65	1.28	-72.47%
unclassified *Flavobacteriaceae*	*Flavobacteriaceae* bacterium Hel1_33_7 (100%)	9.34	8.31	11.4	37.51%
unclassified Gammaproteobacteria	Gamma proteobacterium SCGC AAA160-N17 (100%)	9.36	10.3	7.5	-27.11%
Halioglobus	Bacterium IMCC8513 (100%)	1.15	0.85	1.77	109.47%
Planktomarina	*Rhodobacteraceae* bacterium strain FZCC0042 (100%)	5.02	6.14	2.77	-54.89%
unclassified *Rhodobacteraceae*	*Roseobacter* sp. SB2 (100%)	7.77	7.94	7.44	-6.30%
unclassified *Rhodospirillaceae*	Alpha proteobacterium SCGC AAA158-B04 (100%)	1.92	1.88	2.01	6.91%

Table S3.2: Environmental measurements over all depths (temperature, salinity, and pH; mean ± SE, *n* = 9) and location of sampling. Parenthesis next to each treatment (i.e. ~1.5) represent the time (hours) sampling occurred after slick creation (Zeinstra *et al.*, 2020).

Treatment	Treatment Code	Time	Longitude	Latitude	Temperature (°C)	Salinity (psu)	pH
Seawater Control (~1.5)	"Uncontaminated Seawater"	11:13	52.30805556	3.98388889	9.15 ± 0.18	28.9 ± 1.70	8.42 ± 0.04
Seawater and Oil (~1.5)	"Naturally Dispersed"	11:35	52.38027778	3.99861111			
Seawater, Oil and Slickgone NS (~1.5)	"Slickgone Dispersed"	13:46	52.45638889	3.99250000			
Seawater Control (~5)	"Uncontaminated Seawater"	14:56	52.47805556	3.98222222			
Seawater and Oil (~5)	"Naturally Dispersed"	14:42	52.36027778	4.06194444			
Seawater, Oil and Slickgone NS (~5)	"Slickgone Dispersed"	17:01	52.51472222	4.06138889			
Seawater Control (~25.5)	"Uncontaminated Seawater"	11:46	52.52916667	3.93416667			
Seawater and Oil (~25.5)	"Naturally Dispersed"	11:58	52.50750000	3.88694444	8.97 ± 0.04	32.9	8.4
Seawater, Oil and Slickgone NS (~25.5)	"Slickgone Dispersed"	12:23	52.48250000	3.86722222			

Chapter Four

Bacterial Community Legacy Effects following the Agia Zoni II Oil-Spill, Greece

Abstract

In September 2017 the Agia Zoni II sank in the Saronic Gulf, Greece, releasing approximately 500 tonnes of heavy fuel oil, contaminating the Salamina and Athens coastlines. Effects of the spill, and remediation efforts, on sediment microbial communities were quantified over the following seven months. Five days post-spill, the concentration of measured hydrocarbons within surface sediments of contaminated beaches was 1,093-3,773 μg g^{-1} dry sediment (91% alkanes and 9% polycyclic aromatic hydrocarbons), but measured hydrocarbons decreased rapidly after extensive clean-up operations. Bacterial genera known to contain oil-degrading species increased in abundance, including *Alcanivorax*, *Cycloclasticus*, *Oleibacter, Oleiphilus*, and *Thalassolituus*, and the species *Marinobacter hydrocarbonoclasticus* from approximately 0.02% to >32% (collectively) of the total bacterial community. Abundance of genera with known hydrocarbon-degraders then decreased one month after clean-up. However, a legacy effect was observed within the bacterial community, whereby *Alcanivorax* and *Cycloclasticus* persisted for several months after the oil spill in formerly contaminated sites. This study is the first to evaluate the effect of the Agia Zoni II oil-spill on microbial communities in an oligotrophic sea, where *in-situ* oil-spill studies are rare. The results aid the advancement of post-spill monitoring models, which can predict the capability of environments to naturally attenuate oil.

Introduction

On the 10th of September 2017, the Agia Zoni II tanker sank in the inner Saronic Gulf, Greece, releasing approximately 500 metric tonnes of heavy fuel oil into the waters and contaminating the surrounding coastlines (IOPC, 2017). The Hellenic Coast Guard deployed ~600 meters of oil boom out to sea within 8 hours, which increased to ~9 km of booms and absorbents in the following weeks. Despite this response, the oil had spread far from the spill site and impacted over 4 km of the Salamina coastline and over 25 km of the Athens Riviera including Glyfada and the port of Piraeus, due to a change in the wind direction (Fig. 4.1). An extensive clean-up response was undertaken on all contaminated beaches, including manual removal of tar balls, flushing and trenching, high-powered washing, removal of sediments for either washing/replacement or disposal at landfill, and the use of absorbents (see Fig.

4.1 and Supplementary Material Table S4.1 for sample location and specific treatment/action undertaken at each site). On the 30th November 2017 the shipwreck was removed, and the clean-up operations ceased in February 2018. On the 28th April 2018 the Greek government lifted maritime restrictions.

Oil spills dramatically alter marine microbial community composition, resulting in a decrease in species richness and diversity, in conjunction with selection for oil-degrading Bacteria (Head *et al.*, 2006; McGenity *et al.*, 2012). Certain microbes can degrade a range of hydrocarbons found in crude oil and its derivatives, including obligate hydrocarbonoclastic bacteria (OHCB), which use hydrocarbons as an almost exclusive source of carbon and energy (Yakimov *et al.*, 2007). Whilst OHCB have been demonstrated to degrade other compounds in pure culture (Zadjelovic *et al.*, 2020), there is still limited evidence that the OHCB are competitive for non-hydrocarbon substrates in the environment. This is evidenced by the fact OHCB are typically present in extremely low numbers in uncontaminated environments but rapidly increase in abundance following oil-spills (Yakimov *et al.*, 2004; Atlas and Hazen, 2011; Acosta-González *et al.*, 2015; Nogales and Bosch, 2019). Therefore, whilst it is evident that OHCB use a few other carbon and energy sources, for clarity we refer to them hereafter as “OHCB” to distinguish between these highly adapted and competitive hydrocarbon-degraders and those more metabolically diverse Bacteria, which can also degrade hydrocarbons. Since the Deepwater Horizon well blowout, there has been increased emphasis on understanding oil-spill microbial ecology, with much of the focus on deep sea oil plumes (Hazen *et al.*, 2010; Mason *et al.*, 2012; Redmond and Valentine, 2012), salt marsh sediments (Beazley *et al.*, 2012), or benthic sediments (Mason, Scott, *et al.*, 2014). Though some studies have focused on coastal sediments (Kostka *et al.*, 2011; Lamendella *et al.*, 2014; Huettel *et al.*, 2018) most were conducted either *ex situ* (Röling *et al.*, 2002; Da Silva *et al.*, 2009; Almeida *et al.*, 2013) or retrospectively (De La Huz *et al.*, 2005; Short *et al.*, 2007; Boufadel *et al.*, 2010), and represented a bias towards a single oil-spill event, Deepwater Horizon. Therefore, the *in-situ* establishment and succession of specialised oil-degrading microbial taxa, in the Mediterranean immediately following an oil spill, are less well understood. This is especially true for coastal sediments in the Mediterranean (see Supplementary Material Table. S4.2). Understanding how such ecosystems, and particularly oil-degrading microbial communities, respond to such events will allow for better post-spill monitoring (Kirby *et al.*, 2018). Exposure of environments to oil can also lead to a long-lasting adaptation within the microbial community. This phenomenon of prior exposure can be important in determining the rate at which any subsequent hydrocarbon inputs may be biodegraded (Leahy and Colwell, 1990). Such

knowledge will also assist in designing or improving models such as the Ecological Index of Hydrocarbon Exposure (EIHE) (Lozada *et al.*, 2014) and inform future oil-spill response, such as indicating the thoroughness of clean-up efforts and identifying when tourist/fishing activities can recommence.

The Mediterranean is an oligotrophic sea with extremely low levels of phosphorus (Thingstad *et al.*, 2005) and is virtually an enclosed basin with limited oceanic exchange. Phosphorous is a macronutrient that is vital for microbial growth and especially for hydrocarbon-degradation (Atlas, 1981); and therefore, the availability of these nutrients in the presence of hydrocarbons is vital (Ron and Rosenberg, 2014). From 1977 - 2018 the Mediterranean has been subject to 989 recorded oil-pollution incidents (REMPEC, 2018). Additionally, the Mediterranean has been the location of three of the world's top 20 largest tanker oil spills; including the tankers Haven (1991, 144,000 tonnes, Italy), Irenes Serenade (1980, 100,000 tonnes, Greece), and Independenta (1979, 95,000 tonnes, Turkey) (ITOPF, 2019). The majority of accidents resulting in oil-pollution occur in the Eastern Mediterranean, especially around Greece (Girin and Carpenter, 2019). The Mediterranean currently contains two refineries, two oil terminals, and three oil ports (REMPEC, 2018), with an additional 480 active shipping ports, 50% of which are in located around Greece and Italy (Xue *et al.*, 2004). The Mediterranean is highly socio-politically complex with 21 countries bordering the sea, and future predictions indicate increased levels of oil and gas drilling in the region (Union *et al.*, 2016). Oil pollution in the Mediterranean therefore represents a significant threat to the environment. Despite this, there remains a paucity of information on how oil pollution effects Mediterranean sediment microbial communities.

Our early sampling (five days post spill) of the Agia Zoni II incident allowed a very rare opportunity to investigate the immediate impact on the microbial community and identify the earliest key colonising oil-degrading bacteria from an oil spill that covered a large area of coastal sediment, in a region where fishing and tourism play a pivotal socio-economic role. We quantified hydrocarbon concentrations across seven contaminated and two uncontaminated sites five days post-spill and after remediation. Additionally, we determined oil-spill-induced changes in gene abundance, diversity, and composition of the sediment microbial communities using qPCR and high throughput sequencing of the 16S rRNA gene.

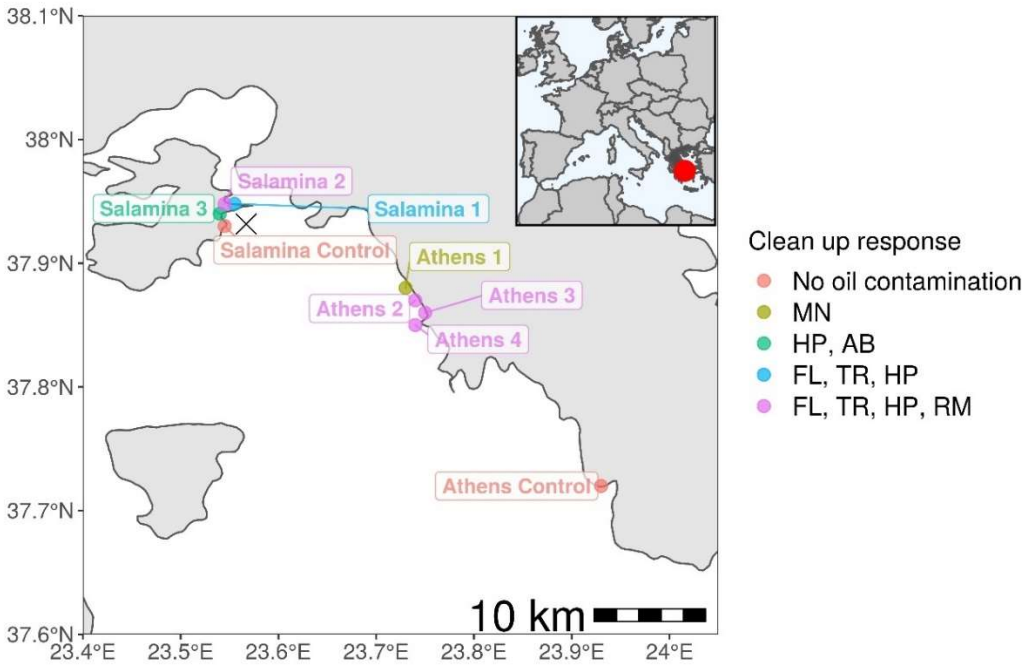

Fig. 4.1: Sampling sites from the Agia Zoni II oil-spill (marked as an X where tanker sank) in Greece (inlet; dark grey; red dot highlights spill-site) and affected Athens Riviera and Salamina coastline. Abbreviations for clean-up response applied at oil-contaminated sample sites (Athens 1-4 and Salamina 1-3): MN (manual removal of tar balls), HP (high-powered washing, to remove oil from hard surfaces), AB (use of absorbents to collect floating oil from the water surface), FL (flushing of sediment with medium pressure water), TR (trenching, used in conjunction with flushing to collect oil), and RM (removal of coastal sediment, either washed and replaced or disposed in landfill).

Results

Sediment Hydrocarbon Concentrations

Five days after the oil spill, the surface sediments at three sample sites on the Athens Riviera were visibly contaminated by hydrocarbons (Fig. 4.2). The concentrations of the aliphatic hydrocarbons fraction including *n*-alkanes from undecane (C_{11}) to dotriacontane (C_{32}) and the branched alkanes, (pristane and phytane) ranged from 1536 ± 557 to 2803 ± 549 μg g^{-1} dry sediment (Fig. 4.2). The concentrations of the aromatic fraction, containing the 2-5 fused-ring polycyclic aromatic hydrocarbons (PAHs), including methylnaphthalenes, dimethylnapthalenes, methylphenanthrenes, and methylanthracenes ranged from 88.20 ± 13.50 to 332 ± 99 μg g^{-1} dry sediment. One-month post-spill, the concentration of total *n*-alkanes, branched alkanes, and PAHs reduced to almost undetectable levels at both the Athens Riviera and Salamina sites (Fig. 4.3). Additionally, we found no significant differences in phosphate, nitrate, and ammonium concentrations between contaminated sites and uncontaminated control sites when compared to coastal water samples (Supplementary Material Fig S4.1).

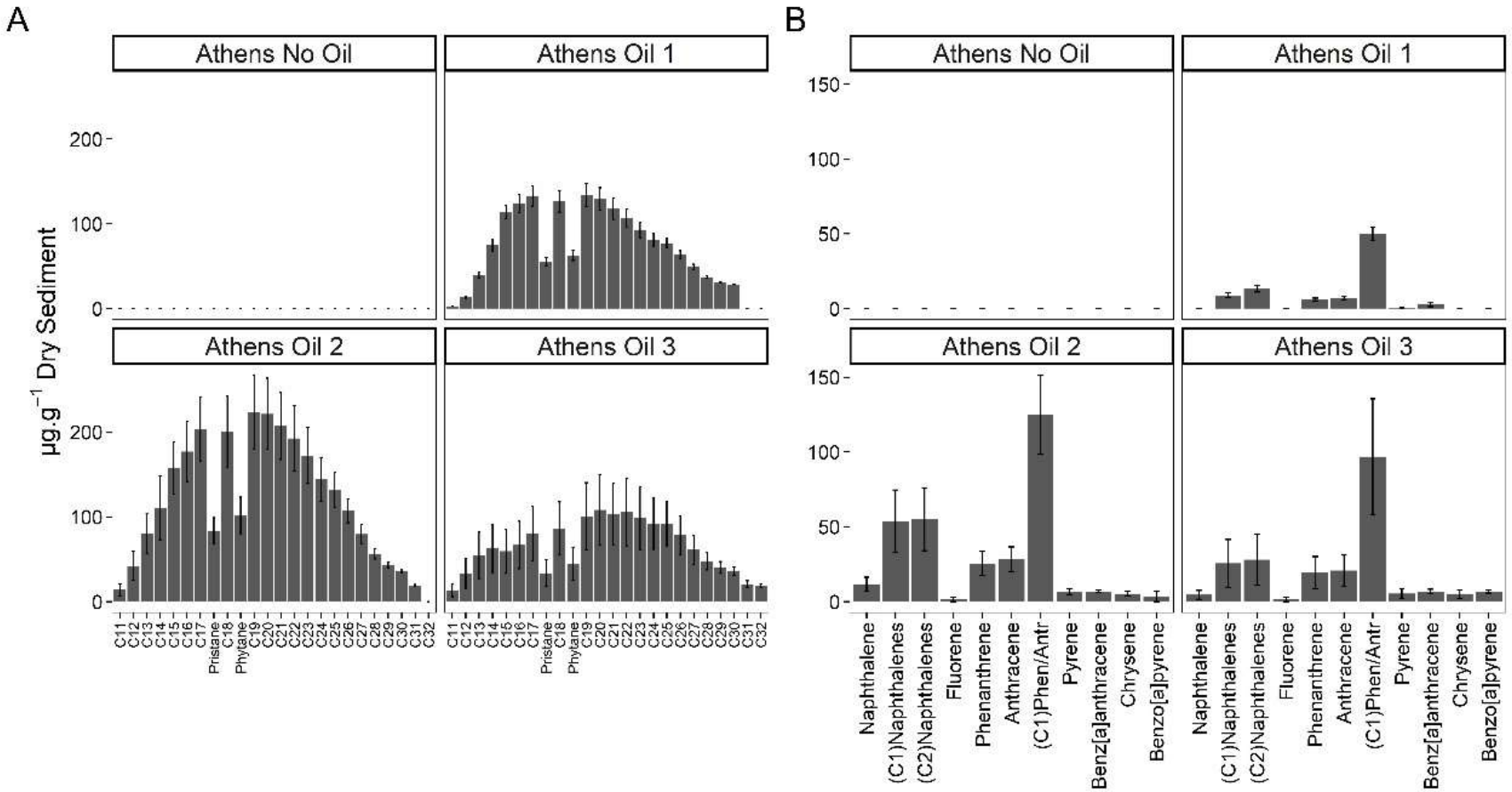

Fig. 4.2: Hydrocarbon concentrations (mean ± SE, *n* = 3) of the three contaminated sites (Athens Oil 1-3) and the uncontaminated control site (Athens No Oil), September 2017. A) *n*-alkanes from C_{11} to C_{32} and the branched alkanes pristane and phytane. B) PAHs from 2-ring naphthalene to 5-ring benzo[*a*]pyrene. No samples were taken for Salamina in September 2017.

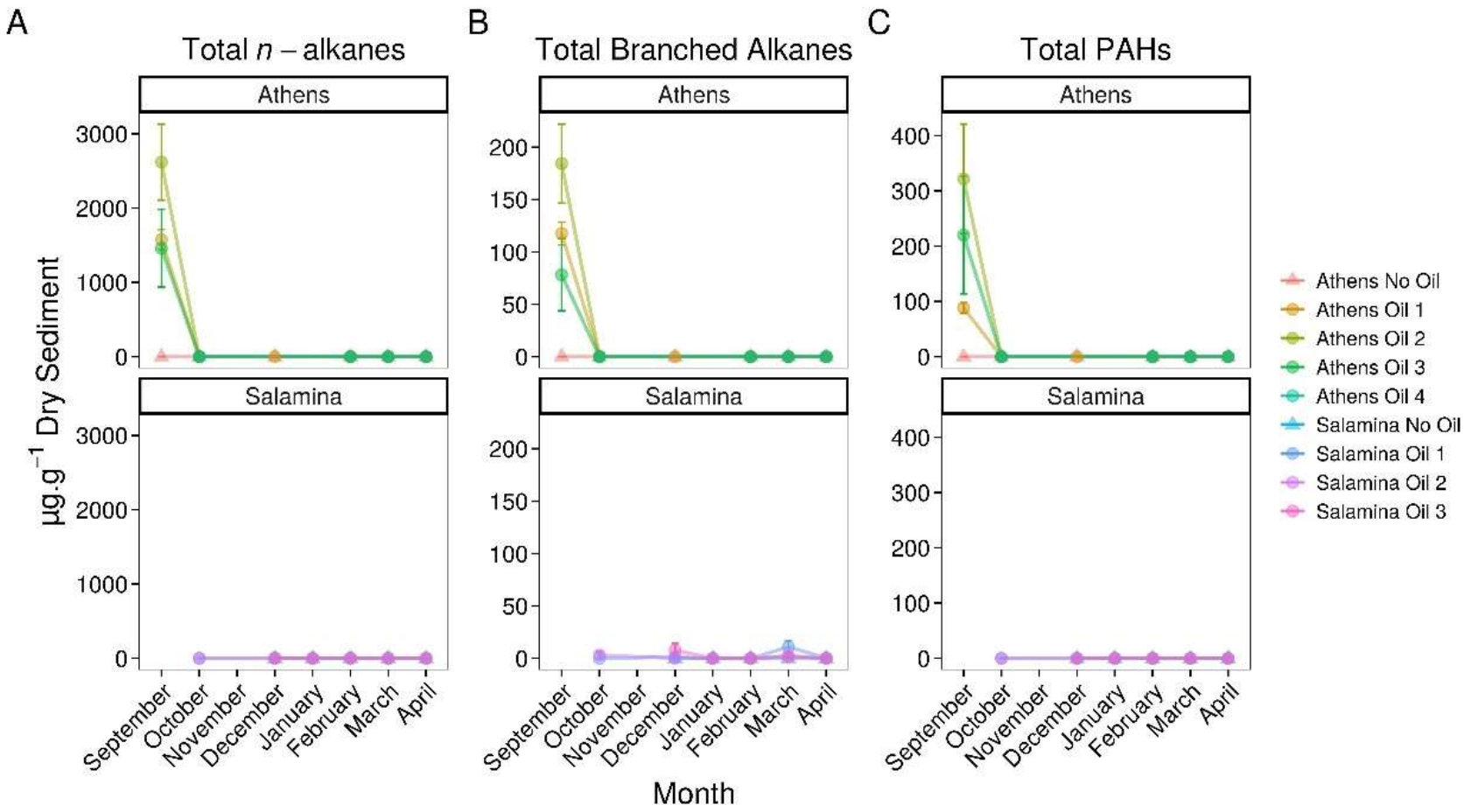

Fig. 4.3: Concentrations (mean ± SE, *n* = 3) of hydrocarbons in control (Suffix "No Oil") and contaminated (Suffix "Oil") sediments along the Athens Riviera and Salamina coastline, sampled from September 2017 to April 2018. A) total *n*-alkanes, B) total branched alkanes (pristane and phytane), and C) total PAHs. No samples were collected for all Salamina sites in September 2017, "Salamina No Oil" in October 2017, or all Salamina and Athens sites in November 2017.

Effects of the Oil-spill on Sediment Microbial Community Composition and Abundance

In order to evaluate any effect that the oil-spill had on microbial community composition or abundance, 16S rRNA bacterial and archaeal genes were analysed by qPCR and amplicon library sequencing. High-throughput 16S rRNA gene sequencing resulted in an average of 55,591 (range 8,093 – 209,105) and 49,983 (range 3,822 – 196,697) sequence reads for *Bacteria* and *Archaea* respectively. Five days post-spill, the mean bacterial 16S rRNA gene abundance (1.6×10^8 copies g^{-1} dry sediment) in Athens contaminated sediments was ~2.5 fold greater, but not statistically significant, than in the uncontaminated control sediments (Supplementary Material Fig. S4.2A). Archaeal 16S rRNA gene abundance was typically two orders of magnitude lower than the *Bacteria* (Supplementary Material Fig. S4.2B) and no significant changes were observed in archaeal 16S rRNA gene abundance in response to the oil spill. Simpson Diversity Index analysis of archaeal and bacterial 16S rRNA gene amplicon libraries revealed no significant difference between contaminated (average across all samples, *Archaea* 0.35 *Bacteria* 0.99) and uncontaminated (*Archaea* 0.26, *Bacteria* 0.99) sites, at any month. Archaeal community analysis revealed a high relative abundance of *Candidatus* Giganthauma and *Nitrosopumilus,* though no significant differences were observed between contaminated and uncontaminated sediment samples. This suggests *Archaea* did not play a significant role in biodegradation of, and were unaffected by, the oil (Supplementary Material Fig. S4.3).

Operational taxonomic units (OTUs) affiliated to numerous OHCB in contaminated sites five days post-spill were significantly more relatively abundant in comparison to uncontaminated control sites. These changes included higher relative abundance of members of *Marinobacter,* closely related to *M. hydrocarbonoclasticus*, *Alcanivorax* spp., *Oleibacter* spp., *Oleiphilus* spp. and *Thalassolituus* spp. (Fig. 4.4) in comparison to uncontaminated sites. In October and December higher relative abundance of *Cycloclasticus*, a known PAH-degrading genus (Dyksterhouse *et al.*, 1995), was also observed in the contaminated site “Salamina Oil 1”. There was also significantly higher relative abundance of sequences affiliated to more catabolically versatile genera or species (i.e. those that use a wider range of substrates than the OHCB whose substrate range in the environment is typically restricted to hydrocarbons) in comparison to uncontaminated sites. These genera have been shown to contain representatives that can degrade hydrocarbons; including *Marinobacter* spp., *Idiomarina* spp., *Alteromonas* spp., *Vibrio* spp., *Erythrobacter* spp., *Roseovarius* spp. (Fig. 4.5; see Supplementary Material Table S4.2). Dissimilarities in bacterial community composition were evident between uncontaminated and

contaminated sites in September 2017 immediately after the oil-spill. However, from October 2017 onwards the bacterial community composition at the oiled sites become increasingly similar to those found at the uncontaminated sites (Supplementary Material Fig. S4.4).

Several of the OTUs that were significantly more relatively abundant at contaminated versus uncontaminated sites were affiliated to OHCB and specifically to known alkane-degraders. For example, OTU-10 (100% 16S rRNA sequence identity to *Marinobacter hydrocarbonoclasticus;* Fig. 4.4 and Fig. 4.6), had significantly higher relative abundance at some contaminated sites (coef. = 10.88, z = 18.13, $p<0.001$) compared to uncontaminated sites. Five days post-spill, OTU-10, represented 15% and 11% at “Athens Oil 2 and 3” respectively, but sharply decreased in relative abundance to virtually undetectable levels from October onwards. The increase in the relative abundance of *M. hydrocarbonoclasticus* represented an increase of 2.14×10^7 16S rRNA gene copies assigned to *M. hydrocarbonoclasticus* compared to uncontaminated Athens sediments. Five OTUs assigned to the OHCB genus *Alcanivorax* (Fig. 4.4 and Fig. 4.6) were significantly more relatively abundant in all contaminated sites (September 2.19% ± 1.52%; coef. = 2.28, z = 6.40, $p<0.001$) compared to uncontaminated sites where it was generally undetectable. From October the relative abundance of *Alcanivorax* OTUs steadily decreased in the contaminated sites, though always remained at least 5- to 297-fold greater than the uncontaminated control sites, where they were often undetectable. Similarly, OTUs from the genus *Oleibacter* (OTU-200 and OTU-265) and OTU-606 from *Oleiphilus* (Fig. 4.4 and Fig. 4.6) were significantly more abundant in “Athens Oil 1” immediately after the oil-spill in September (coef. = 1.44, z = 13.35, $p<0.001$) from uncontaminated control levels, (3.67% ± 0.89% and 1.44% ± 0.83% respectively). However, in April the relative abundance of both genera decreased to levels below 0.01%. Finally, OTU-972 assigned to *Thalassolituus* (Fig. 4.4 and Fig. 4.6), a genus containing species that can degrade a wide range of alkanes (Yakimov *et al.*, 2004; Gregson *et al.*, 2018), was significantly more relatively abundant in sediments from contaminated sites in September (0.74%; coef. = 0.16, z = 7.52, $p<0.001$) compared to uncontaminated control sediments. The relative abundance of *Thalassolituus* decreased in the months thereafter to undetectable levels. The increase in the relative abundance of *Thalassolituus* represented an increase of 1.22×10^6 16S rRNA gene copies compared to uncontaminated Athens sediments, even though *Thalassolituus* was the least abundant OCHB genus.

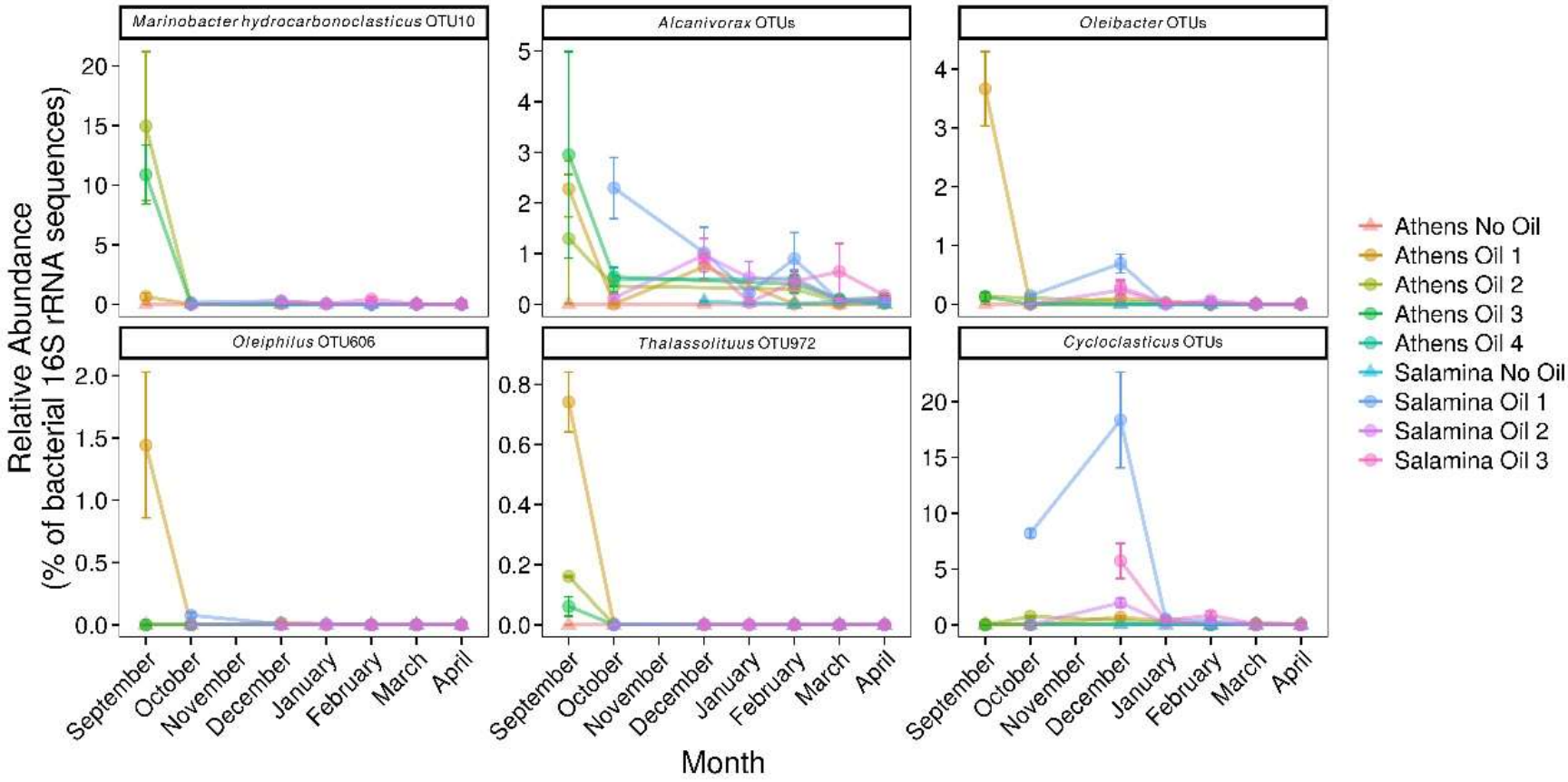

Fig. 4.4: Relative abundance (% of the bacterial community; mean ± SE, *n* = 3) of 16S rRNA gene OTUs assigned to putative obligate hydrocarbonoclastic bacteria (including OTU-10 which has a 100% identity match to M. hydrocarbonoclasticus) in sediments from control (Suffix "No Oil") and contaminated (Suffix "Oil") sites along the Athens Riviera and Salamina coastline, from September 2017 to April 2018. No samples were collected for all Salamina sites in September 2017, "Salamina No Oil" in October 2017, or all Salamina and Athens sites in November 2017.

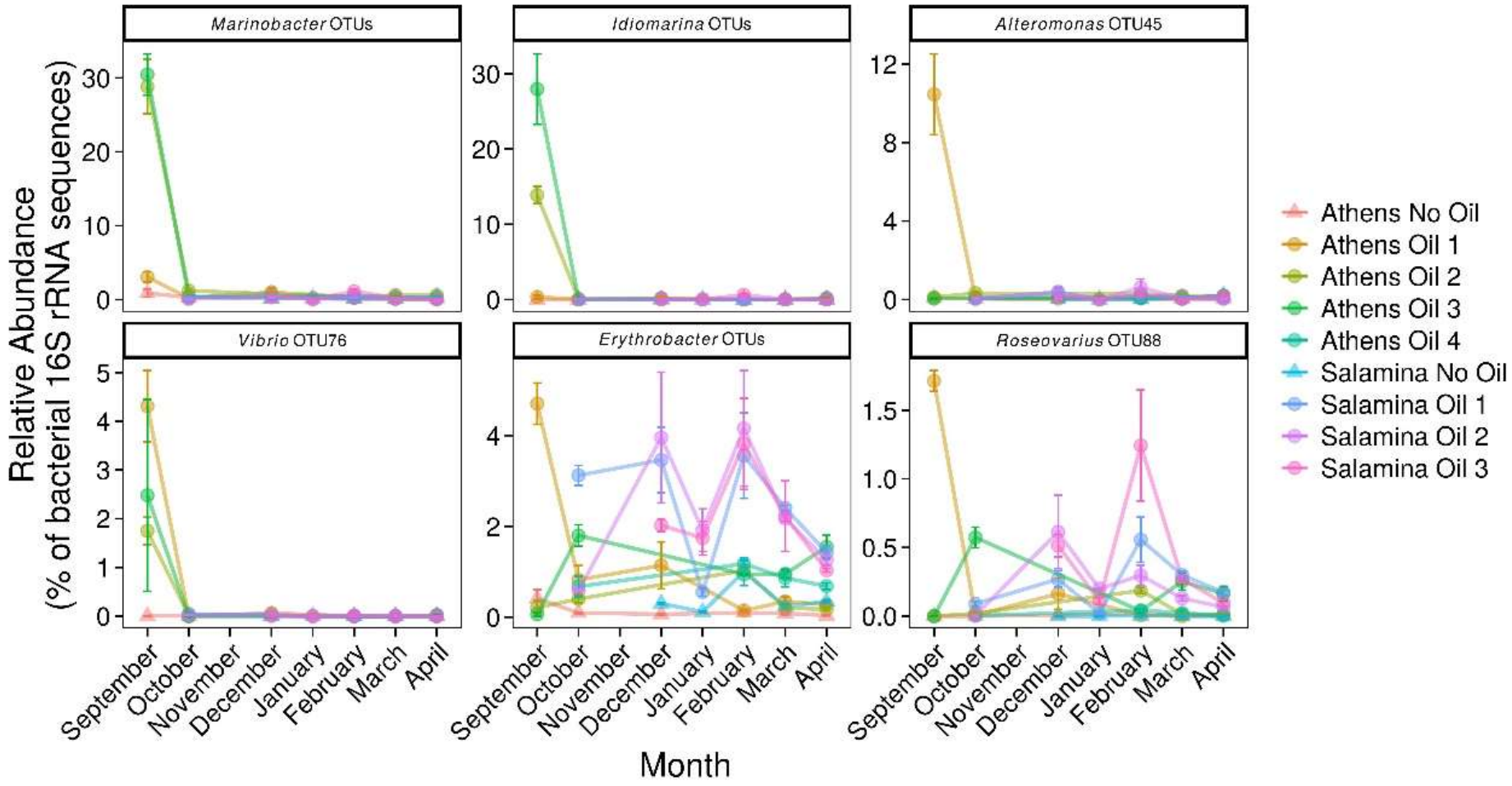

Fig. 4.5: Relative abundance (% of the bacterial community; mean ± SE, *n* = 3) of 16S rRNA gene OTUs assigned to Bacteria associated with oil-degradation, in sediments from control (Suffix "No Oil") and contaminated (Suffix "Oil") sites along the Athens Riviera and Salamina coastline, from September 2017 to April 2018. No samples were collected for all Salamina sites in September 2017, "Salamina No Oil" in October 2017, or all Salamina and Athens sites in November 2017.

No known PAH-degrading OHCB were detected five days post-spill when high PAH concentrations were measured. However, OTUs from more metabolically diverse genera (which have been demonstrated to degrade PAHs; see Supplementary Material Table S4.2) were observed in significantly higher relative abundance (coef. = 1.75, z = 6.06, p<0.001) compared to uncontaminated levels, including *Alteromonas* spp. (10.46% ± 2.91% at "Athens Oil 1"), *Idiomarina* spp. (13.96% ± 11.75% at "Athens Oil 2 and 3"), and *Vibrio* spp. (2.09% ± 2.03% across "Athens Oil 1, 2, and 3"). OTU-31 and OTU-32, assigned to the PAH-degrading genus Cycloclasticus (Fig. 4.4 and Fig. 4.6), had significantly greater relative abundance in some contaminated locations compared with uncontaminated control sites. For example, in October and December they contributed up to 19% of relative abundance at "Salamina Oil 1" (coef. = 18.31, z = 19.21, p<0.001), sharply reducing thereafter.

Ten OTUs belonging to the genus *Marinobacter* (excluding sequences assigned to the OHCB species *M. hydrocarbonoclasticus)* (Fig. 4.5 and Fig. 4. 6), were significantly more relatively abundant in sediments taken in September from "Athens Oil 2 and 3" (30%; coef. = 27.94, z = 43.21, p<0.001) relative to the uncontaminated sites, decreasing sharply from October. Similarly, five OTUs assigned to the genus *Idiomarina* (Fig. 4.5 and Fig. 4.6) were also significantly greater in relative abundance (coef. = 13.88, z = 23.40, p<0.001), at 14% and 28% from sediments in "Athens Oil 2 and 3", respectively, decreasing from October onward. OTU-45 assigned to the genus *Alteromonas* and OTU-76 assigned to the genus *Vibrio* (Fig. 4.5 and Fig. 4.6) significantly increased in relative abundance (coef. = 10.37, z = 26.11, p<0.001), from uncontaminated control levels, particularly at contaminated "Athens Oil 1" to approximately 10% and 3% respectively, before sharply decreasing from October onward.

Two genera from the class Alphaproteobacteria also increased following oil contamination, which included five OTUs assigned the genus *Erythrobacter* and OTU-88 assigned to the species *Roseovarius* spp. (Fig. 4.5 and Fig. 4.6), which were significantly higher in relative abundance at contaminated sites from September to April, relative to levels at the uncontaminated sites.

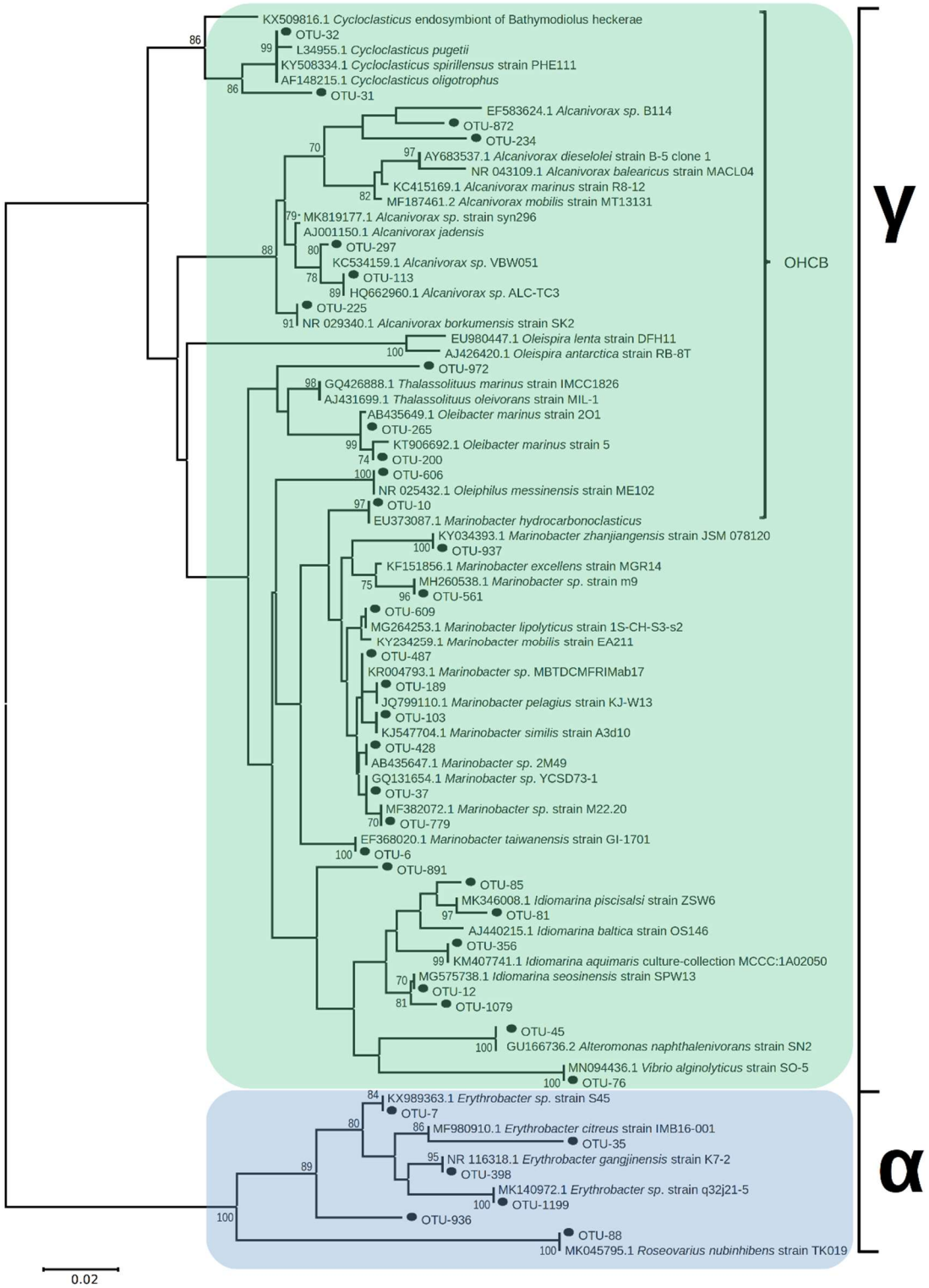

Fig. 4.6: Unrooted Neighbour-Joining phylogeny of 16S rRNA bacterial OTUs, in sediments from contaminated sites along the Athens Riviera and Salamina coastline, from September 2017 to April 2018, aligned with known hydrocarbon-degrading bacteria and closest relatives; bootstrap values >70 displayed (1,000 iterations). Evolutionary distances computed by Maximum Composite Likelihood protocol (using the Tamura-Nei model (Tamura and Nei, 1993)), sum of branch length = 1.15. Analysis involved 82 nucleotide sequences (36 OTUs) with a total of 258 positions in the final dataset. Evolutionary analyses were conducted in MEGA7.

Five days after the oil spill in September there was a strong positive correlation (R^2 = 0.80, $p<0.01$) between the relative abundance of 16S rRNA sequences assigned to hydrocarbon-degrading bacteria (all OTUs displayed in Fig. 4.6) and the concentration of measured hydrocarbons. In addition, the Ecological Index of Hydrocarbon Exposure (EIHE), which quantifies the proportion of the bacterial community with hydrocarbon-bioremediation potential on a scale of 0-1, whereby 1 represents 100% (Lozada *et al.*, 2014), was calculated at 0.52 ± 0.14 in September. This EIHE result was significantly ($p<0.05$) higher than the control site at 0.30 ± 0.11. At the genus level, some correlative relationships between bacterial genera containing hydrocarbon-degraders were observed. OTUs from the genera *Marinobacter* and *Idiomarina* typically co-occurred and were significantly correlated (R^2 = 0.80 $p<0.05$). A difference in the bacterial community composition occurred at different contaminated sites, despite the presence of similar hydrocarbons. For example, at "Athens Oil 2 and 3", when *Marinobacter* and *Idiomarina* were in high relative abundance (collectively 46%) *Alteromonas*, *Oleibacter*, *Oleiphilus*, and *Thalassolituus* had low relative abundance of approximately 0.64%, collectively. In contrast, when *Marinobacter* and *Idiomarina* were in low relative abundance (collectively 4% at "Athens Oil 1" in September) *Alteromonas*, *Oleibacter*, *Oleiphilus*, and *Thalassolituus* had a relative abundance of approximately 16%, collectively, at the same site in September. The full correlation analysis showing the co-occurrence of taxa is provided in Supplementary Material Fig. S4.5.

Discussion

Sediment Hydrocarbon Concentrations and Clean-up Operations

Five days after the oil spill, GC-MS analysis revealed extensive oil contamination in the surface sediments at multiple beaches along the Athens Riviera. This contamination occurred due to rapid transfer of the oil from the water onto the coastal sediments within the first few days of the spill, due to sustained prevailing winds (Parinos *et al.*, 2019). The level of total measured hydrocarbons, 2,158 ± 800 μg g^{-1} dry sediment, was similar to that observed from surface sediments in the Exxon Valdez oil-spill, 4,636 ± 1,628 μg g^{-1} sediment, (Bragg *et al.*, 1994). However, Agia Zoni II hydrocarbon sediment concentrations were much lower than that observed in buried sediments in Pensacola Beach, Florida (11,000 μg g^{-1} sediment total petroleum hydrocarbons) which was impacted by the Macondo oil spill (Huettel *et al.*, 2018). Unbranched alkanes and PAHs from sediments after the Agia Zoni II oil spill were undetected from October 2017 onwards; though some branched alkanes persisted at

low concentrations (primarily at contaminated Salamina sites, Oct – Apr 7.31 ± 7.04 μg g^{-1} sediment).

The near complete removal of hydrocarbons to undetectable levels, from October 2017 onwards, is in line with measurements taken by the Hellenic Centre for Marine Research (HCMR) (Parinos *et al.*, 2019) and is indicative of efficient physical removal and other clean-up operations, which occurred immediately after the oil-spill incident and continued through to February 2018. The preferential removal of the more readily degradable linear *n*-alkanes, as indicated by the presence of branched alkanes and no measurable *n*-alkanes or PAHs from October 2017 onwards, would suggest biodegradation was occurring. The extent to which the removal of hydrocarbons can be attributed to either biodegradation, natural processes, or remediation efforts cannot be determined from our data. However, hydrocarbon data from Parinos et al. (2019) suggested the early onset of biodegradation, which was sustained for 85 days post-oil-spill, especially amongst phenanthrenes.

Whilst absorbents, flushing, and sediment washing were used, a large proportion of the clean-up operations at the study sites consisted of direct sediment removal (whether contaminated or not) (International Oil Pollution Compensation Funds, 2018). Though effective in the removal of oil (Dave and Ghaly, 2011), the bulk removal of coastal sediment can be environmentally damaging (Owens, 1972; Gundlach and Hayes, 1978; Petersen *et al.*, 2002), and, has economic and environmental costs associated with disposal, often to landfill sites. In the case of Agia Zoni II, some sediment-washing and replacement occurred, but these responses were not adopted to the same degree as removal, likely due to the need for a rapid clean up to minimise the economic impact from loss of tourism.

Ecology of Obligate Hydrocarbonoclastic Bacteria (OHCB)

An oil-spill perturbation is indicative of a discrete short term disturbance event (Shade *et al.*, 2012), whereby changes in microbial community are largely trait driven, by the ability of individual species to occupy available niches due to hydrocarbon-degradation processes and pressures. This often manifests as a large increase in the absolute abundance of *Bacteria*, due to selection for hydrocarbon-degrading bacteria (Head *et al.*, 2006), which was observed here with a ~2.5-fold increase, but not significant, in the absolute abundance of the bacterial 16S rRNA gene immediately following the oil-spill. In particular, there was significantly greater relative abundance of genera with known hydrocarbon-degrading bacteria at contaminated sites in comparison to uncontaminated sites. These notable increases, along with a history of hydrocarbon pollution in the Saronic Gulf, indicates an indigenous community of hydrocarbon-degrading bacteria, albeit at mostly very low or undetectable levels,

allowing for rapid colonisation of oiled sediments and growth. Hydrocarbons within sediments five days after the oil spill supported the growth of OHCB, which rapidly became dominant, and were almost undetectable in uncontaminated sediments.

Alcanivorax is preferentially degrades branched- and *n*-alkanes (Yakimov *et al.*, 1998), although it has been shown to enhance degradation of PAHs (McKew *et al.*, 2007). *Alcanivorax* is ubiquitous in the marine environment and is observed in a variety of hydrocarbon polluted environments (see Supplementary Material Table S4.2). In agreement with the results presented here, *Alcanivorax* is often observed to become abundant early on in coastal beach sediments and decrease in abundance as *n*-alkanes are removed from the environment (Head *et al.*, 2006; Kostka *et al.*, 2011; Rodriguez-R *et al.*, 2015). *Alcanivorax* persisted for many months after hydrocarbons (unbranched alkanes and PAHs) were undetected within the environment. This legacy effect could be caused by several processes, including the use of wax esters (Rontani, 2010) or polyhydroxyalkanoates (Możejko-Ciesielska and Kiewisz, 2016) as a carbon and energy store for use when nutrient availability (e.g. N & P) is more favourable for cellular growth. Alternatively, this persistence could be due to the low levels of branched alkanes, such as pristane and phytane, observed within the sediments in the months following September. Unlike most OHCB, certain species of *Alcanivorax* can use branched alkanes, for example, *A. borkumensis* SK2T (Yakimov *et al.*, 1998; Gregson *et al.*, 2019), *A. dieselolei* B-5 (Liu *et al.*, 2011), and *A. hongdengensis* A-11-3 (Wang and Shao, 2012). Additionally, *Alcanivorax* could have persisted in the environment by utilising biogenic-hydrocarbons (Han and Calvin, 1969).

Other alkane-degrading OHCB genera detected included *Oleibacter* (Teramoto *et al.*, 2011), *Oleiphilus* (Golyshin *et al.*, 2002), and *Thalassolituus* (Yakimov *et al.*, 2004; Gregson *et al.*, 2018); though their abundance was primarily restricted to “Athens Oil 1” sediments. *Oleibacter*, *Oleiphilus*, and *Thalassolituus* have all been observed to increase in abundance in oil-contaminated marine environments, though until now evidence is lacking for detection in coastal sandy sediments (see Supplementary Material Table S4.2). Previous studies of oil-contaminated sediment (Coulon *et al.*, 2012) and seawater (Teramoto *et al.*, 2013) observed *Oleibacter* and *Alcanivorax* in similar abundances, in line with our observations. However, in seawater-based laboratory experiments *Thalassolituus* has been observed to outcompete other alkane-degraders such as *Alcanivorax* (McKew *et al.*, 2007), through its use of medium- and long-chained alkanes (Gregson *et al.*, 2019); this was not observed in the sediment samples collected from the Agia Zoni II oil-spill, whereby *Alcanivorax* was in greater abundance.

Cycloclasticus is a PAH-degrading genus (Dyksterhouse *et al.*, 1995), apart from one lineage that degrades very short-chained alkanes (symbiont of *Bathymodiolus,* undetected in this study; Rubin-Blum et al., 2017). *Cycloclasticus*, which has been observed to grow in many marine environments including sandy coastal sediments (see Supplementary Material Table S4.2), was mostly undetected in sediments from Athens, but was observed in high abundance from October through December in Salamina sediments (note that no Salamina samples were taken in September). As found with *Alcanivorax, Cycloclasticus* demonstrated an oil-legacy effect, persisting in the sediments for several months after PAH contamination was undetectable. Once again this could be due to carbon and energy storage, the persistence of trace amounts of high molecular weight PAHs, or biogenic-hydrocarbons. Alternatively, hydrocarbons can be undetected through analytical methods such as GC-MS (McKenna *et al.*, 2013) when weathered hydrocarbons from an oil spill undergo transformation into oxygenated hydrocarbons (though currently there is no evidence that *Cycloclasticus* is able to degrade oxygenated hydrocarbons) (Kiruri *et al.*, 2013), which can persist for years within oil/sand aggregates (Aeppli *et al.*, 2018).

Ecology of Metabolically Versatile Oil-degrading Bacteria and Microbial Interactions

The specialist PAH-degrader, *Cycloclasticus,* was mostly undetected in sediments collected in September from Athens, possibly because it was outcompeted by more metabolically versatile bacteria that can also degrade PAHs. Potential candidates for this PAH-degradation are the genera *Idiomarina* (including OTUs most closely matched to PAH-degraders *I. seosinensis* (Yuan *et al.*, 2015; Gomes *et al.*, 2018) (100% similarity) and *I. piscisalsi* (Nzila *et al.*, 2018) (98.83% similarity)) and *Alteromonas* (including an OTU most closely matched to PAH-degrading *A. naphthalenivorans* (Jin *et al.*, 2011) (100% similarity)). *Idiomarina* and *Alteromonas* can use a range of substrates for growth, including PAHs, and in this region (Athens) may have outcompeted *Cycloclasticus*, in contrast to the latter months in Salamina where *Cycloclasticus* dominated. Given the dominance of *Cycloclasticus* in October/December in Salamina, it could be speculated that this genus was also dominant in September, in contrast to Athens where more metabolically versatile bacteria became established. Alternatively, differences in the clean-up response may partly account for the observed differences in *Cycloclasticus* relative abundance, as, for example, the remediation process of sediment removal did not occur at “Salamina Oil 1 and 3” (see Fig. 4.1 and Supplementary Materials Table S4.1), where an increased relative abundance of *Cycloclasticus* occurred.. This is also the case for

sediments from “Athens Oil 1” where the presence of *Cycloclasticus* was observed, but not in “Athens Oil 2 and 3” sediments.

Idiomarina and *Alteromonas* have been found in a range of oil-contaminated environments, including sandy coastal sediments (see Supplementary Material Table S4.2). In this study it was observed that whilst both these genera increased in abundance in contaminated sites compared to uncontaminated sites, they did not co-occur. *Idiomarina* did however positively correlate with the genus *Marinobacter*; including OTU-10 most closely related to *M. hydrocarbonoclasticus*, which has been shown to degrade a range of alkanes (Gauthier *et al.*, 1992). The co-occurrence of *Idiomarina* and *Marinobacter* was most notable between sediments from “Athens Oil 1” and “Athens Oil 2 and 3” and was to the competitive exclusion of other genera with known oil-degrading Bacteria, including: *Alteromonas, Erythrobacter, Oleibacter, Oleiphilus,* and *Roseovarius,* which co-occurred. *Alteromonas* and *Oleibacter* have been recorded previously to co-occur (Neethu *et al.*, 2019). The dominance of *Idiomarina* and *Marinobacter*, at “Athens Oil 2 and 3”, could potentially be due to indigenous species having a priority effect, providing a competitive advantage, or potentially due to source point pollution events. Alternatively, the absence of *M. hydrocarbonoclasticus* and *Idiomarina* from “Athens Oil 1” sediments could be due to the different remediation efforts at this site, where visible oil contamination was not as evident and thus only manual removal of tar balls occurred (see Fig. 4.1 and Supplementary Materials Table S4.1). The positive relationship between *Marinobacter* and *Idiomarina* has been observed before, including in oil-sludge samples (Albokari *et al.*, 2015) and in sandy coastal sediments from the Macondo oil-spill where these two genera dominated (Joye *et al.*, 2014). Additionally, Joye et al. (2014) observed that *Alcanivorax* was able to co-occur with *Marinobacter* and *Idiomarina*, as also observed in sediments from this study.

This study also demonstrates the ability of *Vibrio* (which is a genus that contains species that can degrade alkanes (Al-Awadhi *et al.*, 2012; Imron and Titah, 2018) and PAHs (Melcher *et al.*, 2002) to grow in several oil-contaminated environments; see Supplementary Material Table S4.2) to also avoid competitive-exclusion by *Marinobacter* and *Idiomarina*. This finding could indicate the ability of certain *Vibrio* to degrade a wide range of hydrocarbons, potentially including branched alkanes, like *Alcanivorax,* which may indicate why these genera are unaffected by the prevailing dominance of *Marinobacter* and *Idiomarina*. Indeed, certain species of *Vibrio* are known to attach to algal cells (Kumazawa *et al.*, 1991; Hood and Winter, 1997) and many algae are known to produce branched alkanes (Binark *et al.*, 2000) so perhaps there is a phototrophic-heterotroph interaction (McGenity *et al.*, 2012)

through the utilisation of branched alkanes by *Vibrio*. However, increased relative abundance in *Vibrio* spp. was not matched with increased branched alkane concentration in Salamina, and therefore this remains unverified. This cooccurrence could also occur due to *Vibrio* using PAHs.

Lastly, species within the genera *Erythrobacter* and *Roseovarius* can degrade a range of hydrocarbons and grow in oil-contaminated marine environments, including sandy coastal sediments (see Supplementary Material Table S4.2). *Erythrobacter* and *Roseovarius* maintained consistently higher abundances at the previously oiled sites in comparison to uncontaminated sites. Suggesting that once the genera have established a presence within the community, through the utilisation of hydrocarbons, they are able to maintain this even in the absence of such carbon and energy sources.

Are Archaea *Affected by Oil-contamination within Coastal Sediments?*

In agreement with many studies, archaeal abundance and diversity was mostly unaffected in the sediment samples taken from after the Agia Zoni II oil-spill (Redmond and Valentine, 2012; Urakawa *et al.*, 2012; King *et al.*, 2015; Sanni *et al.*, 2015). *Archaea* are not commonly considered as hydrocarbon-degraders, apart from certain *Halobacteria (McGenity, 2010; Oren, 2017)* which typically do not prevail in coastal seawater (exception herein being the genera *Haladaptatus* and *Halogranum*). There is growing evidence that growth of nitrifying-Archaea, especially from the genus *Nitrosopumilus*, is inhibited by crude oil (Urakawa *et al.*, 2012, 2019), though some studies do not show any significant inhibition by oil on archaeal populations (Newell *et al.*, 2014; Bernhard *et al.*, 2016). In this study, whilst there were some between-site differences in the relative abundance of OTUs assigned to *Nitrosopumilus* these were not significantly different. By quantifying archaeal species which are sensitive to oil-spill disturbances, post-oil-spill monitoring models can be made more efficient by including them as sentinel species (Kirby *et al.*, 2018).

Post-oil-spill Monitoring of Microbial Communities

The ability of those responding to an oil-spill (oil-spill responders, Government bodies, local authorities, oil-industries, NGOs) to evaluate the efficiency of clean-up operations, and thus provide guidance on future risk-based scenarios, is a vital endeavour to protect the environment and reduce socioeconomic impact. This has been recognised across the globe, and in the UK the cross-government initiative “PREMIAM” was published to this accord (Kirby *et al.*, 2018). Understanding how microbes respond to such perturbations can assist to this regard and has the potential to be incorporated into tools such as the Spill Impact Mitigation Assessment (IPIECA *et al.*, 2017). Combining the data from both hydrocarbon analysis, microbial ecology,

and other environmental sources, a more detailed and holistic understanding can be revealed. Microbial community analysis can highlight whether biodegradation may be taking place and the likelihood of the environment to naturally attenuate the oil-spill. Nutrient concentration analysis would reveal whether the environment is nutrient limited and should therefore be supplemented with fertiliser. Hydrocarbon analysis can detect the proportion of light and heavy molecules that could indicate the need for additional remediation operations.

Using microbial ecology as a post-oil-spill monitoring tool is still in its infancy, however models and indices to assist in this effort are available. Lozada *et al.* (2014) published an "Ecological Index of Hydrocarbon Exposure" (EIHE), whereby hydrocarbon contamination was assumed based on the relative abundance of genera known to contain hydrocarbon-degrading bacteria. The simplicity of this model is both a strength and a weakness. It is simple enough that it can easily be adapted as oil-spill microbial knowledge progresses, but it is too simple to fully establish hydrocarbon exposure. For example, in this study our uncontaminated control sites had an EIHE index of 0.30 ± 0.11 (on a scale of 0 – 1), despite no hydrocarbons being detected. This is due to the model including all species within functionally diverse bacterial genera such as *Pseudomonas* which includes >200 different species, of which only a small minority are known to degrade hydrocarbons. The EIHE could be improved further by analysing microbial community composition at a finer detail, perhaps at a species level, though this would require a tool to phylogenetically match OTUs to known oil-degrading species. Additionally, the inclusion of sentinel microbes, those that are adversely affected by oil-contamination (i.e. ammonia-oxidising archaea, Urakawa et al., 2012, 2019), would also add comprehension to the index. By advancing the knowledge of oil-spill microbial ecology, understanding the genetics and metabolic capabilities of all hydrocarbon-degrading bacteria and their microbial community interactions, and then combining this with hydrocarbon and environmental data, models such as the EIHE can be improved.

Experimental procedures

Sampling Locations and Schedule

Sediments were surveyed at both the surface (0-5 cm) and deeper depths (down to approximately 60 cm) on initial and subsequent site visits. However, only surface sediments were observed to be oil contaminated, so all analyses were focussed on this upper layer. Samples were collected, in triplicate, in sterile 50 ml sterile polypropylene containers from control (uncontaminated) and contaminated (oil contaminated) sites along the Athens Riviera and Salamina Island coast, Greece (see

Fig. 4.1 and Supplementary Materials Table S4.1). Sediments were randomly sampled (*n* = 3) across the distance of each beach. Additionally, coastal seawater samples were collected (we were unable to obtain seawater samples from Athens or Salamina for September 2017) for nutrient analysis (ammonium (NH_4^+), phosphate (PO_4^{3-}), silicate (SiO_2^-), nitrate (NO_3^-), and nitrite (NO_2^-)) using a SEAL Analytical AA3 HR AutoAnalyser tandem JASCO FP-2020 Plus fluorescence detector. Samples were collected in September 2017 five days after the oil-spill, when oiling of sediment was visible, at the Athens sites. However, we were unable to obtain sediment samples from all Salamina site for September 2017. Thereafter, samples were collected over a seven-month period (except for October when no samples for "Salamina No Oil" were collected and November when no samples for all site were collected). Samples were immediately frozen on collection and stored at -20°C.

Hydrocarbon-Degradation (GC-MS)

Hydrocarbons were extracted from thawed sediments. Samples (2 g) were dried with 2 g of anhydrous sodium (Na_2SO_4). Dried samples were extracted with 12 ml of hexane: dichloromethane (50:50) in 20 ml vials with Teflon-lined screw caps by horizontal shaking at 150 oscillations per min over 16 h and finally sonicated for 30 min at 20°C. After centrifugation 12,000 × g for five minutes, extracts were cleaned on Florisil® columns by elution with hexane. Extracts were transferred in conical tubes and evaporated to 0.7 ml over an ice bath to minimise loss of light PAHs. Deuterated alkane (nonadecane $C_{19}d_{40}$ and triacontane $C_{30}d_{62}$ at 10 µg ml^{-1}) and PAH (naphthalene-d_8 and anthrancene-d_{10} at 10 µg ml^{-1}) internal standards were added to each sample and quantification was performed on an Agilent 7890A Gas Chromatography system coupled with a Turbomass Gold Mass Spectrometer with Triple-Axis detector, operating at 70 eV in positive ion mode, using conditions as previously described by Coulon ***et al.*** (2007). External multilevel calibrations were carried out using alkanes (Standard Solution (C_8-C_{40}); Sigma), methylated-PAHs (1-methylnapthalene, 2-methylanthracene, and 9,10-dimethylanthracene; Sigma), and PAH (QTM PAH Mix; Sigma) standards, the concentrations of which ranged from 1.125 to 18 µg ml^{-1}. For quality control, a calibration standard (10 µg ml^{-1}) and a blank were analysed every 10 samples. We quantified alkanes between C_{10} and C_{36} including pristane and phytane and the following PAHs: naphthalene; all isomers of methyl-, dimethyl- and trimethyl-naphthalenes; acenaphthylene; acenaphthene; fluorene; phenanthrene; all isomers of methyl- and dimethyl-phenanthrenes/anthracenes; fluoranthene; pyrene; all isomers of methyl- and dimethyl-pyrene; chrysene; all isomers of methyl- and dimethyl-chrysene. Only those hydrocarbons detected are shown in Fig. 4.3.

qPCR Analysis of Bacterial and Archaeal 16S rRNA Genes

DNA was extracted from 0.25 g of thawed sediment samples with a DNeasy PowerSoil Kit (Qiagen), according to the manufacturer's instructions. The primers used for quantification of archaeal 16S rRNA gene were 344f – ACGGGGYGCAGCAGGCGCGA (Raskin *et al.*, 1994) and 915r – GTGCTCCCCCGCCAATTCCT (Stahl and Amann, 1991), and for bacterial 16S rRNA gene, 341f - CCTACGGGNGGCWGCAG and 785r – GACTACHVGGGTATCTAATCC (Klindworth *et al.*, 2013) were used. These primers have been successfully used to quantify archaeal (Huby *et al.*, 2020) and bacterial (Clark *et al.*, 2020) 16S rRNA gene abundances in environmental samples previously. Furthermore, inspection of standard curves showed that all assays produced satisfactory efficiency (85%) and R^2 values (>0.99). All qPCR reactions were performed using a CFX384™ Real-Time PCR Detection System (BioRad) using reagents, cycle conditions, and standards as previously described (McKew and Smith, 2015; Tatti *et al.*, 2016). It should be noted that qPCR of the 16S rRNA gene, whilst providing a valuable comparison of bacterial growth between samples, does not reflect absolute bacterial biomass, as many species contain multiple copies of the 16S rRNA gene.

Amplicon Sequencing and Bioinformatics

Amplicon libraries were prepared, as per Illumina instructions, by a 25-cycle (*Bacteria*) and 31-cycle (*Archaea*) PCR. PCR primers were the same as those used for qPCR but flanked with Illumina Nextera overhang sequences. A unique combination of Nextera XT Indices (Illumina) were added to PCR products from each sample, via an 8-cycle PCR. PCR products were quantified using PicoGreen and pooled in equimolar concentrations. Quantification of the amplicon libraries was determined via NEBNext® Library Quant Kit for Illumina (New England BioLabs Inc.), prior to sequencing on the Illumina MiSeq® platform, using a MiSeq® 600 cycle v3 reagent kit and 20% PhiX sequencing control standard. Raw sequence datasets have been submitted to the European Nucleotide Archive database under accession number PRJEB33987. Sequence output from the Illumina MiSeq platform were analysed within BioLinux (Field *et al.*, 2006), using a bioinformatics pipeline as described by Dumbrell *et al.* (2016). Forward sequence reads were quality trimmed using Sickle (Joshi and Fass, 2011) prior to error correction within Spades (Nurk *et al.*, 2013) using the BayesHammer algorithm (Nikolenko *et al.*, 2013). The quality filter and error corrected sequence reads were dereplicated, sorted by abundance, and clustered into OTUs (Operational Taxonomic Units) at the 97% sequence identity level via VSEARCH (Rognes *et al.*, 2016). Singleton OTUs were discarded, as well as

chimeras using reference based chimera checking with UCHIME (Edgar *et al.*, 2011). Lastly, taxonomic assignment was conducted with the Ribosomal Database Project (RDP) Classifier (Wang *et al.*, 2007). Non locus-specific, or artefactual, OTUs were discarded prior to statistical analyses, along with any OTUs that had <70% identity with any sequence in the RDP database.

Phylogenetic Analysis

The Neighbour-Joining protocol (Nei and Saitou, 1987) was used to infer the evolutionary history of partial 16S rRNA gene sequence Bacterial OTUs, aligned with known hydrocarbon-degrading bacteria and closest neighbouring accessions using MUSCLE (Edgar, 2004). Bootstrapping analysis (1000 iterations) was conducted to determine the percentage of time associated taxa clustered together in replicate trees (Felsenstein, 1985); only bootstrap values >70% are shown. Evolutionary distances, units in the number of base substitutions per site, were calculated with the use of Maximum Composite Likelihood protocol (Hanson and McElroy, 2015). Phylogenetic analyses were conducted in MEGA7.

Statistical Analysis

Prior to community analysis, sequence data were rarefied to the lowest library sequence value (8,093). Data were first tested for normality (Shapiro-Wilks test), those data which were normally distributed were tested for significance with ANOVAs or appropriate linear models. Non-normally distributed data were analysed using appropriate GLMs (Generalised Linear Models) as follows. The relative abundance of OTUs or genera in relation to oil exposure, site, and sample month were modelled using multivariate negative binomial GLMs (Wang *et al.*, 2010). Here, the number of sequences in each library was accounted for using an offset term, as described previously (Alzarhani *et al.*, 2019). The abundance of archaeal and bacterial 16S rRNA gene copies was also modelled using negative binomial GLMs (Venables and Ripley, 2002). The significance of model terms was assessed via likelihood ratio tests. The EIHE (Lozada *et al.*, 2014) was calculated using the script available at the ecolFudge GitHub page (https://github.com/Dave-Clark/ecolFudge, Clark, 2019) and EIHE values modelled using Poisson GLMs. Correlations were performed using the Pearson's correlation with an alpha of 0.05. All statistical analyses were carried out in R3.6.1 (R Development Core Team, 2011) using a variety of packages available through the references (Venables and Ripley, 2002; Becker *et al.*, 2016; Auguie, 2017; Lenth, 2020). All plots were constructed using the "ggplot2" (Wickham, 2010) and "patchwork" (Pedersen, 2019) R packages.

Supplementary Materials

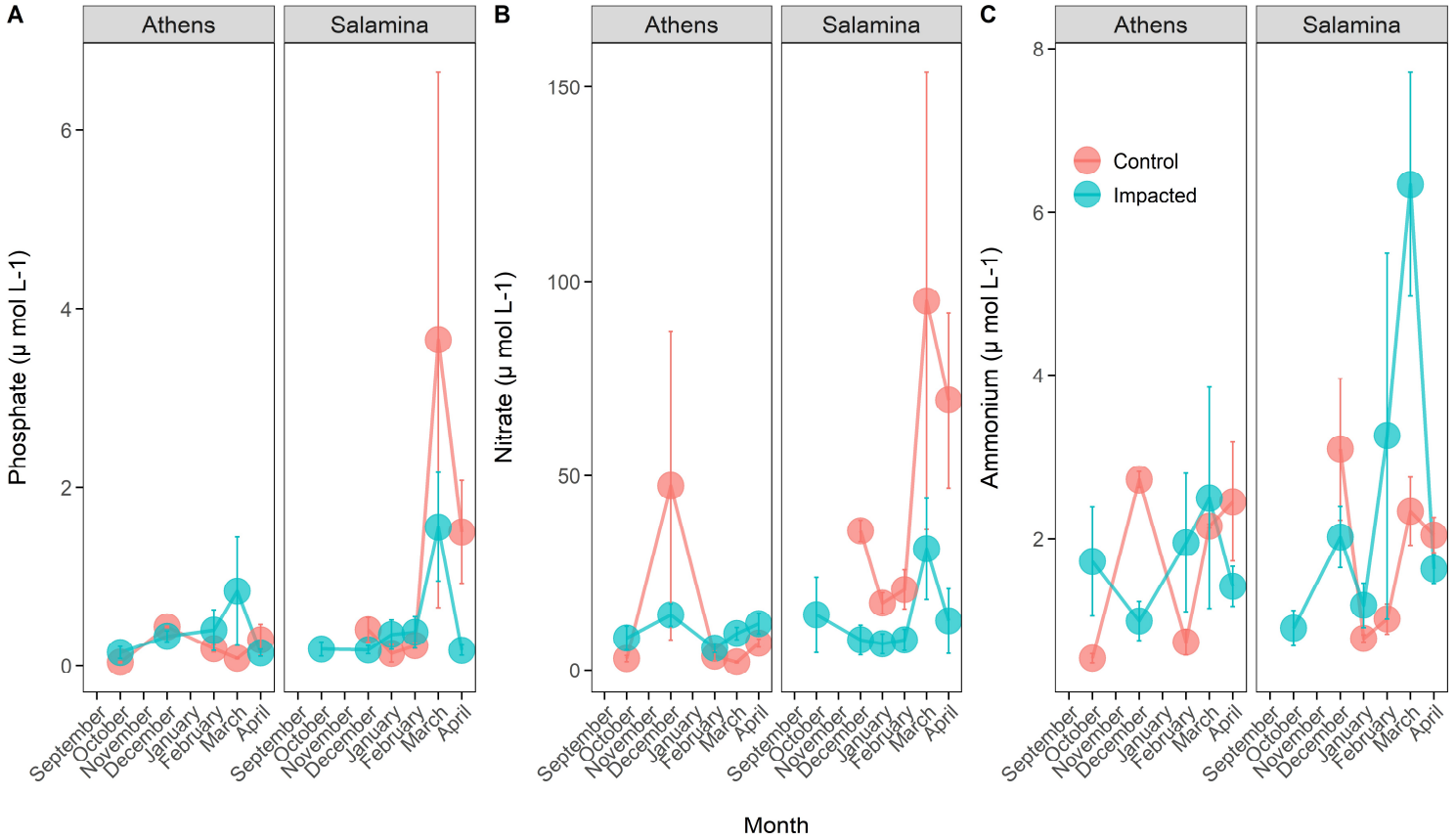

Fig. S4.1: Concentration (mean ± SE, *n* = 3) of phosphate (**A**), nitrate (**B**), and ammonium (**C**) in unimpacted ("Control") and oil-impacted ("Impacted") seawater samples from both the Athens Riviera and Salamina coastlines, sampled from October 2017 to April 2018 (seawater samples not taken in September 2017 at either site).

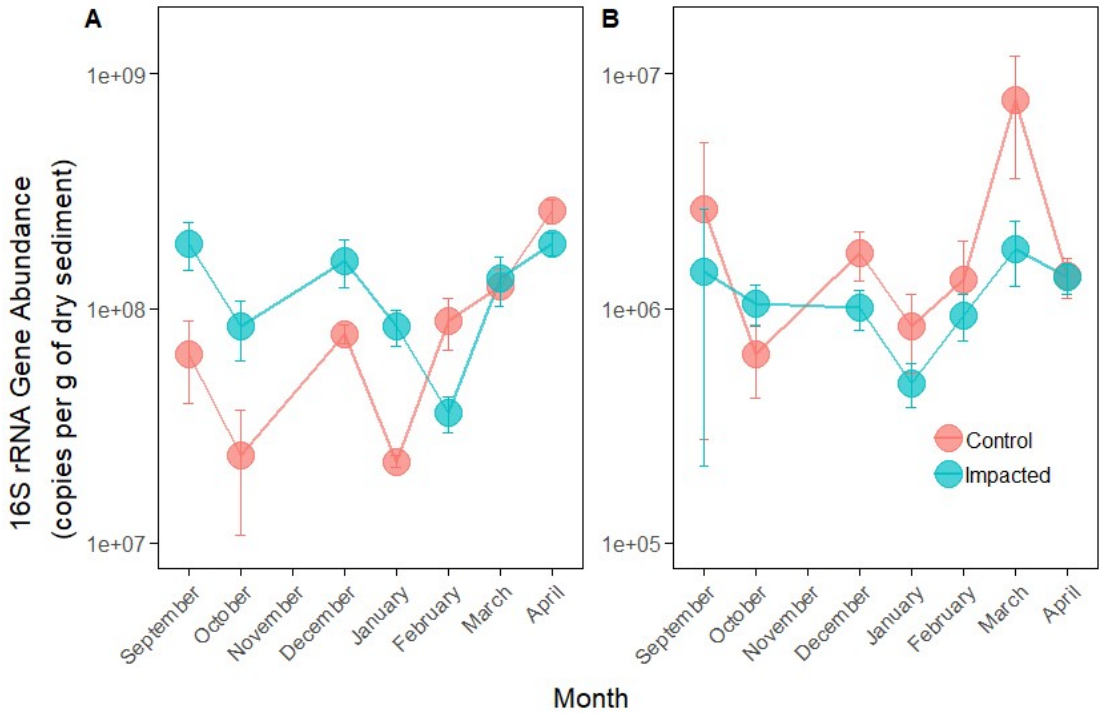

Fig. S4.2: A) bacterial, and B) archaeal, 16S rRNA gene abundance (mean ± SE, *n* = 6 (*n* = 3 for September as Athens only)) in unimpacted ("Control") and oil-impacted ("Impacted") sediments from both the Athens Riviera and Salamina coastlines, between September 2017 and April 2018.

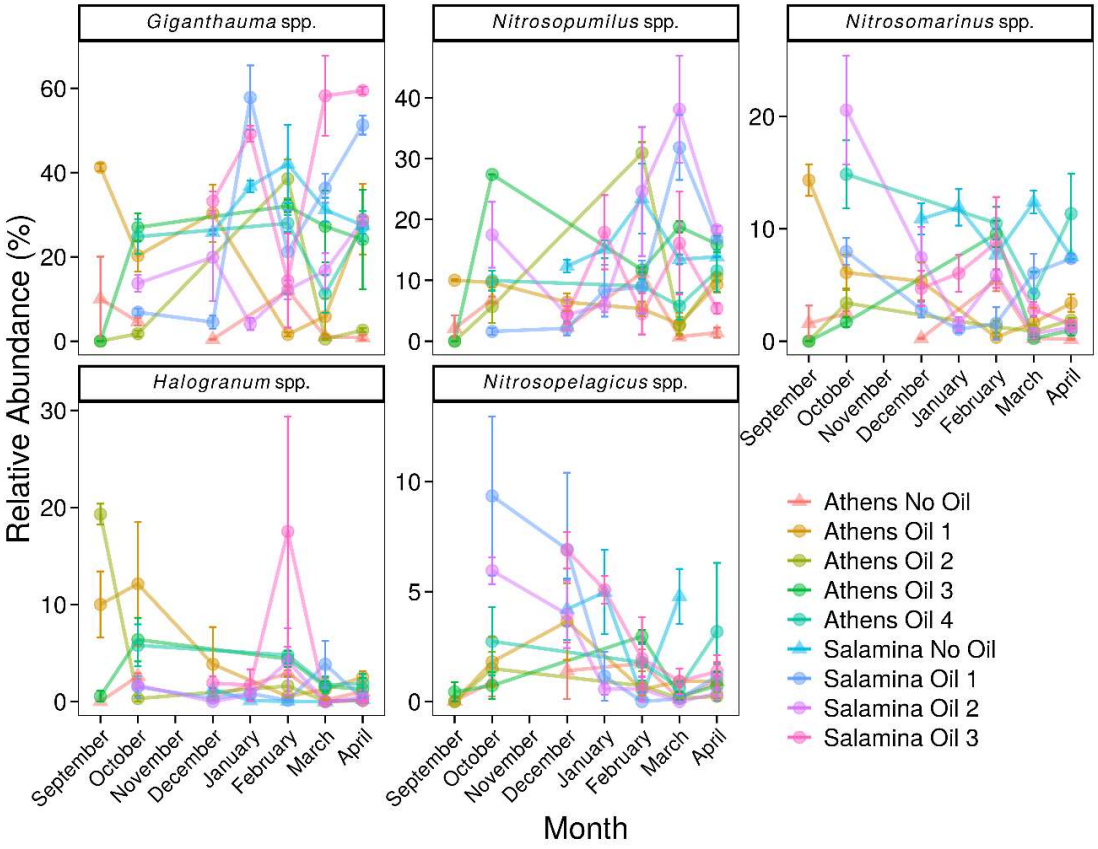

Fig. S4.3: Relative abundance (% of the archaeal community; mean ± SE, *n* = 3) of 16S rRNA gene OTUs assigned to the most abundant *Archaea* in sediments from control (Suffix "No Oil") and oil-impacted (Suffix "Oil") sites along the Athens Riviera and Salamina coastline, from September 2017 to April 2018.

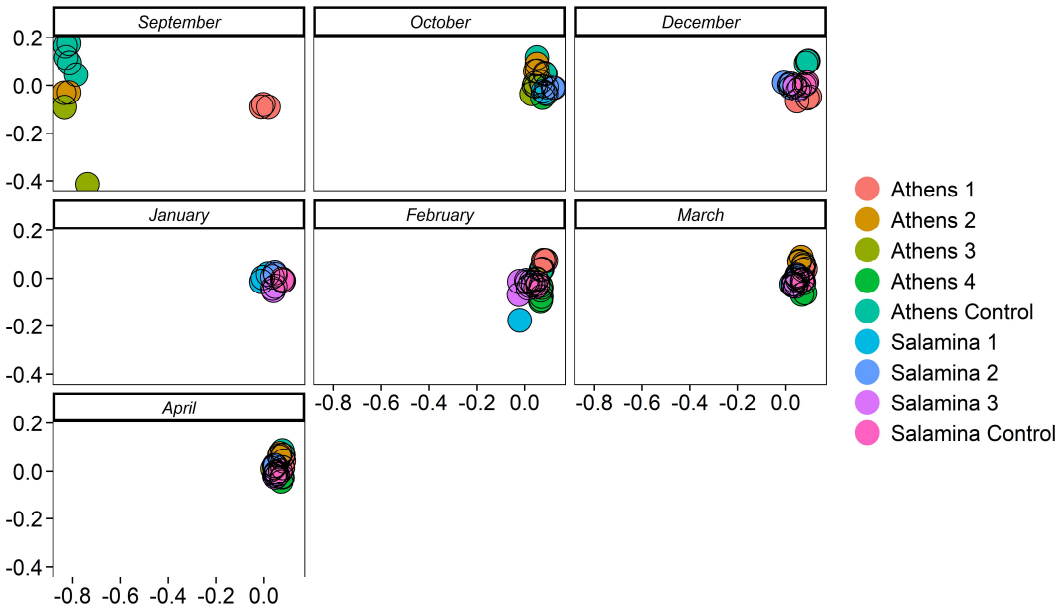

Fig. S4.4: NMDS (non-metric multidimensional scaling) ordination, based on clustered bacterial 16S rRNA OTUs at a 97% similarity threshold, displaying the effect of the Agia Zoni II oil-spill on bacterial community composition from September 2017 until April 2018.

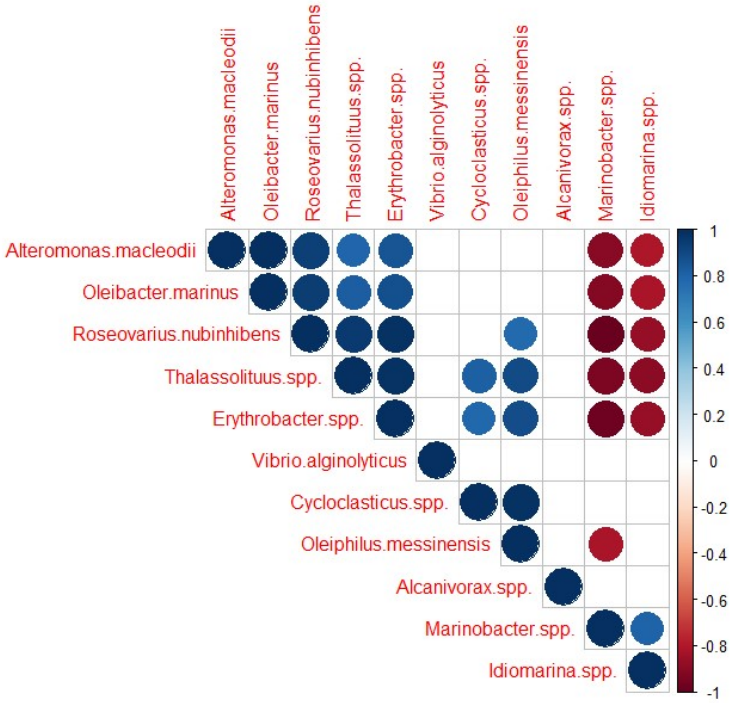

Fig. S4.5: Correlation matrix demonstrating positive (blue) or negative (red) relationships between different oil-degrading genera or species. Blank spaces refer to insignificant relationships.

Table S4.1: Site codes indicate the sampling location as referred to throughout the text and in figures, with exact coordinates (latitude and longitude) and area (either along the Athens Riviera, or, the Salamina coastline).

Site Code	Latitude	Longitude	Area	Response*
Athens No Oil	37°43’1”N	23°55’ E	Athens	No Oil Contamination
Athens Oil 1	37°51’3”N	23°44’55”E	Athens	Manual Removal of Tar Balls
Athens Oil 2	37°51’39”N	23°44’52”E	Athens	Flushing, Trenching, High-powered Washing, Sediment Removal
Athens Oil 3	37°51’54”N	23°44’29”E	Athens	Flushing, Trenching, High-powered Washing, Sediment Removal
Athens Oil 4	37°52’4”N	23°44’13”E	Athens	Flushing, Trenching, High-powered Washing, Sediment Removal
Salamina No Oil	37°55’44”N	23°32’19”E	Salamina	No Oil Contamination
Salamina Oil 1	37°56’31”N	23°33’4”E	Salamina	Flushing, Trenching, High-powered Washing
Salamina Oil 2	37°56’34”N	23°32’34”E	Salamina	Flushing, Trenching, High-powered Washing, Sediment Removal
Salamina Oil 3	37°56’25”N	23°32’17”E	Salamina	High-powered Washing, Absorbents

*Response refers to clean-up operations at the sampling location: Flushing (flushing of sediment with medium pressure water), Trenching (trenching, used in conjunction with flushing to collect oil), High-powered Washing (high-powered washing, to remove oil from hard surfaces), Sediment Removal (removal of coastal sediment, either washed and replace or disposed in landfill), Absorbents (use of absorbents to collect floating oil from the water surface).

Table. S4.2: Evidence demonstrating hydrocarbon-degradation (alkane of PAH) and growth in oil-polluted marine environments (generally or specifically sandy coastal sediments) for certain genera of Bacteria (either OHCB or more metabolically versatile).

Genus	**Hydrocarbon-Degradation Metabolic Capability**	**Isolated Alkane-Degraders**	**Polycyclic Aromatic Hydrocarbon-Degraders**	**Evidence for Increased Abundance in Oiled Marine Environments**[×]	**Evidence for Increased Abundance Oiled Sandy Coastal Sediments**[×]
Alcanivorax spp.	OHCB*	**Yes** – (e.g. Yakimov *et al.*, 1998)	**No –** Clear zone and colour change indicators of PAH-degradation (Yetti et al., 2016) Also, may enhance PAH-degradation utilising alkyl sidechains on methylated PAHs (Yuan et al., 2015; Noh et al., 2018)	**Yes** – (e.g. Kasai *et al.*, 2001; Röling *et al.*, 2004; McKew *et al*., 2007; Wang *et al.*, 2010; Teramoto *et al.*, 2013; Sanni *et al.*, 2015; Lee *et al.*, 2017; Liu *et al.*, 2019)	**Yes** – (e.g. Kostka et al., 2011; Newton *et al.*, 2013; Lamendella et al., 2014; Rodriguez-R *et al.*, 2015; Curtis *et al.*, 2018; Huettel *et al.*, 2018)
Alteromonas spp.	Versatile[±]	**No**	**Yes** – (e.g. *A. distincta (crude oil)* Iwabuchi *et al.*, 2002; ***UD*** *A. naphthalenivorans* strain SN2 Jin *et al.*, 2011)	**Yes** – (e.g. Kasai *et al.*, 2001; Jin *et al*., 2011; Jin *et al.*, 2012; Teramoto *et al.*, 2013; Linda *et al*., 2018)	**Yes** - (e.g. Newton *et al.*, 2013)
Cycloclasticus spp.	OHCB*	**No** (provision; *Cycloclasticus* sp. symbiont of *Bathymodiolus heckerae* – e.g. Rubin-Blum *et al.*, 2017) ***UD***	**Yes** – (e.g. Dyksterhouse *et al.*, 1995)	**Yes** – (e.g. Coulon *et al.*, 2007; Dubinsky *et al.*, 2013; Sanni *et al.*, 2015; Lee *et al.*, 2017; Liu *et al.*, 2017; Linda *et al.*, 2018)	**Yes** – (e.g. Geiselbrecht *et al.*, 1996; Geiselbrecht *et al.*, 1998; Röling *et al.*, 2002)

Erythrobacter spp.	Versatile±	**Yes** – (e.g. *E. flavus* *E. seohaensis* Harwati *et al.*, 2007) ***Both UD***	**Yes** – (e.g. *E. seohaensis* *E. flavus* Harwati *et al.*, 2007 Yuan *et al.*, 2015; *E. atlanticus* Zhuang *et al.*, 2015) ***All UD***	**Yes** – (e.g. McKew *et al.*, 2007; Liu and Liu, 2013; Teramoto *et al.*, 2013; Gao *et al.*, 2015)	**Yes** – (e.g. Macnaughton *et al.*, 1999; Röling *et al.*, 2002; Jiménez *et al.*, 2007)
Idiomarina spp.	Versatile±	**No**	**Yes** – (e.g. *I. baltica* (crude oil) Wang *et al.*, 2010; ***UD*** *I. seosinensis* Yuan *et al.*, 2015; Gomes *et al.*, 2018; *I. piscisalsi* Nzila *et al.*, 2018)	**Yes** – (e.g. Röling *et al.*, 2004; Wang *et al.*, 2010; Albokari *et al.*, 2015)	**Yes** – (e.g. Curtis *et al.*, 2018)
Marinobacter spp.	Versatile±	**Yes** – *(e.g. M. hydrocarbonoclasticus* (Gauthier *et al.*, 1992) *M. flavimaris* ***UD*** e.g. Gomes *et al.*, 2018)	**Yes** – (e.g. *M. flavimaris* *M. alkaliphilus* Yuan *et al.*, 2015; Gomes *et al.*, 2018) ***Both UD***	**Yes** – (e.g. Röling *et al.*, 2004; McKew *et al.*, 2007; Teramoto *et al.*, 2013; Albokari *et al.*, 2015; Sanni *et al.*, 2015; Gao et al., 2015)	**Yes** – (e.g. Kostka et al., 2011; Newton *et al.*, 2013; Lamendella et al., 2014; Rodriguez-R *et al.*, 2015; Curtis *et al.*, 2018; Huettel *et al.*, 2018)
Oleibacter spp.	OHCB*	**Yes** – (e.g. Teramoto *et al.*, 2011)	**No**	**Yes** – (e.g. Teramoto *et al.*, 2013; Sanni *et al.*, 2015; Liu *et al.*, 2017; Liu *et al.*, 2019)	**No**
Oleiphilus spp.	OHCB*	**Yes** – (e.g. Golyshin *et al.*, 2002;	**No**	**Yes** – (e.g. McKew *et al.*, 2007;	**No**

		Toshchakov *et al.*, 2017)		Yang *et al.*, 2016)	
Roseovarius spp.	Versatile[±]	**Yes** – (e.g. *R. crassostreae* (Harwati *et al.*, 2007) ***UD***	**Yes** – (e.g. *R. crassostreae* (Harwati *et al.*, 2007; *R. mucosus* Yuan *et al.*, 2015) ***Both UD***	**Yes** – (e.g. Vila *et al.*, 2010)	**Yes** – (e.g. Gallego *et al.*, 2014; Kappell *et al.*, 2014)
Thalassolituus spp.	OHCB[*]	**Yes** – (e.g. Yakimov *et al.*, 2004)	**No**	**Yes** – (e.g. McKew *et al.*, 2007; Sanni *et al.*, 2015; Lee *et al.*, 2017; Liu *et al.*, 2019)	**No**
Vibrio spp.	Versatile[±]	**Yes** – (e.g. *V. alginolyticus* (Al-Awadhi *et al.*, 2012) Diesel *V. alginolyticus* (Imron and Titah, 2018)	**Yes** – (e.g. *V. cyclotrophicus* (Hedlund and Staley, 2001) ***UD*** *V. anguillarum* (Melcher *et al.*, 2002) Diesel *V. alginolyticus* (Imron and Titah, 2018)	**Yes** – (e.g. Teramoto *et al.*, 2013; Sanni *et al.*, 2015)	**Yes** – (e.g. Geiselbrecht *et al.*, 1996; Rodriguez-R *et al.*, 2015)

***** OHCB – refers to the so called “obligate hydrocarbonoclastic bacteria” (Yakimov *et al.*, 2007)
[±] Versatile – has the metabolic capabilities to grow on a diverse range of substrates
ˣ These lists are by no means exhaustive but are examples of the growth of these genera in either *in situ* or *ex situ* oil-based systems.
UD – this species was not detected in this study

Chapter Five

Evaluation of Polycyclic Aromatic Hydrocarbon Pollution from HMS R*oyal Oak* Shipwreck and Effects on Sediment Microbial Community Structure

Abstract

Given many shipwrecks contain oil products there is a paucity of studies investigating the status of shipwrecks and their surrounding environments. This study evaluates any potential effect the World War II shipwreck HMS *Royal Oak* is having on surrounding benthic sediments in Scapa Flow, Scotland. HMS *Royal Oak* sank in 1939, subsequently leaked oil in the 1960s and 1990s, and is estimated to still hold 697 tonnes of fuel oil. In this study, sediments were analysed, over a 17.5 cm depth profile, along a 50 – 950 m cruciform transect away from the shipwreck. Analysis of polycyclic aromatic hydrocarbons (PAHs) revealed low concentrations (205.91 ± 50.15 μg kg^{-1} of dry sediment), which did not significantly differ with either distance from the shipwreck nor sediment depth. PAH concentrations were well below the ERL (Effects-Range Low) for the OSPAR maritime area and PAHs were confirmed as pyrogenic rather than petrogenic. Moreover, analysis of sediment microbiomes revealed no significant differences in bacterial community structure with distance from the shipwreck, with extremely low levels of obligate hydrocarbonoclasticus bacteria (OHCB; 0.21% ± 0.54%). Both lines of evidence suggest, at the time of sampling, sampled sediments are not currently being impacted by petrogenic hydrocarbons.

Introduction

In the last two decades, the focus on evaluating the environmental impact from shipwrecks has significantly increased (Landquist *et al.*, 2013), especially those from the two World Wars, which constitute >8,600 shipwrecks in the world's seas (Monfils *et al.*, 2006). There is particular concern regarding oil pollution from shipwrecks (Michel *et al.*, 2005; Faksness *et al.*, 2015; Amir-Heidari *et al.*, 2019) because they contain an estimated 2.5 – 20.4 million tonnes of crude oil and petroleum products (Landquist *et al.*, 2017a).

On the 14th October 1939, six weeks after the start of World War II, the British battleship HMS *Royal Oak* was torpedoed by a German submarine and sank to the bottom of Scapa Flow (Orkney Islands, Scotland; Fig. 5.1). As many lives were lost, HMS *Royal Oak* is protected under the Protection of Military Remains Act 1986. The 189 m long and 26,444 tonne battleship lies upside down, approximately 30 m below the surface of the water at its deepest point and 4.9 m at its shallowest point. HMS

Royal Oak sank with approximately 3,000 tonnes of fuel oil on board. It is likely that a large fraction of oil was spilled during the incident, however a significant proportion of oil remained on board. Leaking oil was first observed in the 1960s, and then again during the late 1990s (Hill, 2019). Efforts to remove the fuel oil from the vessel's tanks began in 2006, and by 2010, 1,600 tonnes had been removed (Marine, 2010), though up to 697 tonnes of oil is thought to remain (Hill, 2019). Whilst any visible oil leakage from HMS *Royal Oak* in Scapa Flow has subsided, it is unknown whether there is a legacy of hydrocarbon contamination in the sediments.

Scapa Flow is a large embayment approximately 24 by 13 km, surrounded by the Orkney Islands, situated north east of Scotland, UK (Fig. 5.1) and was the main British fleet base during both World Wars. Much of the marine microbial research conducted in Scapa Flow has focused on microbial mats in sheltered beaches and photosynthetic bacteria (Herbert, 1985; van Gemerden *et al.*, 1989; Wieland *et al.*, 2003). Despite the large number of wrecks (>150; Muir, 2020) and oil pollution events within Scapa Flow, there is a paucity of data on sediment microbial communities of this region. Indeed, there are few studies investigating how shipwrecks impact indigenous microbial communities or evaluating their actual or potential oil pollution. Most of the current literature focuses on archaeological wood (Liu *et al.*, 2018), artefacts (Li *et al.*, 2018), shipwrecks as artificial reefs (Church *et al.*, 2009; Mugge *et al.*, 2019), and microbially induced corrosion (Russell *et al.*, 2004). Hamdan *et al.* (2018) found that World War II and 19th century shipwrecks in the Gulf of Mexico influenced microbial diversity in surface sediments 2 m from the shipwrecks. Sediments around two of the shipwrecks evaluated by Hamdan *et al.* (2018) had no significant effect on microbial diversity and composition. It was suggested that either the greater depths of these shipwrecks, or the fact they were both impacted by the Macondo oil spill, obscured any potential impacts of the shipwrecks on microbial community composition.

A modelling approach (Landquist *et al*. 2013, 2014, 2017a, 2017b) allows the potential for oil leaks from shipwrecks to be predicted. However, *in-situ* sampling of the environment around a shipwreck is ultimately needed to quantify and evaluate whether such shipwrecks pose a threat to the surrounding environment. Furthermore, analyses of *in-situ* microbial communities can provide data that are valuable in the design of post-incident monitoring guidelines (Kirby *et al.*, 2018). This study evaluates historic impact of oil contamination from the shipwreck HMS *Royal Oak* on the surrounding benthic microbial communities. The objective of this study was to determine whether fuel oil from HMS *Royal Oak* displays elevated concentrations in surrounding benthic sediments, using gas chromatography-mass spectrometry to

determine both the concentration and source of sediment PAHs over a 950 m radius of the shipwreck (where those sediments sampled further away act as controls). Furthermore, 16S rRNA gene qPCR and amplicon libraries were used to determine any effects of the shipwreck on sediment bacterial community composition, and to quantify any hydrocarbon-degrading or sentinel bacteria associated with oil pollution.

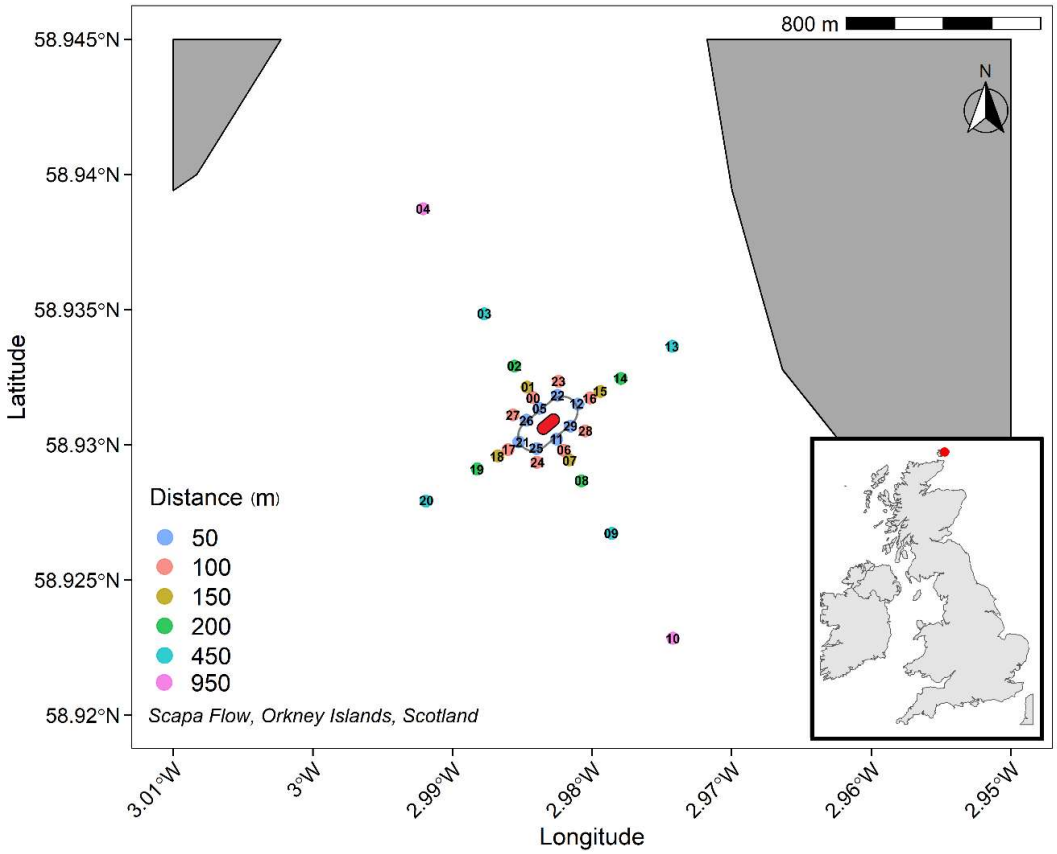

Fig. 5.1: sampling took place between the 3rd and 6th November 2019 in Scapa Flow, Orkney Islands, Scotland, UK (inlet). A 950 m cruciform transect (where those sediments sampled further away act as controls) centred on HMS *Royal Oak* shipwreck (approximation, centre, red), labels refer to sample codes as detailed in Supplementary Material Table S5.1. A safety boundary (grey oval) around HMS *Royal Oak* meant sediment sampling commenced 50 m from the shipwreck.

Results and Discussion

Sediment PAHs Originate from Pyrogenic Sources

Oil-spill hydrocarbon analysis tends to focus on polycyclic aromatic hydrocarbons (PAHs) due to their persistence, carcinogenic, and mutagenic properties (Lehr and Jerina, 1977). The concentration of PAHs (containing 2- to 6-ring parent PAHs and alkylated derivatives (C1-C3)-naphthalenes, (C1-C2)-phenanthrenes, (C1-C3)-dibenzothiophenes, and (C1)-pyrenes) in all sediment samples, around HMS *Royal Oak* shipwreck, ranged from 121 to 348 μg kg^{-1} of dry sediment (Fig. 5.2). There were no significant differences ($p>0.05$) in PAH concentrations between core depths

(2.5, 7.5, 12.5, and 17.5 cm cm) or over distance (50 – 950 m) from the shipwreck, including the transect direction (NE, SE, SW, and NW). There was also no correlation between PAH concentration and distance from the wreck (R^2 = 0.00019 $p>0.05$) nor with sediment depth (R^2 = 0.036 $p>0.05$) (see Supplementary Materials Fig. S5.1). In contrast, sediments near a World War II cargo ship, Nordvard (30 m depth near the Norwegian harbour of Moss), contained PAH concentrations ranging from 3,000 to 25,000 μg kg^{-1} of dry sediment (Ndungu *et al.*, 2017). For comparison, sediment PAH concentrations around both the HMS *Royal Oak* battleship and Nordvard cargo ship were well below those observed in surface coastal sediments contaminated by oil tanker spills such as the Agia Zoni II oil-spill in the Saronic Gulf, Greece (88,000 to 332,000 μg kg^{-1} of dry sediment, Thomas *et al.*, 2020) and the Hebei Spirit oil spill in Daesan Port, South Korea (~71,200 μg kg^{-1} of dry sediment, Kim *et al.*, 2017).

PAH concentrations in sediments around HMS *Royal Oak* were well within typical levels of PAHs found in UK coastal sediments. For example, muddy sediments around Scotland (Woodhead *et al.* 1999), contained PAHs from 75 to 1,212 μg kg^{-1} of dry sediment. Additionally, the observed PAH concentrations within sediments around HMS *Royal Oak* were well below the ERL (Effects-Range Low) and within BC (Background Concentration) levels (3,340 and 212 μg kg^{-1} of dry sediment for ERL and BC, respectively) for sediments in the OSPAR maritime area (North-East Atlantic; Oslo/Paris convention for the Protection of the Marine Environment of the North-East Atlantic; OSPAR Commission, 2009). Therefore, the observed PAH concentrations of sediments around HMS *Royal Oak* would seldom cause negative effects in marine organisms (OSPAR Commission, 2017).

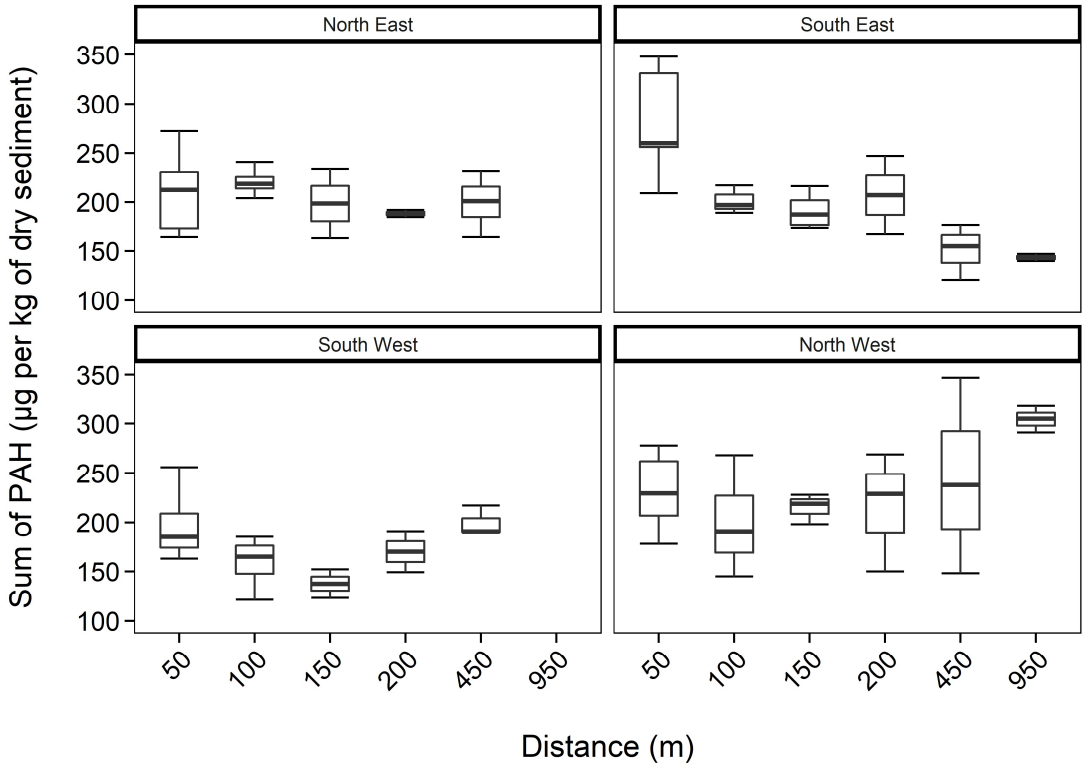

Fig. 5.2: Total PAH concentrations (mean ± SE, *n* = 2) within sediments, including all depths, over 950 m transects (where those sediments sampled further away act as controls) in four different directions from HMS *Royal Oak* shipwreck; located in Scapa Flow, Scotland, UK, November 2019.

As well as evaluating the concentration of environmental PAHs it is also important to determine their origin. PAHs generally enter the environment through three major routes: pyrogenic, petrogenic, or biogenic (Soclo *et al.*, 2000). Pyrogenic PAHs come from the combustion of organic substances at high temperature and low oxygen concentrations, such as industrial thermal cracking and the incomplete combustion of petroleum in motor engines, or from forest fires. Petrogenic PAHs are formed over millions of years at relatively lower temperatures during crude oil maturation and enter the sea from natural seeps or spills and leaks from oil extraction, transportation or storage, or shipwrecks. Finally, biogenic PAHs originate from specific algae and bacteria, or from the degradation of vegetative material (Abdel-Shafy and Mansour, 2016). The evaluation of PAH ratios can provide an accurate identification of the PAH source (Zakaria *et al.*, 2002; Wang and Fingas, 2003; Hussain *et al.*, 2016). Petrogenic PAHs are distinct from pyrogenic PAHs in their chemical composition, with a dominance of C1 to C4 alkylated naphthalenes, phenanthrenes, dibenzothiophenes, fluorenes and chrysenes (Wang and Fingas, 2005). Furthermore, the abundance of LMW (low molecular weight) 2- to 3-ring PAHs is generally much higher than HMW (high molecular weight) 4- to 6-ring PAHs in petrogenic PAHs. Such analysis can determine whether sediment PAHs originated naturally or from anthropogenic inputs

(i.e. shipwrecks) and is important as petrogenic PAHs have increased bioavailability to organisms, especially in filter feeders (Baumard *et al.*, 1998).

Generally, a proportion of LMW (2- and 3-ring) and alkylated (C1-C3 methylnaphthalenes, C1-C2 methylphenanthrenes/anthracenes, C1-C3 methyldibenzothiophenes, C1 methylpyrenes, and C1 methylchrysene) PAHs to total PAHs above 70% would indicate that the PAHs are petrogenic (Law *et al.*, 1999). Our data imply that sediment PAHs around HMS *Royal Oak* were pyrogenic, as the proportion of LMW and alkylated PAHs to total PAHs was significantly below the 70% threshold (coef. 4.02, z 285.5, $p<0.001$); with an overall average of 55% (± 5%) (Fig. 5.3 and see Supplementary Material Table S5.1). Additionally, the proportion of perylene to total 5-ringed aromatics averaged 4% (± 0.6%; Fig. 5.3 and see Supplementary Material Table S5.1); significantly below the 10% threshold (coef. 1.40, z 26.89, $p<0.001$) that is indicative of pyrogenic PAHs (Laflamme and Hites, 1979; Baumard *et al.*, 1998). Only one sample (RO27, 12.5 cm depth) met the 70% threshold (% LMW/alkylated PAHS of total PAHs) for petrogenic PAHs but had a perylene to 5-ringed aromatics ratio of only 4.76%. The accuracy of PAH fingerprinting techniques, such as the above, can be questioned when natural weathering processes and biodegradation may alter PAH distribution patterns. To this regard, Wang et al., (1999) created the "Pyrogenic Index" (PI), which is: ∑(3- to 6-ring EPA priority PAHs)／∑(5 alkylated PAH series); the exact PAHs are available in the original literature. It is suggested this ratio provides better accuracy and less uncertainty than ratios that use individual or LWW PAHs, as the PI is subject to diminutive fluctuation due to changes in individual PAH concentrations. Long-term natural weathering processes and biodegradation have little impact on the ratio, whereas the ratio is significantly altered by combustion. Lighter refined products and most crude oils (i.e. petrogenic) demonstrate a PI of 0.01 while heavy oils and heavy fuel oils range from 0.01 to 0.05. The PI significantly increases for pyrogenic material, for example diesel soot samples were found to be within a range of 0.80 to 2.0 (Wang et al., 1999). The average PI, in sediments around HMS *Royal Oak*, was 1.06 (± 0.34; Fig. 5.3), significantly greater than the thresholds for petrogenic PAHs (coef. 1.04, z 30.67, $p<0.001$). Therefore, considering the results of all three calculations, and the fact none of these results were significantly different over distance from the shipwreck, it can be assumed PAHs detected within sampled sediments around HMS *Royal Oak* were pyrogenic and not from oil that has historically leaked from the shipwreck.

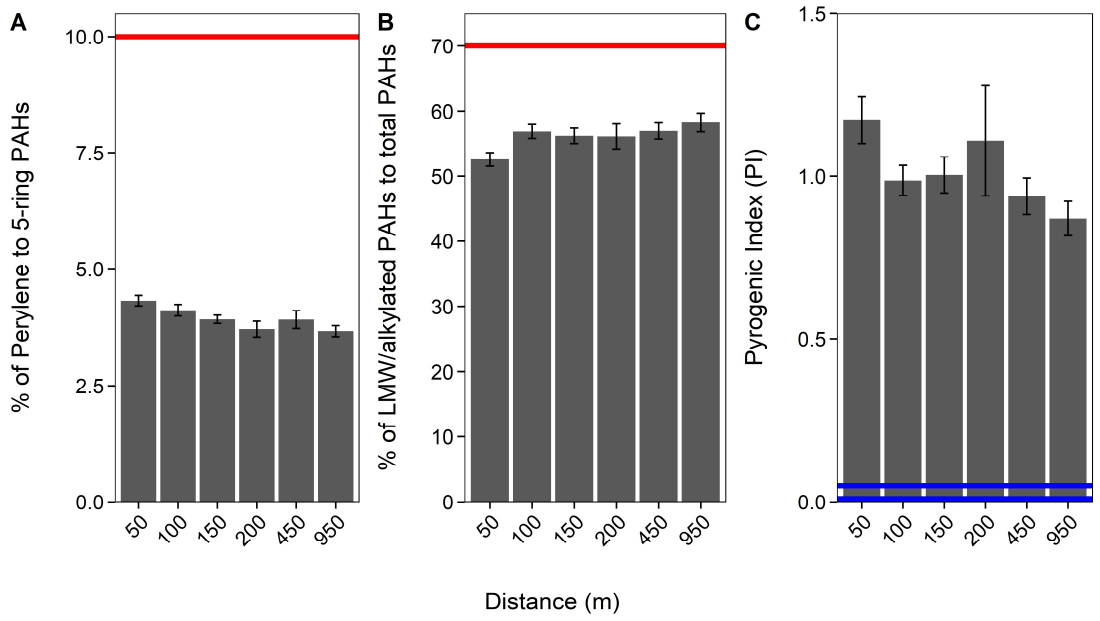

Fig. 5.3: proportion of perylene to 5-ringed aromatics (**A**), of LMW/alkylated PAHs to total PAHs (**B**), and the Pyrogenic Index (PI: ∑(3- to 6-ring EPA priority PAHs)/∑(5 alkylated PAH series)) over a 950 m cruciform transect ("Distance"; where those sediments sampled further away act as controls), from HMS Royal Oak, Scapa Flow, November 2019. Red lines (**A**, **B**) represent the threshold at which PAHs are considered petrogenic. Blue lines (**C**) represent the points below which PAHs are considered petrogenic (0.01 = lighter refined products and most crude oils and 0.01 – 0.05 heavy oil and heavy fuel oils).

Bacterial 16S rRNA Gene Analysis Reveals Low Levels of Hydrocarbon-Degrading Bacteria

Whilst there was no evidence of petrogenic PAHs by GC-MS analysis, evaluating bacterial community composition provides the ability to highlight any localised effects of previous oil-contamination, and reveal any lasting effects caused by previous oil-contamination. Exposure to hydrocarbons can lead to adaptation within indigenous sediment bacterial communities and increases in hydrocarbon oxidising potential, priming the communities for any current or future oil-contamination (Leahy and Colwell, 1990). For example, increased abundance of known hydrocarbon-degrading bacteria (i.e. *Alcanivorax* and *Cycloclasticus*) have been observed in oil-contaminated coastal sediments, many months after hydrocarbons were undetectable (Thomas *et al.*, 2020). Therefore, significantly higher abundance, and a broad diversity, of hydrocarbon-degrading bacteria in sediments close to the shipwreck compared to background levels (i.e. sediments sampled further away from the shipwreck), would indicate that any oil-contamination could be rapidly degraded. Therefore, to determine whether oil from the HMS *Royal Oak* shipwreck has had any effects on sediment bacterial communities, the 16S rRNA gene was analysed by qPCR and amplicon libraries; with an average of 65,239 (range 25,232 – 146,401) sequence reads per sediment sample.

Typically in environments impacted by oil, a large increase in the absolute abundance of Bacteria would be expected due to a selection for hydrocarbon-degrading bacteria, and secondary consumers (Head *et al.*, 2006). For example, bacterial 16S rRNA gene abundance was ~10-fold higher in coastal oiled sediments impacted by the Deep-Water Horizon oil-well-head blowout from Pensacola Beach, Florida, compared to clean sand samples (Kostka *et al.*, 2011). In sediments across the 950 m transects, around HMS *Royal Oak*, the mean bacterial 16S rRNA gene abundance was $1.31 \times 10^8 \pm 7.04 \times 10^7$ copies per g of dry sediment. There were no significant differences ($p>0.05$) observed over the 950m distance from the shipwreck, nor by any transect direction (Supplementary Material Fig. S5.2A/B), providing additional evidence that sediments localised around the ship, were not currently being contaminated with oil. There was, however, a significant increase in 16S rRNA gene abundance (1.57-fold; coef. 0.26, t 2.60, $p<0.05$) at 2.5 cm depth compared to the deeper sediments at 7.5, 12.5, and 17.5 cm (Supplementary Material Fig. S5.2A).

Differences in 16S rRNA gene bacterial sequence diversity (assigned to OTUs at a 97% similarity threshold) was driven primarily by sediment depth ($R^2 = 0.15$, $p<0.001$, $n = 4$; Fig. 5.4). As sediments transitioned from aerobic to anaerobic beyond 2.5 cm depth, the bacterial community differences between 2.5 cm and the deeper sediments (7.5 to 17.5 cm) were primarily driven by significant increases in the relative abundance of anaerobic sulphate-reducing bacteria (e.g. *Desulfatiglans* spp., coef. 1.87, t 7.17, $p<0.001$) and significant decreases in the relative abundance of aerobic ammonia-oxidising bacteria (e.g. *Nitrosospira* spp., coef. -1.72, t -12.18, $p<0.001$). Proximity to the shipwreck had no significant effect on bacterial community composition ($p>0.05$, $n = 4$; Supplementary Material Fig. S5.3), suggesting no evidence of oil-related community changes and adaption within the sediments.

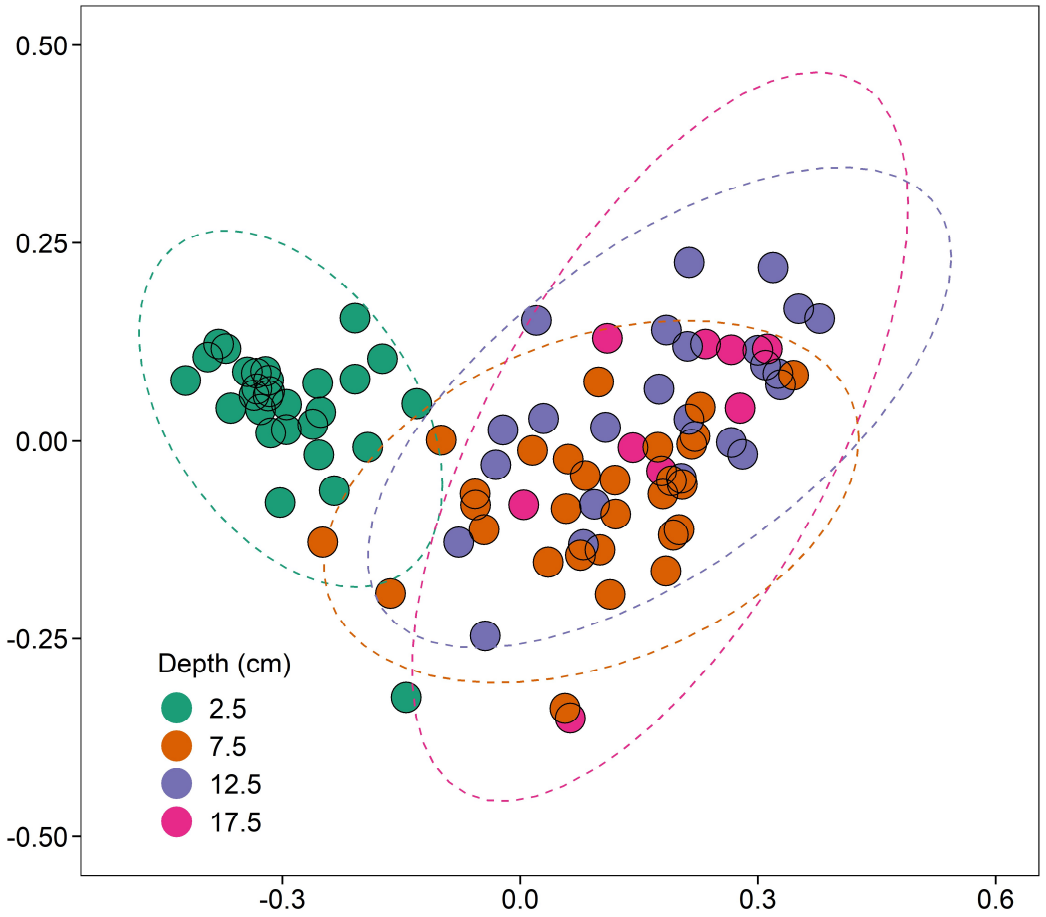

Fig. 5.4: NMDS (non-metric multidimensional scaling) ordination (stress = 0.10), based on clustered bacterial 16S rRNA OTUs at a 97% similarity threshold, displaying the effect of depth (cm) on bacterial community composition (R^2 = 0.15, p<0.001, *n* = 4).

The Ecological Index of Hydrocarbon Exposure (EIHE) is an index from 0 – 1, whereby 1 represents 100% of 16S rRNA gene sequences assigned to bacterial genera with hydrocarbon-biodegradation potential (Lozada *et al.*, 2014). The EIHE, within sediments around HMS *Royal Oak*, was on average 0.008 (± 0.022) over all sediment depths and distances from the shipwreck (Fig. 5.5A-C). There were no significant differences (p>0.05) in the EIHE between sediment depth, distance from the shipwreck, or direction of the transect (Fig. 5.5A-C). The low index (0.012 ± 0.018) at the surface (2.5 cm) would suggest that the greater abundance of the bacterial 16S rRNA gene was not driven by the presence of hydrocarbon-degrading bacteria. The EIHE contains 63 genera, and in sediment samples from this study 36 of these genera were present, although often only in very low relative abundance. The genera *Bacillus*, *Mycobacterium*, *Shewanella*, *Sulfitobacter*, and *Vibrio* made up a large proportion of sequences assigned to the EIHE (87%), in sediments around HMS *Royal Oak*, all of which are genera that primarily contain species that do not degrade hydrocarbons. Compared to other studies of oil-polluted environments, an EIHE of 0.012 (± 0.018) in

surface sediments is exceptionally low (see Fig. 5.5D and Supplementary Material Table S5.2). Comparatively, a study within the Gulf of Mexico revealed that sediments around the shipwreck of the oil-tanker “Halo” (sunk May 1942) contained PAH concentrations ranging approximately 0 to 1,400 μg kg^{-1} of dry sediment respectively, resulting in an EIHE of 0.025 (see Fig. 5.5 and Supplementary Material Table S5.2; Hamdan *et al.*, 2018), two-fold higher than the EIHE observed in surface sediments around HMS *Royal Oak*. Additionally, contaminated sediments sampled five days after the Agia Zoni II oil-spill, which contained average PAH concentrations of 210,000 μg kg^{-1} of dry sediment, resulted in an EIHE of 0.52, 42-fold higher than the EIHE observed in surface sediments of the present study (see Fig. 5.5D and Supplementary Material Table S5.2; Thomas *et al.*, 2020).

Only a minority (5 out of 63) of the genera within the EIHE are assigned to the OHCB (obligate hydrocarbonoclastic bacteria), a group of widely distributed marine bacteria that use hydrocarbons as an almost exclusive source of carbon and energy (Yakimov *et al.*, 2007). Analysis of OHCB genera revealed only a sporadic and very low abundance of *Alcanivorax*, *Oleispira*, *Oleibacter*, and *Thalassolituus* sequences, accounting for only 0.002% relative abundance of the bacterial community. OHCB are typically present in low numbers in uncontaminated environments but rapidly increase in abundance following oil spills (Head *et al.*, 2006). The OHCB are aerobic and so would not be expected to grow in the anaerobic sediments (7.5 to 17.5 cm; see Supplementary Material Fig. S5.4). Whilst many OHCB can use alternative electron acceptors, they cannot degrade oil under anoxic conditions, as activation of hydrocarbons by their oxygenase enzymes requires molecular oxygen (van Beilen *et al.*, 2003). The EIHE does however also include genera that contain known anaerobic hydrocarbon-degraders (Lozada *et al.*, 2014), including for example the genera *Desulfococcus*, *Desulfatibacillum*, *Desulfatiferula*, and *Desulfobacterium*, which were detected only in very low abundance in sampled sediments. *Desulfococcus oleovorans* strain Hxd3 was the first described organism capable of anaerobic hydrocarbon-degradation (Aeckersberg *et al.*, 1991) and others have since been described, including alkane-degraders (e.g. *Desulfatibacillum alkanivorans* strain AK-01; So and Young, 1999). However, there are numerous strains of anaerobic hydrocarbon-degraders that are yet to be assigned to any known genus (e.g. see Rabus *et al.*, 2016), such as the PAH-degrading sulphate-reducing *Deltaproteobacteria* strain NaphS2 (Galushko *et al.*, 1999). Furthermore, certain anaerobic hydrocarbon-degrading bacteria are missing from the EIHE reference list (e.g. *Desulfatiglans* (Jochum *et al.*, 2018) , *Desulfosarcina* (Watanabe *et al.*, 2017), and *Desulfobacula* (Rabus *et al.*, 1993)). These issues, coupled with the fact that in

comparison to aerobic hydrocarbon-degradation there are many anaerobic hydrocarbon-degradation pathways (Widdel *et al.*, 2010; Rabus *et al.*, 2016; Davidova *et al.*, 2018), means that assessments of anaerobic marine environments with the EIHE is much more problematic, and as such, analysis of sediments around HMS *Royal Oak* could potentially underestimate biosignatures for hydrocarbon presence. To this end, the abundance of missing anaerobic hydrocarbon-degrading sulphate-reducing bacteria was calculated separately and constituted 15% of overall sulphate-reducing bacteria. Whilst these hydrocarbon-degrading sulphate-reducing bacteria may have been utilising buried pyrogenic PAHs there was no significant ($p>0.05$) difference in abundance with distance from the shipwreck. The extremely low EIHE, and a low abundance of OHCB and other genera associated with hydrocarbon-degrading (both aerobic and anaerobic), in sediments around HMS *Royal Oak*, suggest an absence of hydrocarbons required to support the growth of hydrocarbon-degrading bacteria.

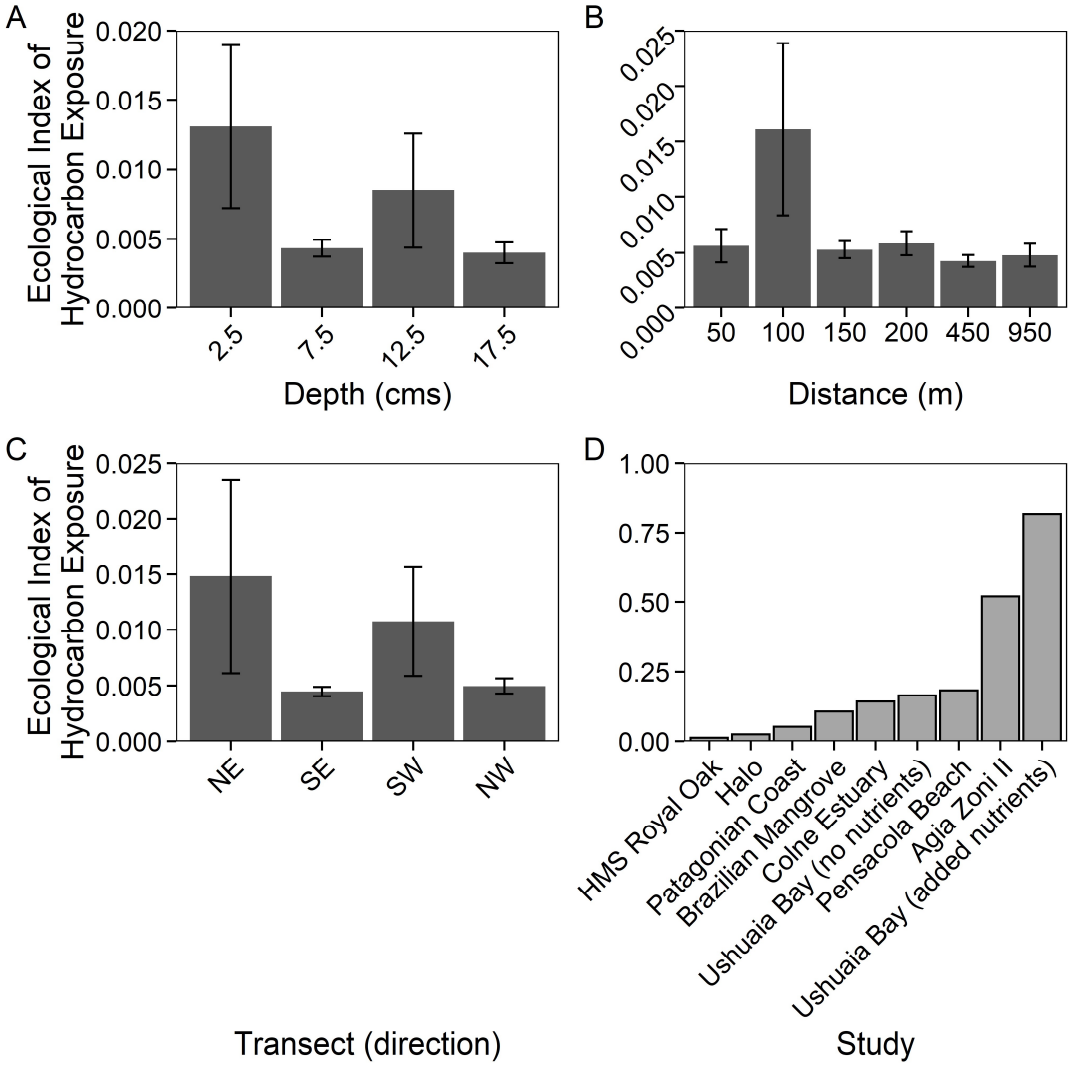

Fig. 5.5: Ecological Index of Hydrocarbon Exposure (EIHE) (ratio up to 1) representing relative abundance of oil-degrading/associated Bacteria, (Lozada et al., 2014) measurements (± SE, *n* = 4), for sediments sampled around the shipwreck HMS *Royal Oak* (located in Scapa Flow, Scotland, UK, November 2019), over a 17.5 cm depth profile (**A**), a 950 m transect (where sediments further away act as controls) (**B**), and given the transect direction (**C**). Additionally, a comparison between the HMS *Royal Oak* EIHE and other studies investigating oil-polluted environments (**D**): "HMS *Royal Oak*" (present study, surface sediments), "Halo" (Hamdan *et al.*, 2018), "Patagonian Coast" (Lozada *et al.*, 2014), "Brazilian Mangrove" (Dos Santos *et al.*, 2011), "Colne Estuary" (Coulon *et al.*, 2012), "Ushuaia Bay (no nutrients)", "Pensacola Beach" (Kostka *et al.*, 2011), "Agia Zoni II" (Thomas *et al.*, 2020) and "Ushuaia Bay (added nutrients)" (Guibert *et al.*, 2012).

Is there Evidence of Historic Oil-Spills, from HMS Royal Oak *Shipwreck, Impacting Surrounding Sediment?*

The low levels of sediment PAHs around the HMS *Royal Oak* were deemed to originate from pyrogenic sources. Bacterial community analysis also revealed extremely low abundances of OHCB and other potential aerobic or anaerobic oil-degrading genera both within the EIHE and those not included. Both lines of evidence therefore suggest that the sampled sediments (50 – 950 m from HMS *Royal Oak*) show no impacts from current oil leaks. Moreover, there is no evidence of impact by the reported historical oil-spills by HMS *Royal Oak*. There remains the possibility of more localised pollution within a 50 m radius, but this region was not sampled in this study due to a 50 m safety boundary. However, should this be the case, it would infer that any pollution would be highly localised to the immediate vicinity around the shipwreck, and this study confirms minimal impacts from leaking oil to the wider surrounding environment.

Experimental Procedures

Sampling Campaign

Sediment cores were sampled using an OSIL extended box corer from 30 sites located on a cruciform transect (four transects: North East, South East, South West, North West) centred around HMS *Royal Oak* shipwreck, employed to capture the dispersion trajectory of any sediment contaminants. Samples were taken 50, 100, 150, 200, 450, and 950 m from the shipwreck along the transects (Scapa Flow, Scotland, UK; 58 55 50N, 002 58 58W), between the 3rd and 6th November 2019 (Fig. 5.1). HMS *Royal Oak* is protected under the Protection of Military Remains Act 1986; therefore a 50 m safety boundary was placed around the shipwreck. Transects were to 950 m, allowing for sufficient sampling coverage and comparison between those closer to the shipwreck and control sediments further away (i.e. 450 – 950 m). At each of the 30 sites, samples were taken from 2.5, 7.5, 12.5, and 17.5 cm sediment depth. See Supplementary Material Table S5.1 for full sample details. The box corer and all

subsampling equipment were pentane-rinsed between sites to prevent cross-station contamination. A CTD was deployed at each sampling site; no significant temporal or spatial differences were recorded regarding temperature (10.35ºC) or salinity (35.27 PSU). Sediments within the survey area comprised poorly sorted fine muddy sands. These findings support the notion that this area of Scapa Flow experiences limited tidal and/or wind-generated water flows. Sediment Profile Imagery (SPI) provided accompanying evidence of this (Supplementary Material Fig. S5.4) and revealed that oxidised sediments were limited to the surficial region (0 to ~2.5 to 5 cm), with clear anoxia below. The SPI imagery further evidenced the presence of both epifauna and infauna species, and associated bioturbative activity, present within the sediment layers. There were no signs of oil contamination during the survey, either visible on the sea surface or in the sediment samples collected.

PAH Analysis

Homogenised sediment samples were extracted using alkaline saponification prior to filtering and subsequent liquid-liquid extraction into pentane. Samples were passed through an alumina chromatography column to remove residual polar compounds and concentrated to 1 ml. Deuterated PAH (naphthalene$_{d8}$, acenaphthylene$_{d8}$, anthracene$_{d10}$, dibenzothiophene$_{d8}$, pyrene$_{d10}$, benzo[*a*]anthracene$_{d12}$, benzo[a]pyrene$_{d12}$, and dibenz[a,h]anthracene$_{d14}$) internal standards were added to each sample and quantification was performed on an Agilent 6890 Gas Chromatography system coupled with an Agilent 5975 Mass Spectrometer with Triple-Axis detector, operating at 70 eV in positive ion mode, using conditions as previously described by Kelly *et al.* (2000). Quantification for PAHs was performed using surrogate standards and five calibrations levels (range 25 – 500 ng ml^{-1}). A suite of alkylated and parent polycyclic aromatic hydrocarbons (PAHs), including compounds with both petrogenic and combustion sources, were then determined. This suite comprised naphthalene and the C1-C3 methylnaphthalenes, acenaphthylene, acenaphthene, fluorene, phenanthrene, anthracene, C1-C2 methylphenanthrenes/ anthracenes, dibenzothiophene and C1-C3 methyldibenzothiophenes, fluoranthene, pyrene, C1 methylpyrenes, benz[a]anthracene, chrysene, C1 methylchrysene, 1,2-benzodiphenylene sulphide, benzo[b]fluoranthene, benzo[k]fluoranthene, benzo[e]pyrene, benzo[a]pyrene, perylene, indeno[1,2,3-cd]pyrene, benzo[ghi]perylene and dibenz[a,h]anthracene. The % oil, within a sample, is calculated by the proportion of low molecular weight (2- and 3-ring) and alkylated (C1-C3 methylnaphthalenes, C1-C2 methylphenanthrenes/anthracenes, C1-C3 methyldibenzothiophenes, C1 methylpyrenes, and C1 methylchrysene) PAHs. The % combustion is the remaining proportion of PAHs within the sample.

qPCR analysis of Bacterial 16S rRNA genes

DNA was extracted from 0.25 g of thawed sediment samples with a DNeasy PowerSoil Kit (Qiagen), according to the manufacturer's instructions. The primers used for quantification of bacterial 16S rRNA were 341f - CCTACGGGNGGCWGCAG and 785r – GACTACHVGGGTATCTAATCC (Klindworth *et al.*, 2013). qPCR reactions were performed using a CFX384™ Real-Time PCR Detection System (BioRad) using reagents, cycle conditions, and standards as previously described (McKew and Smith, 2015; Tatti *et al.*, 2016). Inspection of standard curves showed that all assays produced satisfactory efficiency (74%) and R2 values (>0.99). It should be noted that qPCR of the 16S rRNA gene, whilst providing a valuable comparison of bacterial growth between samples, does not reflect absolute bacterial biomass, as many species contain multiple copies of the 16S rRNA gene.

Amplicon Sequencing and Bioinformatics

Amplicon libraries were prepared, as per Illumina instructions by a 25-cycle PCR. PCR primers were the same as those used for qPCR but flanked with Illumina overhang sequences. A unique combination of Nextera XT v2 Indices (Illumina) were added to PCR products from each sample, via an 8-cycle PCR. PCR products were quantified using Quant-iT PicoGreen dsDNA Assay Kit (TheromFisher Scientific) and pooled in equimolar concentrations. Quantification of the amplicon libraries was determined via NEBNext® Library Quant Kit for Illumina (New England BioLabs Inc.), prior to sequencing on the Illumina MiSeq® platform, using a MiSeq® 600 cycle v3 reagent kit and 20% PhiX sequencing control standard. Raw sequence data have been submitted to the European Nucleotide Archive database under accession number PRJEB37440. Sequence output from the Illumina MiSeq platform were analysed within BioLinux (Field *et al.*, 2006), using a bioinformatics pipeline as described by Dumbrell *et al.*, (2016). Forward sequence reads were quality trimmed using Sickle (Davies and Evans, 1980) prior to error correction within SPades (Nurk *et al.*, 2013) using the BayesHammer algorithm (Nikolenko *et al.*, 2013). The quality filter and error corrected sequence reads were dereplicated, sorted by abundance, and clustered into OTUs (Operational Taxonomic Units) at the 97% level via VSEARCH (Rognes *et al.*, 2016). Singleton OTUs were discarded, as well as chimeras using reference based chimera checking with UCHIME (Edgar *et al.*, 2011). Taxonomic assignment was conducted with RDP Classifier (Wang *et al.*, 2007). Non locus-specific, or artefactual, OTUs were discarded prior to statistical analyses, along with any OTUs that had <70% identity with any sequence in the RDP database.

Statistical Analysis

Prior to community analysis, sequence data were rarefied to the lowest library sequence value (25,232). Data were first tested for normality (Shapiro-Wilks test), those data which were normally distributed were tested for significance with ANOVAs or appropriate linear models. Non-normally distributed data were analysed using appropriate GLMs (Generalised Linear Models) as follows. The relative abundance of OTUs or genera in relation depth, distance, or transect were modelled using multivariate negative binomial GLMs (W. Wang *et al.*, 2010). Here, the number of sequences in each library was accounted for using an offset term, as described previously (Alzarhani *et al.*, 2019). The abundance of bacterial 16S rRNA gene copies was modelled using negative binomial GLMs. The concentration of PAHs, and the difference between means and threshold values, was also modelled using negative binomial GLMs (Venables and Ripley, 2002). The significance of model terms was assessed via likelihood ratio tests. Correlations were performed using Spearman rank correlation with an alpha of 0.05. The Ecological Index of Hydrocarbon Exposure (Lozada *et al.*, 2014) was calculated using the script available at the ecolFudge GitHub page (https://github.com/Dave-Clark/ecolFudge, Clark, 2019) and EIHE values modelled using poisson GLMs. It should be noted that samples from the compared studies (Fig. 5.5D) come from aerobic surface sediments and thus only surface sediments from this study were used in the comparison.

All statistical analyses were carried out in R3.6.1 (R Development Core Team, 2011) using a variety of packages available through the references (Venables and Ripley, 2002; Csardi and Nepusz, 2006; Hope, 2013; Wilke, 2015, 2020; Becker *et al.*, 2016; Auguie, 2017; Oksanen *et al.*, 2019; Hvitfeldt, 2020; Kassambara, 2020; Lenth, 2020; Pedersen, 2020). All plots were constructed using the “ggplot2” (Bodenhofer *et al.*, 2011) and “patchwork” (Pedersen, 2019) R packages.

Supplementary Materials

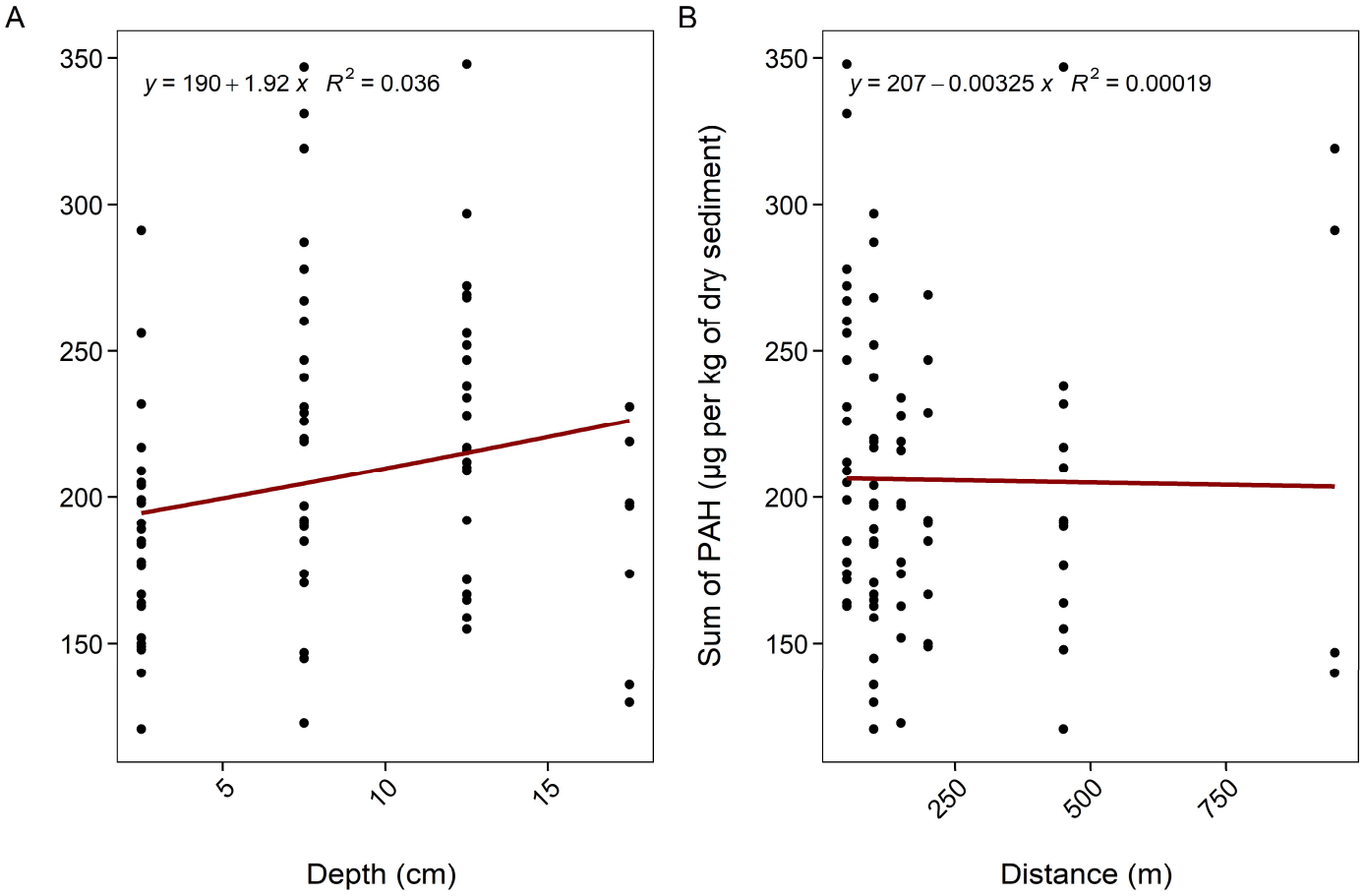

Fig. S5.1: correlations between PAH concentrations (µg kg-^{1} of dry sediment) and depth (cm) (**A**) measured from sediment core samples taken over a 950 m cruciform transect ("Distance"; where 950 m samples represent controls) (**B**), from HMS Royal Oak, Scapa Flow, November 2019.

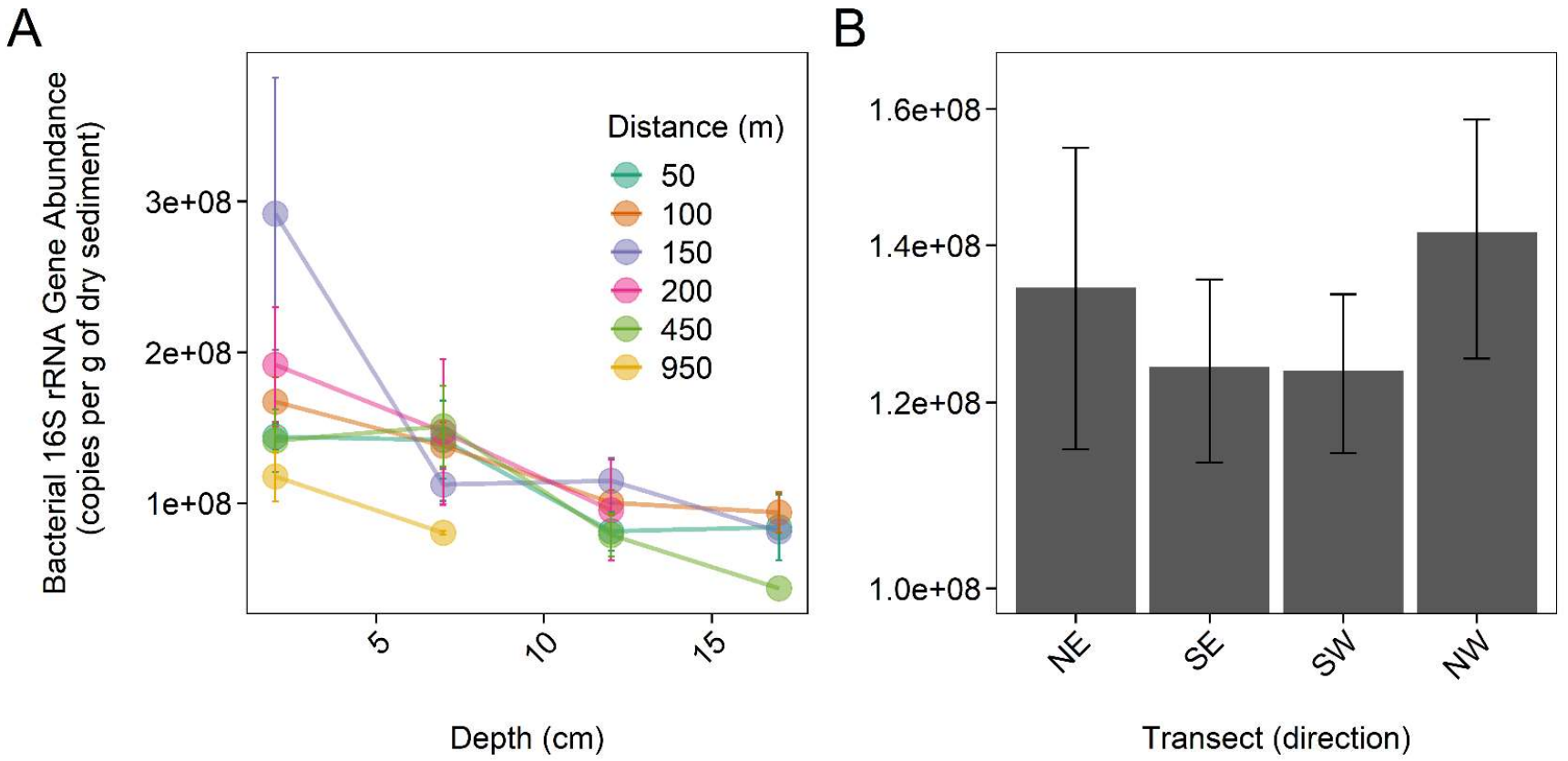

Fig. S5.2: Bacterial 16S rRNA gene abundance (mean ± SE, *n* = 4) at (**A**) increasing depth (cm) measured from sediment core samples taken along a 950 m cruciform transect ("Distance"; where 950 m samples represent controls), and (**B**) between the different transect directions, from HMS *Royal Oak*, Scapa Flow, November 2019.

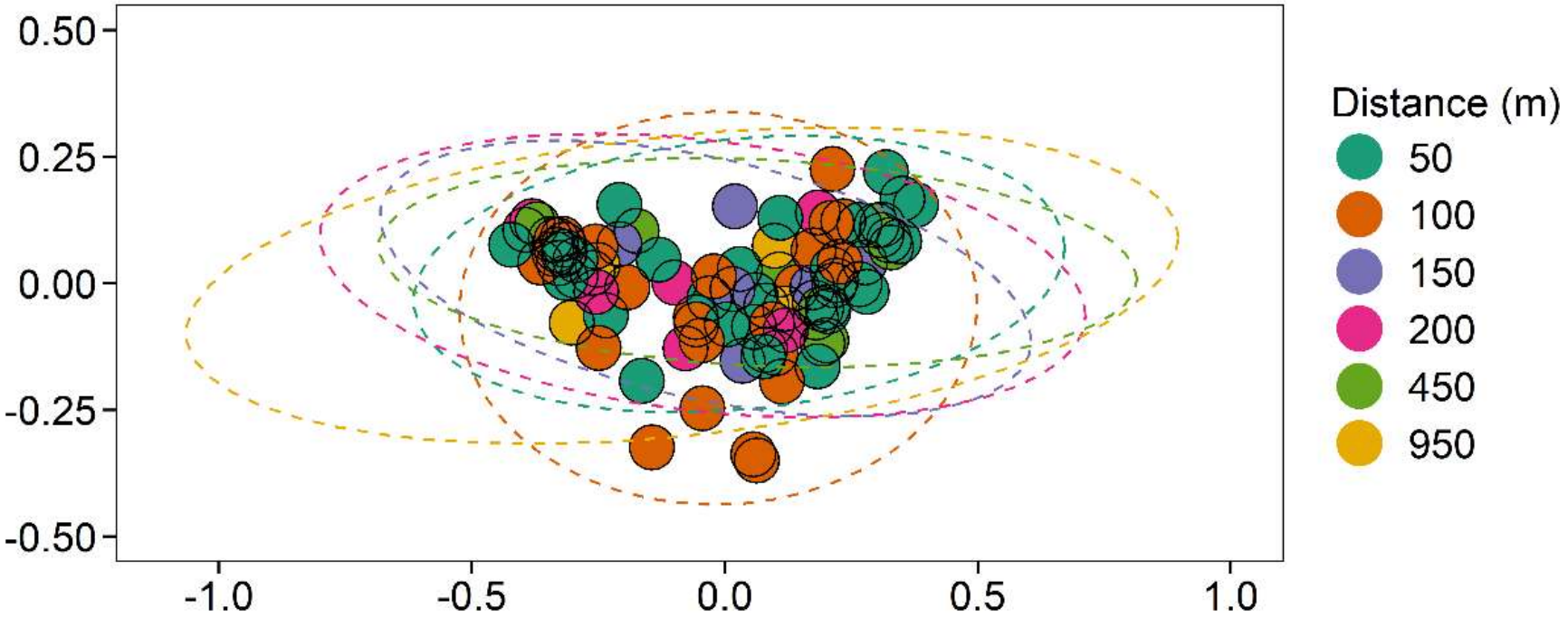

Fig. S5.3: NMDS (non-metric multidimensional scaling) ordination (stress = 0.10), based on clustered bacterial 16S rRNA OTUs at a 97% similarity threshold, displaying the effect of a 950 m transect ("Distance"; where 950 m samples represent controls) from HMS *Royal Oak* on bacterial community composition ($p>0.05$, $n = 4$).

Fig. S5.4: Sediment Profile Imagery (Left) and representative sampled sediment (Right) demonstrates sediments were comprised of poorly sorted fine muddy sands. Oxidised sediments were limited to the superficial region (0 to ~2.5 to 5 cm), with clear anoxia below.

Table S5.1: Oil versus combustion contribution to ∑PAH, concentrations per dry weight sediment. Generally, 70-80% of ∑Oil to ∑PAH (%Oil column) indicates a petrogenic signature (Law *et al.*, 1999). The % oil is calculated by the proportion of low molecular weight (2- and 3-ring) and alkylated (C1-C3 methylnaphthalenes, C1-C2 methylphenanthrenes/anthracenes, C1-C3 methyldibenzothiophenes, C1 methylpyrenes, and C1 methylchrysene) PAHs. The % combustion is the remaining proportion of PAHs within the sample.

Depth (cm)	Distance (m)	Transect	Station	THC (mg kg^{-1})	∑PAH (µg kg^{-1})	∑Oil (µg kg^{-1})	∑Combustion (µg kg^{-1})	%Oil	%Combustion	Ratio (%) of Perylene to five-ringed PAHs
2.50	100	NW	RO00	40.3	184	106	78	58	42	4.56%
7.50	100	NW	RO00	42.7	171	107	64	63	37	4.28%
12.50	100	NW	RO00	59.7	252	145	107	58	42	3.78%
17.50	100	NW	RO00	40.7	198	114	84	58	42	4.18%
2.50	150	NW	RO01	45.4	198	119	79	60	40	3.87%
7.50	150	NW	RO01	56	219	125	94	57	43	3.38%
12.50	150	NW	RO01	56.5	228	116	112	51	49	3.24%
2.50	200	NW	RO02	32.5	150	87	63	58	42	5.31%
7.50	200	NW	RO02	57.2	229	129	100	56	44	3.88%
12.50	200	NW	RO02	56.7	269	145	124	54	46	3.75%
2.50	450	NW	RO03	37	148	84	64	57	43	3.89%
7.50	450	NW	RO03	81.6	347	237	110	68	32	3.76%
12.50	450	NW	RO03	75.1	238	143	95	60	40	3.90%
2.50	950	NW	RO04	62.7	291	170	121	58	42	3.96%
7.50	950	NW	RO04	63.1	319	198	121	62	38	3.74%
2.50	50	NW	RO05	39.6	205	109	96	53	47	4.41%
7.50	50	NW	RO05	72	278	141	137	51	49	4.44%
12.50	50	NW	RO05	61	212	113	99	53	47	3.90%
2.50	100	SE	RO06	41.2	198	109	89	55	45	4.16%
7.50	100	SE	RO06	58.4	197	104	93	53	47	3.93%
12.50	100	SE	RO06	58.2	217	109	108	50	50	3.83%
17.50	100	SE	RO06	35.5	130	71	59	55	45	4.06%

2.50	150	SE	RO07	35.7	178	100	78	56	44	3.94%
7.50	150	SE	RO07	45.8	174	103	71	59	41	3.83%
12.50	150	SE	RO07	55.3	216	116	100	54	46	3.96%
17.50	150	SE	RO07	93.2	197	107	90	54	46	3.75%
2.50	200	SE	RO08	35.5	805	529	276	66	34	3.59%
7.50	200	SE	RO08	65.4	247	134	113	54	46	4.24%
12.50	200	SE	RO08	40.4	167	92	75	55	45	3.28%
2.50	450	SE	RO09	28.4	121	69	52	57	43	3.49%
12.50	450	SE	RO09	41.2	155	80	75	52	48	3.24%
2.50	950	SE	RO10	31.4	140	81	59	58	42	3.56%
7.50	950	SE	RO10	36.4	147	81	66	55	45	3.40%
2.50	50	SE	RO11	57.3	256	120	136	47	53	4.98%
7.50	50	SE	RO11	78.2	331	144	187	44	56	4.62%
12.50	50	SE	RO11	153	348	168	180	48	52	4.25%
2.50	50	NE	RO12	37.4	164	84	80	51	49	4.42%
7.50	50	NE	RO12	61.8	231	109	122	47	53	3.71%
12.50	50	NE	RO12	67.9	272	135	137	50	50	3.70%
17.50	50	NE	RO12	65.3	231	116	115	50	50	4.07%
2.50	450	NE	RO13	35.2	164	97	67	59	41	4.60%
7.50	450	NE	RO13	58.5	616	278	338	45	55	5.56%
12.50	450	NE	RO13	52.6	210	114	96	54	46	3.56%
17.50	450	NE	RO13	37	197	105	92	53	47	3.37%
2.50	200	NE	RO14	46.2	232	140	92	60	40	3.26%
7.50	200	NE	RO14	42.6	192	113	79	59	41	3.67%
12.50	200	NE	RO14	42.8	192	113	79	59	41	3.53%
2.50	150	NE	RO15	36.3	185	115	70	62	38	4.13%
7.50	150	NE	RO15	62.2	966	383	583	40	60	5.93%
2.50	100	NE	RO16	34.5	163	102	61	63	37	4.34%
7.50	100	NE	RO16	52.5	220	131	89	60	40	3.76%
12.50	100	NE	RO16	59.2	234	140	94	60	40	3.85%
2.50	100	SW	RO17	53.3	204	103	101	50	50	4.36%
7.50	100	SW	RO17	36.1	185	113	72	61	39	3.96%

12.50	100	SW	RO17	40.1	159	86	73	54	46	3.67%
17.50	100	SW	RO17	47.1	136	66	70	49	51	3.55%
2.50	150	SW	RO18	30.9	121	68	53	56	44	4.47%
7.50	150	SW	RO18	43.3	123	63	60	51	49	3.33%
2.50	200	SW	RO19	40.5	152	80	72	53	47	3.72%
7.50	200	SW	RO19	53.9	191	106	85	55	45	3.60%
2.50	450	SW	RO20	34.5	149	87	62	58	42	4.57%
7.50	450	SW	RO20	53.5	190	102	88	54	46	3.35%
12.50	450	SW	RO20	60.3	217	119	98	55	45	2.98%
2.50	50	SW	RO21	56.4	191	95	96	50	50	3.51%
7.50	50	SW	RO21	44.8	185	104	81	56	44	4.40%
12.50	50	SW	RO21	48	209	108	101	52	48	4.13%
17.50	50	SW	RO21	50.8	174	89	85	51	49	3.49%
2.50	50	NE	RO22	31.4	163	96	67	59	41	4.41%
7.50	50	NE	RO22	56.6	226	135	91	60	40	4.39%
12.50	50	NE	RO22	45.6	172	99	73	58	42	5.21%
17.50	50	NE	RO22	37.8	174	111	63	64	36	5.94%
2.50	100	NE	RO23	41	199	118	81	59	41	4.44%
7.50	100	NE	RO23	52.6	241	130	111	54	46	4.92%
2.50	100	SW	RO24	36.9	217	143	74	66	34	3.90%
7.50	100	SW	RO24	62.6	287	145	142	51	49	3.88%
12.50	100	SW	RO24	46.8	165	85	80	52	48	3.18%
2.50	50	SW	RO25	32.2	167	96	71	57	43	4.30%
7.50	50	SW	RO25	51.6	404	216	188	53	47	4.66%
12.50	50	SW	RO25	41.6	256	156	100	61	39	3.85%
2.50	50	NW	RO26	41.6	178	93	85	52	48	4.50%
7.50	50	NW	RO26	79.2	267	136	131	51	49	4.18%
12.50	50	NW	RO26	67.4	247	128	119	52	48	3.67%
2.50	100	NW	RO27	29	163	99	64	61	39	4.77%
7.50	100	NW	RO27	29.2	145	88	57	61	39	5.12%
12.50	100	NW	RO27	40.9	268	188	80	70	30	4.76%
17.50	100	NW	RO27	42	219	125	94	57	43	4.36%

2.50	100	SE	RO28	51.1	189	99	90	52	48	4.44%
7.50	100	SE	RO28	58.7	197	101	96	51	49	4.03%
12.50	100	SE	RO28	64.8	297	195	102	66	34	3.55%
2.50	50	SE	RO29	35	209	107	102	51	49	4.60%
7.50	50	SE	RO29	80.8	260	134	126	52	48	4.08%
12.50	50	SE	RO29	303	765	312	453	41	59	5.03%

Table S5.2: comparison of Ecological Index of Hydrocarbon Exposure results, (ratio %) representing relative abundance of oil-degrading/associated bacteria, Lozada et al., 2014) measurements (± SE, *n* = 4), between this study and other oil-polluted environments. *µg per kg of dry sediment; na = not available.

Study	Matrix	EIHE	PAH*	Total Aliphatic Hydrocarbons*	Total Petroleum Hydrocarbons*	Reference	Notes
HMS *Royal Oak*	**Benthic Sediment**	**0.008**	**229**	**na**	**na**	**Current study**	**Avg. over all samples**
Agia Zoni II	Beach Sediment	**0.52**	210,000	2,170,000	na	Thomas *et al.*, 2020	Sediments from the Athens coastline five days after being contaminated by an oil-spill
Brazilian Mangrove	Mangrove Sediment	**0.107**	na	na	1,500,000 to 2,000,000	Dos Santos *et al.*, 2011	Sediment exposed to crude oil (5% v/w) after 23 days
Colne Estuary	Mudflat Sediment	**0.143**	671,000	1,717,000	2,388,000	Coulon *et al.*, 2012	Sediment and crude oil spiked (300 ml m^{-2}) experiment after 2 days
Halo	Benthic Sediment	**0.025**	0 to 1,500	750 to 3,000	2,000,000 to 17,000,000	Hamdan *et al.*, 2018	Ranges overall all depths and distances from Halo shipwreck
Patagonian Coast	Intertidal Sediment	**0.052**	1,054	5,002,000	na	Lozada *et al.*, 2014	Cordova Cove (CC08-1) sediments contaminated by oil-spill 100 days before hand
Pensacola Beach	Beach Sediment	**0.183**	na	na	1,900,000 to 4,500,000	Kostka *et al.*, 2011	Sediments collected had been exposed to oil-contamination from Deep-Water Horizon, collected July 2010
Ushuaia Bay (no nutrients)	Intertidal Sediment	**0.165**	na	19,700 to 347,000	na	Guibert *et al.*, 2012	Sediment-in-seawater slurry spiked with crude oil (0.4% v/v) OS08.oil (no additional nutrients)
Ushuaia Bay (added nutrients)	Intertidal Sediment	**0.817**	na	19,700 to 347,000	na	Guibert *et al.*, 2012	Sediment-in-seawater slurry spiked with crude oil (0.4% v/v) OS08.oilnut (additional nutrients)

Chapter Six

Concluding Remarks

This thesis has evaluated the effects of oil-spills, remediation strategies, and shipwrecks on the structure and succession of hydrocarbon-degrading bacteria (HCB), as well as hydrocarbon-biodegradation, within different marine environments.

The Importance of Experimental Conditions and Sampling Methodology

In chapter two a very clear succession pattern of obligate hydrocarbonoclastic bacteria (OHCB) was observed. Importantly, this succession revealed how the OHCB *Oleispira*, hitherto considered to be a psychrophile, can dominate in the early stages of oil-spill response (1 and 3 days), outcompeting all other OHCB at the relatively high temperature of 16ºC. Multiple theories were suggested as to why *Oleispira* dominated in the first few days, from competitive advantage to a mesophilic phenotype, but it was the early sampling (1 and 3 days) that revealed this novel occurrence. Many *ex situ* oil-spill experiments, and studies of real *in situ* oil spills, neglect sampling the early phase and evaluate HCB response over weeks, months, and even years after oil contamination. Understanding how HCB, and indigenous microbial communities, respond over the long-term is obviously crucial, as it allows for an environment's response and resilience to such disturbances to be evaluated, but the immediate early phase response is equally important, as it allows for the environment's natural ability to attenuate oil to be predicted. Chapter Four highlighted the importance of sampling the early and later phases of an oil-spill. Immediate (five days) sediment sampling after the Agia Zoni II oil-spill revealed a high abundance of HCB, which highlighted the environment's natural ability to attenuate oil whilst uncovering novel microbial relationships. Additionally, the subsequent seven month sampling campaign revealed a legacy effect of HCB within sedimental microbial communities.

Chapter Two not only highlighted the importance of early sampling but also highlighted a number of other significant considerations regarding experimental conditions. Many experimental setups adopt the use of WAF (water-accommodated fractions) and CEWAF (chemically-enhanced water-accommodated fractions) to evaluate the use of dispersants on oil-spills. Fundamentally, oil is stirred into seawater for a set period of time, allowed to settle (i.e. those hydrocarbon fractions not accommodated into the seawater resurface), and then the WAF is sampled from below the water's surface. CEWAF are very similar, except they include the addition of a dispersant which is applied to the surface prior to mixing. Essentially, using these

methodologies means you are comparing a chemically/mechanically dispersed oil (CEWAF) to a mechanically dispersed oil (WAF) and not to a floating surface oil-slick, which is what would occur in the real-world. Moreover, CEWAF can have significantly different concentrations of soluble compounds and tiny oil droplets, the concentration of which is dependent upon mixing energy and time, in comparison to WAF. Additionally, often the increased surface area of oil produced in CEWAF means hydrocarbon concentrations are often higher than WAF. Thus, these methodologies are not truly replicable or comparable. Chapter Two revealed that chemically dispersed oil-slicks, in comparison to a floating oil-slick, significantly increased the abundance of HCB and the rate of alkane-biodegradation in the first 24 hours. Whereas, many experiments which find no effect of dispersant application, or even that dispersant application inhibits the growth of HCB and hydrocarbon-biodegradation, use WAF and CEWAF.

In addition to WAF/CEWAF limitations, *ex situ* oil-spill experiments have received a significant amount of criticism due to their confined nature, which does not allow dispersed oil to rapidly dilute to sub-ppm, which can inhibit hydrocarbon-degradation. Lower concentrations of oil, and dispersion over a wider area, may allow access to further inorganic nutrients which in turn leads to faster hydrocarbon-biodegradation compared to undispersed oil on the surface. However, the results in Chapter Two demonstrated that even with a relatively high oil concentration (1000 ppm), and the confined nature of microcosms, both dispersants and biosurfactants significantly increased the rate of hydrocarbon-degradation and the abundance of HCB in the first 24 hours. Perhaps the initial nutrient loading provided an advantageous environment in which microbes were able to proliferate, whilst overcoming any disadvantages of *ex situ* microcosms. However, Chapter Two also demonstrated that from day three bacterial growth in the microcosms was limited by nitrogen, which may not occur *in situ* where oil can disperse to much wider areas and thus allow access to further inorganic nutrients, which in turn could mean growth is not limited. This once again highlights the importance of sampling the early phase, as the initial advantage of using a dispersant over a floating oil-slick would have otherwise been missed. Conceivably, if growth was not limited, as predicted would happen *in situ*, it may mean hydrocarbon-biodegradation would have not been limited too. Thus, dispersants may have maintained significantly increased alkane-biodegradation, in comparison to the oil-only control, for a longer period of time, which could have translated into significant PAH-biodegradation, which did not occur in the nutrient limited microcosms.

It is vitally important that any *ex situ* oil-spill experiment aims to replicate the environmental conditions observed in the target environment. For example, seawater in Chapter Three (North Sea, Holland) and sediments in Chapter Four (Athens and Salamina, Greece) were found to be oligotrophic, with extremely limited phosphorous, thus, high levels of nutrient loading would be unacceptable in any *ex situ* experiment trying to replicate those environments at that particular time. *In situ* oil-spill experiments should be the gold standard, as they provide real-world environmental conditions, however they undoubtedly come with many logistical, legislative, cultural, and financial barriers. Therefore, *ex situ* experiments will be the adopted methodology the majority of the time and indeed have many benefits, for example control over ecological parameters (chemical, physical, or biological) and their spatial and temporal interactions, providing greater reproducibility and replication. However, potential biases of *ex situ* experiments, especially reduced spatial and temporal scales, should be considered when evaluating results. Future work could focus on evaluating microbial communities, and hydrocarbon-biodegradation rates, whilst comparing a wide range of oil concentrations while using different methodological approaches (WAF, floating slick, micro- and mesocosms, wave tanks, and *in situ*). These comparisons should not only systematically compare spatial scales but also temporal scales, as *ex situ* experiments are often reduced in comparison to real-world scenarios. Furthermore, it would be worthwhile identifying scaling patterns in the design of *ex situ* oil-spill experiments from the literature. Conducting these comparisons would highlight which methodological biases require the most attention when conducting oil-spill research.

Evaluating Microbial Community Response to Oil-spills will Advance and Refine Post-oil-spill Monitoring Models and Guidelines

The Ecological Index of Hydrocarbon Exposure (EIHE), which aims to establish hydrocarbon exposure in an environmental sample based on the relative abundance of bacteria with hydrocarbon-biodegradation potential, was evaluated and discussed in all the chapters of this thesis. Evaluating bacterial communities to this end, whilst in its infancy, can provide insightful outputs which can: 1) provide a baseline of uncontaminated samples to which target samples can be compared, thus providing a proxy for hydrocarbon exposure, and 2) evaluate the potential for an oil-contaminated environment to naturally attenuate oil.

These two outputs were demonstrated in the *in situ* oil-slick experiment in Chapter Three. Firstly, the EIHE score was obtained for “control samples”, in this case from uncontaminated seawater, thus providing a baseline for comparison. Secondly,

the EIHE score from the oil-slicks was extremely low (~0.012), and no different to uncontaminated seawater, even when hydrocarbons were measured at an average of 221 ppm. The lack of HCB growth was potentially due to phosphorous limitation, but regardless, the low EIHE score demonstrated that at the time of sampling the environment had a limited capacity to attenuate oil, and thus other intervention measures (e.g. dispersant application and physical removal) to clean-up the oil would be advised. It is worth noting however that samples were collected up to a maximum of 25.5 hours after oil-slick creation, and therefore HCB growth could have been missed due to a growth lag-phase; though this was not observed in the *ex situ* oil-spill experiment in Chapter Two, where HCB growth was several orders of magnitude within 24 hours when nutrients were plentiful.

Chapter Three highlighted a positive benefit of using the EIHE in oil-polluted environments, however, there are a series of limitations to the EIHE. Firstly, as demonstrated in Chapter Three, the EIHE fails to reveal hydrocarbon exposure in environments where HCB growth is limited by nutrients. Secondly, key genera of bacteria known to contain species able to degrade-hydrocarbons (e.g. *Colwellia*, *Glaciecola*, *Arcobacter*) are absent from the reference list. Lastly, is the overestimation of hydrocarbon exposure in an environment, as the EIHE tool is incapable of species differentiation (i.e. those species within a metabolically-diverse genus able to degrade-hydrocarbons compared to those which cannot). This limitation was demonstrated in Chapter Four where uncontaminated beach sediment samples, with no measurable hydrocarbons, had an EIHE score of 0.30, and was likely due to an overestimation of the genera *Pseudomonas* which contains >200 species of which only a fraction can degrade-hydrocarbons. There are many other genera within the reference list which also contain only a fraction of HCB in relation to more metabolically-diverse species which do not degrade hydrocarbons, and thus overestimation is a clear drawback of the EHIE.

It's evident therefore, improvement and refinement of the EIHE concept, and indeed the creation of a new index all together, is required. Improvements can be achieved through development of the reference list to include all genera which contain HCB. Moreover, the inclusion of any known hydrocarbon-degrading archaea and fungi would also be valuable, though this presents a series of challenges. For example, there are no efficient universal primers to account for all three domains and thus separate sequencing runs would be required, meaning three separate data frames of relative abundances, which could not be combined as members of the domain *Bacteria* are often orders of magnitude more abundant than *Archaea*. Therefore, the new tool could potentially produce three scores, one for each domain, which could

then be compared to uncontaminated samples. This would require considerable literature review but ultimately would make the tool more comprehensive. Testing would be required to determine how beneficial the inclusion of *Archaea* and *Fungi* to the index would be in balance with additional financial and time expenditure (i.e. sequencing). It is worth noting that the selection of primers should carefully be considered whenever taxonomic analysis is being conducted; aiming for a balance between efficiency, specificity, and sensitivity. This is because bacterial primers, frequently used in this type of analysis, were often developed some time ago, whereby they were referenced against redundant phylogenetic databases or originated from *in vitro* cultured species. Using suboptimal primer pairs can cause under-representation of certain taxa or amplification of non-target sequences.

To address the issue of overestimation, samples could be compared to a reference list not at the genus level but at a species level. To achieve this would be a difficult undertaking and would require comparing a samples 16S rRNA sequence to an internal reference database; which would be required to contain all the 16S rRNA sequences of all HCB as well as all non-hydrocarbon-degrading bacterial species within the same genus. Subsequently, the index would require comprehensive testing, to determine whether the new index was able to better reveal hydrocarbon exposure and an environments ability to naturally attenuate oil, in comparison to the current EIHE tool. Testing could involve a range of matrices (e.g. seawater and sediment), environmental conditions (e.g. nutrient and mixing energy), and a broad range of oil concentrations to determine if the current EIHE limitations had been overcome. Once these limitations have been corrected, such a tool would prove impactful in not only revealing the presence of hydrocarbons but also in highlighting an environment's ability to naturally attenuate oil. Such a tool could be included in post-oil-spill assessment (such as being incorporated into the Spill Impact Mitigation Assessment, SIMA), thus adding valuable information to oil-spill-response management when assessing intervention measures.

References

Abbasian, F., Lockington, R., Mallavarapu, M., and Naidu, R. (2015) A Comprehensive Review of Aliphatic Hydrocarbon Biodegradation by Bacteria. *Appl Biochem Biotechnol* **176**: 670–699.

Abdel-Shafy, H.I. and Mansour, M.S.M. (2016) A review on polycyclic aromatic hydrocarbons: Source, environmental impact, effect on human health and remediation. *Egypt J Pet* **25**: 107–123.

Abraham, W.R., Meyer, H., and Yakimov, M. (1998) Novel glycine containing glucolipids from the alkane using bacterium Alcanivorax borkumensis. *Biochim Biophys Acta - Lipids Lipid Metab* **1393**: 57–62.

Acosta-González, A., Martirani-von Abercron, S.M., Rosselló-Móra, R., Wittich, R.M., and Marqués, S. (2015) The effect of oil spills on the bacterial diversity and catabolic function in coastal sediments: a case study on the Prestige oil spill. *Environ Sci Pollut Res* **22**: 15200–15214.

Aeckersberg, F., Bak, F., and Widdel, F. (1991) Anaerobic oxidation of saturated hydrocarbons to CO2 by a new type of sulfate-reducing bacterium. *Arch Microbiol* **156**: 5–14.

Aeppli, C., Swarthout, R.F., O'Neil, G.W., Katz, S.D., Nabi, D., Ward, C.P., et al. (2018) How Persistent and Bioavailable Are Oxygenated Deepwater Horizon Oil Transformation Products? *Environ Sci Technol* **52**: 7250–7258.

Afshar-Mohajer, N., Fox, M.A., and Koehler, K. (2019) The human health risk estimation of inhaled oil spill emissions with and without adding dispersant. *Sci Total Environ* **654**: 924–932.

Al-Awadhi, H., Dashti, N., Kansour, M., Sorkhoh, N., and Radwan, S. (2012) Hydrocarbon-utilizing bacteria associated with biofouling materials from offshore waters of the Arabian Gulf. *Int Biodeterior Biodegrad* **69**: 10–16.

Al-Mallah, M., Goutx, M., Mille, G., and Bertrand, J.C. (1990) Production of emulsifying agents during growth of a marine Alteromonas in sea water with eicosane as carbon source, a solid hydrocarbon. *Oil Chem Pollut* **6**: 289–305.

Albokari, M., Mashhour, I., Alshehri, M., Boothman, C., and Al-Enezi, M. (2015) Characterization of microbial communities in heavy crude oil from Saudi Arabia. *Ann Microbiol* **65**: 95–104.

Alexander, F.J., King, C.K., Reichelt-Brushett, A.J., and Harrison, P.L. (2017) Fuel oil and dispersant toxicity to the Antarctic sea urchin (Sterechinus neumayeri). *Environ Toxicol Chem* **36**: 1563–1571.

Almeida, C.M.R., Reis, I., Couto, M.N., Bordalo, A.A., and Mucha, A.P. (2013)

Potential of the microbial community present in an unimpacted beach sediment to remediate petroleum hydrocarbons. *Environ Sci Pollut Res* **20**: 3176–3184.

Alonso-Gutiérrez, J., Costa, M.M., Figueras, A., Albaigés, J., Viñas, M., Solanas, A.M., and Novoa, B. (2008) Alcanivorax strain detected among the cultured bacterial community from sediments affected by the “Prestige” oil spill. *Mar Ecol Prog Ser* **362**: 25–36.

Alzarhani, A.K., Clark, D.R., Underwood, G.J.C., Ford, H., Cotton, T.E.A., and Dumbrell, A.J. (2019) Are drivers of root-associated fungal community structure context specific? *ISME J* **13**: 1330–1344.

Amir-Heidari, P., Arneborg, L., Lindgren, J.F., Lindhe, A., Rosén, L., Raie, M., et al. (2019) A state-of-the-art model for spatial and stochastic oil spill risk assessment: A case study of oil spill from a shipwreck. *Environ Int* **126**: 309–320.

Andelman, J.B. and Suess, M.J. (1970) Polynuclear aromatic hydrocarbons in the water environment. *Bull World Health Organ* **43**: 479–508.

Ashby, R.D., Solaiman, D.K.Y., and Foglia, T.A. (2008) Property control of sophorolipids: Influence of fatty acid substrate and blending. *Biotechnol Lett* **30**: 1093–1100.

Atlas, R.M. (1981) Microbial degradation of petroleum hydrocarbons: An environmental perspective. *Microbiol Rev* **45**: 180–209.

Atlas, R.M. and Hazen, T.C. (2011) Oil biodegradation and bioremediation: A tale of the two worst spills in U.S. history. *Environ Sci Technol* **45**: 6709–6715.

Auguie, B. (2017) gridExtra: functions in Grid graphics. R Package Version 2.3. *CRAN Proj*.

Bacosa, H.P., Erdner, D.L., Rosenheim, B.E., Shetty, P., Seitz, K.W., Baker, B.J., and Liu, Z. (2018) Hydrocarbon degradation and response of seafloor sediment bacterial community in the northern Gulf of Mexico to light Louisiana sweet crude oil. *ISME J* **12**: 2532–2543.

Bælum, J., Borglin, S., Chakraborty, R., Fortney, J.L., Lamendella, R., Mason, O.U., et al. (2012) Deep-sea bacteria enriched by oil and dispersant from the Deepwater Horizon spill. *Environ Microbiol* **14**: 2405–2416.

Banat, I.M. (1995) Biosurfactants production and possible uses in microbial enhanced oil recovery and oil pollution remediation: A review. *Bioresour Technol* **51**: 1–12.

Banat, I.M., Franzetti, A., Gandolfi, I., Bestetti, G., Martinotti, M.G., Fracchia, L., et al. (2010) Microbial biosurfactants production, applications and future potential. *Appl Microbiol Biotechnol* **87**: 427–444.

Banat, I.M., Makkar, R.S., and Cameotra, S.S. (2000) Potential commercial applications of microbial surfactants. *Appl Microbiol Biotechnol* **53**: 495–508.

Banat, I.M., Satpute, S.K., Cameotra, S.S., Patil, R., and Nyayanit, N. V. (2014) Cost effective technologies and renewable substrates for biosurfactants' production. *Front Microbiol* **5**: 1–18.

Barnsley, E.A. (1976) Naphthalene metabolism by pseudomonads: The oxidation of 1,2-dihydroxynaphthalene to 2-hydroxychromene-2-carboxylic acid and the formation of 2′-hydroxybenzalpyruvate. *Biochem Biophys Res Commun* **72**: 1116–1121.

Baumard, P., Budzinski, H., Michon, Q., Garrigues, P., Burgeot, T., and Bellocq, J. (1998) Origin and bioavailability of PAHs in the Mediterranean Sea from mussel and sediment records. *Estuar Coast Shelf Sci* **47**: 77–90.

Beazley, M.J., Martinez, R.J., Rajan, S., Powell, J., Piceno, Y.M., Tom, L.M., et al. (2012) Microbial community analysis of a coastal salt marsh affected by the Deepwater Horizon oil spill. *PLoS One* **7**:.

Becker, R.A., Wilks, A.R., Brownrigg, R., Minka, T.P., and Deckmyn, A. (2016) Package "maps": Draw Geographical Maps. *R Packag version 23-6*.

Van Beilen, J.B., Funhoff, E.G., Van Loon, A., Just, A., Kaysser, L., Bouza, M., et al. (2006) Cytochrome P450 alkane hydroxylases of the CYP153 family are common in alkane-degrading eubacteria lacking integral membrane alkane hydroxylases. *Appl Environ Microbiol* **72**: 59–65.

van Beilen, J.B., Li, Z., Duetz, W.A., Smits, T.H.M., and Witholt, B. (2003) Diversité des systèmes alcane hydroxylase dans l'environnement. *Oil Gas Sci Technol* **58**: 427–440.

Van Beilen, J.B., Marín, M.M., Smits, T.H.M., Röthlisberger, M., Franchini, A.G., Witholt, B., and Rojo, F. (2004) Characterization of two alkane hydroxylase genes from the marine hydrocarbonoclastic bacterium Alcanivorax borkumensis. *Environ Microbiol* **6**: 264–273.

van Beilen, J.B., Panke, S., Lucchini, S., Franchini, A.G., Röthlisberger, M., and Witholt, B. (2001) Analysis of Pseudomonas putida alkane-degradation gene clusters and flanking insertion sequences: Evolution and regulation of the alk genes. *Microbiology* **147**: 1621–1630.

Bejarano, A.C., Clark, J.R., and Coelho, G.M. (2014) Issues and challenges with oil toxicity data and implications for their use in decision making: A quantitative review. *Environ Toxicol Chem* **33**: 732–742.

Bejarano, A.C., Levine, E., and Mearns, A.J. (2013) Effectiveness and potential ecological effects of offshore surface dispersant use during the Deepwater Horizon oil spill: A retrospective analysis of monitoring data. *Environ Monit Assess* **185**: 10281–10295.

Bellamy, D.J., Clarke, P.H., John, D.M., Jones, D., Whittick, A., and Darke, T. (1967) Effects of pollution from the Torrey Canyon on littoral and sublittoral ecosystems. *Nature* **216**: 1170–1173.

Bernhard, A.E., Sheffer, R., Giblin, A.E., Marton, J.M., and Roberts, B.J. (2016) Population dynamics and community composition of ammonia oxidizers in salt marshes after the Deepwater Horizon oil spill. *Front Microbiol* **7**:.

Binark, N., Güven, K.C., Gezgin, T., and Ünlü, S. (2000) Oil pollution of marine algae. *Bull Environ Contam Toxicol* **64**: 866–872.

Blumer, M. (1971) Scientific aspects of the oil spill problem. *Environ Aff* **54**: 54–77.

Boccadoro, C., Krolicka, A., Receveur, J., Aeppli, C., and Le Floch, S. (2018) Microbial community response and migration of petroleum compounds during a sea-ice oil spill experiment in Svalbard. *Mar Environ Res* **142**: 214–233.

Bodenhofer, U., Kothmeier, A., and Hochreiter, S. (2011) Apcluster: An R package for affinity propagation clustering. *Bioinformatics* **27**: 2463–2464.

Bossert, I. and Bartha, R. (1984) Fate of Petroleum in Soil Ecosystems., New York, US: Macmillan Publishing Co.

Boufadel, M.C., Sharifi, Y., Van Aken, B., Wrenn, B.A., and Lee, K. (2010) Nutrient and oxygen concentrations within the sediments of an Alaskan beach polluted with the Exxon Valdez oil spill. *Environ Sci Technol* **44**: 7418–7424.

Bousso, R. (2018) BP Deepwater Horizon costs balloon to $65 billion. *Reuters*.

Bragg, J.R., Prince, R.C., Harner, E.J., and Atlas, R.M. (1994) Effectiveness of bioremediation for the Exxon Valdez oil spill. *Nature* **368**: 413–418.

Brakstad, O.G., Daling, P.S., Faksness, L.G., Almås, I.K., Vang, S.H., Syslak, L., and Leirvik, F. (2014) Depletion and biodegradation of hydrocarbons in dispersions and emulsions of the Macondo 252 oil generated in an oil-on-seawater mesocosm flume basin. *Mar Pollut Bull* **84**: 125–134.

Brakstad, O.G., Nonstad, I., Faksness, L.G., and Brandvik, P.J. (2008) Responses of microbial communities in Arctic sea ice after contamination by crude petroleum oil. *Microb Ecol* **55**: 540–552.

Brakstad, O.G., Nordtug, T., and Throne-Holst, M. (2015) Biodegradation of dispersed Macondo oil in seawater at low temperature and different oil droplet sizes. *Mar Pollut Bull* **93**: 144–152.

Brakstad, Odd G., Ribicic, D., Winkler, A., and Netzer, R. (2018) Biodegradation of dispersed oil in seawater is not inhibited by a commercial oil spill dispersant. *Mar Pollut Bull* **129**: 555–561.

Brakstad, Odd Gunnar, Størseth, T.R., Brunsvik, A., Bonaunet, K., and Faksness, L.G. (2018) Biodegradation of oil spill dispersant surfactants in cold seawater.

Chemosphere **204**: 290–293.

Brandvik, P.J., Johansen, Ø., Davies, E.J., Leirvik, F., Krause, D.F., Daling, P.S., et al. (2017) Subsea Dispersant Injection (SSDI) - Summary Findings from a Multi-Year Research and Development Industry Initiative. *Int Oil Spill Conf Proc*.

Brandvik, P.J., Resby, J.L.M., Daling, P.S., Leirvik, F., and Fritt-Rasmussen, J. (2010) Meso-Scale Weathering of Oil as a Function of Ice Conditions. Oil Properties, Dispersibility, and In Situ Burnability of Weathered Oil as a Function of Time. JIP Report no. 19 (SINTEF A15563), Trondheim, Norway.

Bretherton, L., Kamalanathan, M., Genzer, J., Hillhouse, J., Setta, S., Liang, Y., et al. (2019) Response of natural phytoplankton communities exposed to crude oil and chemical dispersants during a mesocosm experiment. *Aquat Toxicol* **206**: 43–53.

Brion, N., Baeyens, W., De Galan, S., Elskens, M., and Laane, R.W.P.M. (2004) The North Sea: Source or sink for nitrogen and phosphorus to the Atlantic Ocean? *Biogeochemistry* **68**: 277–296.

Bristow, L.A., Mohr, W., Ahmerkamp, S., and Kuypers, M.M.M. (2017) Nutrients that limit growth in the ocean. *Curr Biol* **27**: R474–R478.

Brockmann, U.H., Laane, R.W.P.M., and Postma, J. (1990) Cycling of nutrient elements in the North Sea. *Netherlands J Sea Res* **26**: 239–264.

Broman, D., Ganning, B., and Lindblad, C. (1983) Effects of high pressure, hot water shore cleaning after oil spills on shore ecosystems in the Northern Baltic proper. *Mar Environ Res* **10**: 173–187.

Buist, I., Potter, S., Nedwed, T., and Mullin, J. (2011) Herding surfactants to contract and thicken oil spills in pack ice for in situ burning. *Cold Reg Sci Technol* **67**: 3–23.

Burger, J. (1997) Oil Spills, New Brunswick: Rutgers University Press.

Burns, K.A., Garrity, S.D., and Levings, S.C. (1993) How many years until mangrove ecosystems recover from catastrophic oil spills? *Mar Pollut Bull* **26**: 239–248.

Cai, Z., Liu, W., Fu, J., O'Reilly, S.E., and Zhao, D. (2017) Effects of oil dispersants on photodegradation of parent and alkylated anthracene in seawater. *Environ Pollut* **229**: 272–280.

Caiazza, N.C., Shanks, R.M.Q., and O'Toole, G.A. (2005) Rhamnolipids modulate swarming motility patterns of Pseudomonas aeruginosa. *J Bacteriol* **187**: 7351–7361.

Cappello, S., Caruso, G., Zampino, D., Monticelli, L.S., Maimone, G., Denaro, R., et al. (2007) Microbial community dynamics during assays of harbour oil spill bioremediation: A microscale simulation study. *J Appl Microbiol* **102**: 184–194.

Cappello, S. and Yakimov, M. (2010) Alcanivorax. In *Handbook of Hydrocarbon and*

Lipid Microbiology. McGenity, T.J. (ed). Berlin Heidelberg: Springer-Verlag, pp. 1737–1748.

Caruso, G., Denaro, R., Genovese, M., Giuliano, L., Mancuso, M., and Yakimov, M. (2004) New methodological strategies for detecting bacterial indicators. *Chem Ecol* **20**: 167–181.

Ceresana (2015) Market Study on Surfactants, Konstanz, Germany.

Chandrasekar, S., Sorial, G.A., and Weaver, J.W. (2006) Dispersant effectiveness on oil spills - impact of salinity. *ICES J Mar Sci* **63**: 1418–1430.

Chandrasekar, S., Sorial, G.A., and Weaver, J.W. (2005) Dispersant effectiveness on three oils under various simulated environmental conditions. *Environ Eng Sci* **22**: 324–336.

Chang, J.S., Radosevich, M., Jin, Y., and Cha, D.K. (2004) Enhancement of phenanthrene solubilization and biodegradation by trehalose lipid biosurfactants. *Environ Toxicol Chem* **23**: 2816–2822.

Chebbi, A., Hentati, D., Zaghden, H., Baccar, N., Rezgui, F., Chalbi, M., et al. (2017) Polycyclic aromatic hydrocarbon degradation and biosurfactant production by a newly isolated Pseudomonas sp. strain from used motor oil-contaminated soil. *Int Biodeterior Biodegrad* **122**: 128–140.

Chong, H. and Li, Q. (2017) Microbial production of rhamnolipids: Opportunities, challenges and strategies. *Microb Cell Fact* **16**:.

Chronopoulou, P.M., Sanni, G.O., Silas-Olu, D.I., van der Meer, J.R., Timmis, K.N., Brussaard, C.P.D., and McGenity, T.J. (2015) Generalist hydrocarbon-degrading bacterial communities in the oil-polluted water column of the North Sea. *Microb Biotechnol* **8**: 434–447.

Chrzanowski, Ł., Ławniczak, Ł., and Czaczyk, K. (2012) Why do microorganisms produce rhamnolipids? *World J Microbiol Biotechnol* **28**: 401–419.

Chung, W.K. and King, G.M. (2001) Isolation, Characterization, and Polyaromatic Hydrocarbon Degradation Potential of Aerobic Bacteria from Marine Macrofaunal Burrow Sediments and Description of Lutibacterium anuloederans gen. nov., sp. nov., and Cycloclasticus spirillensus sp. nov. *Appl Environ Microbiol* **67**: 5585–5592.

Church, R.A., Warren, D.J., and Irion, J.B. (2009) Analysis of Deepwater Shipwrecks in the Gulf of Mexico Artificial Reef Effect of Six World War II Shipwrecks. *Oceanography* **22**: 50–63.

Clark, D.R. (2019) ecolFudge.

Clark, D.R., McKew, B.A., Dong, L.F., Leung, G., Dumbrell, A.J., Stott, A., et al. (2020) Mineralization and nitrification: Archaea dominate ammonia-oxidising

communities in grassland soils. *Soil Biol Biochem* **143**:.

Clayton Jr, J.R., Payne, J.R., and Farlow, J.S. (1993) Oil Spill Dispersants: Mechanisms of Action and Laboratory Tests. In *Oil Spill Dispersants: Mechanisms of Action and Laboratory Tests*. Boca Raton, FL.

Colvin, K.A., Lewis, C., and Galloway, T.S. (2020) Current issues confounding the rapid toxicological assessment of oil spills. *Chemosphere* **245**:.

Commendatore, M.G. and Esteves, J.L. (2004) Natural and anthropogenic hydrocarbons in sediments from the Chubut River (Patagonia, Argentina). *Mar Pollut Bull* **48**: 910–918.

Commendatore, M.G., Esteves, J.L., and Colombo, J.C. (2000) Hydrocarbons in coastal sediments of Patagonia, Argentina: Levels and probable sources. *Mar Pollut Bull* **40**: 989–998.

Coolbaugh, T., Hague, E., Cox, R., and Varghese, G. (2017) Joint Industry Sponsored Effort to Evaluate Post-Macondo Dispersant Research. *Int Oil Spill Conf Proc*.

Cooper, D.G. and Paddock, D.A. (1984) Production of a biosurfactant from Torulopsis bombicola. *Appl Environ Microbiol* **47**: 173–176.

Cormack, D. (2013) Response to Marine Oil Pollution: Review and Assessment, Dordrecht: Springer Netherlands.

Couillard, C.M., Lee, K., Légaré, B., and King, T.L. (2005) Effect of dispersant on the composition of the water-accommodated fraction of crude oil and its toxicity to larval marine fish. *Environ Toxicol Chem* **24**: 1496–1504.

Coulon, F., Chronopoulou, P.M., Fahy, A., Païssé, S., Goñi-Urriza, M., Peperzak, L., et al. (2012) Central role of dynamic tidal biofilms dominated by aerobic hydrocarbonoclastic bacteria and diatoms in the biodegradation of hydrocarbons in coastal mudflats. *Appl Environ Microbiol* **78**: 3638–3648.

Coulon, F., McKew, B.A., Osborn, A.M., McGenity, T.J., and Timmis, K.N. (2007) Effects of temperature and biostimulation on oil-degrading microbial communities in temperate estuarine waters. *Environ Microbiol* **9**: 177–186.

Crisafi, F., Genovese, M., Smedile, F., Russo, D., Catalfamo, M., Yakimov, M., et al. (2016) Bioremediation technologies for polluted seawater sampled after an oil-spill in Taranto Gulf (Italy): A comparison of biostimulation, bioaugmentation and use of a washing agent in microcosm studies. *Mar Pollut Bull* **106**: 119–126.

Croome, A. (1999) Sinking Fast. *New Sci* 49.

Csardi, G. and Nepusz, T. (2006) The igraph software package for complex network research. *InterJournal Complex Syst*.

Curtis, D., Elango, V., Collins, A.W., Rodrigue, M., and Pardue, J.H. (2018) Transport of crude oil and associated microbial populations by washover events on coastal

headland beaches. *Mar Pollut Bull* **130**: 229–239.

D'Auria, M., Racioppi, R., and Velluzzi, V. (2008) Photodegradation of crude oil: Liquid injection and headspace solid-phase microextraction for crude oil analysis by gas chromatography with mass spectrometer detector. *J Chromatogr Sci* **46**: 339–344.

Das, K. and Mukherjee, A.K. (2007) Crude petroleum-oil biodegradation efficiency of Bacillus subtilis and Pseudomonas aeruginosa strains isolated from a petroleum-oil contaminated soil from North-East India. *Bioresour Technol* **98**: 1339–1345.

DASIC-International (2002) Slickgone NS Data Safety Sheet, Hampshire, UK.

Dave, D. and Ghaly, A.E. (2011) Remediation technologies for marine oil spills: A critical review and comparative analysis. *Am J Environ Sci* **7**: 424–440.

Daverey, A. and Pakshirajan, K. (2010) Sophorolipids from Candida bombicola using mixed hydrophilic substrates: Production, purification and characterization. *Colloids Surfaces B Biointerfaces* **79**: 246–253.

Davidova, I.A., Marks, C.R., and Suflita, J.M. (2018) Anaerobic Hydrocarbon-Degrading Deltaproteobacteria. In *Taxonomy, Genomics and Ecophysiology of Hydrocarbon-Degrading Microbes*. pp. 1–38.

Davies, A.J. and Evans, J.G. (1980) An analysis of the one-dimensional steady-state glow discharge. *J Phys D Appl Phys* **13**:.

Davila, A.M., Marchal, R., and Vandecasteele, J.P. (1994) Sophorose lipid production from lipidic precursors: Predictive evaluation of industrial substrates. *J Ind Microbiol* **13**: 249–257.

Delille, D., Bassères, A., and Dessommes, A. (1998) Effectiveness of bioremediation for oil-polluted antarctic seawater. *Polar Biol* **19**: 237–241.

DeLorenzo, M.E., Key, P.B., Chung, K.W., Pisarski, E., Shaddrix, B., Wirth, E.F., et al. (2018) Comparative Toxicity of Two Chemical Dispersants and Dispersed Oil in Estuarine Organisms. *Arch Environ Contam Toxicol* **74**: 414–430.

Al Disi, Z., Jaoua, S., Al-Thani, D., Al-Meer, S., and Zouari, N. (2017) Considering the Specific Impact of Harsh Conditions and Oil Weathering on Diversity, Adaptation, and Activity of Hydrocarbon-Degrading Bacteria in Strategies of Bioremediation of Harsh Oily-Polluted Soils. *Biomed Res Int* **2017**:.

Dombrowski, N., Donaho, J.A., Gutierrez, T., Seitz, K.W., Teske, A.P., and Baker, B.J. (2016) Reconstructing metabolic pathways of hydrocarbon-degrading bacteria from the Deepwater Horizon oil spill. *Nat Microbiol* **1**: 1–7.

Dong, C., Bai, X., Sheng, H., Jiao, L., Zhou, H., and Shao, Z. (2015) Distribution of PAHs and the PAH-degrading bacteria in the deep-sea sediments of the high-latitude Arctic Ocean. *Biogeosciences* **12**: 2163–2177.

Dorsett, M. (2010) Exxon Valdez Oil Spill Continued Effects On The Alaskan Economy. *Colon Acad Alliance Undergrad Res J* **1**: 1–17.

Doyle, S.M., Whitaker, E.A., De Pascuale, V., Wade, T.L., Knap, A.H., Santschi, P.H., et al. (2018) Rapid formation of microbe-oil aggregates and changes in community composition in coastal surface water following exposure to oil and the dispersant corexit. *Front Microbiol* **9**: 1–16.

Duarte, M., Jauregui, R., Vilchez-Vargas, R., Junca, H., and Pieper, D.H. (2014) AromaDeg, a novel database for phylogenomics of aerobic bacterial degradation of aromatics. *Database* **2014**:.

Dubinsky, E.A., Conrad, M.E., Chakraborty, R., Bill, M., Borglin, S.E., Hollibaugh, J.T., et al. (2013) Succession of hydrocarbon-degrading bacteria in the aftermath of the deepwater horizon oil spill in the gulf of Mexico. *Environ Sci Technol* **47**: 10860–10867.

Dumbrell, A.J., Ferguson, R.M.W., and Clark, D.R. (2016) Microbial Community Analysis by Single-Amplicon High-Throughput Next Generation Sequencing: Data Analysis – From Raw Output to Ecology. In *Hydrocarbon and Lipid Microbiology Protocols*. McGenity, T.J., Timmis, K.N., and Nogales, B. (eds). Berlin, Heidelberg, Heidelberg: Springer Protocols Handbooks, pp. 155–206.

Dyksterhouse, S.E., GRAY, J.P., HERWIG, R.P., LARA, J.C., and STALEY, J.T. (1995) Cycloclasticus pugetti gen. nov., sp. nov., an aromatic hydrocarbon-degrading bacterium from marine sediments. *Int J Syst Bacteriol* **45**: 116-123.

Edgar, R.C. (2004) MUSCLE: Multiple sequence alignment with high accuracy and high throughput. *Nucleic Acids Res* **32**: 1792–1797.

Edgar, R.C., Haas, B.J., Clemente, J.C., Quince, C., and Knight, R. (2011) UCHIME improves sensitivity and speed of chimera detection. *Bioinformatics* **27**: 2194–2200.

Edwards, E.A. and Grbic-Galic, D. (1994) Anaerobic degradation of toluene and o-xylene by a methanogenic consortium. *Appl Environ Microbiol* **60**: 313–322.

Edwards, J.R. and Hayashi, J.A. (1965) Structure of a rhamnolipid from Pseudomonas aeruginosa. *Arch Biochem Biophys* **111**: 415–421.

Etkin, D.S. (2000) Worldwide analysis of marine oil spill cleanup cost factors. In *Environment Canada Arctic and Marine Oil Spill Program Technical Seminar (AMOP) Proceedings*.

European Maritime Safety Agency (2009) Manual on the Applicability of Oil Spill Dispersants - Version 2, Lisbon, Portgual.

Exton, D.A., Suggett, D.J., Steinke, M., and McGenity, T.J. (2012) Spatial and temporal variability of biogenic isoprene emissions from a temperate estuary.

Global Biogeochem Cycles **26**:.

Faksness, L.G., Daling, P., Altin, D., Dolva, H., Fosbæk, B., and Bergstrøm, R. (2015) Relative bioavailability and toxicity of fuel oils leaking from World War II shipwrecks. *Mar Pollut Bull* **94**: 123–130.

El Fantroussi, S. and Agathos, S.N. (2005) Is bioaugmentation a feasible strategy for pollutant removal and site remediation? *Curr Opin Microbiol* **8**: 268–275.

Feldman, D. (1987) Surfactants in consumer products, theory, technology and application, J. Falbe, Ed., Springer-Verlag, Berlin, 1987 547. *J Polym Sci Part C Polym Lett* **25**: 461–462.

Felsenstein, J. (1985) Confidence Limits on Phylogenies: an Approach Using the Bootstrap. *Evolution (N Y)* **39**: 783–791.

Ferguson, R.M.W., Gontikaki, E., Anderson, J.A., and Witte, U. (2017) The variable influence of dispersant on degradation of oil hydrocarbons in subarctic deep-sea sediments at low temperatures (0-5 °C). *Sci Rep* **7**: 2253.

Field, D., Tiwari, B., Booth, T., Houten, S., Swan, D., Bertrand, N., and Thurston, M. (2006) Open software for biologists: From famine to feast. *Nat Biotechnol* **24**: 801–803.

Fingas, M. (2011a) An Overview of In-Situ Burning. In *Oil Spill Science and Technology*. pp. 737–903.

Fingas, M. (2011b) Oil Spill Dispersants: A Technical Summary. In *Oil Spill Science and Technology*. pp. 435–582.

Fingas, M. (2000) The Basics of Oil Spill Cleanup, CRC Press.

Fingas, M.F. (1995) The Evaporation of Oil Spills. In *Proceedings of the 18th Arctic Marine Oilspill Program Technical Seminar*.

Fiocco, R.J. and Lewis, A. (1999) Oil spill dispersants, Washington, D.C.: National Academies Press.

Fisheries and Oceans Canada (2001) In situ Oil Burning Policy and Decision Guidelines, British Columbia.

Floch Le, S., Dussauze, M., François-Xavier, M., Claireaux, G., Theron, M., Le Maire, P., and Nicolas-Kopec, A. (2014) DISCOBIOL: Assessment of the Impact of Dispersant Use for Oil Spill Response in Coastal or Estuarine Areas. In *International Oil Spill Conference Proceedings*. pp. 491–503.

Foght, J.M., Fedorak, P.M., and Westlake, D.W.S. (1983) Effect of the dispersant Corexit 9527 on the microbial degradation of sulfur heterocycles in Prudhoe Bay oil. *Can J Microbiol* **29**: 623–627.

French-McCay, D.P. (2004) Oil spill impact modeling: Development and validation. *Environ Toxicol Chem* **23**: 2441–2456.

Gallego, S., Vila, J., Tauler, M., Nieto, J.M., Breugelmans, P., Springael, D., and Grifoll, M. (2014) Community structure and PAH ring-hydroxylating dioxygenase genes of a marine pyrene-degrading microbial consortium. *Biodegradation* **25**: 543–556.

Galushko, A., Minz, D., Schink, B., and Widdel, F. (1999) Anaerobic degradation of naphthalene by a pure culture of a novel type of marine sulphate-reducing bacterium. *Environ Microbiol* **1**: 415–420.

Gao, X., Gao, W., Cui, Z., Han, B., Yang, P., Sun, C., and Zheng, L. (2015) Biodiversity and degradation potential of oil-degrading bacteria isolated from deep-sea sediments of South Mid-Atlantic Ridge. *Mar Pollut Bull* **97**: 373–380.

Garneau, M.É., Michel, C., Meisterhans, G., Fortin, N., King, T.L., Greer, C.W., and Lee, K. (2016) Hydrocarbon biodegradation by Arctic sea-ice and sub-ice microbial communities during microcosm experiments, Northwest Passage (Nunavut, Canada). *FEMS Microbiol Ecol* **92**:.

Garrett, R.M., Pickering, I.J., Haith, C.E., and Prince, R.C. (1998) Photooxidation of crude oils. *Environ Sci Technol* **32**: 3719–3723.

Gauthier, M.J., Lafay, B., Christen, R., Fernandez, L., Acquaviva, M., Bonin, P., and Bertrand, J.-C. (1992) Marinobacter hydrocarbonoclasticus gen. nov., sp. nov., a New, Extremely Halotolerant, Hydrocarbon-Degrading Marine Bacterium. *Int J Syst Bacteriol* **42**: 568–576.

Geiselbrecht, A.D., Hedlund, B.P., Tichi, M.A., and Staley, J.T. (1998) Isolation of marine polycyclic aromatic hydrocarbon (PAH)-degrading Cycloclasticus strains from the Gulf of Mexico and comparison of their PAH degradation ability with that of Puget Sound Cycloclasticus strains. *Appl Environ Microbiol* **64**: 4703–4710.

Geiselbrecht, A.D., Herwig, R.P., Deming, J.W., and Staley, J.T. (1996) Enumeration and phylogenetic analysis of polycyclic aromatic hydrocarbon-degrading marine bacteria from Puget Sound sediments. *Appl Environ Microbiol* **62**: 3344–3349.

van Gemerden, H., Tughan, C.S., de Wit, R., and Herbert, R.A. (1989) Laminated microbial ecosystems on sheltered beaches in Scapa Flow, Orkney Islands. *FEMS Microbiol Lett* **62**: 87–101.

Geraci, J.R. and St Aubin, D.J. (1991) Sea mammals and oil: confronting the risks. *Desalination* **82**: 403.

Geys, R., Soetaert, W., and Van Bogaert, I. (2014) Biotechnological opportunities in biosurfactant production. *Curr Opin Biotechnol* **30**: 66–72.

Gilson, D. (2006) Report on the Non-Mechanical Response for the T/V Exxon Valdez Oil Spill.

Girin, M. and Carpenter, A. (2019) Shipping and Oil Transportation in the

Mediterranean Sea. In *Pollution in the Mediterranean Sea: Part I - The International Context*. Carpenter, A. and Kostianoy, A.G. (eds). Springer International Publishing.

Global Market Insights (2018) Global Market Insights.

Göbbert, U., Lang, S., and Wagner, F. (1984) Sophorose lipid formation by resting cells of Torulopsis bombicola. *Biotechnol Lett* **6**: 225–230.

Golyshin, P.N., Chernikova, Ta.N., Abraham, W.R., Lünsdorf, H., Timmis, K.N., and Yakimov, M.M. (2002) Oleiphilaceae fam. nov., to include Oleiphilus messinensis gen. nov., sp. nov., a novel marine bacterium that obligately utilizes hydrocarbons. *Int J Syst Evol Microbiol* **52**: 901–911.

Gomes, M.B., Gonzales-Limache, E.E., Sousa, S.T.P., Dellagnezze, B.M., Sartoratto, A., Silva, L.C.F., et al. (2018) Exploring the potential of halophilic bacteria from oil terminal environments for biosurfactant production and hydrocarbon degradation under high-salinity conditions. *Int Biodeterior Biodegrad* **126**: 231–242.

Gontikaki, E., Potts, L.D., Anderson, J.A., and Witte, U. (2018) Hydrocarbon-degrading bacteria in deep-water subarctic sediments (Faroe-Shetland Channel). *J Appl Microbiol* **125**: 1040–1053.

Gonzini, O., Plaza, A., Di Palma, L., and Lobo, M.C. (2010) Electrokinetic remediation of gasoil contaminated soil enhanced by rhamnolipid. *J Appl Electrochem* **40**: 1239–1248.

Goodlad, J. (1996) Effects of the Braer oil spill on the Shetland seafood industry. *Sci Total Environ* **186**: 127–133.

Gopalan, B. and Katz, J. (2010) Turbulent shearing of crude oil mixed with dispersants generates long microthreads and microdroplets. *Phys Rev Lett* **104**:.

Green, D.H., Bowman, J.P., Smith, E.A., Gutierrez, T., and Bolch, C.J.S. (2006) Marinobacter algicola sp. nov., isolated from laboratory cultures of paralytic shellfish toxin-producing dinoflagellates. *Int J Syst Evol Microbiol* **56**: 523–527.

Green, D.H., Echavarri-Bravo, V., Brennan, D., and Hart, M.C. (2015) Bacterial diversity associated with the coccolithophorid algae emiliania huxleyi and coccolithus pelagicus f. braarudii. *Biomed Res Int* **2015**:.

Green, D.H., Llewellyn, L.E., Negri, A.P., Blackburn, S.I., and Bolch, C.J.S. (2004) Phylogenetic and functional diversity of the cultivable bacterial community associated with the paralytic shellfish poisoning dinoflagellate Gymnodinium catenatum. *FEMS Microbiol Ecol* **47**: 345–357.

Greenwood, N., Devlin, M.J., Best, M., Fronkova, L., Graves, C., Milligan, A., et al. (2019) Utilising eutrophication assessment directives from freshwater to marine

systems in the Thames estuary and Liverpool Bay, UK. *Front Mar Sci* **6**:.

Gregson, B.H., Metodieva, G., Metodiev, M. V., Golyshin, P.N., and McKew, B.A. (2018) Differential Protein Expression During Growth on Medium Versus Long-Chain Alkanes in the Obligate Marine Hydrocarbon-Degrading Bacterium Thalassolituus oleivorans MIL-1. *Front Microbiol* **9**: 1–14.

Gregson, B.H., Metodieva, G., Metodiev, M. V., Golyshin, P.N., and McKew, B.A. (2020) Protein expression in the obligate hydrocarbon-degrading psychrophile Oleispira antarctica RB-8 during alkane degradation and cold tolerance. *Environ Microbiol* **22**: 1870–1883.

Gregson, B.H., Metodieva, G., Metodiev, M. V., and McKew, B.A. (2019) Differential protein expression during growth on linear versus branched alkanes in the obligate marine hydrocarbon-degrading bacterium Alcanivorax borkumensis SK2T. *Environ Microbiol* **21**: 2347–2359.

Grimaud, R., Ghiglione, J.F., Cagnon, C., Lauga, B., Vaysse, P.J., Rodriguez-Blanco, A., et al. (2012) Genome sequence of the marine bacterium Marinobacter hydrocarbonoclasticus SP17, which forms biofilms on hydrophobic organic compounds. *J Bacteriol* **194**: 3539–3540.

Gros, J., Nabi, D., Würz, B., Wick, L.Y., Brussaard, C.P.D., Huisman, J., et al. (2014) First day of an oil spill on the open sea: Early mass transfers of hydrocarbons to air and water. *Environ Sci Technol* **48**: 9400–9411.

Gudiña, E.J., Rodrigues, A.I., Alves, E., Domingues, M.R., Teixeira, J.A., and Rodrigues, L.R. (2015) Bioconversion of agro-industrial by-products in rhamnolipids toward applications in enhanced oil recovery and bioremediation. *Bioresour Technol* **177**: 87–93.

Guibert, L.M., Loviso, C.L., Marcos, M.S., Commendatore, M.G., Dionisi, H.M., and Lozada, M. (2012) Alkane Biodegradation Genes from Chronically Polluted Subantarctic Coastal Sediments and Their Shifts in Response to Oil Exposure. *Microb Ecol* **64**: 605–616.

Gundlach, E.R. and Hayes, M.O. (1978) Vulnerability of coastal environments to oil spill impacts. *Mar Technol Soc J* **12**: 18–27.

Gunnison, D. and Alexander, M. (1975) Basis for the Resistance of Several Algae to Microbial Decomposition. *Appl Microbiol* **29**: 729–738.

Gutierrez, T., Green, D.H., Nichols, P.D., Whitman, W.B., Semple, K.T., and Aitken, M.D. (2013) Polycyclovorans algicola gen. nov., sp. nov., an aromatic-hydrocarbon- degrading marine bacterium found associated with laboratory cultures of marine phytoplankton. *Appl Environ Microbiol* **79**: 205–214.

Gutierrez, T., Green, D.H., Whitman, W.B., Nichols, P.D., Semple, K.T., and Aitken,

M.D. (2012) Algiphilus aromaticivorans gen. nov., sp. nov., an aromatic hydrocarbon-degrading bacterium isolated from a culture of the marine dinoflagellate Lingulodinium polyedrum, and proposal of Algiphilaceae fam. nov. *Int J Syst Evol Microbiol* **62**: 2743–2749.

Gutierrez, T., Nichols, P.D., Whitman, W.B., and Aitken, M.D. (2012) Porticoccus hydrocarbonoclasticus sp. nov., an aromatic hydrocarbon-degrading bacterium identified in laboratory cultures of marine phytoplankton. *Appl Environ Microbiol* **78**: 628–637.

Gutierrez, T., Rhodes, G., Mishamandani, S., Berry, D., Whitman, W.B., Nichols, P.D., et al. (2014) Polycyclic aromatic hydrocarbon degradation of phytoplankton-associated Arenibacter spp. and description of Arenibacter algicola sp. nov., an aromatic hydrocarbon-degrading bacterium. *Appl Environ Microbiol* **80**: 618–628.

Gutierrez, T., Singleton, D.R., Berry, D., Yang, T., Aitken, M.D., and Teske, A. (2013) Hydrocarbon-degrading bacteria enriched by the Deepwater Horizon oil spill identified by cultivation and DNA-SIP. *ISME J* **7**: 2091–2104.

Haba, E., Pinazo, A., Jauregui, O., Espuny, M.J., Infante, M.R., and Manresa, A. (2003) Physicochemical characterization and antimicrobial properties of rhamnolipids produced by Pseudomonas aeruginosa 47T2 NCBIM 40044. *Biotechnol Bioeng* **81**: 316–322.

Hall, G.B. (1994) Biology of Freshwater Pollution, 4th ed. Essex: Prentice Hall.

Hamdan, L.J. and Fulmer, P.A. (2011) Effects of COREXIT® EC9500A on bacteria from a beach oiled by the Deepwater Horizon spill. *Aquat Microb Ecol* **63**: 101–109.

Hamdan, L.J., Salerno, J.L., Reed, A., Joye, S.B., and Damour, M. (2018) The impact of the Deepwater Horizon blowout on historic shipwreck-associated sediment microbiomes in the northern Gulf of Mexico. *Sci Rep* **8**:.

Han, J. and Calvin, M. (1969) Hydrocarbon distribution of algae and bacteria, and microbiological activity in sediments. *Proc Natl Acad Sci U S A* **64**: 436–443.

Hanson, K.M. and McElroy, E.J. (2015) Anthropogenic impacts and long-term changes in herpetofaunal diversity and community composition on a barrier island in the Southeastern United States. *Herpetol Conserv Biol* **10**: 765–780.

Harayama, S., Kishira, H., Kasai, Y., and Shutsubo, K. (1999) Petroleum biodegradation in marine environments. *J Mol Microbiol Biotechnol* **1**: 63–70.

Harwati, T.U., Kasai, Y., Kodama, Y., Susilaningsih, D., and Watanabe, K. (2007) Characterization of Diverse Hydrocarbon-Degrading Bacteria Isolated from Indonesian Seawater. *Microbes Environ* **22**: 412–415.

Hassanshahian, M., Bayat, Z., Cappello, S., Smedile, F., and Yakimov, M. (2016)

Comparison the effects of bioaugmentation versus biostimulation on marine microbial community by PCR-DGGE: A mesocosm scale. *J Environ Sci (China)* **43**: 136–146.

Hassanshahian, M. and Cappello, S. (2013) Crude Oil Biodegradation in the Marine Environments. *Biodegrad - Eng Technol* 101–135.

Hazen, T.C., Dubinsky, E.A., DeSantis, T.Z., Andersen, G.L., Piceno, Y.M., Singh, N., et al. (2010) Deep-sea oil plume enriches indigenous oil-degrading bacteria. *Science (80-)* **330**: 204–208.

Hazen, T.C., Prince, R.C., and Mahmoudi, N. (2016) Marine Oil Biodegradation. *Environ Sci Technol* **50**: 2121–2129.

Head, I.M., Jones, D.M., and Larter, S.R. (2003) Biological activity in the deep subsurface and the origin of heavy oil. *Nature* **426**: 344–352.

Head, I.M., Jones, D.M., and Röling, W.F.M. (2006) Marine microorganisms make a meal of oil. *Nat Rev Microbiol* **4**: 173–182.

Hedlund, B.P. and Staley, J.T. (2001) Vibrio cyclotrophicus sp. nov., a polycyclic aromatic hydrocarbon (PAH)-degrading marine bacterium. *Int J Syst Evol Microbiol* **51**: 61–66.

Heider, J., Spormann, A.M., Beller, H.R., and Widdel, F. (1998) Anaerobic bacterial metabolism of hydrocarbons. *FEMS Microbiol Rev* **22**: 459–473.

Henkel, J.R., Sigel, B.J., and Taylor, C.M. (2014) Oiling rates and condition indices of shorebirds on the northern gulf of mexico following the deepwater horizon oil spill. *J F Ornithol* **85**: 408–420.

Herbert, R.A. (1985) Development of mass blooms of photosynthetic bacteria on sheltered beaches in Scapa Flow, Orkney Islands. *Proc R Soc Edinburgh Sect B Biol Sci* **87**: 15–25.

Hill, P. (2019) Managing the Wreck of HMS Royal Oak.

Hisatsuka, K.I., Nakahara, T., Sano, N., and Yamada, K. (1971) Formation of rhamnolipid by pseudomonas aerugznosa and its function in hydrocarbon fermentation. *Agric Biol Chem* **35**: 686–692.

Hodson, P. V., Adams, J., and Brown, R.S. (2019) Oil toxicity test methods must be improved. *Environ Toxicol Chem* **38**: 302–311.

Hood, M.A. and Winter, P.A. (1997) Attachment of Vibrio cholerae under various environmental conditions and to selected substrates. *FEMS Microbiol Ecol* **22**: 215–223.

Hope, R.M. (2013) Rmisc: Ryan Miscellaneous.

Hosokawa, R., Nagai, M., Kondo, H., Teragaki, J., and Okuyama, H. (2011) Application of autochthonous bioaugmentation in cold regions of Japan. In

Contaminated Soils: Environmental Impact, Disposal and Treatment. pp. 463–472.

Hosokawa, R., Nagai, M., Morikawa, M., and Okuyama, H. (2009) Autochthonous bioaugmentation and its possible application to oil spills. *World J Microbiol Biotechnol* **25**: 1519–1528.

Hubert, C.R.J., Oldenburg, T.B.P., Fustic, M., Gray, N.D., Larter, S.R., Penn, K., et al. (2012) Massive dominance of Epsilonproteobacteria in formation waters from a Canadian oil sands reservoir containing severely biodegraded oil. *Environ Microbiol* **14**: 387–404.

Huby, T.J.C., Clark, D.R., McKew, B.A., and McGenity, T.J. (2020) Extremely halophilic archaeal communities are resilient to short-term entombment in halite. *Environ Microbiol*.

Huettel, M., Overholt, W.A., Kostka, J.E., Hagan, C., Kaba, J., Wells, W.B., and Dudley, S. (2018) Degradation of Deepwater Horizon oil buried in a Florida beach influenced by tidal pumping. *Mar Pollut Bull* **126**: 488–500.

Huggett, M.J., Williamson, J.E., De Nys, R., Kjelleberg, S., and Steinberg, P.D. (2006) Larval settlement of the common Australian sea urchin Heliocidaris erythrogramma in response to bacteria from the surface of coralline algae. *Oecologia* **149**: 604–619.

Hussain, J., Zhao, Z., Pang, Y., Xia, L., Hussain, I., and Jiang, X. (2016) Effects of Different Water Seasons on the Residual Characteristics and Ecological Risk of Polycyclic Aromatic Hydrocarbons in Sediments from Changdang Lake, China. *J Chem* **2016**:.

Hvitfeldt, E. (2020) paletteer: Comprehensive Collection of Color Palettes. R package version 1.2.0.

IARC (1987) Overall evaluations of carcinogenicity: an updating of IARC Monographs volumes 1 to 42. *IARC Monogr Eval Carcinog Risks Hum Suppl* **7**: 1–440.

Ibrar, M. and Zhang, H. (2020) Construction of a hydrocarbon-degrading consortium and characterization of two new lipopeptides biosurfactants. *Sci Total Environ* **714**:.

Imron, M.F. and Titah, H.S. (2018) Optimization of diesel biodegradation by vibrio alginolyticus using Box-Behnken design. *Environ Eng Res* **23**: 374–382.

International Oil Pollution Compensation Funds (2018) Agia Zoni II.

IOPC (2017) Incident report: Agia Zoni II. 1–5.

IPIECA, IOGP, and API (2017) Guidelines on implementing Spill Impact Mitigation Assessment, SIMA. *IPIECA/IOGP Oil Spill Response JIP*.

Isaac, P., Sánchez, L.A., Bourguignon, N., Cabral, M.E., and Ferrero, M.A. (2013)

Indigenous PAH-degrading bacteria from oil-polluted sediments in Caleta Cordova, Patagonia Argentina. *Int Biodeterior Biodegrad* **82**: 207–214.

ITOPF (2013a) Effects of oil pollution on the marine environment.

ITOPF (2011a) Fate of marine oil spills.

ITOPF (2019) Oil Tanker Spill Statistics 2019, London.

ITOPF (2011b) Use of Dispersants to Treat Oil Spills, London.

ITOPF (2013b) Use of Skimmers in Oil Pollution Response.

ITOPF (2014) Weathering.

Iwabuchi, N., Sunairi, M., Urai, M., Itoh, C., Anzai, H., Nakajima, M., and Harayama, S. (2002) Extracellular polysaccharides of Rhodococcus rhodochrous S-2 stimulate the degradation of aromatic components in crude oil by indigenous marine bacteria. *Appl Environ Microbiol* **68**: 2337–2343.

Jagadevan, S. and Mukherji, S. (2004) Successful in situ oil bioremediation programmes - Key parameters. *Indian J Biotechnol* **3**: 495–501.

Jarvis, F.G. and Johnson, M.J. (1949) A Glyco-lipide Produced by Pseudomonas Aeruginosa. *J Am Chem Soc* **71**: 4124–4126.

Ji, Y., Mao, G., Wang, Y., and Bartlam, M. (2013) Structural insights into diversity and n-alkane biodegradation mechanisms of alkane hydroxylases. *Front Microbiol* **4**: 58.

Jiménez, N., Viñas, M., Bayona, J.M., Albaiges, J., and Solanas, A.M. (2007) The Prestige oil spill: Bacterial community dynamics during a field biostimulation assay. *Appl Microbiol Biotechnol* **77**: 935–945.

Jin, H.M., Jeong, H., Moon, E.J., Math, R.K., Lee, K., Kim, H.J., et al. (2011) Complete genome sequence of the polycyclic aromatic hydrocarbon-degrading bacterium Alteromonas sp. strain SN2. *J Bacteriol* **193**: 4292–4293.

Jin, H.M., Kim, J.M., Lee, H.J., Madsen, E.L., and Jeon, C.O. (2012) Alteromonas as a key agent of polycyclic aromatic hydrocarbon biodegradation in crude oil-contaminated coastal sediment. *Environ Sci Technol* **46**: 7731–7740.

Jochum, L.M., Schreiber, L., Marshall, I.P.G., Jørgensen, B.B., Schramm, A., and Kjeldsen, K.U. (2018) Single-cell genomics reveals a diverse metabolic potential of uncultivated Desulfatiglans-related deltaproteobacteria widely distributed in marine sediment. *Front Microbiol* **9**: 1–16.

John, V., Arnosti, C., Field, J., Kujawinski, E., MacCormick, A., and McCormick, A. (2016) The Role of Dispersants in Oil Spill Remediation: Fundamental Concepts, Rationale for Use, Fate, and Transport Issues. *Oceanography* **29**: 108–117.

Joshi, N.A. and Fass, J.N. (2011) Sickle: A sliding-window, adaptive, quality-based trimming tool for FastQ files (Version 1.33).

Joye, S.B., Teske, A.P., and Kostka, J.E. (2014) Microbial dynamics following the macondo oil well blowout across gulf of Mexico environments. *Bioscience* **64**: 766–777.

Kaczorek, E. and Olszanowski, A. (2011) Uptake of hydrocarbon by Pseudomonas fluorescens (P1) and Pseudomonas putida (K1) strains in the presence of surfactants: A cell surface modification. *Water Air Soil Pollut* **214**: 451–459.

Kang, S.W., Kim, Y.B., Shin, J.D., and Kim, E.K. (2010) Enhanced biodegradation of hydrocarbons in soil by microbial biosurfactant, sophorolipid. *Appl Biochem Biotechnol* **160**: 780–790.

Kapellos, G.E. (2017) Microbial Strategies for Oil Biodegradation. *Model Microscale Transp Biol Process* 19–39.

Kappell, A.D., Wei, Y., Newton, R.J., van Nostrand, J.D., Zhou, J., McLellan, S.L., and Hristova, K.R. (2014) The polycyclic aromatic hydrocarbon degradation potential of Gulf of Mexico native coastal microbial communities after the Deepwater Horizon oil spill. *Front Microbiol* **5**: 1–13.

Kasai, Y., Kishira, H., and Harayama, S. (2002) Bacteria Belonging to the Genus. *Appl Environ Microbiol* **68**: 5625–5633.

Kasai, Y., Kishira, H., Syutsubo, K., and Harayama, S. (2001) Molecular detection of marine bacterial populations on beaches contaminated by the Nakhodka tanker oil-spill accident. *Environ Microbiol* **3**: 246–255.

Kassambara, A. (2020) 'ggpubr': "ggplot2" Based Publication Ready Plots. R package version 0.3.0.

Kauppi, B., Lee, K., Carredano, E., Parales, R.E., Gibson, D.T., Eklund, H., and Ramaswamy, S. (1998) Structure of an aromatic-ring-hydroxylating dioxygenasenaphthalene 1,2-dioxygenase. *Structure* **6**: 571–586.

Kearns, D.B. (2010) A field guide to bacterial swarming motility. *Nat Rev Microbiol* **8**: 634–644.

Kelly, C.A., Law, R.J., and Emerson, H.S. (2000) Methods for analysis for hydrocarbons and polycyclic aromatic hydrocarbons (PAH) in marine samples. *Aquat Environ Prot Anal Methods* **12**: 18.

Kim, M., Jung, J.H., Ha, S.Y., An, J.G., Shim, W.J., and Yim, U.H. (2017) Long-Term Monitoring of PAH Contamination in Sediment and Recovery After the Hebei Spirit Oil Spill. *Arch Environ Contam Toxicol* **73**: 93–102.

King, G.M., Kostka, J.E., Hazen, T.C., and Sobecky, P.A. (2015) Microbial Responses to the Deepwater Horizon Oil Spill: From Coastal Wetlands to the Deep Sea. *Ann Rev Mar Sci* **7**: 377–401.

Kingston, P.F. (1992) Impact of offshore oil production installations on the benthos of

the north sea. *ICES J Mar Sci* **49**: 45–53.

Kirby, M., Neall, P., Rooke, J., and Yardley, H. (2011) Formulation Changes in Oil Spill Dispersants: Are They Toxicologically Significant? In *Oil Spill Science and Technology*. pp. 629–642.

Kirby, M.F., Brant, J., Moore, J., and Lincoln, S. (2018) PREMIAM – Pollution Response in Emergencies – Marine Impact Assessment and Monitoring: Post-incident monitoring guidelines. Secone Edition. Science Series Technical Report., Lowestoft.

Kiruri, L.W., Dellinger, B., and Lomnicki, S. (2013) Tar balls from deep water horizon oil spill: Environmentally persistent free radicals (EPFR) formation during crude weathering. *Environ Sci Technol* **47**: 4220–4226.

Kleindienst, S., Paul, J.H., and Joye, S.B. (2015) Using dispersants after oil spills: Impacts on the composition and activity of microbial communities. *Nat Rev Microbiol* **13**: 388–396.

Kleindienst, S., Seidel, M., Ziervogel, K., Grim, S., Loftis, K., Harrison, S., et al. (2015) Chemical dispersants can suppress the activity of natural oil-degrading microorganisms. *Proc Natl Acad Sci* **112**: 14900–14905.

Klindworth, A., Pruesse, E., Schweer, T., Peplies, J., Quast, C., Horn, M., and Glöckner, F.O. (2013) Evaluation of general 16S ribosomal RNA gene PCR primers for classical and next-generation sequencing-based diversity studies. *Nucleic Acids Res* **41**: 1–11.

Konishi, M., Yoshida, Y., and Horiuchi, J. ichi (2015) Efficient production of sophorolipids by Starmerella bombicola using a corncob hydrolysate medium. *J Biosci Bioeng* **119**: 317–322.

Kostka, J.E., Prakash, O., Overholt, W.A., Green, S.J., Freyer, G., Canion, A., et al. (2011) Hydrocarbon-degrading bacteria and the bacterial community response in Gulf of Mexico beach sands impacted by the deepwater horizon oil spill. *Appl Environ Microbiol* **77**: 7962–7974.

Krell, T., Lacal, J., Reyes-Darias, J.A., Jimenez-Sanchez, C., Sungthong, R., and Ortega-Calvo, J.J. (2013) Bioavailability of pollutants and chemotaxis. *Curr Opin Biotechnol* **24**: 451–456.

Kretschmer, A., Bock, H., and Wagner, F. (1982) Chemical and physical characterization of interfacial-active lipids from Rhodococcus erythropolis grown on n-alkanes. *Appl Environ Microbiol* **44**: 864–870.

Krolicka, A., Boccadoro, C., Mæland, M., Preston, C., Birch, J., Scholin, C., and Baussant, T. (2014) Detection of oil leaks by quantifying hydrocarbonoclastic bacteria in cold marine environments using the Environmental Sample

Processor. In *Proceedings of the 37th AMOP Technical Seminar on Environmental Contamination and Response*. pp. 791–807.

Krolicka, A., Boccadoro, C., Nilsen, M.M., Demir-Hilton, E., Birch, J., Preston, C., et al. (2019) Identification of microbial key-indicators of oil contamination at sea through tracking of oil biotransformation: An Arctic field and laboratory study. *Sci Total Environ* **696**:.

Kronberg, B., Holmberg, K., and Lindman, B. (2014) Surface Chemistry of Surfactants and Polymers, Wiley.

Kube, M., Chernikova, T.N., Al-Ramahi, Y., Beloqui, A., Lopez-Cortez, N., Guazzaroni, M.E., et al. (2013) Genome sequence and functional genomic analysis of the oil-degrading bacterium Oleispira antarctica. *Nat Commun* **4**:.

Kujawinski, E.B., Kido Soule, M.C., Valentine, D.L., Boysen, A.K., Longnecker, K., and Redmond, M.C. (2011) Fate of dispersants associated with the Deepwater Horizon oil spill. *Environ Sci Technol* **45**: 1298–1306.

Kumazawa, N.H., Fukuma, N., and Komoda, Y. (1991) Attachment of Vibrio parahaemolyticus Strains to Estuarine Algae. *J Vet Med Sci* **53**: 201–205.

Kurtz, Z.D., Müller, C.L., Miraldi, E.R., Littman, D.R., Blaser, M.J., and Bonneau, R.A. (2015) Sparse and Compositionally Robust Inference of Microbial Ecological Networks. *PLoS Comput Biol* **11**:.

De La Huz, R., Lastra, M., Junoy, J., Castellanos, C., and Viéitez, J.M. (2005) Biological impacts of oil pollution and cleaning in the intertidal zone of exposed sandy beaches: Preliminary study of the “prestige” oil spill. *Estuar Coast Shelf Sci* **65**: 19–29.

Lacaze, J.C. and Villedon de Naïde, O. (1976) Influence of illumination on phytotoxicity of crude oil. *Mar Pollut Bull* **7**: 73–76.

Laflamme, R.E. and Hites, R.A. (1979) Tetra- and pentacyclic, naturally-occurring, aromatic hydrocarbons in recent sediments. *Geochim Cosmochim Acta* **43**: 1687–1691.

Laidler, K.J. (1985) Chemical kinetics and the origins of physical chemistry. *Arch Hist Exact Sci* **32**: 43–75.

Lamendella, R., Strutt, S., Borglin, S., Chakraborty, R., Tas, N., Mason, O.U., et al. (2014) Assessment of the deepwater horizon oil spill impact on gulf coast microbial communities. *Front Microbiol* **5**: 1–13.

Landquist, H., Hassellöv, I.M., Rosén, L., Lindgren, J.F., and Dahllöf, I. (2013) Evaluating the needs of risk assessment methods of potentially polluting shipwrecks. *J Environ Manage* **119**: 85–92.

Landquist, H., Norrman, J., Lindhe, A., Norberg, T., Hassellöv, I.M., Lindgren, J.F.,

and Rosén, L. (2017) Expert elicitation for deriving input data for probabilistic risk assessment of shipwrecks. *Mar Pollut Bull* **125**: 399–415.

Landquist, H., Rosén, L., Lindhe, A., Norberg, T., and Hassellöv, I.M. (2017) Bayesian updating in a fault tree model for shipwreck risk assessment. *Sci Total Environ* **590**–**591**: 80–91.

Landquist, H., Rosén, L., Lindhe, A., Norberg, T., Hassellöv, I.M., Lindgren, J.F., and Dahllöf, I. (2014) A fault tree model to assess probability of contaminant discharge from shipwrecks. *Mar Pollut Bull* **88**: 239–248.

Lang, S. and Wullbrandt, D. (1999) Rhamnose lipids - Biosynthesis, microbial production and application potential. *Appl Microbiol Biotechnol* **51**: 22–32.

LaRoche, G., Eisler, R., and Tarzwell, C.M. (1970) Bioassay procedures for oil and oil dispersant toxicity evaluation. *J (Water Pollut Control Fed* **42**: 1982–1989.

Law, R.J., Kelly, C.A., and Nicholson, M.D. (1999) Polycyclic aromatic hydrocarbons (PAH) in shellfish affected by the Sea Empress oil spill in Wales in 1996. *Polycycl Aromat Compd* **17**: 229–239.

Lea-Smith, D.J., Biller, S.J., Davey, M.P., Cotton, C.A.R.R., Perez Sepulveda, B.M., Turchyn, A. V., et al. (2015) Contribution of cyanobacterial alkane production to the ocean hydrocarbon cycle. *Proc Natl Acad Sci* **112**: 13591–13596.

Leahy, J.G. and Colwell, R.R. (1990) Microbial degradation of hydrocarbons in the environment. *Microbiol Rev* **54**: 305–315.

Lebaron, P., Servais, P., Troussellier, M., Courties, C., Vives-Rego, J., Muyzer, G., et al. (1999) Changes in bacterial community structure in seawater mesocosms differing in their nutrient status. *Aquat Microb Ecol* **19**: 255–267.

Lecomte Du Noüy, P. (1919) A new apparatus for measuring surface tension. *J Gen Physiol* **1**: 521–524.

Lee, J., Han, I., Kang, B.R., Kim, S.H., Sul, W.J., and Lee, T.K. (2017) Degradation of crude oil in a contaminated tidal flat area and the resilience of bacterial community. *Mar Pollut Bull* **114**: 296–301.

Lee, K., Nedwed, T., Prince, R.C., and Palandro, D. (2013) Lab tests on the biodegradation of chemically dispersed oil should consider the rapid dilution that occurs at sea. *Mar Pollut Bull* **73**: 314–318.

Lee, R.F. (2003) Photo-oxidation and Photo-toxicity of Crude and Refined Oils. *Spill Sci Technol Bull* **8**: 157–162.

Lee, S.C., Lee, S.J., Kim, S.H., Park, I.H., Lee, Y.S., Chung, S.Y., and Choi, Y.L. (2008) Characterization of new biosurfactant produced by Klebsiella sp. Y6-1 isolated from waste soybean oil. *Bioresour Technol* **99**: 2288–2292.

Lehr, R.E. and Jerina, D.M. (1977) Metabolic activations of polycyclic hydrocarbons -

Structure-activity relationships. *Arch Toxicol* **39**: 1–6.

Lenth, R. (2020) emmeans: Estimated Marginal Means, aka Least-Squares Means. R package version 1.4.7. *https://CRANR-project.org/package=emmeans*.

Li, Q., Cao, L., Wang, W., Tan, H., Jin, T., Wang, G., et al. (2018) Analysis of the bacterial communities in the waterlogged wooden cultural relics of the Xiaobaijiao No. 1 shipwreck via high-throughput sequencing technology. *Holzforschung* **72**: 609–619.

Li, Z., Lee, K., King, T., Boufadel, M.C., and Venosa, A.D. (2008) Assessment of chemical dispersant effectiveness in a wave tank under regular non-breaking and breaking wave conditions. *Mar Pollut Bull* **56**: 903–912.

Linda, A., Hernado, P.B., and Yuewen, D. (2018) Response of microbial communities to oil spill in the Gulf of Mexico: A review. *African J Microbiol Res* **12**: 536–545.

Lindstrom, J.E. and Braddock, J.F. (2002) Biodegradation of petroleum hydrocarbons at low temperature in the presence of the dispersant Corexit 9500. *Mar Pollut Bull* **44**: 739–747.

Little, D.I. and Little, A.E. (1991) Estuarine oil spill effects in the context of dispersant use changes. *nternational Oil Spill Conf Proc* **1**: 507–518.

Liu, C., Wang, W., Wu, Y., Zhou, Z., Lai, Q., and Shao, Z. (2011) Multiple alkane hydroxylase systems in a marine alkane degrader, Alcanivorax dieselolei B-5. *Environ Microbiol* **13**: 1168–1178.

Liu, J., Bacosa, H.P., and Liu, Z. (2017) Potential environmental factors affecting oil-degrading bacterial populations in deep and surface waters of the Northern Gulf of Mexico. *Front Microbiol* **7**: 1–14.

Liu, J., Zheng, Y., Lin, H., Wang, X., Li, M., Liu, Y., et al. (2019) Proliferation of hydrocarbon-degrading microbes at the bottom of the Mariana Trench. *Microbiome* **7**: 1–13.

Liu, Z., Fu, T., Hu, C., Shen, D., Macchioni, N., Sozzi, L., et al. (2018) Microbial community analysis and biodeterioration of waterlogged archaeological wood from the Nanhai No. 1 shipwreck during storage. *Sci Rep* **8**:.

Liu, Z. and Liu, J. (2013) Evaluating bacterial community structures in oil collected from the sea surface and sediment in the northern Gulf of Mexico after the Deepwater Horizon oil spill. *Microbiologyopen* **2**: 492–504.

Lormières, F. and Oger, P.M. (2017) Epsilonproteobacteria dominate bacterial diversity at a natural tar seep. *Comptes Rendus - Biol* **340**: 238–243.

Lozada, M., Marcos, M.S., Commendatore, M.G., Gil, M.N., and Dionisi, H.M. (2014) The Bacterial Community Structure of Hydrocarbon-Polluted Marine Environments as the Basis for the Definition of an Ecological Index of

Hydrocarbon Exposure. *Microbes Environ* **29**: 269–276.

Luna, J.M., Rufino, R.D., Sarubbo, L.A., and Campos-Takaki, G.M. (2013) Characterisation, surface properties and biological activity of a biosurfactant produced from industrial waste by Candida sphaerica UCP0995 for application in the petroleum industry. *Colloids Surfaces B Biointerfaces* **102**: 202–209.

Al Maawali, W., Al Naabi, A., Al Yaruubi, M., Saleem, A., and Al Maashri, A. (2019) Design and Implementation of an Unmanned Surface Vehicle for Oil Spill Handling. In *1st International Conference on Unmanned Vehicle Systems-Oman, UVS 2019*.

Macnaughton, S.J., Stephen, J.R., Venosa, A.D., Davis, G.A., Chang, Y.J., and White, D.C. (1999) Microbial population changes during bioremediation of an experimental oil spill. *Appl Environ Microbiol* **65**: 3566–3574.

Madigan, M., Martinko, J., Dunlap, P., and Clark, D. (2008) Brock Biology of microorganisms 12th edn. *Int Microbiol* **11**: 65–73.

Major, D., Zhang, Q., Wang, G., and Wang, H. (2012) Oil-dispersant mixtures: Understanding chemical composition and its relation to human toxicity. *Toxicol Environ Chem* **94**: 1832–1845.

Mann, K.H. and Lazier, J.R.N. (2013) Dynamics of Marine Ecosystems: Biological-Physical Interactions in the Oceans: Third Edition.

Manzetti, S. (2013) Polycyclic Aromatic Hydrocarbons in the Environment: Environmental Fate and Transformation. *Polycycl Aromat Compd* **33**: 311–330.

Marchant, R. and Banat, I.M. (2012) Microbial biosurfactants: Challenges and opportunities for future exploitation. *Trends Biotechnol* **30**: 558–565.

Marine, B. (2010) Royal Oak Oil Removal Programme.

Maritime and Coastguard Agency (2020) Maritime and Coastguard Agency Counter Pollution Stockpiles.

Markets and Markets (2017) Markets and Markets.

Marlowe, I.T., Green, J.C., Neal, A.C., Brassell, S.C., Eglinton, G., and Course, P.A. (1984) Long chain (n-c37-c39) alkenones in the prymnesiophyceae. distribution of alkenones and other lipids and their taxonomic significance. *Br Phycol J* **19**: 203–216.

Marshall, A.G. and Rodgers, R.P. (2008) Petroleomics: Chemistry of the underworld. *Proc Natl Acad Sci* **105**: 18090–18095.

Marx, R.B. and Aitken, M.D. (2000) Bacterial chemotaxis enhances naphthalene degradation in a heterogeneous aqueous system. *Environ Sci Technol* **34**: 3379–3383.

Mason, O.U., Han, J., Woyke, T., and Jansson, J.K. (2014) Single-cell genomics

reveals features of a Colwellia species that was dominant during the Deepwater Horizon oil spill. *Front Microbiol* **5**:.

Mason, O.U., Hazen, T.C., Borglin, S., Chain, P.S.G., Dubinsky, E.A., Fortney, J.L., et al. (2012) Metagenome, metatranscriptome and single-cell sequencing reveal microbial response to Deepwater Horizon oil spill. *ISME J* **6**: 1715–1727.

Mason, O.U., Scott, N.M., Gonzalez, A., Robbins-Pianka, A., Bælum, J., Kimbrel, J., et al. (2014) Metagenomics reveals sediment microbial community response to Deepwater Horizon oil spill. *ISME J* **8**: 1464–1475.

McFarlin, K.M., Prince, R.C., Perkins, R., and Leigh, M.B. (2014) Biodegradation of dispersed oil in Arctic seawater at -1°C. *PLoS One* **9**:.

McGenity, T.J. (2010) Halophilic Hydrocarbon Degraders. In *Handbook of Hydrocarbon and Lipid Microbiology*.

McGenity, T.J., Folwell, B.D., McKew, B.A., and Sanni, G.O. (2012) Marine crude-oil biodegradation: a central role for interspecies interactions. *Aquat Biosyst* **8**: 1–19.

McKenna, A.M., Nelson, R.K., Reddy, C.M., Savory, J.J., Kaiser, N.K., Fitzsimmons, J.E., et al. (2013) Expansion of the analytical window for oil spill characterization by ultrahigh resolution mass spectrometry: Beyond gas chromatography. *Environ Sci Technol* **47**: 7530–7539.

McKew, B.A., Coulon, F., Osborn, A.M., Timmis, K.N., and McGenity, T.J. (2007) Determining the identity and roles of oil-metabolizing marine bacteria from the Thames estuary, UK. *Environ Microbiol* **9**: 165–176.

McKew, B.A., Coulon, F., Yakimov, M.M., Denaro, R., Genovese, M., Smith, C.J., et al. (2007) Efficacy of intervention strategies for bioremediation of crude oil in marine systems and effects on indigenous hydrocarbonoclastic bacteria. *Environ Microbiol* **9**: 1562–1571.

McKew, B.A. and Smith, C.J. (2015) Real-Time PCR Approaches for Analysis of Hydrocarbon-Degrading Bacterial Communities. In *Hydrocarbon and Lipid Microbiology Protocols*. McGenity, T.J., Timmis, K.N., and Fernandez, B.N. (eds). Berlin, Heidelberg: Springer Protocols Handbooks.

McNaught, A.D. and Wilkinson, A. (1997) IUPAC. Compendium of Chemical Terminology, 2nd ed. (the “Gold Book”).

Melcher, R.J., Apitz, S.E., and Hemmingsen, B.B. (2002) Impact of irradiation and polycyclic aromatic hydrocarbon spiking on microbial populations in marine sediment for future aging and biodegradability studies. *Appl Environ Microbiol* **68**: 2858–2868.

Meng, L., Liu, H., Bao, M., and Sun, P. (2016) Microbial community structure shifts are

associated with temperature, dispersants and nutrients in crude oil-contaminated seawaters. *Mar Pollut Bull* **111**: 203–212.

Messina, E., Denaro, R., Crisafi, F., Smedile, F., Cappello, S., Genovese, M., et al. (2016) Genome sequence of obligate marine polycyclic aromatic hydrocarbons-degrading bacterium Cycloclasticus sp. 78-ME, isolated from petroleum deposits of the sunken tanker Amoco Milford Haven, Mediterranean Sea. *Mar Genomics* **25**: 11–13.

Michel, J., Gilbert, T., Etkin, D.S., Urban, R., Waldron, J., and Blocksidge, C.T. (2005) Potentially polluting wrecks in Marine waters. *2005 Int Oil Spill Conf IOSC 2005* 11590–11629.

Milton, S.L., Lutz, P.L., Shigenaka, G., Hoff, R.Z., Yender, R.A., and Mearns, A.J. (2010) Oil and sea turtles: biology, planning and response.

Minucelli, T., Ribeiro-Viana, R.M., Borsato, D., Andrade, G., Cely, M.V.T., de Oliveira, M.R., et al. (2017) Sophorolipids Production by Candida bombicola ATCC 22214 and Its Potential Application in Soil Bioremediation. *Waste and Biomass Valorization* **8**: 743–753.

Monfils, R., Gilbert, T., and Nawadra, S. (2006) Sunken WWII shipwrecks of the Pacific and East Asia: The need for regional collaboration to address the potential marine pollution threat. *Ocean Coast Manag* **49**: 779–788.

Moya Ramírez, I., Altmajer Vaz, D., Banat, I.M., Marchant, R., Jurado Alameda, E., and García Román, M. (2016) Hydrolysis of olive mill waste to enhance rhamnolipids and surfactin production. *Bioresour Technol* **205**: 1–6.

Możejko-Ciesielska, J. and Kiewisz, R. (2016) Bacterial polyhydroxyalkanoates: Still fabulous? *Microbiol Res* **192**: 271–282.

Mugge, R.L., Brock, M.L., Salerno, J.L., Damour, M., Church, R.A., Lee, J.S., and Hamdan, L.J. (2019) Deep-sea biofilms, historic shipwreck preservation and the Deepwater Horizon spill. *Front Mar Sci* **6**:.

Muir, T. (2020) Scapa Flow Historic Wreck Site.

Mulligan, C.N. (2005) Environmental applications for biosurfactants. *Environ Pollut* **133**: 183–198.

Mulligan, C.N. and Gibbs, B.F. (1993) Factors influencing the economics of biosurfactant, N. Kosaric. New York, US: Marcel Dekker.

Nagashima, H., Zulkharnain, A. Bin, Maeda, R., Fuse, H., Iwata, K., and Omori, T. (2010) Cloning and Nucleotide Sequences of Carbazole Degradation Genes from Marine Bacterium Neptuniibacter sp. Strain CAR-SF. *Curr Microbiol* **61**: 50–56.

Nakama, Y. (2017) Surfactants, Ullmann.

Nalco Environmental Solutions (2014) Safety Data Sheet Corexit ® Ec9500a, Texas,

US.

NASA (2019) April 1, 2019 - Phytoplankton Bloom in North Sea.

National Oceanic and Atmospheric Administration (2010) Characteristics of Response Strategies: A Guide for Spill Response Planning in Marine Environments.

National Research Council (2014) Responding to Oil Spills in the U.S. Arctic marine environment, Washington, D.C: National Academy of Sciences.

National Toxicology Program (2011) NTP 12th Report on Carcinogens. *Rep Carcinog* **12**:.

Naysim, L.O., Kang, H.J., and Jeon, C.O. (2014) Zhongshania aliphaticivorans sp. nov., an aliphatic hydrocarbon-degrading bacterium isolated from marine sediment, And transfer of Spongiibacter borealis Jang et al. 2011 to the genus Zhongshania as Zhongshania borealis comb. nov. *Int J Syst Evol Microbiol* **64**: 3768–3774.

NCBI Taxonomy Browser (2020a) Alcanivorax.

NCBI Taxonomy Browser (2020b) Pseudomonas.

Ndungu, K., Beylich, B.A., Staalstrøm, A., Øxnevad, S., Berge, J.A., Braaten, H.F.V., et al. (2017) Petroleum oil and mercury pollution from shipwrecks in Norwegian coastal waters. *Sci Total Environ* **593**–**594**: 624–633.

Nedwed, T. and Coolbaugh, T. (2008) Do basins and beakers negatively bias dispersant-effectiveness tests? In *International Oil Spill Conference - IOSC 2008, Proceedings*. pp. 835–842.

Neethu, C.S., Saravanakumar, C., Purvaja, R., Robin, R.S., and Ramesh, R. (2019) Oil-Spill Triggered Shift in Indigenous Microbial Structure and Functional Dynamics in Different Marine Environmental Matrices. *Sci Rep* **9**:.

Nei, M. and Saitou, N. (1987) The neighbor-joining method: a new method for reco... [Mol Biol Evol. 1987] - PubMed result. *Mol Biol Evol*.

Newell, S.E., Eveillard, D., Mccarthy, M.J., Gardner, W.S., Liu, Z., and Ward, B.B. (2014) A shift in the archaeal nitrifier community in response to natural and anthropogenic disturbances in the northern Gulf of Mexico. *Environ Microbiol Rep* **6**: 106–112.

Newton, R.J., Huse, S.M., Morrison, H.G., Peake, C.S., Sogin, M.L., and McLellan, S.L. (2013) Shifts in the Microbial Community Composition of Gulf Coast Beaches Following Beach Oiling. *PLoS One* **8**: 1–13.

Niepceron, M., Portet-Koltalo, F., Merlin, C., Motelay-Massei, A., Barray, S., and Bodilis, J. (2010) Both Cycloclasticus spp. and Pseudomonas spp. as PAH-degrading bacteria in the Seine estuary (France). *FEMS Microbiol Ecol* **71**: 137–147.

Nikolenko, S.I., Korobeynikov, A.I., and Alekseyev, M.A. (2013) BayesHammer: Bayesian clustering for error correction in single-cell sequencing. *BMC Genomics* **14**:.

Nikolopoulou, M., Eickenbusch, P., Pasadakis, N., Venieri, D., and Kalogerakis, N. (2013) Microcosm evaluation of autochthonous bioaugmentation to combat marine oil spills. *N Biotechnol* **30**: 734–742.

Nitz, H., Duarte, M., Jauregui, R., Pieper, D.H., Müller, J.A., and Kästner, M. (2020) Identification of benzene-degrading Proteobacteria in a constructed wetland by employing in situ microcosms and RNA-stable isotope probing. *Appl Microbiol Biotechnol* **104**: 1809–1820.

Nogales, B. and Bosch, R. (2019) Microbial Communities in Hydrocarbon-Polluted Harbors and Marinas. In *Microbial Communities Utilizing Hydrocarbons and Lipids: Members, Metagenomics and Ecophysiology*.

Noh, J., Kim, H., Lee, C., Yoon, S.J., Chu, S., Kwon, B.O., et al. (2018) Bioaccumulation of Polycyclic Aromatic Hydrocarbons (PAHs) by the Marine Clam, Mactra veneriformis, Chronically Exposed to Oil-Suspended Particulate Matter Aggregates. *Environ Sci Technol* **52**: 7910–7920.

Noirungsee, N., Hackbusch, S., Viamonte, J., Bubenheim, P., Liese, A., and Müller, R. (2020) Influence of oil, dispersant, and pressure on microbial communities from the Gulf of Mexico. *Sci Rep* **10**: 7079.

Norcorss, B.E. (1988) Advanced organic chemistry: reactions mechanisms, and structure, 7th ed. ohn Wiley and Sons, New York.

Norman, R.S., Frontera-Suau, R., and Morris, P.J. (2002) Variability in Pseudomonas aeruginosa lipopolysaccharide expression during crude oil degradation. *Appl Environ Microbiol* **68**: 5096–5103.

North, E.W., Adams, E.E., Thessen, A.E., Schlag, Z., He, R., Socolofsky, S.A., et al. (2015) The influence of droplet size and biodegradation on the transport of subsurface oil droplets during the Deepwater Horizon spill: A model sensitivity study. *Environ Res Lett* **10**:.

Nurk, S., Bankevich, A., Antipov, D., Gurevich, A., Korobeynikov, A., Lapidus, A., et al. (2013) Assembling genomes and mini-metagenomes from highly chimeric reads. In *Lecture Notes in Computer Science (including subseries Lecture Notes in Artificial Intelligence and Lecture Notes in Bioinformatics)*. pp. 158–170.

Nzila, A., Jung, B.K., Kim, M.C., Ibal, J.C., Budiyanto, F., Musa, M.M., et al. (2018) Complete genome sequence of the polycyclic aromatic hydrocarbons biodegrading bacterium Idiomarina piscisalsi strain 10PY1A isolated from oil-contaminated soil. *Korean J Microbiol* **54**: 289–292.

O'Laughlin, C.M., Law, B.A., Zions, V.S., King, T.L., Robinson, B., and Wu, Y. (2017) Settling of dilbit-derived oil-mineral aggregates (OMAs) & transport parameters for oil spill modelling. *Mar Pollut Bull* **124**: 292–302.

Oil-Slick-Dispersants (2015) Safety Data Sheet Superdispersant 25, Elvington, UK.

Oksanen, J., Blanchet, F.G., Friendly, M., Kindt, R., Legendre, P., McGlinn, D., et al. (2019) vegan: Community Ecology Package. R package version 2.5.6. **254**:.

Oren, A. (2017) Aerobic Hydrocarbon-Degrading Archaea. In *Taxonomy, Genomics and Ecophysiology of Hydrocarbon-Degrading Microbes. Handbook of Hydrocarbon and Lipid Microbiology.* McGenity, T.J. (ed). Springer, Cham, pp. 1–12.

OSPAR Commission (2009) Agreement on CEMP Assessment Criteria for the QSR 2010.

OSPAR Commission (2017) Status and Trends in the Concentrations of Polycyclic Aromatic Hydrocarbons (PAHs) in Sediment.

Owens, E.H. (1972) The Cleaning of Gravel Beaches Polluted By Oil. *Coast Eng Proc* **1**: 143.

Pacwa-Płociniczak, M., Płaza, G.A., Piotrowska-Seget, Z., and Cameotra, S.S. (2011) Environmental applications of biosurfactants: Recent advances. *Int J Mol Sci* **12**: 633–654.

Parinos, C., Hatzianestis, I., Chourdaki, S., Plakidi, E., and Gogou, A. (2019) Imprint and short-term fate of the Agia Zoni II tanker oil spill on the marine ecosystem of Saronikos Gulf. *Sci Total Environ* **693**: 133568.

Passeri, A., Schmidt, M., Haffner, T., Wray, V., Lang, S., and Wagner, F. (1992) Marine biosurfactants. IV. Production, characterization and biosynthesis of an anionic glucose lipid from the marine bacterial strain MM1. *Appl Microbiol Biotechnol* **37**: 281–286.

Passow, U. (2016) Formation of rapidly-sinking, oil-associated marine snow. *Deep Res Part II Top Stud Oceanogr* **129**: 232–240.

Passow, U., Sweet, J., and Quigg, A. (2017) How the dispersant Corexit impacts the formation of sinking marine oil snow. *Mar Pollut Bull* **125**: 139–145.

Pedersen, T.L. (2020) ggraph: An Implementation of Grammar of Graphics for Graphs and Networks. R package version 2.0.3.

Pedersen, T.L. (2019) patchwork: The Composer of Plots. *Cran*.

Peeters, J.C.H., Haas, H., Peperzak, L., and Wetsteyn, L.P.M.J. (1991) Limiting factors for phytoplankton in the North Sea. *Water Sci Technol* **24**: 261–267.

Petersen, J., Michel, J., Zengel, S., White, M., Lord, C., and Plank, C. (2002) Environmental Sensitivity Index Guidelines. Version 3.0. *NOAA Tech Memo NOS*

OR&R.

Philp, R.P. (1985) Petroleum Formation and Occurrence.

Piatt, J.F., Lensink, C.J., Butler, W., and Nysewander, D.R. (1990) Immediate Impact of the “Exxon Valdez” Oil Spill on Marine Birds. *Auk* **107**: 387–397.

Potter, D.L. and Simmons, K.E. (1998) Analysis of Petroleum Hydrocarbons in Environmental Media, Amherst Scientific Publishers.

Prince, R.C. and Butler, J.D. (2014) A protocol for assessing the effectiveness of oil spill dispersants in stimulating the biodegradation of oil. *Environ Sci Pollut Res* **21**: 9506–9510.

Prince, R.C., Coolbaugh, T.S., and Parkerton, T.F. (2016) Oil dispersants do facilitate biodegradation of spilled oil. *Proc Natl Acad Sci* **113**: E1421–E1421.

Prince, R.C., Kelley, B.A., and Butler, J.D. (2015) Three Widely-Available Dispersants Substantially Increase the Biodegradation of otherwise Undispersed Oil. *J Mar Sci Res Dev* **06**: 1–4.

Prince, R.C., McFarlin, K.M., Butler, J.D., Febbo, E.J., Wang, F.C.Y., and Nedwed, T. (2013) The primary biodegradation of dispersed crude oil in the sea. *Chemosphere* **90**: 521–526.

Prince, R.C., Nash, G.W., and Hill, S.J. (2016) The biodegradation of crude oil in the deep ocean. *Mar Pollut Bull* **111**: 354–357.

Pruthi, V. and Cameotra, S.S. (1997) Rapid identification of biosurfactant-producing bacterial strains using a cell surface hydrophobicity technique. *Biotechnol Tech* **11**: 671–674.

Quigg, A., Passow, U., Daly, K.L., Burd, A., Hollander, D.J., Schwing, P.T., and Lee, K. (2020) Marine Oil Snow Sedimentation and Flocculent Accumulation (MOSSFA) Events: Learning from the Past to Predict the Future. In *Deep Oil Spills*. pp. 196–220.

R Development Core Team, R. (2011) R: A Language and Environment for Statistical Computing.

Rabus, R., Boll, M., Heider, J., Meckenstock, R.U., Buckel, W., Einsle, O., et al. (2016) Anaerobic microbial degradation of hydrocarbons: From enzymatic reactions to the environment. *J Mol Microbiol Biotechnol* **26**: 5–28.

Rabus, R., Nordhaus, R., Ludwig, W., and Widdel, F. (1993) Complete oxidation of toluene under strictly anoxic conditions by a new sulfate-reducing bacterium. *Appl Environ Microbiol* **59**: 1444–1451.

Rahim, R., Ochsner, U.A., Olvera, C., Graninger, M., Messner, P., Lam, J.S., and Soberón-Chávez, G. (2001) Cloning and functional characterization of the Pseudomonas aeruginosa rhlC gene that encodes rhamnosyltransferase 2, an

enzyme responsible for di-rhamnolipid biosynthesis. *Mol Microbiol* **40**: 708–718.

Rahsepar, S., Smit, M.P.J., Murk, A.J., Rijnaarts, H.H.M., and Langenhoff, A.A.M. (2016) Chemical dispersants: Oil biodegradation friend or foe? *Mar Pollut Bull* **108**: 113–119.

Ramya, C., Lakshmi, R., Asha, D., Sivamurugan, V., Vasudevan, V., and Krishnan, M. (2018) Demonstration of bioprocess factors optimization for enhanced mono-rhamnolipid production by a marine Pseudomonas guguanensis. *Int J Biol Macromol* **108**: 531–540.

Rapp, P., Bock, H., Wray, V., and Wagner, F. (1979) Formation, Isolation and Characterization of Trehalose Dimycolates from Rhodococcus erythropolis Grown on n-Alkanes. *J Gen Microbiol* **115**: 491–503.

Raskin, L., Stromley, J.M., Rittmann, B.E., and Stahl, D.A. (1994) Group-specific 16S rRNA hybridization probes to describe natural communities of methanogens. *Appl Environ Microbiol* **60**: 1232–1240.

Rawe, J., Krietemeyer, S., and Meagher-Hartzell, E. (1993) Guide for Conducting Treatability Studies under CERCLA: Biodegradation Remedy Selection—Interim Guidance. U.S. Environmental Protection Agency, Washington, D.C.

Redmond, M.C. and Valentine, D.L. (2012) Natural gas and temperature structured a microbial community response to the Deepwater Horizon oil spill. *Proc Natl Acad Sci* **109**: 20292–20297.

Redmond, M.C., Valentine, D.L., and Sessions, A.L. (2010) Identification of novel methane-, ethane-, and propane-oxidizing bacteria at marine hydrocarbon seeps by stable isotope probing. *Appl Environ Microbiol* **76**: 6412–6422.

Reijnhart, R. and Rose, R. (1982) Evaporation of crude oil at sea. *Water Res* **16**: 1319–1325.

REMPEC (2018) Mediterranean Integrated GIS on Marine Pollution Risk Assessment and Response.

Rial, D., Murado, M.A., Beiras, R., and Vázquez, J.A. (2014) Toxicity of four spill-treating agents on bacterial growth and sea urchin embryogenesis. *Chemosphere* **104**: 57–62.

Ribicic, D., Netzer, R., Hazen, T.C., Techtmann, S.M., Drabløs, F., and Brakstad, O.G. (2018) Microbial community and metagenome dynamics during biodegradation of dispersed oil reveals potential key-players in cold Norwegian seawater. *Mar Pollut Bull* **129**: 370–378.

Ribicic, D., Netzer, R., Winkler, A., and Brakstad, O.G. (2018) Microbial communities in seawater from an Arctic and a temperate Norwegian fjord and their potentials for biodegradation of chemically dispersed oil at low seawater temperatures. *Mar*

Pollut Bull **129**: 308–317.

Risdon, G.C., Pollard, S.J.T., Brassington, K.J., McEwan, J.N., Paton, G.I., Semple, K.T., and Coulon, F. (2008) Development of an analytical procedure for weathered hydrocarbon contaminated soils within a UK risk-based framework. *Anal Chem* **80**: 7090–7096.

Rivers, A.R., Sharma, S., Tringe, S.G., Martin, J., Joye, S.B., and Moran, M.A. (2013) Transcriptional response of bathypelagic marine bacterioplankton to the Deepwater Horizon oil spill. *ISME J* **7**: 2315–2329.

Robertson, B.R. and Button, D.K. (1999) Determination of Bacterial Biomass from Flow Cytometric Measurements of Forward Light Scatter Intensity. *Curr Protoc Cytom* **9**: Unit 11.9.

Rodriguez-R, L.M., Overholt, W.A., Hagan, C., Huettel, M., Kostka, J.E., and Konstantinidis, K.T. (2015) Microbial community successional patterns in beach sands impacted by the Deepwater Horizon oil spill. *ISME J* **9**: 1928–1940.

Rognes, T., Flouri, T., Nichols, B., Quince, C., and Mahé, F. (2016) VSEARCH: a versatile open source tool for metagenomics. *PeerJ* **4**: e2584.

Röling, W.F.M. and Van Bodegom, P.M. (2014) Toward quantitative understanding on microbial community structure and functioning: A modeling-centered approach using degradation of marine oil spills as example. *Front Microbiol* **5**: 1–12.

Röling, W.F.M., Milner, M.G., Jones, D.M., Fratepietro, F., Swannell, R.P.J., Daniel, F., and Head, I.M. (2004) Bacterial community dynamics and hydrocarbon degradation during a field-scale evaluation of bioremediation on a mudflat beach contaminated with buried oil. *Appl Environ Microbiol* **70**: 2603–2613.

Röling, W.F.M., Milner, M.G., Jones, D.M., Lee, K., Daniel, F., Swannell, R.J.P., and Head, I.M. (2002) Robust hydrocarbon degradation and dynamics of bacterial communities during nutrient-enhanced oil spill bioremediation. *Appl Environ Microbiol* **68**: 5537–5548.

Ron, E.Z. and Rosenberg, E. (2014) Enhanced bioremediation of oil spills in the sea. *Curr Opin Biotechnol* **27**: 191–194.

Rongsayamanont, W., Soonglerdsongpha, S., Khondee, N., Pinyakong, O., Tongcumpou, C., Sabatini, D.A., and Luepromchai, E. (2017) Formulation of crude oil spill dispersants based on the HLD concept and using a lipopeptide biosurfactant. *J Hazard Mater* **334**: 168–177.

Rontani, J.-F. (2010) Production of Wax Esters by Bacteria. In *Handbook of Hydrocarbon and Lipid Microbiology*. Timmis, K. (ed). Berlin, Heidelberg, pp. 459–470.

Rosen, M.J. and Kunjappu, J.T. (2012) Surfactants and Interfacial Phenomena: Fourth

Edition.

Rosenberg, E. and Ron, E.Z. (1999) High- and low-molecular-mass microbial surfactants. *Appl Microbiol Biotechnol* **52**: 154–162.

Rubin-Blum, M., Antony, C.P., Borowski, C., Sayavedra, L., Pape, T., Sahling, H., et al. (2017) Short-chain alkanes fuel mussel and sponge Cycloclasticus symbionts from deep-sea gas and oil seeps. *Nat Microbiol* **2**:.

Russell, M.A., Murphy, L.E., Johnson, D.L., Foecke, T.J., Morris, P.J., and Mitchell, R. (2004) Science for stewardship: Multidisciplinary research on USS Arizona. *Mar Technol Soc J* **38**: 54–63.

Rystad Energy (2020) Global oil and gas discoveries reach four-year high in 2019, boosted by ExxonMobil's Guyana success.

Saborimanesh, N. and Mulligan, C.N. (2015) Effect of Sophorolipid Biosurfactant on Oil Biodegradation by the Natural Oil-Degrading Bacteria on the Weathered Biodiesel, Diesel and Light Crude Oil. *J Bioremediation Biodegrad* **06**:

Sambles, C.M. and White, D.A. (2015) Genome sequence of Rhodococcus sp. strain PML026, a trehalolipid biosurfactant producer and biodegrader of oil and alkanes. *Genome Announc* **3**:.

Sanni, G.O., Coulon, F., and McGenity, T.J. (2015) Dynamics and distribution of bacterial and archaeal communities in oil-contaminated temperate coastal mudflat mesocosms. *Environ Sci Pollut Res* **22**: 15230–15247.

Santos, D.K.F., Meira, H.M., Rufino, R.D., Luna, J.M., and Sarubbo, L.A. (2017) Biosurfactant production from Candida lipolytica in bioreactor and evaluation of its toxicity for application as a bioremediation agent. *Process Biochem* **54**: 20–27.

Dos Santos, H.F., Cury, J.C., do Carmo, F.L., Dos Santos, A.L., Tiedje, J., van Elsas, J.D., et al. (2011) Mangrove bacterial diversity and the impact of oil contamination revealed by pyrosequencing: Bacterial proxies for oil pollution. *PLoS One* **6**:.

Schneiker, S., Dos Santos, V.A.P.M., Bartels, D., Bekel, T., Brecht, M., Buhrmester, J., et al. (2006) Genome sequence of the ubiquitous hydrocarbon-degrading marine bacterium Alcanivorax borkumensis. *Nat Biotechnol* **24**: 997–1004.

Sevilla, E., Yuste, L., Moreno, R., and Rojo, F. (2017) Differential expression of the three Alcanivorax borkumensis SK2 genes coding for the P450 cytochromes involved in the assimilation of hydrocarbons. *Environ Microbiol Rep* **9**: 797–808.

Shade, A., Peter, H., Allison, S.D., Baho, D.L., Berga, M., Bürgmann, H., et al. (2012) Fundamentals of microbial community resistance and resilience. *Front Microbiol* **3**: 1–19.

Shaw, S.L., Chisholm, S.W., and Prinn, R.G. (2003) Isoprene production by

Prochlorococcus, a marine cyanobacterium, and other phytoplankton. *Mar Chem* **80**: 227–245.

Shekhar, S., Sundaramanickam, A., and Balasubramanian, T. (2015) Biosurfactant producing microbes and their potential applications: A review. *Crit Rev Environ Sci Technol* **45**: 1522–1554.

Short, J.W., Irvine, G. V., Mann, D.H., Maselko, J.M., Pella, J.J., Lindeberg, M.R., et al. (2007) Slightly weathered Exxon Valdez oil persists in Gulf of Alaska beach sediments after 16 years. *Environ Sci Technol* **41**: 1245–1250.

Da Silva, A.C., De Oliveira, F.J.S., Bernardes, D.S., and De França, F.P. (2009) Bioremediation of marine sediments impacted by petroleum. *Appl Biochem Biotechnol* **153**: 58–66.

Simarro, R., González, N., Bautista, L.F., Molina, M.C., and Schiavi, E. (2012) Evaluation of the influence of multiple environmental factors on the biodegradation of dibenzofuran, phenanthrene, and pyrene by a bacterial consortium using an orthogonal experimental design. *Water Air Soil Pollut* **223**: 3437–3444.

Singh, P., Patil, Y., and Rale, V. (2019) Biosurfactant production: emerging trends and promising strategies. *J Appl Microbiol* **126**: 2–13.

Smith, M.B. and March, J. (2006) March's Advanced Organic Chemistry: Reactions, Mechanisms, and Structure: Sixth Edition, Edition, 3rd (ed) W. W. Norton & Company.

So, C.M., Phelps, C.D., and Young, L.Y. (2003) Anaerobic transformation of alkanes to fatty acids by a sulfate-reducing bacterium, strain Hxd3. *Appl Environ Microbiol* **69**: 3892–3900.

So, C.M. and Young, L.Y. (1999) Isolation and characterization of a sulfate-reducing bacterium that anaerobically degrades alkanes. *Appl Environ Microbiol* **65**: 2969–2976.

Soclo, H.H., Garrigues, P., and Ewald, M. (2000) Origin of polycyclic aromatic hydrocarbons (PAHs) in coastal marine sediments: Case studies in Cotonou (Benin) and Aquitaine (France) Areas. *Mar Pollut Bull* **40**: 387–396.

Sönnichsen, N. (2020) Number of offshore rigs worldwide 2018 by region.

Southward, A.J. and Southward, E.C. (1978) Recolonization of Rocky Shores in Cornwall After Use of Toxic Dispersants to Clean Up the Torrey Canyon Spill . *J Fish Res Board Canada* **35**: 682–706.

Souza, E.C., Vessoni-Penna, T.C., and De Souza Oliveira, R.P. (2014) Biosurfactant-enhanced hydrocarbon bioremediation: An overview. *Int Biodeterior Biodegrad* **89**: 88–94.

Speight, J.G. (2004) Petroleum asphaltenes - Part 1: Asphaltenes, resins and the structure of petroleum. *Oil Gas Sci Technol* **59**: 467–477.

Sperandio, G.J. (1965) Reviews. *J Pharm Sci* **54**: 1227.

Stahl, D.A. and Amann, R. (1991) Development and application of nucleic acid probes in bacterial systematics. In *Nucleic Acid Techniques in Bacterial Systematics*. pp. 205–248.

Stevens, L. and Wardrop, J. (2005) Oil spill monitoring handbook, South Victoria, Australia: CSIRO Publishing.

Suja, L.D., Summers, S., and Gutierrez, T. (2017) Role of EPS, dispersant and nutrients on the microbial response and MOS formation in the subarctic Northeast Atlantic. *Front Microbiol* **8**: 1–15.

Suwansukho, P., Rukachisirikul, V., Kawai, F., and H-Kittikun, A. (2008) Production and applications of biosurfactant from Bacillus subtilis MUV4. *Songklanakarin J Sci Technol* **30**: 87–93.

Svane, I. and Petersen, J.K. (2001) On the problems of epibioses, fouling and artificial reefs, a review. *Mar Ecol* **22**: 169–188.

Tamura, K. and Nei, M. (1993) Estimation of the number of nucleotide substitutions in the control region of mitochondrial DNA in humans and chimpanzees. *Mol Biol Evol* **10**: 512–526.

Tatti, E., McKew, B.A., Whitby, C., and Smith, C.J. (2016) Simultaneous dna-rna extraction from coastal sediments and quantification of 16S rRNA genes and transcripts by real-time PCR. *J Vis Exp* **2016**:.

Techtmann, S.M., Zhuang, M., Campo, P., Holder, E., Elk, M., Hazen, T.C., et al. (2017) Corexit 9500 enhances oil biodegradation and changes active bacterial community structure of oil enriched microcosms. *Appl Environ Microbiol* **83**: 1–14.

Teramoto, M., Ohuchi, M., Hatmanti, A., Darmayati, Y., Widyastuti, Y., Harayama, S., and Fukunaga, Y. (2011) Oleibacter marinus gen. nov., sp. nov., a bacterium that degrades petroleum aliphatic hydrocarbons in a tropical marine environment. *Int J Syst Evol Microbiol* **61**: 375–380.

Teramoto, M., Queck, S.Y., and Ohnishi, K. (2013) Specialized Hydrocarbonoclastic Bacteria Prevailing in Seawater around a Port in the Strait of Malacca. *PLoS One* **8**: 2–8.

Tett, P. and Walne, A. (1995) Observations and simulations of hydrography, nutrients and plankton in the southern north sea. *Ophelia* **42**: 371–416.

Thingstad, T.F., Krom, M.D., Mantoura, R.F.C., Flaten, C.A.F., Groom, S., Herut, B., et al. (2005) Nature of phosphorus limitation in the ultraoligotrophic eastern

Mediterranean. *Science (80-)* **309**: 1068–1071.

Thomas, G.E., Cameron, T.C., Campo, P., Clark, D.R., Coulon, F., Gregson, B.H., et al. (2020) Bacterial Community Legacy Effects Following the Agia Zoni II Oil-Spill, Greece. *Front Microbiol* **11**: 1–15.

Throne-Holst, M., Markussen, S., Winnberg, A., Ellingsen, T.E., Kotlar, H.K., and Zotchev, S.B. (2006) Utilization of n-alkanes by a newly isolated strain of Acinetobacter venetianus: The role of two AlkB-type alkane hydroxylases. *Appl Microbiol Biotechnol* **72**: 353–360.

Throne-Holst, M., Wentzel, A., Ellingsen, T.E., Kotlar, H.K., and Zotchev, S.B. (2007) Identification of novel genes involved in long-chain n-alkane degradation by Acinetobacter sp. strain DSM 17874. *Appl Environ Microbiol* **73**: 3327–3332.

Topouzelis, K.N. (2008) Oil spill detection by SAR images: Dark formation detection, feature extraction and classification algorithms. *Sensors* **8**: 6642–6659.

Toshchakov, S. V., Korzhenkov, A.A., Chernikova, T.N., Ferrer, M., Golyshina, O. V., Yakimov, M.M., and Golyshin, P.N. (2017) The genome analysis of Oleiphilus messinensis ME102 (DSM 13489T) reveals backgrounds of its obligate alkane-devouring marine lifestyle. *Mar Genomics* **36**: 41–47.

Total-Fluides (2012) Safety Data Sheet Finasol OSR 52, Puteaux, France.

Tremblay, J., Fortin, N., Elias, M., Wasserscheid, J., King, T.L., Lee, K., and Greer, C.W. (2019) Metagenomic and metatranscriptomic responses of natural oil degrading bacteria in the presence of dispersants. *Environ Microbiol* **21**: 2307–2319.

Tremblay, J., Yergeau, E., Fortin, N., Cobanli, S., Elias, M., King, T.L., et al. (2017) Chemical dispersants enhance the activity of oil- and gas condensate-degrading marine bacteria. *ISME J* **11**: 2793–2808.

Trudel, K., Belore, R.C., Mullin, J. V., and Guarino, A. (2010) Oil viscosity limitation on dispersibility of crude oil under simulated at-sea conditions in a large wave tank. *Mar Pollut Bull* **60**: 1606–1614.

U.S. Energy Information Administration (2020) Short-Term Energy Outlook (STEO).

Union, E.U.E., Ttf, D., and International Association of Oil & Gas (2016) Europe Exploration and Production Trends 2016.

Urakawa, H., Garcia, J.C., Barreto, P.D., Molina, G.A., and Barreto, J.C. (2012) A sensitive crude oil bioassay indicates that oil spills potentially induce a change of major nitrifying prokaryotes from the Archaea to the Bacteria. *Environ Pollut* **164**: 42–45.

Urakawa, H., Rajan, S., Feeney, M.E., Sobecky, P.A., and Mortazavi, B. (2019) Ecological response of nitrification to oil spills and its impact on the nitrogen cycle.

Environ Microbiol **21**: 18–33.

Varjani, S.J. and Upasani, V.N. (2016) Biodegradation of petroleum hydrocarbons by oleophilic strain of Pseudomonas aeruginosa NCIM 5514. *Bioresour Technol* **222**: 195–201.

Varjani, S.J. and Upasani, V.N. (2017) Critical review on biosurfactant analysis, purification and characterization using rhamnolipid as a model biosurfactant. *Bioresour Technol* **232**: 389–397.

Venables, W.N. and Ripley, B.D. (2002) Modern Applied Statistics with S (Fourth Edition).

Vijayakumar, S. and Saravanan, V. (2015) Biosurfactants-types, sources and applications. *Res J Microbiol* **10**: 181–192.

Vila, J., Nieto, J.M., Mertens, J., Springael, D., and Grifoll, M. (2010) Microbial community structure of a heavy fuel oil-degrading marine consortium: Linking microbial dynamics with polycyclic aromatic hydrocarbon utilization. *FEMS Microbiol Ecol* **73**: 349–362.

Vogel, T.M. (1996) Bioaugmentation as a soil bioremediation approach. *Curr Opin Biotechnol* **7**: 311–316.

Walker, C.D., Deschamps, S., Proulx, K., Tu, M., Salzman, C., Woodside, B., et al. (2004) Mother to infant or infant to mother? Reciprocal regulation of responsiveness to stress in rodents and the implications for humans. *J Psychiatry Neurosci* **29**: 364–382.

Wang, J. and Wang, S. (2018) Microbial degradation of sulfamethoxazole in the environment. *Appl Microbiol Biotechnol* **102**: 3573–3582.

Wang, L., Wang, W., Lai, Q., and Shao, Z. (2010) Gene diversity of CYP153A and AlkB alkane hydroxylases in oil-degrading bacteria isolated from the Atlantic Ocean. *Environ Microbiol* **12**: 1230–1242.

Wang, L.Y., Ke, W.J., Sun, X.B., Liu, J.F., Gu, J.D., and Mu, B.Z. (2014) Comparison of bacterial community in aqueous and oil phases of water-flooded petroleum reservoirs using pyrosequencing and clone library approaches. *Appl Microbiol Biotechnol* **98**: 4209–4221.

Wang, Q., Garrity, G.M., Tiedje, J.M., and Cole, J.R. (2007) Naïve Bayesian classifier for rapid assignment of rRNA sequences into the new bacterial taxonomy. *Appl Environ Microbiol* **73**: 5261–5267.

Wang, W. and Shao, Z. (2012) Genes involved in alkane degradation in the alcanivorax hongdengensis strain A-11-3. *Appl Microbiol Biotechnol* **94**: 437–448.

Wang, W. and Shao, Z. (2014) The long-chain alkane metabolism network of

Alcanivorax dieselolei. *Nat Commun* **5**:.

Wang, W., Wang, L., and Shao, Z. (2010) Diversity and Abundance of Oil-Degrading Bacteria and Alkane Hydroxylase (alkB) Genes in the Subtropical Seawater of Xiamen Island. *Microb Ecol* **60**: 429–439.

Wang, W., Wang, L., and Shao, Z. (2018) Polycyclic aromatic hydrocarbon (PAH) degradation pathways of the obligate marine PAH degrader Cycloclasticus sp. strain P1. *Appl Environ Microbiol* **84**:.

Wang, Y., Lau, P.C.K., and Button, D.K. (1996) A marine oligobacterium harboring genes known to be part of aromatic hydrocarbon degradation pathways of soil pseudomonads. *Appl Environ Microbiol* **62**: 2169–2173.

Wang, Z. and Fingas, M. (2005) Oil and Petroleum Product Fingerprinting Analysis by Gas Chromatographic Techniques. In *Chromatographic Analysis of the Environment*. pp. 1027–1101.

Wang, Z., Fingas, M., Shu, Y.Y., Sigouin, L., Landriault, M., Lambert, P., et al. (1999) Quantitative characterization of PAHs in burn residue and soot samples and differentiation of pyrogenic PAH1 from petrogenic PAHs - The 1994 mobile burn study. *Environ Sci Technol* **33**: 3100–3109.

Wang, Z. and Fingas, M.F. (2003) Development of oil hydrocarbon fingerprinting and identification techniques. In *Marine Pollution Bulletin*.

Ward, C.P. and Overton, E.B. (2020) How the 2010 Deepwater Horizon spill reshaped our understanding of crude oil photochemical weathering at sea: a past, present, and future perspective. *Environ Sci Process Impacts* **22**: 1125–1138.

Wardley-Smith, J. (1980) Oil in the sea. *Mar Pollut Bull* **11**: 303–304.

Watanabe, M., Higashioka, Y., Kojima, H., and Fukui, M. (2017) Desulfosarcina widdelii sp. nov. and Desulfosarcina alkanivorans sp. nov., hydrocarbon-degrading sulfate-reducing bacteria isolated from marine sediment and emended description of the genus Desulfosarcina. *Int J Syst Evol Microbiol* **67**: 2994–2997.

White, D.A., Hird, L.C., and Ali, S.T. (2013) Production and characterization of a trehalolipid biosurfactant produced by the novel marine bacterium Rhodococcus sp., strain PML026. *J Appl Microbiol* **115**: 744–755.

White, H.K., Lyons, S.L., Harrison, S.J., Findley, D.M., Liu, Y., and Kujawinski, E.B. (2014) Long-Term Persistence of Dispersants following the Deepwater Horizon Oil Spill. *Environ Sci Technol Lett* **1**: 295–299.

Whitehead, A., Dubansky, B., Bodinier, C., Garcia, T.I., Miles, S., Pilley, C., et al. (2012) Genomic and physiological footprint of the Deepwater Horizon oil spill on resident marsh fishes. *Proc Natl Acad Sci U S A* **109**: 20298–20302.

Whyte, L.G., Hawari, J., Zhou, E., Bourbonnière, L., Inniss, W.E., and Greer, C.W.

(1998) Biodegradation of variable-chain-length alkanes at low temperatures by a psychrotrophic Rhodococcus sp. *Appl Environ Microbiol* **64**: 2578–2584.

Wickham, H. (2010) A Layered grammar of graphics. *J Comput Graph Stat* **19**: 3–28.

Widdel, F., Knittel, K., and Galushko, A. (2010) Anaerobic Hydrocarbon-Degrading Microorganisms: An Overview. In *Handbook of Hydrocarbon and Lipid Microbiology*. pp. 1997–2021.

Wieland, A., Kühl, M., McGowan, L., Fourçans, A., Duran, R., Caumette, P., et al. (2003) Microbial Mats on the Orkney Islands Revisited: Microenvironment and Microbial Community Composition. *Microb Ecol*.

Wilke, C.O. (2015) Cowplot: streamlined plot theme and plot annotations for ggplot2. *R Packag version 050 Available https//cran.rproject.org/web/packages/cowplot/index.html*.

Wilke, C.O. (2020) ggtext: Improved Text Rendering Support for “ggplot2”. R package version 0.1.0.

Wirth, M.A., Passow, U., Jeschek, J., Hand, I., and Schulz-Bull, D.E. (2018) Partitioning of oil compounds into marine oil snow: Insights into prevailing mechanisms and dispersant effects. *Mar Chem* **206**: 62–73.

Woodhead, R.J., Law, R.J., and Matthiessen, P. (1999) Polycyclic aromatic hydrocarbons in surface sediments around England and Wales, and their possible biological significance. *Mar Pollut Bull* **38**: 773–790.

Xu, E.G., Mager, E.M., Grosell, M., Pasparakis, C., Schlenker, L.S., Stieglitz, J.D., et al. (2016) Time- and Oil-Dependent Transcriptomic and Physiological Responses to Deepwater Horizon Oil in Mahi-Mahi (Coryphaena hippurus) Embryos and Larvae. *Environ Sci Technol* **50**: 7842–7851.

Xue, X., Hong, H., and Charles, A.T. (2004) Cumulative environmental impacts and integrated coastal management: The case of Xiamen, China. *J Environ Manage* **71**: 271–283.

Yakimov, M.M., Gentile, G., Bruni, V., Cappello, S., D’Auria, G., Golyshin, P.N., and Giuliano, L. (2004) Crude oil-induced structural shift of coastal bacterial communities of rod bay (Terra Nova Bay, Ross Sea, Antarctica) and characterization of cultured cold-adapted hydrocarbonoclastic bacteria. *FEMS Microbiol Ecol* **49**: 419–432.

Yakimov, M.M., Giuliano, L., Denaro, R., Crisafi, E., Chernikova, T.N., Abraham, W.R., et al. (2004) Thalassolituus oleivorans gen. nov., sp. nov., a novel marine bacterium that obligately utilizes hydrocarbons. *Int J Syst Evol Microbiol* **54**: 141–148.

Yakimov, M.M., Giuliano, L., Gentile, G., Crisafi, E., Chernikova, T.N., Abraham, W.R.,

et al. (2003) Oleispira antarctica gen. nov., sp. nov., a novel hydrocarbonoclastic marine bacterium isolated from Antarctic coastal sea water. *Int J Syst Evol Microbiol* **53**: 779–785.

Yakimov, M.M., Golyshin, P.N., Lang, S., Moore, E.R.B., Abraham, W.R., Lünsdorf, H., and Timmis, K.N. (1998) Alcanivorax borkumensis gen. nov., sp. nov., a new, hydrocarbon- degrading and surfactant-producing marine bacterium. *Int J Syst Bacteriol* **48**: 339–348.

Yakimov, M.M., Timmis, K.N., and Golyshin, P.N. (2007) Obligate oil-degrading marine bacteria. *Curr Opin Biotechnol* **18**: 257–266.

Yang, T., Nigro, L.M., Gutierrez, T., D'Ambrosio, L., Joye, S.B., Highsmith, R., and Teske, A. (2016) Pulsed blooms and persistent oil-degrading bacterial populations in the water column during and after the Deepwater Horizon blowout. *Deep Res Part II Top Stud Oceanogr* **129**: 282–291.

Yergeau, E., Maynard, C., Sanschagrin, S., Champagne, J., Juck, D., Lee, K., and Greer, C.W. (2015) Microbial community composition, functions, and activities in the gulf of mexico 1 year after the deepwater horizon accident. *Appl Environ Microbiol* **81**: 5855–5866.

Yetti, E., Thontowi, A., and Yopi (2016) Polycyclic aromatic hydrocarbon degrading bacteria from the Indonesian marine environment. *Biodiversitas* **17**: 857–864.

Yuan, J., Lai, Q., Sun, F., Zheng, T., and Shao, Z. (2015) The diversity of PAH-degrading bacteria in a deep-sea water column above the southwest Indian ridge. *Front Microbiol* **6**: 1–12.

Zadjelovic, V., Chhun, A., Quareshy, M., Silvano, E., Hernandez-Fernaud, J.R., Aguilo-Ferretjans, M.M., et al. (2020) Beyond oil degradation: enzymatic potential of Alcanivorax to degrade natural and synthetic polyesters. *Environ Microbiol* **22**: 1356–1369.

Zajic, J.E., Guignard, H., and Gerson, D.F. (1977) Properties and biodegradation of a bioemulsifier from Corynebacterium hydrocarboclastus. *Biotechnol Bioeng* **19**: 1303–1320.

Zakaria, M.P., Takada, H., Tsutsumi, S., Ohno, K., Yamada, J., Kouno, E., and Kumata, H. (2002) Distribution of polycyclic aromatic hydrocarbons (PAHs) in rivers and estuaries in Malaysia: A widespread input of petrogenic PAHs. *Environ Sci Technol* **36**: 1907–1918.

Zeinstra, M., Brussaard, C., McGenity, T.J., McKew, B.A., Thomas, G.E., Murk, T., et al. (2020) ExpOS'D: Experimental Oil Spill Data-sharing.

Zhang, G., Wu, Y., Qian, X., and Meng, Q. (2005) Biodegradation of crude oil by *Pseudomonas aeruginosa* in the presence of rhamnolipids. *J Zhejiang Univ Sci*

6B: 725–730.

Zhang, Z., Hou, Z., Yang, C., Ma, C., Tao, F., and Xu, P. (2011) Degradation of n-alkanes and polycyclic aromatic hydrocarbons in petroleum by a newly isolated Pseudomonas aeruginosa DQ8. *Bioresour Technol* **102**: 4111–4116.

Zhuang, L., Liu, Y., Wang, L., Wang, W., and Shao, Z. (2015) Erythrobacter atlanticus sp. nov., a bacterium from ocean sediment able to degrade polycyclic aromatic hydrocarbons. *Int J Syst Evol Microbiol* **65**: 3714–3719.

Appendix

Appendix 1: Published Technical Report – ExpOS'D: Experimental Oil Spill Data-sharing

Zeinstra, M., Brussaard, C., McGenity, T.J., McKew, B.A., **Thomas, G.E.**, Murk, T., et al. (2020) ExpOS'D: Experimental Oil Spill Data-sharing.

ITOPF R&D Award 2018
Final Report

ExpOS'D

Experimental Oil Spill Data-sharing

Experimental oil spill

April 16th – April 18th 2019

Marieke Zeinstra	NHL Stenden University of Applied sciences
Corina Brussaard	NIOZ
Terry McGenity	University of Essex
Boyd McKew	University of Essex
Gareth Thomas	University of Essex
Tinka Murk	Wageningen University and Research
Martine van den Heuvel Greve	Wageningen University and Research
Michiel Visser	Rijkswaterstaat Zee & Delta

Acknowledgements

We express thanks to Rijkswaterstaat Zee & Delta, Michiel Visser in particular, for their extensive efforts in organizing this research opportunity. Furthermore, we thank the crew of the involved vessels ARCA, ROTTERDAM and HEBO-CAT 7, as well as the organization providing the aerial surveillance aircraft (Dutch Coastguard, MUMM Belgium, Havariekommando CCME) for their assistance. Furthermore we thank the Belgian authorities (directorate-general Environment of the federal public service health, food chains safety and environment) for the use of their dispersant application equipment.

We thank ITOPF for funding the research activities with the R&D Award 2018. B McKew also acknowledges funding from the Eastern Academic Research council and G Thomas' participation was also supported by The Natural Environmental Research Council EnvEast Doctoral Training Partnership.

Dedication

In memory of Sjon Huisman, whose extensive efforts have been crucial in initiating this experiment.

Contents

Reading Guide

To accommodate for the various nature of the studies performed, the report is divided into different sections:

In chapter 1 the goal of the project and the plans are outlined, as well as the process towards actually performing the experiment.

Chapter 2 describes the experimental oil spill as performed in April 2019 in detail.

In chapters 3 and 4, you'll find a separate chapter per research topic, describing methods, results and conclusions.

1 Introduction

1.1 Description of the project

Like any spill-response option, the goal of dispersant application is to minimize the impacts of the oil. To better predict these impacts and aid decision making, scientists work towards a better understanding of the effectiveness and effects of dispersion of oil under different conditions.
Rijkswaterstaat (the Dutch government agency responsible for oil spill response) has organised an experimental oil spill in the North Sea comparing two different dispersion options (natural and chemical) on separate oil slicks under similar conditions.
The ExpOS'D project was initiated to enable researchers from different international institutes and with different research focus, to collect data from these oil slicks, yielding a uniquely comprehensive and integrated dataset for current and future research. Planned observations included: 1) The behaviour (size, shape, thickness profile) of the different slicks on the water surface over time and spatiotemporal water column hydrocarbon profiles as an indication of the effect of the treatments on the fate of oil and as validation for underlying mechanisms. 2) Analysis of microbial and planktonic community compositions over time, providing an indication of the impact of the treatments on key biogeochemical processes and potential for oil biodegradation. 3) Measurement of concentrations of precursors of aggregate formation (TEP/EPS) to provide insights in the potential of different treatments to induce enhanced marine snow formation or even MOSSFA effects (marine oil-snow sedimentation and flocculent accumulation).
The resulting data-set will be shared publicly to allow a broad application of the obtained data.

1.2 Experimental design

Weather conditions are crucial in this experiment: The wind speed should be at least 5 m/s, to be able to observe the dispersion process (this will not occur with insufficient wind energy). Furthermore, with these conditions, the light oil that is planned for the experiment is expected to disappear on its own without residues. A maximum wind speed of 10 m/s was chosen. Above this wind speed the slicks could disappear too quickly, and the safety during the experiment cannot be guaranteed (especially for sampling with the RHIB).

The project proposal consisted of the following experimental design:
Two dispersant conditions are compared natural dispersion (no treatment) and chemical dispersion (ship based dispersant application). For each of the conditions, two oil slicks are released: one crosswind slick and one into the wind direction. Each slick is a single straight line, released with a controlled outflow from a ship sailing at a fixed speed (Table 1).

Table 1. Slick summaries

	Alpha	*Bravo*	*Charlie*	*Delta*
	Day 1	Day 1	Day 2	Day 2
	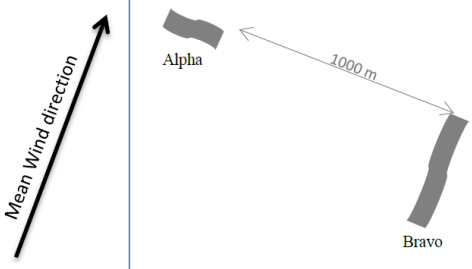		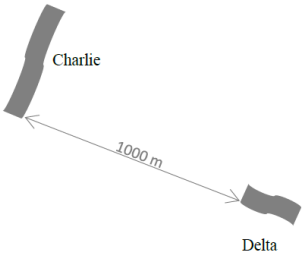	
Oriëntation	Crosswind	Into the wind direction	Into the wind direction	crosswind
Oil Volume	1,5 m^3	3,5 m^3	3,5 m^3	1,5 m^3
Length	215 m	500 m	500 m	215 m
Treatment	None (natural disp.)	None (natural disp.)	Chemical dispersion	Chemical dispersion
	Aerial observation	Aerial observation	Aerial observation	Aerial observation
	Ship based radar	Ship based radar	Ship based radar	Ship based radar
		Sampling oil & water	Sampling oil & water	

After the slicks are deposited, their transport, shape and size are monitored by means of ship-based radar as well as aerial observation.

For the two larger, crosswind, slicks, samples of the oil slick and the water beneath the oil slick are collected at four time intervals, to be analysed for different purposes (Table 2).

Table 2. sampling summary based on original logistics plan (13-04-2018)

Measurement	Institution	Oil Slicks	Locations	Depths	TimePoint	Total number of samples
Water - toxicity test	WUR	Bravo-Charlie	Out -Centre	1,5m-5m	T1-T2	36
Water - phytoplankton pigments (HPLC)	NIOZ	Bravo-Charlie	Out-Edge-Centre	1,5m-5m	T1-T2-T3-T4	48
Water - microbe abundances (FCM)	NIOZ	Bravo-Charlie	Out-Edge-Centre	1,5m-5m	T1-T2-T3-T4	48
Water - nutrients	NIOZ	Bravo-Charlie	Out-Edge-Centre	1,5m-5m	T1-T2-T3-T4	48
Water - zooplankton qualitative analysis	NIOZ	Bravo-Charlie	Out-Edge-Centre	1,5m-5m	T1-T2-T3-T4	48
Water - TEP	NIOZ	Bravo-Charlie	Out-Edge-Centre	1,5m-5m	T1-T2-T3-T4	96
Water- for DNA extraction, qPCR abundance and NGS Miseq amplicon libraries & nutrient analysis	Uessex	Bravo-Charlie	Out-Edge-Centre	surface-1,5m-5m	T1-T2-T3-T4	120
Water - GC/MS hydrocarbon analysis	Uessex	Bravo-Charlie	Out-Edge-Centre	surface-1,5m-5m	T1-T2-T3-T4	192
Oil layer - Dispersant residue	Rijkswaterstaat	Charlie	Centre	surface	T1-T2-T3-T4	8

In addition, laboratory verification experiments are performed with the same oil and dispersant as the field experiment, studying:

- Impact of dispersant on hydrocarbon degradation and microbial communities.
- Formation of Extracellular Polymeric Substances

1.3 Materials

The oil type used was a Light/Medium Arabian Crude (table 3).

Table 3. General properties of the test oil, determined upon first delivery (April 2018)

Name	Method	Units	Result (Temperature)	
Kinematic viscosity	ASTM D445	mm^2/s	10.76 (15 °C)	7.597 (25 °C)
Density	ASTM D5002	kg/m^3	879.4 (15 °C)	872.6 (25 °C)
API gravity	calculated	-	29.32	
Oil-seawater interfacial tension	ASTM D1331	Dynes/cm	14.8 (13 °C)	

Dispersant used was: Dasic Slickgone NS dispersant, from the stock of the Belgian operational spill response organisation.

1.4 Performing the experimental oil spill

The first attempt was planned for April 17th-20th 2018. As weather conditions seemed appropriate, all ships, equipment, materials, observation airplanes and people were mobilized for the execution of the experiment. On the first test day, we sailed out to the test location although expected wind speeds were slightly below optimal. Upon arrival at the test location we were faced with conditions even more quiet than expected, rendering execution of the experiment not useful as well as potentially harmful to the environment due to the persistence of the slick in such conditions. Under the assumption that more suitable conditions might come up in the next days, the equipment and procedures necessary in the experiment were tested.
Later that day, the decision was made to cancel the efforts for this attempt as weather reports did not indicate suitable conditions for the following days.

A new attempt at performing the experiment was planned for September 18th-21st 2018. Our experience during the April attempt was used to make minor adjustment of plans and procedures. Sampling and sample processing procedures were adjusted to adapt to the conditions on board. A separate aerial observations plan was performed to eliminate a centralized briefing with the aircraft crews from different countries and allow them to fly from their home base. However, the weather posed a problem again: due to a tropical storm in the region (ex-hurricane Helene) and the uncertainties in predicting its path, the weather predictions were very uncertain in the week prior to the experiment (at the formal Go/No-go moment).
As a result, the organizers decided to not commence mobilization of ships and materials and cancel this attempt.

The experimental oil spill was performed the third, and final, attempt in April 2019. Because project funds had been lost in (preparations & logistics surrounding) the two previous attempts, the experimental design of the sampling had to be limited.

2 Experimental oil spill April 2019

The third attempt for the experimental oil spill was planned for 16th and 17th of April 2019. As mentioned, some aspects were removed from the sampling plan (table 4).

Table 4. Adjusted sampling plan for April 2019

Measurement	Institution	Oil Slicks	Locations	Depths	TimePoint	Total number of samples
Water - toxicity test	WUR	Bravo-Charlie	Out -Centre	1,5m-5m	T1-T2	36
Water- for DNA extraction, qPCR abundance and NGS Miseq amplicon libraries & nutrient analysis	Uessex	Bravo-Charlie	Out -Centre	surface-1,5m-5m	T1-T2-T3-T4	144
Water - GC/MS hydrocarbon analysis	Uessex	Bravo-Charlie	Out -Centre	surface-1,5m-5m	T1-T2-T3-T4	144
Oil layer - Dispersant residue	Rijkswaterstaat	Charlie	Centre	surface	T1-T2-T3-T4	8

On the day prior to the experiment, we decided to perform a condensed experimental design, as the expected wind speed for the 2nd test day would be insufficient. The condensed plan meant releasing three oil slicks on the same day (Alpha, Bravo and Charlie; table 1), so that the majority of the planned data and observations could still be collected within the 1-day window of suitable conditions.

Table 5. Participants involved in the experimental oil spill in April 2019

Name	Organisation	Role	
Michiel Visser	RWS Zee & Delta	On Scene Commander	ARCA
Bert van Angeren	RWS Zee & Delta	Assistant OCS	ARCA
Marieke Zeinstra	NHL Stenden University of Applied Sciences	Research Leader	ARCA
Sanne Steenbrink	NHL Stenden University of Applied Sciences	Oil deposition obs.	HEBOCAT
Tim Leijssen		Radar Observations	ARCA
Claus van de Weem		Radar Observations	ARCA
Terry McGenity	University of Essex	Principal Investigator	-
Boyd McKew	University of Essex	Principal Investigator Water sampling	ARCA
Gareth Thomas	University of Essex	Water sampling	ARCA
Corina Brussaard	NIOZ	Principal Investigator	-
Anna Noordeloos	NIOZ	Logistics	-
Gianluca Bizzarro	NIOZ	Water sampling	ARCA
Tinka Murk	WUR	Principal Investigator	-
Martine van den Heuvel	WUR	Principal Investigator	-
Vincent Escarvage	WUR	Logistics of samples	-
Eric Donnay	FPS-DG Environment Belgium	Dispersant application	ARCA
Philip Durieux	FPS-DG Environment Belgium	Dispersant application	ARCA
Richard Hill	OSSC	Dispersant application	ARCA
Jon Rees	CEFAS	Modelling	-

2.1 Activities Log

Date	Time (local)	Action
16-04-2019		
	9:00	All ships on site
	9:15	HEBOCAT releases slick Alpha
	9:36	Measurement of environmental conditions (water)
	10:25	HEBOCAT releases slick Bravo
		Sampling outside of slick, T1
	11:12	Measurement of environmental conditions (water)
	11:35	Sampling inside slick Bravo, T1
	11:40	HEBOCAT releases slick Charlie
	12:15-13:17	Dispersant application on slick Charlie
	13:39	Alpha and Bravo slick are merging: Aerial observations indicate initial contact upwind edge of Alpha and downwind tip of Bravo.
	13:46	Sampling inside slick Charlie, T1
	14:13	Measurement of environmental conditions (water)
	14:42	Sampling inside slick Bravo, T2
		Sampling outside of slick, T2
	17:01	Sampling inside slick Charlie, T2
17-04-2019		
	7:52 (5:52 UTC)	EMSA CleanSeaNet detects potential oil slick near original test area. 52° 26' 51" N 003° 50' 44" E
	11:25	ARCA arrives on spill location; The oil slicks have drifted to the shipping lane, some ship trails through them are observed. Small patches of sheen are ominous in the area.
		1st larger slick observed by radar: Shape (long), orientation (East-West) and size (2 km long), give strong indication this is one of the main slicks (either Bravo or Charlie).
	11:41	Measurement of environmental conditions (water)
	11:42	Sampling outside of slick, T3
	11:58	Sampling 1st observed slick, with bottles labelled 'Bravo', T3
	12:12	2nd larger slick observed by radar, to the south of 1st observed slick: Shape, orientation and size, indicate this is one of the main slicks. Distance and orientation towards the other slick (to the south of, and slightly tilted compared to each other) give strong indication that this is the Bravo slick.
	12:23	Sampling 2nd observed slick with bottles labelled 'Charlie', T3
	13:00	Mechanical dispersion/scattering of remaining oil with ARCA
	15:00	Return to port
	19:33 (17:33 UTC)	EMSA CleanSeaNet detects no potential oil slicks in the vicinity of the test location.

The following sub-sections will explain the activities in more detail.

2.1.1 Oil Slick deposition (16-04-18)

Oil was pumped directly out of a tank container on deck of the HEBOCAT 7. To ensure a constant initial thickness within and between slicks, the deposition occurred at a fixed pump-rate (24 m^3/h), with a fixed sailing speed relative to the water (2 knots). The oil was released from a 2"hose, trailing 20 meters behind the ship on flotation bladders, thereby avoiding agitation of the oil slick by the ship itself.

Oil slick Bravo was deposited Northeast of Alpha at that time, at a distance of 2100 m. Crosswind spacing (North-South) was 1000 m, as planned.

Oil slick Charlie was deposited parallel to Bravo, 1500 meters to the North (the spacing was increased based on observed spreading of the existing slicks).

	Deposition start			**Deposition end**		
	Time	**Coordinates**		**Time**	**Coordinates**	
Alpha (crosswind)	09:12			09:18	52°15,129' N	3°59,527' E
Bravo	10:20			10:29	52°14,991' N	3°59,514' E
Charlie	11:34			11:43	52°15,929' N	3°56,520' E

The weight of the container was recorded from the crane on board the ship:

Weight of container+oil before experiment	13,5 tonnes
Weight of container+oil after experiment	8,2 tonnes
Amount of oil deposited	**5,3 tonnes**

With our oil density of 879,4 (15 °C), this means a total of 6,03 m^3 oil was released.

Deposition using the diaphragm pump should be consistent over time, this means slick Alpha is 1,51 m^3 and Bravo and Charlie are 2,26 m^3 each.

2.1.2 Dispersant application (16-04-18)

Dispersant was applied via the ship-borne application system (MARKLEEN Dispersant spray system) installed on the ARCA specifically for this experiment. The dispersant spray arms were fitted on either side of the aft deck. Drop hoses were used to bring the spray nozzles closer to the water surface.

The ARCA sailed through the oil slick with a speed of 3 knots. A constant flow of seawater (110-120 l/min) was maintained through the system. The dispersant flow (9-11 l/min) was started when entering the oil slick and stopped when exiting it. With the sailing speed of 3 knots this would ensure a dispersant dosage of 40 - 50 l per 10 000 m^2 of oiled area, consistent with dispersant manufacturer recommendation.

	Dispersant flow ON			**Dispersant flow OFF**		
	Time	**Coordinates**		**Time**	**Coordinates**	
Track 1 (against the wind)	12:20	52°16,225' N	3°55,643' E	12:28	52°16,668' N	3°56,340' E
Track 2 (with the wind)	12:35	52°16,914' N	3°56,399' E	12:51	52°16,981' N	3°55,190' E
Track 3 (against the wind)	12:59	52°17,188' N	3°55,234' E	13:16	52°18,062' N	3°56,710' E

During the experiment, the dispersant application digital flow meter reading was fairly constant and did not drop below 9 l/min. This would suggest, in the 41 minutes of dispersant application, between 369 and 451 litres of dispersant were applied. However, the calibration of the flowmeter wasn't checked before the experiment and is therefore only indicative. The dispersant used was contained in a standard cubitainer of 600 l. According to the level indications observed at the start (600 l) and end of the experiment (400 l) of the dispersant tank, approximately 200 litres of dispersant were applied on the Charlie slick. This suggests that the values of the flowrate of dispersant indicated by the flowmeter where overestimated. Both values are less than the theoretical recommended maximum amount of (3,5 m^3 x 0,20 = 700 litre).

More spray passes would be advised in case of a real spill situation. For this experiment, it was decided not to do so as it would leave insufficient time for observing the slick behaviour and sampling.

Visually, the dispersion application appeared to work on the treated areas: The treated area seemed clear from oil. However visual observations did not show a visible dispersion effect on the patches of emulsified oil after treatment by dispersants.

For future application of dispersant spray arms on the ARCA, it was advised to fit them more to the front of the ship where the oil film is not pushed away of ship's sides, increasing the oil encounter rate.

2.1.3 Sampling stations

Sampling was performed from the RHIB at three different water depths. Water was sampled at 1,5 and 5 meters below the surface, using a sampling device specialized for sampling beneath floating oil slicks[1]. Surface samples were collected by manually filling a bottle at the water surface .

Label	Notes	Time	Coordinates	
	16-04-19			
Control T1		11:13	52°14'26,6"N	3°59'00,2"E
Bravo T1		11:35	52°14'52,9"N	3°57'17,5"E
Charlie T1		13:46	52°18'56,3"N	3°56'21,3"E
Bravo T2		14:42	52°20'09,7"N	3°57'40,3"E
Control T2		14:56	52°21'01,8"N	3°58'40,5"E
Charlie T2		17:01	52°24'41,3"N	4°01'16,1"E
	17-04-19			
Control T3		11:46	52°25'40,5"N	3°51'30,3"E
Bravo T3	1st observed slick (must be Charlie)	11:58	52°25'23,7"N	3°51'06,2"E
Charlie T3	2nd observed slick, south of first (thus is Bravo)	12:23	52°24'38,7"N	3°49'25,3"E

Oil slick identification on day 2 proved a challenge as a lot of smaller patches were found in the area. After aerial observations guided the ARCA to the most heavily oiled area, the ship-based radar was used to identify oil slicks as 'major' slicks based on expected orientation and elongated shape.

Two major slicks were identified, each around 2 km long, oriented roughly east-west, positioned parallel to one another with a distance of approximately 1,5 kilometres.

Aerial observations for this time confirm these two slicks are the most substantial slicks in the area: They are indicated as the thickest oil observed. Other slick instances identified in the area are a long thin streak of sheen, and spill fragments around the anchorage area.

2.1.4 Measurement of environmental conditions (water)

Using the integrated sensors of the (Seabird) CTD sampler available on board of the ARCA, water column conditions were measured at different times during the experiment.

Used sensors: Temperature (Serial# 1643), Conductivity (Serial# 1443) and Ph (Serial# 0717).

Date	Local Time	Latitude	Longitude	Depth (m)	Temperature (°C)	Conductivity (S/m)	Salinity (PSU)	pH
Apr 16 2019	9:39:38	52,2445	3,9872	1,47	9,08	3,021	27,8	8,4
	11:12:45	52,2370	3,9826	6,96	9,17	3,076	28,3	8,4
	11:17:50	52,2365	3,9794	4,78	9,27	3,014	27,5	8,4

[1] L. Peperzak, P. Kienhuis, C. P. D. Brussaard, and J. Huisman, "Accidental and Deliberate Oil Spills in Europe: Detection, Sampling and Subsequent Analyses," in *Handbook of Hydrocarbon and Lipid Microbiology*, Ed Timmis KN and van der Meer J-R, vol. 78, no. January, Berlin, Heidelberg: Springer Berlin Heidelberg, 2010, pp. 3471–3489.

	14:16:50	52,3245	3,9550	1,31	9,39	3,137	28,7	8,5
	14:18:06	52,3250	3,9553	5,87	8,85	3,438	32,2	8,4
Apr 17 2019	11:47:17	52,4292	3,8544	1,27	9,01	3,514	32,9	8,4
	11:48:49	52,4290	3,8540	4,31	8,93	3,509	32,9	8,4

2.1.5 Radar observations

On board of the MV Arca, a ship-borne oil radar was used to observe the oil slicks in the area around the ship. (Working principle of this radar is similar to that of the SLAR and SAR radars used in aerial and satellite observations: A floating substance can dampen the capillary waves that are normally present on the water surface. The radar picks up the capillary waves and thereby the lack of them is visible as a darker area.) The field of view the first day was roughly 3 km, the second day the wind speed declined and the result was a range of roughly 2 km. The radar operator manually added & edited polygons outlining the slick extent visible on the radar image. The polygons were subsequently saved. Raw data from both days is stored and the operations are summarised as time compressed movie 1 for each day (https://doi.pangaea.de/10.1594/PANGAEA.902609).

The radar image was visible for the crew on board, allowing for the researchers to observe the slicks in real time as well as guiding the ship's crew in operational tasks such as chemical dispersion on day one and mechanically dispersing the remaining slicks on day 2.

2.1.6 Aerial observations

The trials were monitored by different aircraft. A flight schedule was devised to have a continuous view on the oil slick:

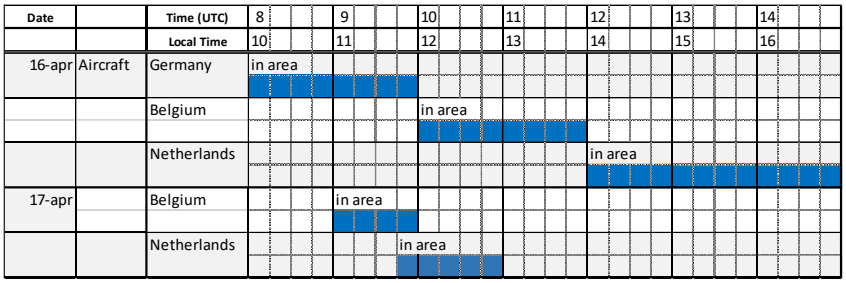

Observers were asked to record oil slick characteristics during the lifetime of the slicks:

- Slick Length
- Slick Width
- Orientation of slick relative to North
- Coordinates of the slick (downwind edge (centre of width))
- Mass distribution within the slick: Is the thickest part down-wind, central, or elsewhere?

In addition, they collected imagery with the different sensors available in the different aircraft (SLAR images, photos, IR/UV images).

2.2 General observations and remarks

The adjustment of the plan to make three of the oil slicks on one day, did have some effect on the data collection:

Not all three slicks could be observed by the oil-radar on the ARCA at the same time as the total size of the test area extended the range of this specific radar. Furthermore, the workload of the sampling crew was high as they had to sample two slicks the same day.

2.2.1 Qualitative observations during the experiment

During dispersant application, the ARCA sailed through the relatively fresh (1-2u) Charlie slick. (Each traverse was through a previously untreated portion of the oil slick.) The participants on board the ARCA had a unique view on this fresh oil layer from the height of the bridge.

- The oil slick was generally thin (metallic), with small irregular streamers of black oil.
- Streamers of light-brown coloured oil were visible within the slick, suggesting emulsification already occurring on this short time-scale.
- Wave breaking in the slick would result in a local clean patch that subsequently gradually built up in thickness through the colours sheen-rainbow-metallic.
- Little black globules of oil were observed in the slick.

3 Research based on the experimental spill

Oil slick elongation and transport as a result of dispersion

Zeinstra-Helfrich M, Marieke

This section describes the behaviour of the oil slicks over time based on observations from the sky as well as the ship based radar. In addition the slick behaviour is compared with oil slick elongation model results.
The oil slicks very clearly elongate in the wind direction, with a rate that is approximately the same for all three slicks, meaning that the crosswind slick Alpha relatively elongates much faster.
The elongation model overestimates the dispersion, thereby making the slicks disappear too quick. The extrapolation of the layer thickness-droplet size relation should be reassessed, as they were not measured for the layer thicknesses that were observed in the field. Furthermore the overestimation of dispersion can partly be attributed to the environmental conditions; the specific situation (wind from over a large landmass) meant the sea was less energetic than our simple wind speed relation predicted.

1. Introduction

One goal of the experimental oil spill was to investigate the manner in which the oil slicks disappear from the water surface over time. Basis of the experiments was comparing the behaviour of 2 long slicks, one of which is placed parallel to wind direction and the second perpendicular to the wind direction. This configuration would allow comparison of the lengthwise dilution process depending on slick size (cross section in wind direction). Furthermore the behaviour of a long wind-wise naturally dispersed slick could be compared with a chemically dispersed slick in the same configuration.

1.1. Theory

Breaking waves submerge local patches of oil. This process (entrainment) occurs at a rate depending on the amount of breaking waves. The submerged oil is broken into droplets with a size dependent on mixing energy, oil properties and oil layer thickness. The droplets rise back to the water surface; their time under the water surface depends on how deep they were entrained (wind speed), density difference between oil and seawater, but mostly on droplet size. As the oil slick is transported by the wind, oil that has been submerged for sufficiently long can resurface upwind of the original slick, causing an elongation (dilution) of the oil slick in the wind direction.

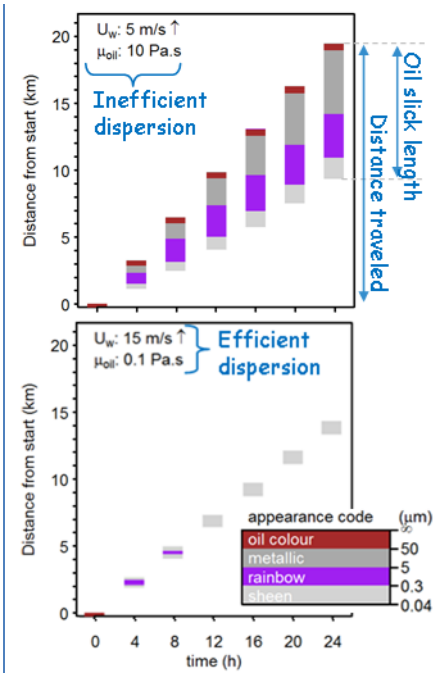

When modelling this phenomenon, two distinct mechanisms show up (Fig. 1):

Fig. 1. Modelled oil slick elongation for two extreme cases. Wind direction is up, colours indicate oil slick thickness, adapted from (Zeinstra-Helfrich et al. 2017)

In case of sub-optimal dispersion, the main slick remains largely intact (in size an thickness) and forms a long tail with decreasing thickness in the upwind direction. Over time, more oil is gradually transported to the tail, which increases in length while the thickness of the main slick very slowly decreases. The downwind edge of the oil slick is displaced in the wind direction with the chosen wind drift factor.

In case of optimal conditions for (natural or chemical) dispersion, a more vertical process occurs. A lot of entrainment is occurring, and entrained oil is broken up into droplets that are very well suspended. As a result, a lot of the oil is moved to the water column in the first hours. As the resulting slick becomes thinner, this process goes increasingly fast. Visible on the water surface is a relatively small oil slick that contains only a small fraction of the original spilled oil. The thickest part of this slick is in de middle, and as most oil is suspended below the surface, the slick movement by wind is much less than the modelled wind drift factor.

For situations between those extremes, a combination of these both processes occurs: in which the slick elongates until the main slick has decreased sufficiently to transition into the vertical behaviour of 'optimal' conditions.

2. Methods

The execution of the experimental oil spill itself has been described in chapters one and two of the main report. This section describes the methods specifically for the investigation of oil slick behaviour and transport.

2.1. Data processing

The observations recorded by the aerial observers (mostly provided in the 'standard Bonn Agreement Pollution forms') were aggregated into one large table.

The oil slick polygons that were collected with the ship-based oil radar, were read & processed using Python. The observations were aggregated into the same table:

- Observation time (corrected from local time to UTC, as well as the 15 minute offset of the radar PC.)
- The polygon itself
- Slick length: length of the polygon's bounding box (The bounding box, is the smallest rectangle that can completely enclose the polygon)
- Slick width: width of the polygon bounding box
- Oiled area: polygon area.
- Orientation: the orientation of the polygon's bounding box, in degrees compared to North.

For slick Alpha, the initial length & width (the first 30 minutes), needed a bit more consideration: The longest axis of the slick (length) is crosswind at the time of deposition and a brief period afterwards, later on the longest axis orients in the wind direction (similar to oil slick B and C). In our analysis we're interested in elongation in the wind-direction, and therefore this is the 'length' we are looking for.

To accommodate this, the characteristics of the first 30 minutes of slick Alpha are calculated separately:

- The width of the slick is the distance between the most Northern and Southern tip of the slick polygon.
- The length of the slick is the distance between the Eastern and Western edge of the slick cross-section in the middle between the North and South tip.

Upon returning to the slicks on the 2nd test day, more oil slick observations were made. These observations are not included in this analysis as the slicks were not undisturbed (they passed shipping).

2.2. Oil Slick elongation modelling

The test conditions were replicated using the Oil Slick Elongation model (Zeinstra-Helfrich et al. 2017).

- Slick Alpha & Bravo were modelled from (just after) deposition: using length as observed at that time & oil volume/slick area as thickness.
- Slick Bravo & Charlie were modelled starting 1,5 hour after deposition (the time chemical dispersion was finished). The simulations use length as observed at that time & oil volume/slick area as thickness.

		A	B	B > 1,5 h	C > 1,5 h
L_0	m	241	1067	2019	1851
H_0	m	1,26E-05	3,68E-05	3,31E-06	4,37E-06

Oil properties of the fresh oil were based on the measurements as performed in April 2018. Oil properties of weathered oil were based on weathering calculations for an amount of 3,5 m^3 of our oil for 1,5 hours.

		Fresh	Weathered	Weathered + dispersant
ρ_{oil}	kg/m^3	879,4	937	937
μ_{oil}	Pa.s	9,46E-03	2,21E-01	2,21E-01
$\sigma_{oil\text{-}sw}$	N/m	0,0148	0,0148	0,00148

The model was run with different settings for wind speeds. (7,5, 8,9 and 6,5 m/s)

3. Results

The data table of oil slick observations is stored available via PANGAEA (https://doi.pangaea.de/10.1594/PANGAEA.902311). The data was used to produce images per oil slick. In this chapter we describe the results, the images can be found in the appendix (pages 24 to 28).

3.1. General observations on the slick behaviour over time

Slick *Alpha* (p24-25)was deposited at 7:12u UTC, and can only be observed for a little over 5 hours before merging with Bravo. It was deposited across the wind: On the first radar observation, 13 minutes after deposition, its angle is 29° compared to North. The Alpha slick very clearly develops a tail in the upwind direction (east). As a result, the longest axis soon shifts towards an orientation around 90°.

From 9:30, the aerial observers consistently report a greater oil slick length than the ship-based radar. The mismatch appears to occur in pinpointing the western tip of the oil slick. As the ARCA was sailing near slick Bravo at that time, the western tip was our far side: there is a possibility we underestimated the western tip of slick alpha as it neared the edge of the radar range. Oil slick width observations show better agreement between aerial reporting and radar observations.

The (crosswind) width of the slick gradually increases from just below 0,5 km to 1,21 km. The length (in wind direction) of increases up to 3,700 km in 4,32 hours. This is an increase of 3,5 km compared to the first observed length of 215 meters.

The IR images made by the German Coastguard over a period of two hours (8-10 UTC) very clearly show a thick 'streak' in the downwind edge of the oil slick. The thick portion starts off as a 50-100 m wide crosswind band, visible 1 hour after deposition (IR image 8:16UTC), developing a progressively longer tail over time (Fig. 13, p25). The thick portion slowly appears to decrease in thickness and size.
Subsequent aerial observations by the Belgian Coastguard record the same phenomenon: at 10:32 and 11:15 they record a long slick oriented around 90°, with the thickest portion at or near the downwind edge. In their final observation (11:44), no specific thickest part can be observed and the slick area is 60% sheen and 40% metallic (Fig. 12, p24).

Slick *Bravo* (p26-27) was deposited at 8:25 UTC, into the wind direction (69° compared to North). The orientation quickly shifts to 80° and remains so fairly constant.

In the first 3 hours of the slick lifetime, radar and aerial observations of length, width and location are in good agreement. After 12 UTC, it is presumed that the aerial observers included the former slick Alpha in their observations of slick Bravo. There is a big jump in slick length, width and area at that time, largely consisting of sheen- oil thicknesses (0,04 – 0,30 µm).

Slick bravo starts of 212 meter wide and spreads to 1518 m wide. Ship-based radar observations, indicate length increased from 1,02 to 5,26 km in 6,79 hours (for comparison with Alpha: Bravo elongates to 3,44 km in 4,29 h).

The thick part of slick Bravo is an elongated wind-wise shape: In the IR images of 9:15, 9:35 and 9:59, the thick portion of slick Bravo is 1,3 to 1,4 km long, and a thinner sheen is forming on the upwind (right) side. Subsequent Aerial observations (10:36, 11:13), indicate the thick portion on the downwind side in the form of an elongated shape of 1,3 and 1,5 km long (reported as the downwind 50% of the 2,6 km long slick, the downwind 50% of the 3,0 km long slick respectively). In the last observation (11:48), the thick portion has an undefined length and is positioned at 30% of the slick length.

Thickness observations until 12:00 UTC indicate show the slick is spreading out: The area of thickest oil (true oil colour, class 4&5) decreases, while area of the thinner oil increases. (After 12 UTC, this graph is affected by slick Alpha.)

Oil slick *Charlie* (p28) was deposited at 11:34 UTC, dispersants were applied over the period 10:20 - 11:16 UTC. The initial orientation the slick was 55°, the angle increases to 65-70°, but settles down around 55° at the end of test day 1.

Radar and aerial observations of oil slick length match very well for slick Charlie. There is some disagreement between the width observations, however. This could be due to the generally irregular shape of the oil slick. (The polygons show more 'jagged' edges, compared to the 'smoother' slick Bravo).

Slick Charlie spreads from 117 meter to 951 meter in width. The length increases from 878 meters to 4,20 km in 5,51 hours. (In 4,32 and 4,38 hours the slick elongates to 3,89 km (Ship Radar) and 3,30 km (Aerial observation)).

Thickness observations of slick Charlie are a bit less clear than for the other slicks, in part because IR observations were no longer available at that time. Aerial observations indicate the thickest portion of the slick to be in the centre of the width, subsequently:

- in 3 patches, starting at 30% of slick length (10:38)
- from start until width of the slick (11:13)
- at 40% of length starting downwind (11:42): 40% of 2,6 km long = 1,3 km long.

Slick Charlie spreads out: over time, the area of thinner slick (sheen, rainbow & metallic) increases while the true oil colour decreases.

3.2. Model results

The initial model runs were based on wind speed of 7,5 meters per second and oil thicknesses based on observations. The outputs of these runs (Fig. 4 and Fig. 5, page 21), clearly show the behaviour of the oil slicks matches that for very efficient dispersion (favourable conditions): the oil slick length does not increase very much, the thick part remains central to the slick.

The models were run with some variations of inputs (wind speed & oil thickness) to investigate to what extend a better match with observations can be obtained. In order to easily compare different model results with the observed behaviour of the oil slicks, we've plotted visible oil slick length over time as observed (coloured markers) versus the different model outputs (lines) in Fig. 6, page 21. As expected, a lower wind speed and a higher oil layer thickness result in less efficient dispersion and a larger slick length.

To check the intermediate calculations in the model, like wave height, breaking wave coverage etc., we've looked up observed values during our test period:

- Unfortunately, the calculated white-cap coverage cannot be compared with satellite obtained white cap coverage (Salisbury *et al.*, 2014) as wind-sat overpasses did not match our test-times and locations.
- Measured significant wave heights near the test site (Fig. 3, page 20) only briefly reach up to 90 cm, but are mostly below that value. The model does calculate higher wave heights at the wind speeds used as input (Tab. 1, page 20).

4. Discussion

All methods combined, a great number observations were made of the oil slicks.

For the radar observations, the vicinity to the oil slick was crucial in capturing the outlines of the slicks correctly. Differences between aerial observations and radar observations indicate the 'far side' of the oil slick was not always captured correctly, especially if the ARCA was a bit further off (the radar observations of slick Alpha after 9:00 UTC). At the end of the first test-day the ARCA performed an extra transect of the entire slick-length between slick Bravo & Charlie, to completely capture their outlines at this time.

The aerial observations vary with time, based on the sensor techniques available on the aircraft, as well as on the 'experience' of the crew with these oil slicks.

The observations of slick Alpha & Bravo are most clear, partly because of the available sensor systems at that time, and partly because they were observed for the longest period of time. Unfortunately the merging of the slicks didn't allow for longer comparison of their behaviour.

Observations of slick Charlie were a little less abundant. It could only be observed 'unobstructed' for a brief period: Deposition of this slick was last in the row, and applying dispersants took quite some time. Furthermore, at that time, IR observations which have proven very valuable in analysing the other slicks, were no longer available. Of course, the three transverses of the ARCA through the slick for dispersant application probably affected the slicks behaviour and may have caused some additional scattering.

Model results

The model results overestimate the dispersion compared to what was observed. Of course, the elongation model is a simplification of reality and only considers the mechanism of dispersion over a lengthwise cross-section.

The oil slick elongation model is very sensitive to layer thickness, as this parameter influences the droplet size distribution. With input of a layer thicknesses realistic in this field exercise, the slick disappears too quickly. This means that the extrapolation of the droplet size calculations to these minute thicknesses should be re-assessed.

The significant wave height as measured at a representative location, is much lower than the significant wave height the model calculates for the observed wind speed. Of course, in reality, wave generation is much more complex than our parameterization with wind speed only. The wind direction from the east (from across the European land mass) meant that there has not been much room for wave build-up. This could explain the lower significant wave height and can indicate the conditions were less energetic than the wind-speed parameterizations in the model predict.

Slick behaviour

The observations of oil slick behaviour support the theory of an oil slick elongating (diluting) in the wind direction. The thick portion of both slicks Alpha and Bravo remains downwind and largely the same size, while the length of the oil slick increases trough a thinner tail upwind.
The oil slick initial orientation had a very big influence on the elongation of the slick. (Note that all three slicks were deposited with the same speed of sailing and pump-speed, and therefore an equal initial thickness.) The cross-wind slick (Alpha), despite its smaller volume and initial length, becomes just as long as the other slicks in the same timeframe. This means that the (absolute) increase in length in the wind direction on this time-scale was roughly the same for the slicks, indicating that the elongation of the oil slick happened at a fixed rate (for these conditions and oil properties) and was not affected by initial length. For all three slicks, ignoring suspicious measurements, the increase in length occurs approximately the same rate from the start to the end of the observation period.
Relatively, the elongation of slick Alpha is much larger. As a result, the thick portion of the slick is visibly declining and disappears altogether in the end. This suggests that his slick is successfully 'diluting' by elongation and would disappear later on.

The theory that the downwind portion of the slick feeds the tail is further supported by the observation that a thickness gap in the slick Alpha, is translated down the entire slick tail length: In the thick downwind edge of slick Alpha, a thinner region can be seen in the IR images (Fig. 13, p25). Over time, the upwind tail of this region remains slightly thinner than the remainder of the tail.

6. Appendix:

6.1. Environmental conditions

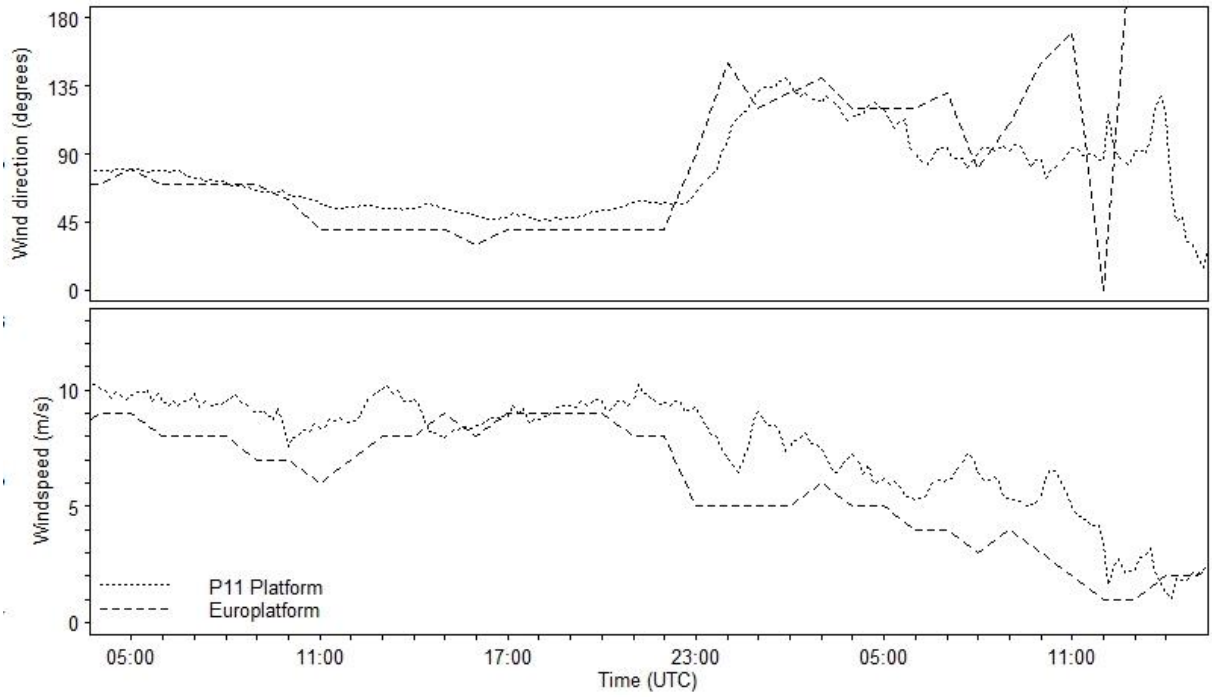

Fig. 2. Wind speed during the first test day, as observed by 2 offshore stations. (P11 platform position is 3,342°E, 52,359°N, 45 kilometres Northwest of our test site. Europlatform position is 3,275°E, 51,998°N, 55 kilometres Southwest of our test site.) Data downloaded from https://waterinfo.rws.nl/#!/nav/index/ and https://www.knmi.nl/nederland-nu/klimatologie/uurgegevens_Noordzee.

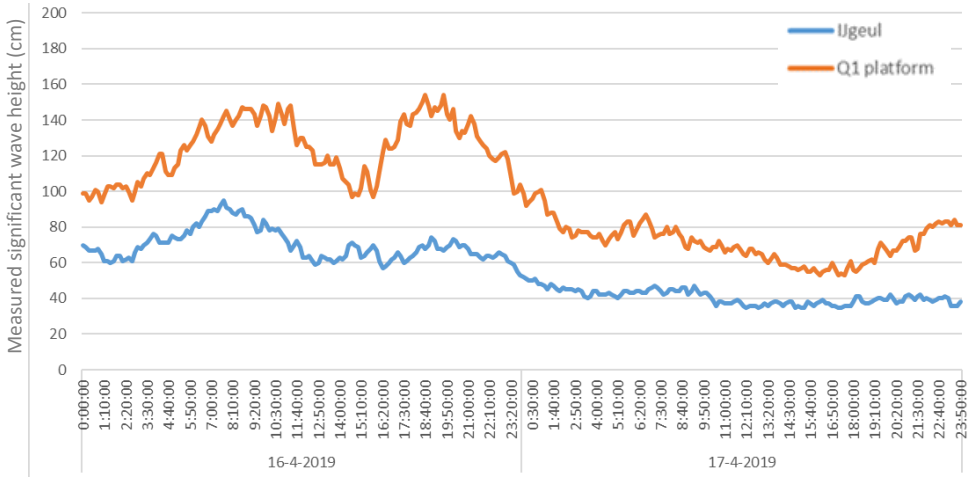

Fig. 3. Significant wave height measured at station 2 stations: Bleu line: 'IJgeul 1' Position of this station: 4,264°E, 52,488°N, located 31 km Northeast of our test position. Orange line 'Q1 platform', position 4,150°E, 52,925°N, located 75 km North northeast of our test site.
Distance from the coast: test site: 24,1 km, IJgeul1: 21,1 km, Q1 platform: 55,2 km.

Wind speed (m/s)	Significant wave height (m)
5,0	0,6
5,5	0,7
6,0	0,8
6,5	0,9
7,0	1,1
7,5	1,3
8,0	1,4
8,5	1,6
9,0	1,8

Tab. 1. Significant wave height as calculated by the model for each wind speed.

6.2. Model results

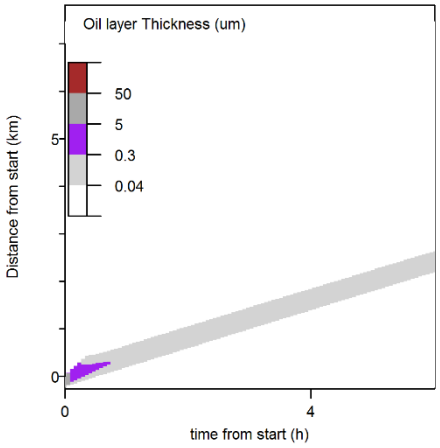

Fig. 4. Model output, slick Alpha. Wind speed 7,5 m/s (upwards)

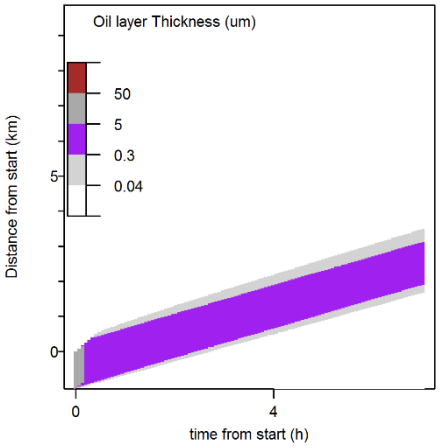

Fig. 5. Model output, slick Bravo. Wind speed 7,5 m/s (upwards)

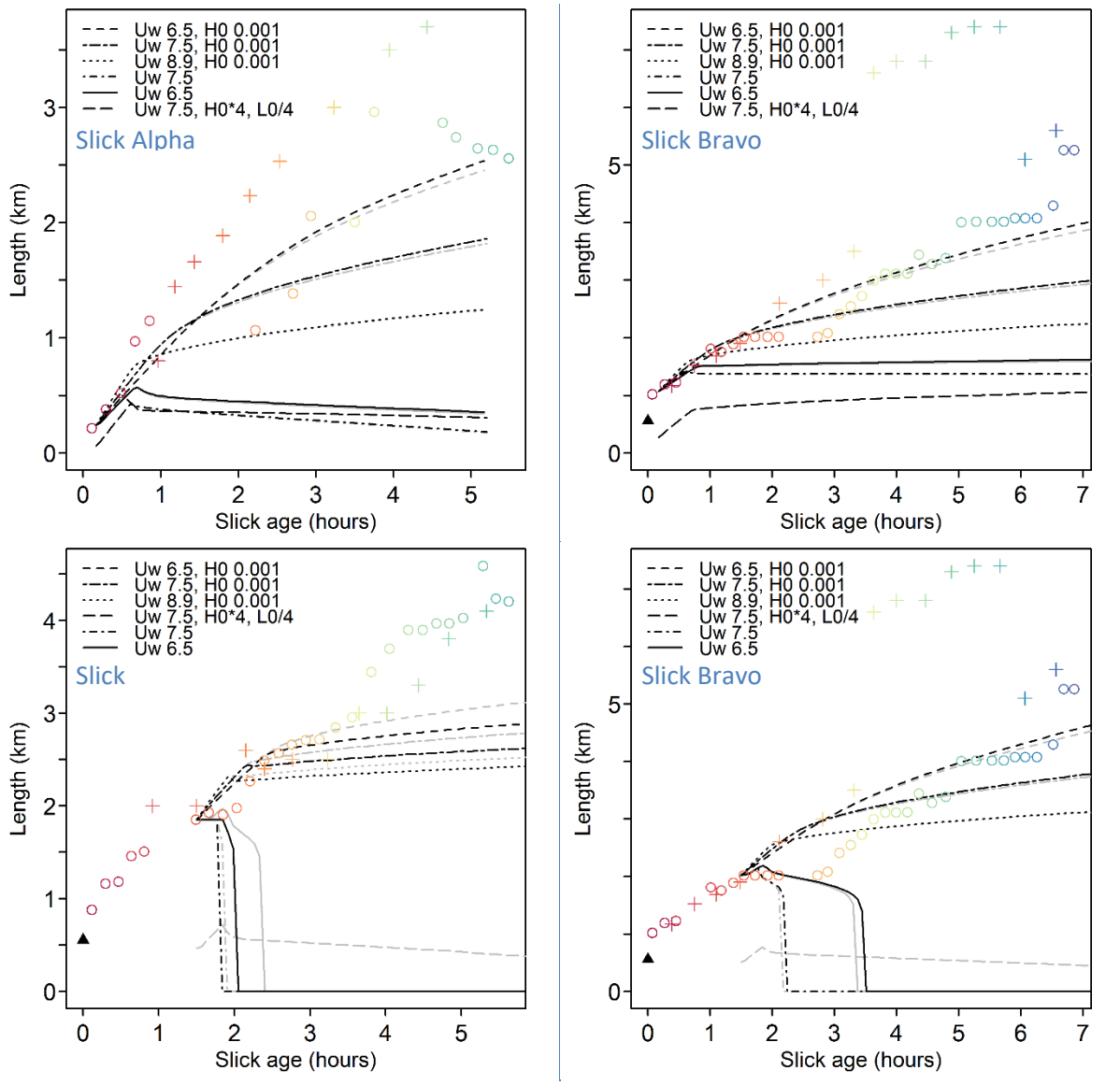

Fig. 6. Combined elongation model output (lines) compared to slick observations (markers) of oil slick length. Black lines are simulations based on un-weathered oil properties, grey lines are simulations based on weathered oil properties. Other model settings are given in the legend: wind speed (Uw in m/s) and layer thicknesses H0 in meters, if other than originally planned.

6.3. Appendix: Oil slick observations

Slick alpha and Bravo merging

The aerial observation images indicate initial contact between slick Alpha and Bravo took place between 11:23 and 11:48 (Fig.1 & Fig.3).

Using the ship based radar, the slick extent of Alpha and Bravo were recorded separately until 12:47 UTC (Fig.2). Because the operator had followed both slicks during their lifetime, he could distinguish the wider shape of A from the narrower, longer shape of B.

The aerial observers recorded slick data for Alpha and Bravo separately until 12:00 UTC. The new aerial observations crew starting at 12:00 UTC could not distinguish the different slicks (Fig.4 & Fig.5).

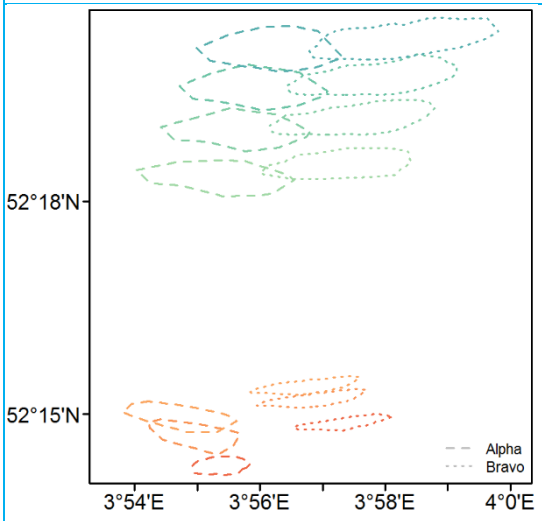

Fig. 8. Slick outlines obtained from the ship based radar. For each of the 7 time points (colour) a set of both Alpha and Bravo is shown (line types).

Fig. 7. 11:23 UTC. slick Bravo in the foreground, slick Alpha on the left hand border, slick Charlie in the background (right).

Fig. 9. 11:48 UTC: slick Alpha in the foreground. In the background slick Charlie (left) and Bravo (right)

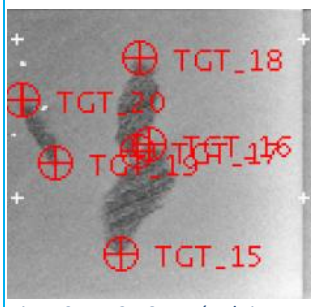

Fig. 10. 11:34 SLAR (Belgium CG).

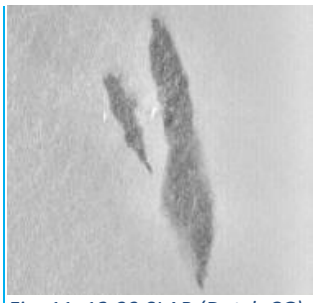

Fig. 11. 12:39 SLAR (Dutch CG)

In both these SLAR images: Slick Charlie to the left. On the right hand side, slick Alpha (bottom) connected to slick Bravo (top)

Individual oil slick observations

The following pages contain an overview of the observations of each oil slick. These consist of a combination graph of the characteristics the slick. The graph layout is as follows:

<table>
<tr><td>Name of the oil slick</td><td rowspan="2">Graphs on the left hand side for the evolution of characteristic oil slick properties over time.
Symbols indicate observation types. From top to bottom:
- Slick length: The longest axis of the slick, as reported on the observation forms (aerial observation) or calculated from the polygons.
- Oil Slick width: The shortest axis of the slick, as reported on the observation forms (aerial observation) or calculated from the polygons.
- Total oil slick surface area.
- Surface area of the oil slick in each of the Bonn Agreement Colour Codes (obtained from aerial observations only)
- Oil slick orientation, in degrees compared to North.</td></tr>
<tr><td>Legend: Across the graph:
Colours indicate the slick age since deposition, ranging from red to blue.
Symbols indicate the type of observation.</td></tr>
<tr><td>The large graph on the right hand side, shows slick extent & position over time:
- Radar observations of the slick outline are plotted as polygons.
- Symbols (x and +) connected by dotted lines are the starting & end positions coordinates of the slick as reported by the aerial observations crew. An additional (◊ or □) on the same line, indicates the position of the thickest part inside the slick.</td><td></td></tr>
<tr><td></td><td>In the small box on the bottom right, significant timing information is given:
For slick A & B, three vertical lines indicate timing of their merger: 11:48 confirmed contact; 12:00u final aerial observation that considers them separate; 12:47 final separate radar observation</td></tr>
</table>

In addition, some characteristic images of the oil slick are provided. For all images, see https://doi.pangaea.de/10.1594/PANGAEA.902608.

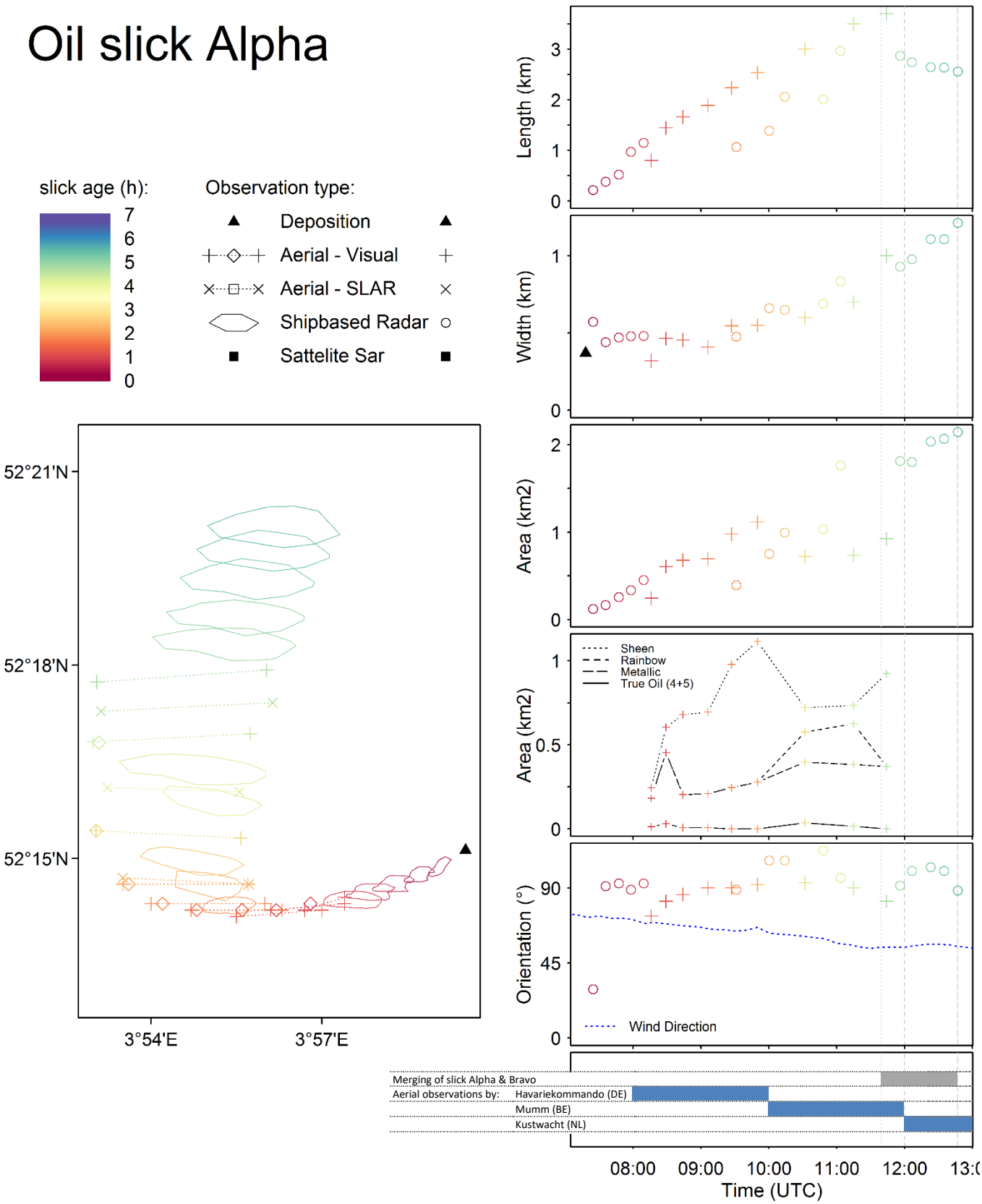

Fig. 12. Combined plot of all observations of slick Alpha over time.

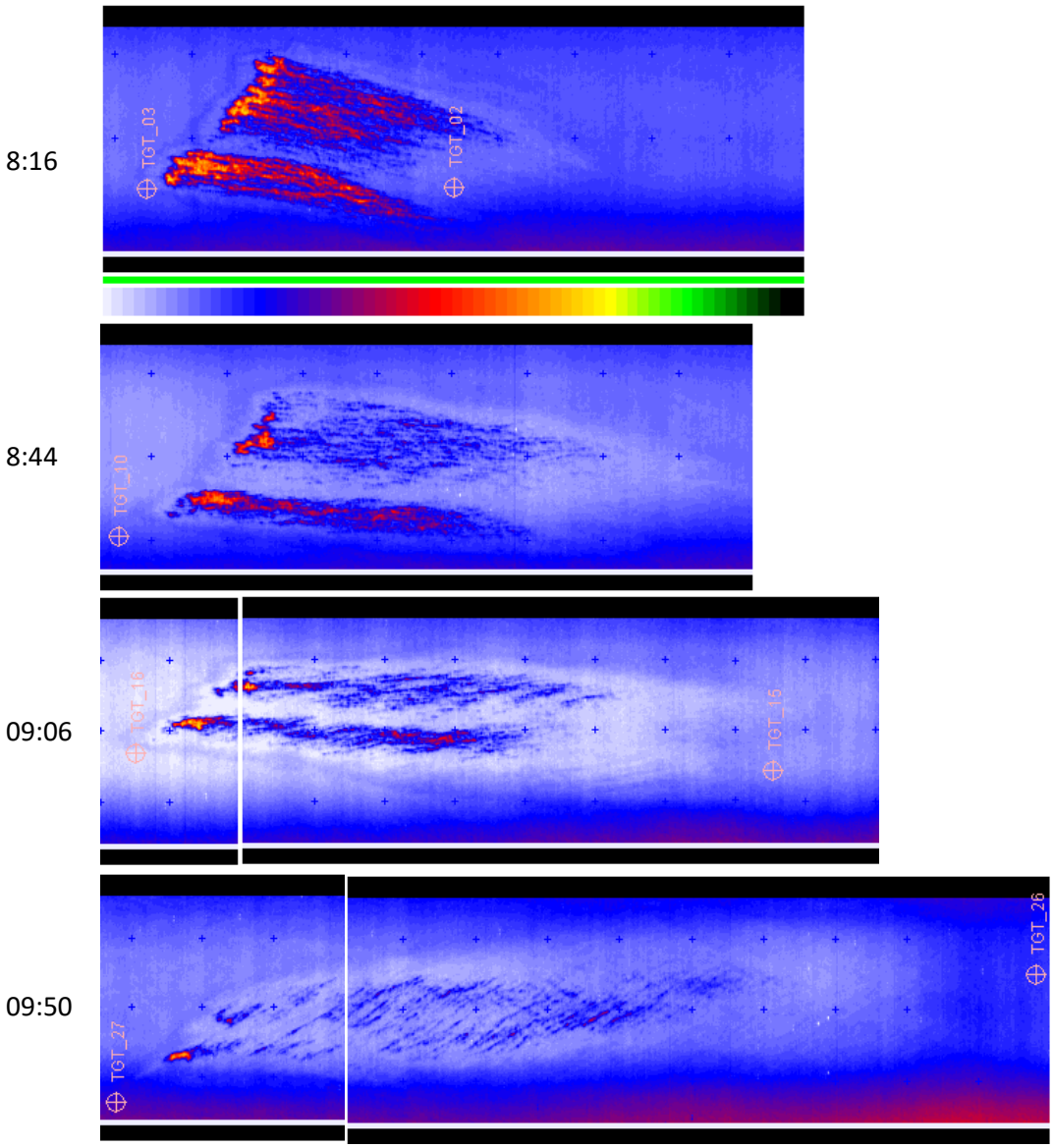

Fig. 13. IR images of slick Alpha, at different time points, made by the German Coastguard. Grid: 200 m

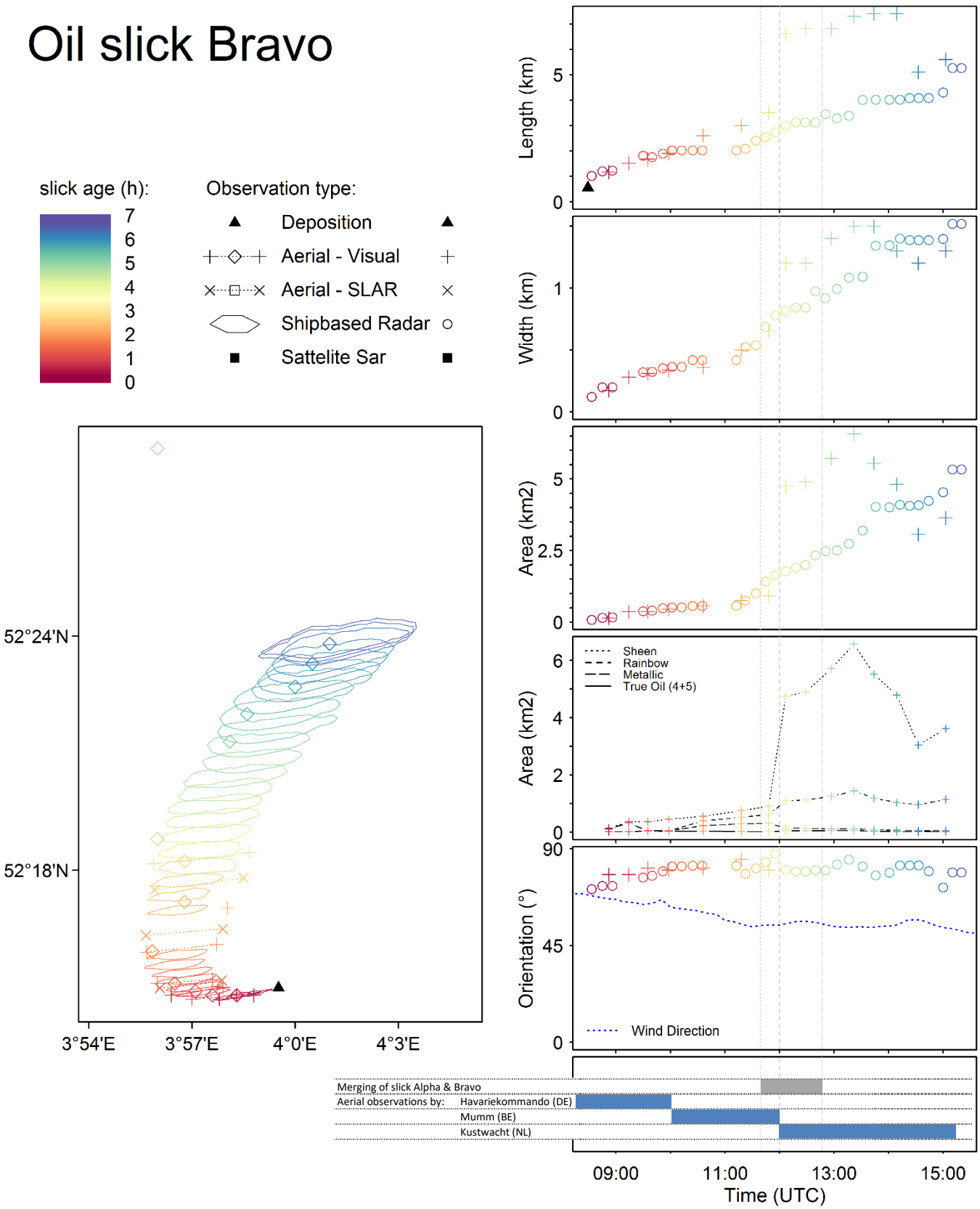

Fig. 14. Combined plot of all observations of slick Bravo over time.

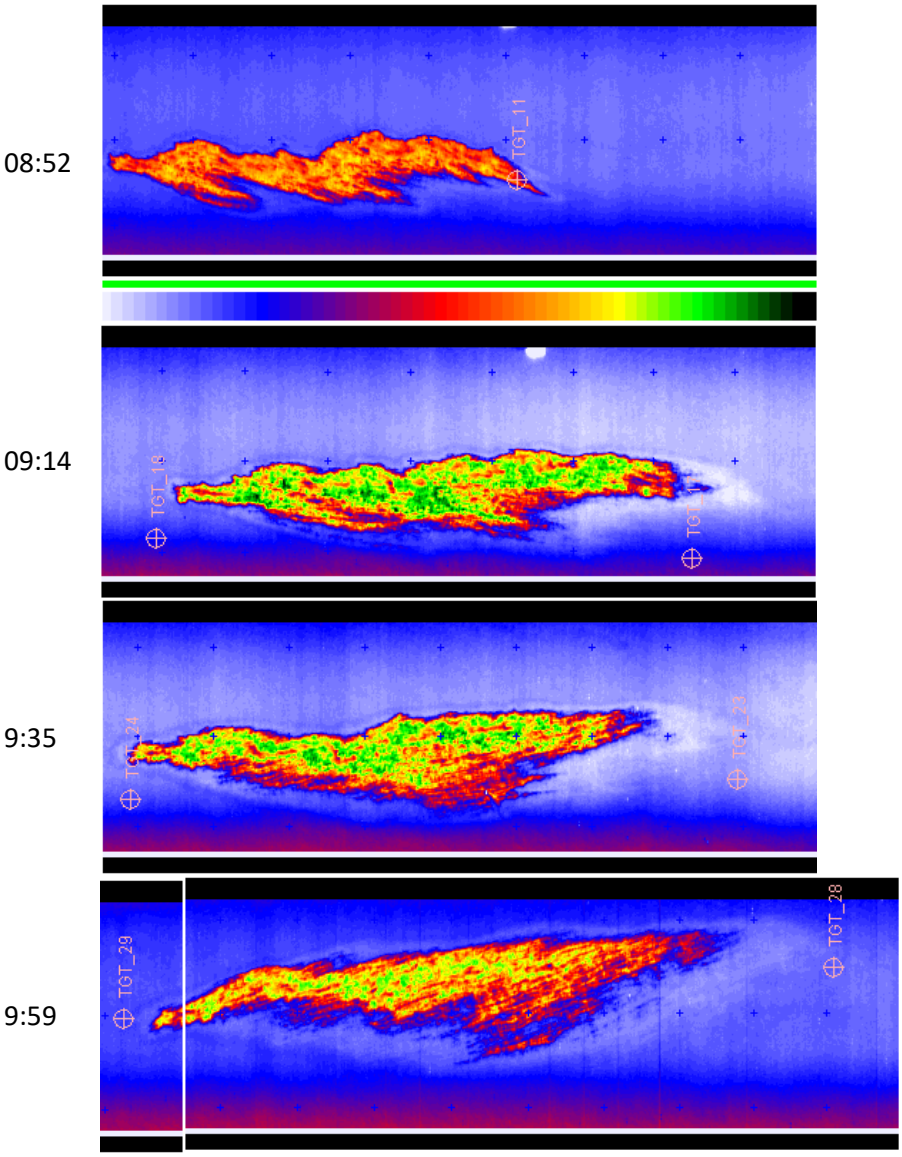

Fig. 15. IR images of slick Bravo, at different time points, made by the German Coastguard. Grid: 200 m

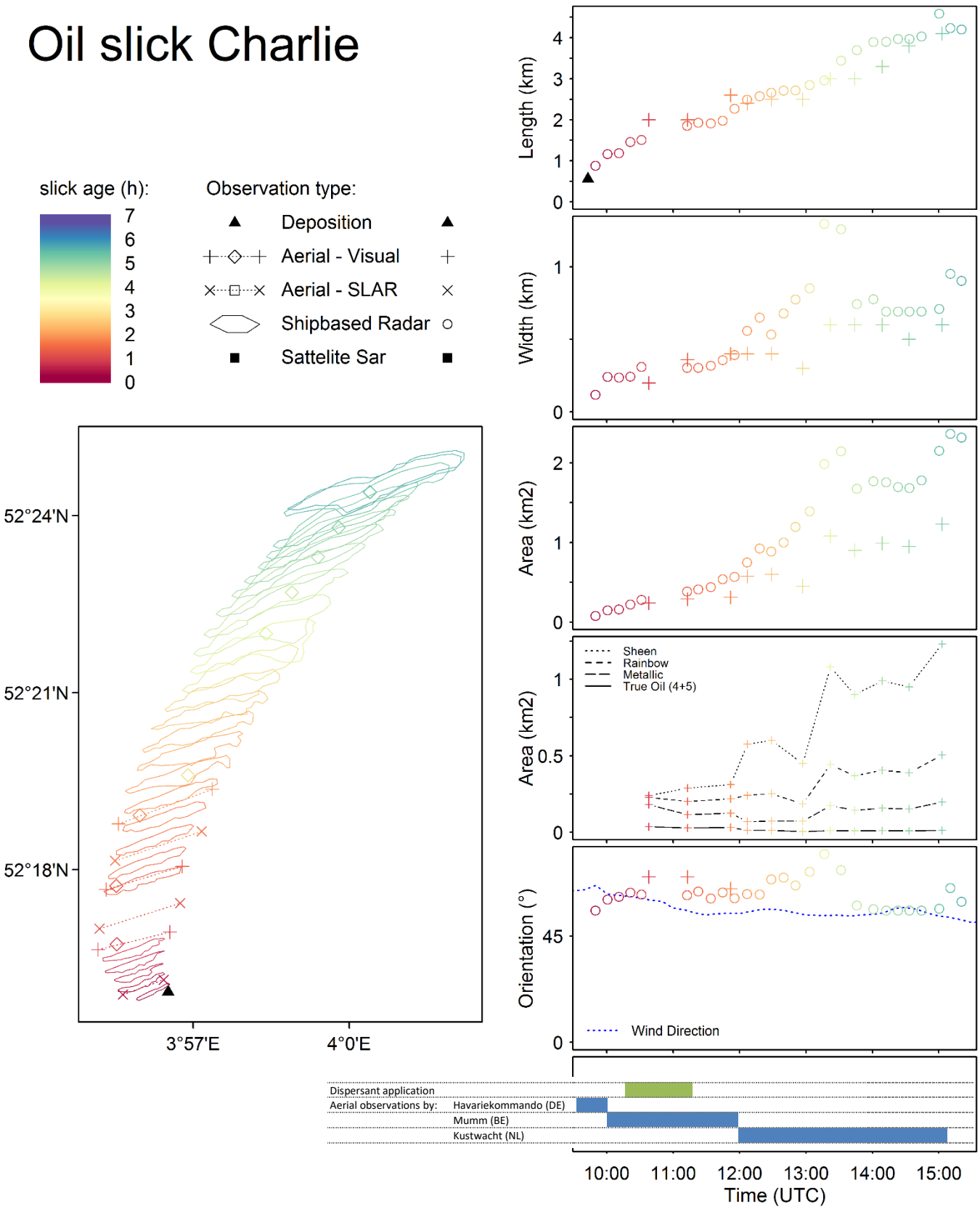

Fig. 16. Combined plot of all observations of slick Charlie over time.

Chemical vs Natural Dispersion: Impacts on microbial communities and hydrocarbon biodegradation

Thomas, Gareth; McGenity, Terry J; McKew, Boyd A

Materials & Methods

These methods describe what will be (and some have been) taking place on the ExpOS'D samples and are therefore subject to slight alterations where required.

Nutrient Analysis

Nutrient analysis was conducted on all samples to determine concentrations of ammonia (NH_{4+}), phosphate ($PO4_{3-}$), silicate (SiO_{2-}), nitrate (NO_{3-}), and nitrite (NO_{2-}). Ammonia concentrations were measured by protocol G-327-05 Rev.6, phosphate by protocol G-297-03 Rev.5, silicate by protocol G-177-96 Rev.10, and nitrate and nitrite via protocol G-172-96 Rev.13 on a SEAL Analytical AA3 HR AutoAnalyzer tandem JASCO FP-2020 Plus fluorescence detector.

Hydrocarbon Degradation

Hydrocarbons were extracted from 50 ml brown-glass vials (collected *in situ*) using a 6 ml solvent extraction of 1:1 hexane and dichloromethane, vigorously shaken for 30 seconds, and placed in an ultrasonic bath for 30 minutes. Deuterated alkanes (nonadecane $C_{19}d_{40}$ and triacontane $C_{30}d_{62}$ at 10 µg ml^{-1}) and PAH (naphthalene-d_8 and anthrancene-d_{10} at 10 µg ml^{-1}) internal standards were added to each sample and quantification was performed on an Agilent 7890A Gas Chromatography system coupled with a Turbomass Gold Mass Spectrometer with Triple-Axis detector, operating at 70 eV in positive ion mode, using conditions as previously described by Coulon *et al.*, (2007). External multilevel calibrations were carried out using alkanes (Standard Solution (C^8-C^{40}); Sigma), methylated-PAHs (1-methylnapthalene, 2-methylanthracene, and 9,10-dimethylanthracene; Sigma), and PAH (QTM PAH Mix; Sigma) standards, the concentrations of which ranged from 1.125 to 18 µg ml^{-1}. For quality control, a 2.0 ng l^{-1} diesel standard solution (ASTM C12-C60 quantitative, Supelco) and a 1.0 ng l^{-1} PAH Mix Standard solution (Supelco) were analysed every 15 samples. The variation of the reproducibility of extraction and quantification of water samples were determined by successive extractions and injections (n = 6) of the same sample and estimated to be ± 8%. All alkanes between C_{10} and C_{36} including pristane and phytane and the following PAHs were quantified (naphthalene; all isomers of methyl-, dimethyl- and trimethyl-naphthalenes; acenaphthylene; acenaphthene; fluorine; phenanthrene; all isomers of methyl- and dimethyl-phenanthrenes/anthracenes; fluoranthene; pyrene; all isomers of methyl- and dimethyl-pyrene; chrysene; all isomers of methyl- and dimethyl-chrysene). Only those hydrocarbons detected are shown in Fig. 6.

qPCR analysis of Bacterial 16S rRNA genes

DNA was extracted from *in situ* seawater samples from the thawed Millipore® Sterivex™ filters with a DNeasy PowerWater Sterivex Kit (Qiagen) according to the manufacturer's instructions. The primers used for quantification of bacterial 16S rRNA were 341f - CCTACGGGNGGCWGCAG and 785r – GACTACHVGGGTATCTAATCC (Klindworth *et al.*, 2013). qPCR reactions were performed using a CFX384™ Real-Time PCR Detection System (BioRad) with a PCR using reagents, cycle conditions, and standards as previously described (McKew and Smith, 2015; Tatti *et al.*, 2016). Inspection of standard curves showed that all assays produced satisfactory efficiency (74%) and R^2 values (>0.99).

Amplicon Sequencing and Bioinformatics

Amplicon libraries were prepared, as per Illumina instructions by a 25-cycle PCR. PCR primers were the same as those used for qPCR but flanked with Illumina overhang sequences. A unique combination of Nextera XT v2 Indices (Illumina) were added to PCR products from each sample, via an 8-cycle PCR. PCR products were quantified using Quant-iT PicoGreen dsDNA Assay Kit (TheromFisher Scientific) and pooled in equimolar concentrations. Quantification of the amplicon libraries was determined via NEBNext® Library Quant Kit for Illumina (New England BioLabs Inc.), prior to sequencing on the Illumina MiSeq® platform, using a MiSeq® 600 cycle v3 reagent kit and 20% PhiX sequencing control standard. Sequence output from the Illumina MiSeq platform were analysed within BioLinux (Field *et al.*, 2006), using a bioinformatics pipeline as described by Dumbrell *et al.*, (2016). Forward sequence reads were quality trimmed using Sickle (Joshi and Fass, 2011) prior to error correction within SPades (Nurk *et al.*, 2013) using the BayesHammer algorithm (Nikolenko *et al.*, 2013). The quality filter and error corrected sequence reads were dereplicated, sorted by abundance, and clustered into OTUs (Operational Taxonomic Units) at the 97% level via VSEARCH (Rognes *et al.*, 2016). Singleton OTUs were discarded, as well as chimeras using reference-based chimera checking with UCHIME (Edgar *et al.*, 2011). Taxonomic assignment was conducted with RDP Classifier (Wang *et al.*, 2007). Non locus-specific, or artefactual, OTUs were discarded prior to statistical analyses, along with any OTUs that had <70% identity with any sequence in the RDP database.

Statistical Analysis

Data were first tested for normality (Shapiro-Wilks test), those data which were normally distributed were tested for significance with ANOVAs or appropriate linear models. Non-normally distributed data were analysed using appropriate GLMs (Generalised Linear Models) as follows. The relative abundance of OTUs or genera in relation depth, treatment, or time were modelled using multivariate negative binomial GLMs (Wang *et al.*, 2010). Here, the number of sequences in each library was accounted for using an offset term, as described previously (Alzarhani *et al.*, 2019). The abundance of bacterial 16S rRNA gene copies was also modelled using negative binomial GLMs (Venables and Ripley, 2002). The significance of model terms was assessed via likelihood ratio tests. The Environmental Index of Hydrocarbon Exposure (Lozada *et al.*, 2014) was calculated using the script available at the ecolFudge GitHub page (https://github.com/Dave-Clark/ecolFudge, Clark, 2019) and EIHE values modelled using poisson GLMs. All statistical analyses were carried out in R3.6.1 (R Development Core Team, 2011) using a variety of packages available through the references (Searle *et al.*, 1980; Venables and Ripley, 2002; Becker *et al.*, 2016; Auguie, 2017). All plots were constructed using the “ggplot2” (Bodenhofer *et al.*, 2011) and “patchwork” (Pedersen, 2019) R packages.

Results

Background bacterial 16S rRNA gene abundance in the surface of seawater was 86,293 (± 44,098) copies per ml of seawater, at 1.5 meters this was 98,438 (± 23,383) copies per ml of seawater, and at 5 meters was 84,725 (± 25,164) copies per ml of seawater (Fig. 1). Whilst there were no statistically significant results in the absolute abundance of bacterial copies, there are some temporal trends observed whereby a reduction is observed after 24 hours across all depths. With an average of 55% reduction at surface, 82% reduction at 1.5 meters, and 21% reduction at 5 meters in background bacterial gene copies. There are no observable significant differences between treatments.

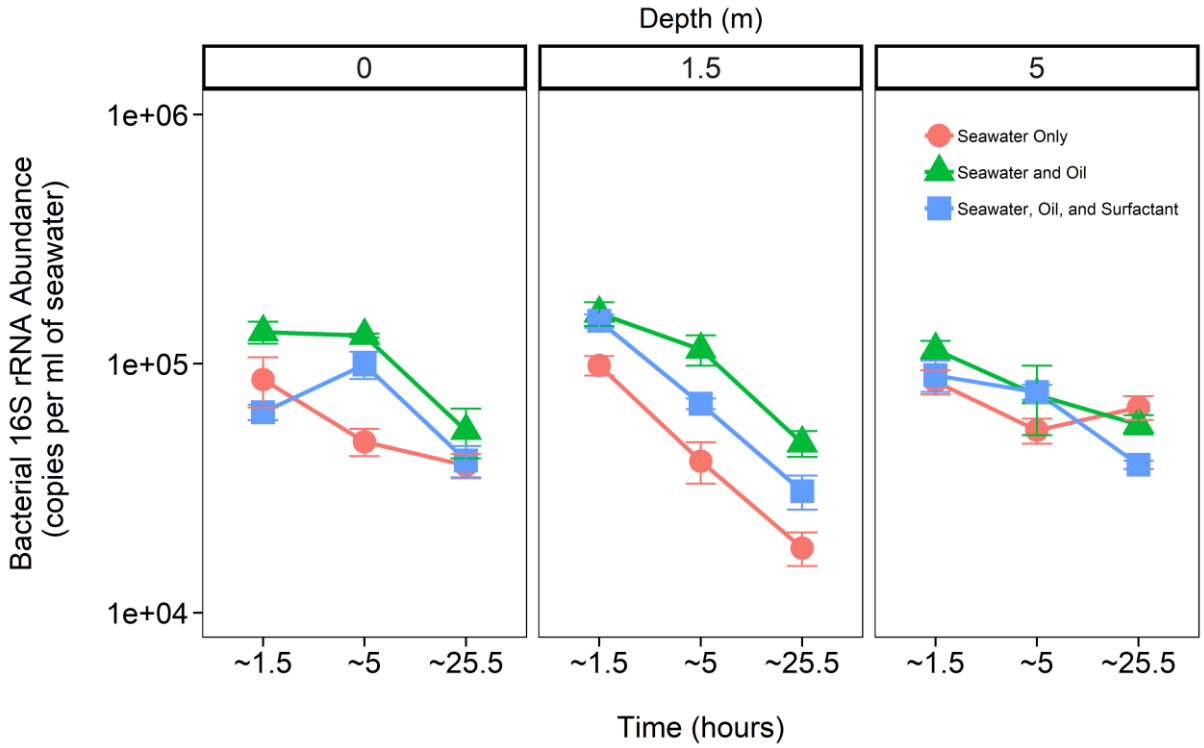

Fig 1: Bacterial 16S rRNA gene abundance (mean ± SE, *n* = 3) ~1.5 hours, ~5 hours, and ~ 25.5 hours after oil deposition. Measured within three treatments (Seawater Only, Seawater and Oil, and Seawater, Oil and Slickgone NS Dispersant) at surface level (0) and depths of 1.5 and 5 meters.

Temporal selection demonstrated the largest effect on the bacterial community composition (Fig. 2; R^2 = 0.28, F = 15.90, P<0.001) with depth and treatment demonstrating no significant effect (P>0.05).

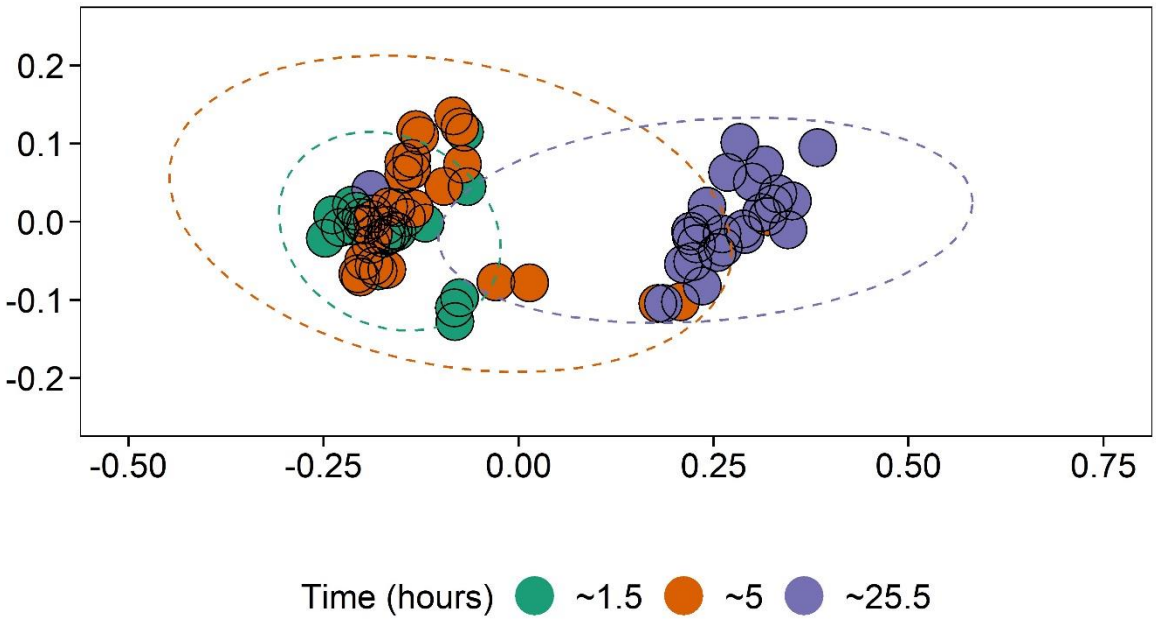

Fig. 2: NMDS (non-metric multidimensional scaling) ordination, based on clustered bacterial 16S rRNA OTUs at a 97% confidence level, displaying the effect of time (hours) on bacterial community composition (R^2 = 0.28, F = 15.90, P<0.001).

Whilst there was little effect on the overall community composition between treatments, based on preliminary analysis, some operational taxonomic units (OTUs) did demonstrate differences (Fig. 3). Most notably are the OTUs assigned to *Candidatus Pelagibacter* spp. and *Plankomarina* spp. (Fig. 3). OTU1, assigned to *Candidatus Pelagibacter* spp., represented the most abundant OTU in the bacterial 16S rRNA amplicon library. Approximately 24 hours after initial sampling, both treatments that contained oil demonstrated a significant decrease in relative abundance of OTU1 (coef. -6.02, z -3.53, P<0.05). Though at approximately 5 hours the treatment with Oil and Slickgone NS maintained significantly increased relative abundance in comparison to seawater only (coef. 7.07, z 4.15, P<0.01). At both 1 hour after oil deposit and 24 hours after initial sampling, the relative abundance of OTU4, assigned to *Plankomarina* spp., remained similar between all treatments. However, approximately 5 hours after oil deposit, whilst OTU4 had increased to 7% in the seawater control, this growth was significantly (coef. -4.18, z -9.19, P<0.001) inhibited in the treatment containing only oil (4.43 ± 0.51%) and more so with oil and Slickgone NS (2.94 ± 0.34%).

Analysis of bacterial 16S rRNA OTU sequences as a function of the Ecological Index of Hydrocarbon Exposure (Lozada *et al.*, 2014) revealed no significant differences between treatments, time points, or depths (Fig. 4). Moreover, with the index averaging less than 0.02, and the relative abundance of Obligate Hydrocarbonclastic Bacteria (OHCB) less than 1*10-6, it revealed the oil (with or without Slickgone NS) treatments did not promote the growth of oil-degrading bacteria within approximately 25 hours. This is likely due to the sampling not capturing the oil/water interface efficiently.

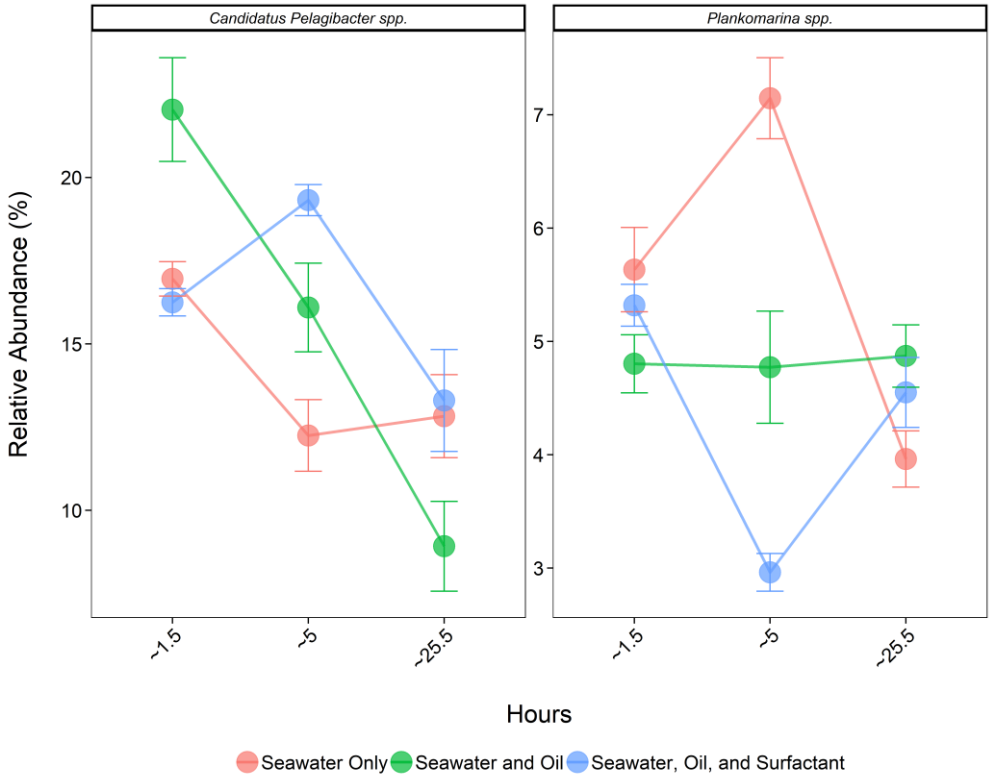

Fig. 3: Relative abundance (% of the bacterial community; mean ± SE, *n* = 3) of bacterial 16S rRNA gene, of OTUs belonging to the genera *Candidatus Pelagibacter* spp., and *Plankomarina* spp. ~1.5 hours, ~5

hours, and ~ 25.5 hours after oil deposition. Measured within three treatments (Seawater Only, Seawater and Oil, and Seawater, Oil and Slickgone NS Dispersant).

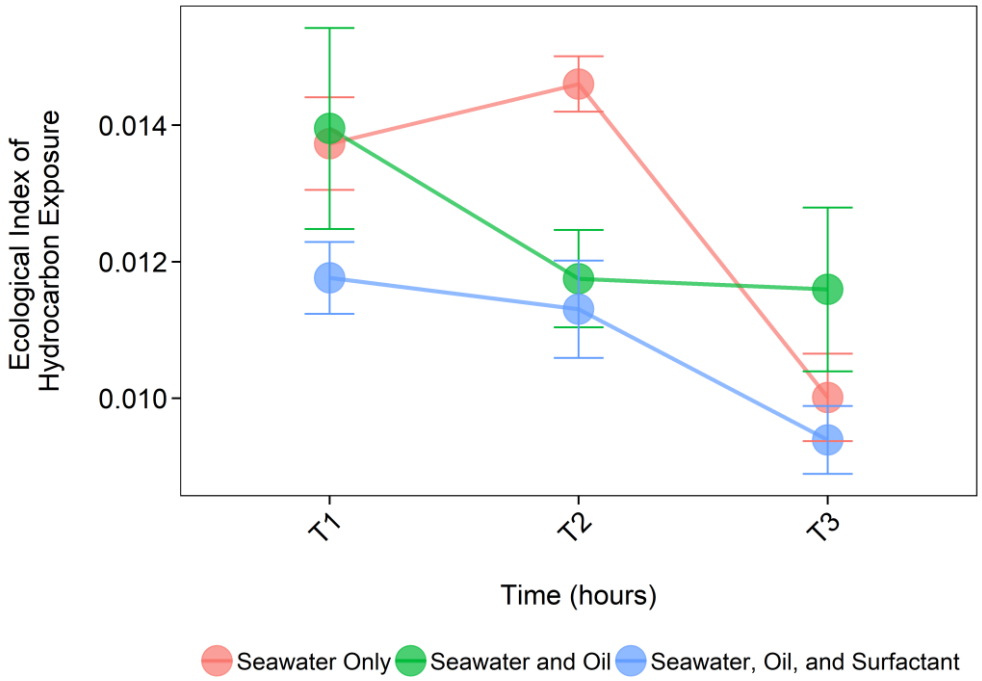

Fig. 4: Mean Environmental Index of Hydrocarbon Exposure (ratio %) representing relative abundance of Bacteria with hydrocarbon bioremediation potential (Lozada et al., 2014; mean ± SE, *n* = 3). ~1.5 hours (T1), ~5 hours (T2), and ~ 25.5 hours (T3) after oil deposition. Measured within three treatments (Seawater Only, Seawater and Oil, and Seawater, Oil and Slickgone NS Dispersant).

Analysis of nutrients (Fig. 5) revealed no significant difference between treatments 1 hour after the oil-slicks were released; with total N concentrations ranging from 8.45 – 9.37 µMol. Approximately 5.5 hours after oil-slick deposits, total N tended to decrease across all treatments, with ammonia (coef. -0.42, z -3.98, P<0.01) and nitrate (coef. -9.09, z -3.42, P<0.05) significantly decreased in the treatment containg oil and surfactant in comparison to oil only treatment. Approximately 25.5 hours after oil-slick deposits, total N significantly (coef. -14.70, z -5.42, P<0.001) decreased across all treatments from both other time points, to a range of 1.51 – 1.77 µMol. Phospherous was undetecable across all treatments and at all time points.

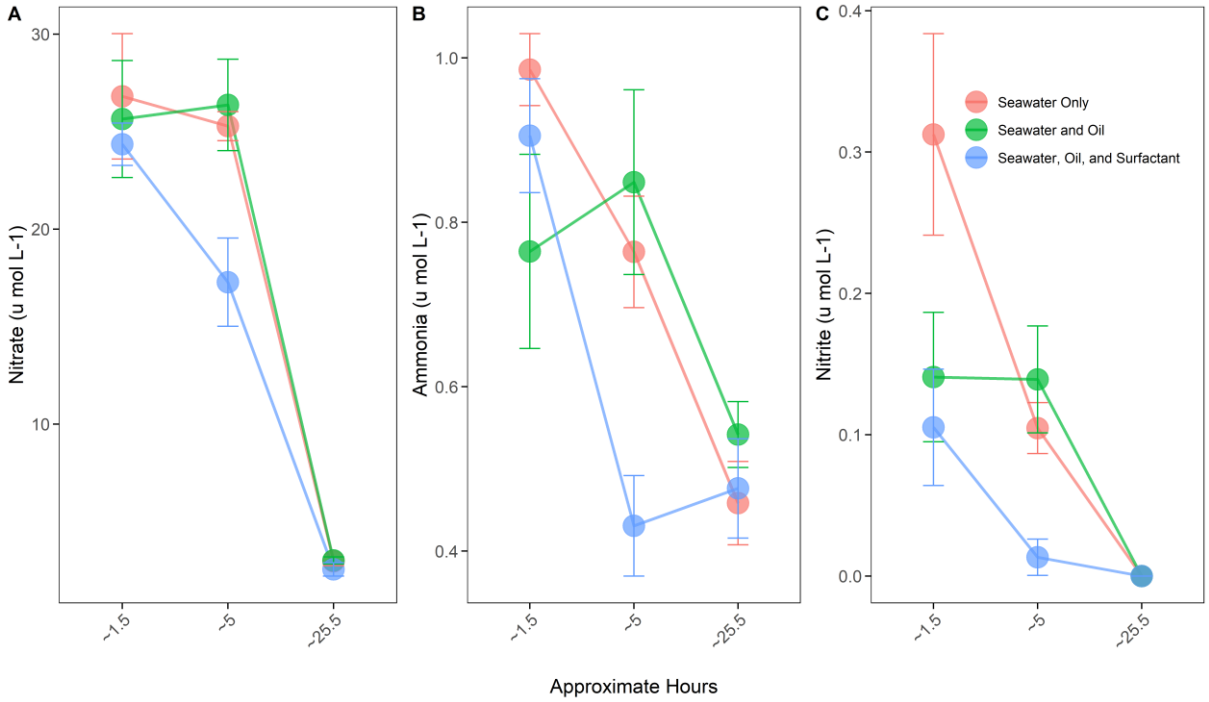

Fig. 5: Nitrate (A), ammonia (B), and nitrite (C) concentrations (mean ± SE, *n* = 3) from samples taken ~1.5 hours, ~5 hours, and ~ 25.5 hours after oil-deposition. Measured within three treatments (Seawater Only, Seawater and Oil, and Seawater, Oil and Slickgone NS Dispersant).

Apart from two samples no hydrocarbons were measured in sampled seawater. This further reflects the fact the sampling methodology did not capture the oil/water interface. The samples which did have measurable hydrocarbons were taken from the surface in the oil and Slickgone NS treatment ("Charlie") after 25.5 hours. Measurable hydrocarbons included an average concentration of *n*-alkanes (C^{14}-C^{31}) 188.13 (± 76.91) µg ml^{-1} seawater, branched alkanes (pristane and phytane) 27.20 (± 11.91) µg ml^{-1} seawater, and PAHs (phenanthrene and 2methyl-anthracene) 5.84 (± 3.13) µg ml^{-1} seawater.

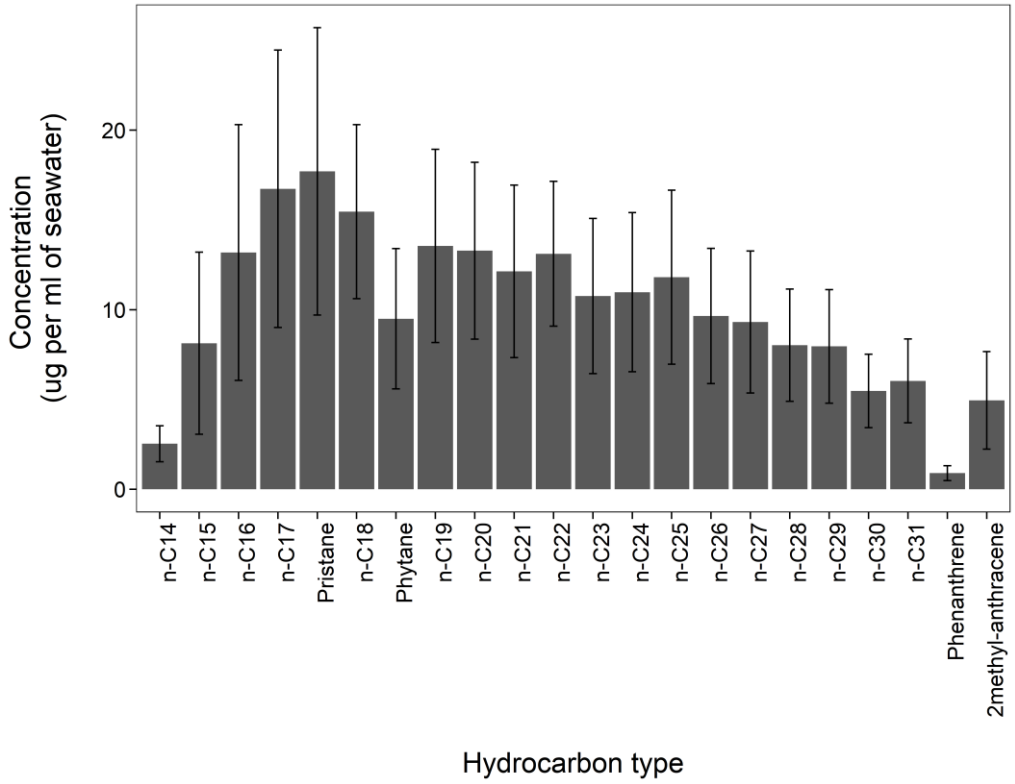

Fig. 6: Seawater samples taken from the "Oil and Slickgone NS" treatment ("Charlie") after 25.5 hours. Measured hydrocarbon concentrations (mean ± SE, *n* = 2) include *n*-alkanes (C^{14} to C^{31}), branched alkanes pristane and phytane, and PAHs (phenanthrene and 2-methyl-anthracene).

References

Alzarhani, A.K., Clark, D.R., Underwood, G.J.C., Ford, H., Cotton, T.E.A., and Dumbrell, A.J. (2019) Are drivers of root-associated fungal community structure context specific? *ISME J* **13**: 1330–1344.

Auguie, B. (2017) gridExtra: functions in Grid graphics. R Package Version 2.3. *CRAN Proj*.

Becker, R.A., Wilks, A.R., Brownrigg, R., Minka, T.P., and Deckmyn, A. (2016) Package "maps": Draw Geographical Maps. *R Packag version 23-6*.

Bodenhofer, U., Kothmeier, A., and Hochreiter, S. (2011) Apcluster: An R package for affinity propagation clustering. *Bioinformatics* **27**: 2463–2464.

Clark, D.R. (2019) ecolFudge.

Coulon, F., McKew, B.A., Osborn, A.M., McGenity, T.J., and Timmis, K.N. (2007) Effects of temperature and biostimulation on oil-degrading microbial communities in temperate estuarine waters. *Environ Microbiol* **9**: 177–186.

Dumbrell, A.J., Ferguson, R.M.W., and Clark, D.R. (2016) Microbial Community Analysis by Single-Amplicon High-Throughput Next Generation Sequencing: Data Analysis – From Raw Output to Ecology. In *Hydrocarbon and Lipid Microbiology Protocols*. McGenity, T.J., Timmis, K.N., and Nogales, B. (eds). Berlin, Heidelberg, Heidelberg: Springer Protocols Handbooks, pp. 155–206.

Edgar, R.C., Haas, B.J., Clemente, J.C., Quince, C., and Knight, R. (2011) UCHIME improves sensitivity and speed of chimera detection. *Bioinformatics* **27**: 2194–2200.

Field, D., Houten, S., Thurston, M., Swan, D., Tiwari, B., Booth, T., and Bertrand, N. (2006) Open software for biologists: from famine to feast. *Nat Biotechnol*.

Joshi, N. and Fass, J. (2011) sickle - A windowed adaptive trimming tool for FASTQ files using quality. *(Version 133)* [Software].

Klindworth, A., Pruesse, E., Schweer, T., Peplies, J., Quast, C., Horn, M., and Glöckner, F.O. (2013) Evaluation of general 16S ribosomal RNA gene PCR primers for classical and next-generation sequencing-based diversity studies. *Nucleic Acids Res* **41**: 1–11.

Lozada, M., Marcos, M.S., Commendatore, M.G., Gil, M.N., and Dionisi, H.M. (2014) The Bacterial Community Structure of Hydrocarbon-Polluted Marine Environments as the Basis for the Definition of an Ecological Index of Hydrocarbon Exposure. *Microbes Environ* **29**: 269–276.

McKew, B.A. and Smith, C.J. (2015) Real-Time PCR Approaches for Analysis of Hydrocarbon-Degrading Bacterial Communities. In *Hydrocarbon and Lipid Microbiology Protocols*. McGenity, T.J., Timmis, K.N., and Fernandez, B.N. (eds). Berlin, Heidelberg: Springer Protocols Handbooks.

Nikolenko, S.I., Korobeynikov, A.I., and Alekseyev, M.A. (2013) BayesHammer: Bayesian clustering for error correction in single-cell sequencing. *BMC Genomics* **14**:.

Nurk, S., Bankevich, A., Antipov, D., Gurevich, A., Korobeynikov, A., Lapidus, A., et al. (2013) Assembling genomes and mini-metagenomes from highly chimeric reads. In *Lecture Notes in Computer Science (including subseries Lecture Notes in Artificial Intelligence and Lecture Notes in Bioinformatics)*. pp. 158–170.

Pedersen, T.L. (2019) patchwork: The Composer of Plots. *Cran*.

R Development Core Team, R. (2011) R: A Language and Environment for Statistical Computing.

Rognes, T., Flouri, T., Nichols, B., Quince, C., and Mahé, F. (2016) VSEARCH: a versatile open source tool for metagenomics. *PeerJ* **4**: e2584.

Salisbury, D.J., Anguelova, M.D., and Brooks, I.M. (2014) Global distribution and seasonal dependence of satellite-based whitecap fraction. *Geophys Res Lett* **41**: 1616–1623.

Searle, S.R., Speed, F.M., and Milliken, G.A. (1980) Population marginal means in the linear model: An alternative to least squares means. *Am Stat* **34**: 216–221.

Tatti, E., McKew, B.A., Whitby, C., and Smith, C.J. (2016) Simultaneous dna-rna extraction from coastal sediments and quantification of 16S rRNA genes and transcripts by real-time PCR. *J Vis Exp* **2016**: e54067.

Venables, W.N. and Ripley, B.D. (2002) Modern Applied Statistics with S (Fourth Edition).

Wang, Q., Garrity, G.M., Tiedje, J.M., and Cole, J.R. (2007) Naïve Bayesian classifier for rapid assignment of rRNA sequences into the new bacterial taxonomy. *Appl Environ Microbiol* **73**: 5261–5267.

Wang, W., Wang, L., and Shao, Z. (2010) Diversity and Abundance of Oil-Degrading Bacteria and Alkane Hydroxylase (alkB) Genes in the Subtropical Seawater of Xiamen Island. *Microb Ecol* **60**: 429–439.

Zeinstra-Helfrich, M., Koops, W., and Murk, A.J. (2017) Predicting the consequence of natural and chemical dispersion for oil slick size over time. *J Geophys Res Ocean* **122**: 7312–7324.

Acute toxicity of oil and dispersed oil in water to a temperate amphipod

van den Heuvel-Greve, Martine J; de Vlieger, O; Abbenis, S; Murk, Albertinka J

Abstract

To assess the acute toxicity of water directly below the two oil slicks, water samples from the field tests were tested with the marine amphipod, *Gammarus locusta* at 9°C. No toxicity was observed after five days of exposure. Additionally worst case standard toxicity tests were conducted with the same oil and oil dispersed with the same dispersant as used in the field tests. Oil in water fractions were prepared by stirring floating oil on water for 48 hrs in a closed glass jar in the dark. The average LC50 value of these standard toxicity tests with *G. locusta* were 0.13 ml oil/L for Arabian light crude oil and 0.11 ml oil/L for Arabian light crude oil dispersed with SLICKGONE NS (in a 1:25 dispersant:oil ratio based on volume), resulting in a slightly enhanced toxicity of the dispersed oil (factor 1.2) compared to the non-dispersed oil. Comparison of the field tests with the standard laboratory tests showed that the field samples contained oil in water concentrations below the No Observed Effect Concentration for both the oil and the dispersed oil.

Materials & Methods

Test species

Toxicity tests were conducted using the epibenthic marine amphipod, *Gammarus locusta* (Costa et al., 1998). *G. locusta* is widely spread along the European Atlantic coast and can be found in Portugal, all the way up to Iceland (Lincon, 1979). The species is mostly abundant in high salinity areas but can prevail in brackish waters as well (Costa et al., 1998; Costa & Costa, 1999). They can be found from the intertidal zone to a depth of 30 meters (Hartog den, 1963; Costa et al., 1998; Costa & Costa, 1999).

Individual *G. locusta* were collected from the wild. They were collected 1-5 days prior to each experiment. Collection took place in an intertidal area in the Dutch Oosterschelde near Goese Sas (51°32’43.36”N; 3°55’28.79”E). Gammarids were collected in the period from February till April 2019, and kept in an aquarium at test temperature until the start of the tests. They were fed with Tetra Wafer MiniMax food prior to the test. Species ranging from 6-15 mm in length were selected for testing.

Test chemicals

The tested oil was Arabian light crude oil (after 48 hrs of stirring, see below) and the applied dispersant was SLICKGONE NS, and identical to the oil and dispersants used in the field experiments.

Laboratory tests

Toxicity tests were performed in the laboratory to assess the LC50 value for both the oil and dispersed oil, during February-April 2019 (prior to the field test). The tests were executed with water-accommodated fractions of both the oil (WAF) and the dispersed oil (the chemically enhanced water-accommodated fractions - CEWAF). The WAF and CEWAF were prepared with artificial seawater (ASW) using Pro Reef Salt Mix (Colombo®) mixed with Milli-Q water to obtain a salinity of 34-36‰, which is comparable to Oosterschelde seawater.

WAF and CEWAF preparation took place in a climate room in 5L glass Duran® bottles. First 5.2 L of ASW was added to each of the bottles. Then oil or oil and dispersant was added to each of the

bottles. The concentration of dispersant was 1:25 dispersant:oil ratio based on volume. The ASW in combination with oil, or oil and dispersant was stirred for 48 hour using a stir bar and a stir plate. The test temperature was measured for test weeks 6-12 using a temperature logger placed in a water bottle. The average test temperature was 9.34˚C ±0.38 (based on test weeks 6-12), which was comparable to the temperature of the field experiment (see 2.1.4.).

A set of eight bottles with individually dosed concentrations were tested during each test. Increasing concentrations were added to each of these bottles to be able to draft a concentration curve (Tables 2A/2B). A range finding test was conducted first to get a first indication of the oil's toxicity prior to the ultimate tests.

Table 2A. Nominal oil concentrations used in the toxicity studies with Arabian light crude oil during subsequent Test Weeks (TW).

		TW0	TW1	TW2	TW3	TW4
Tx	Oil (ml/L)	Range Finding	LC_{50} Oil	LC_{50} Oil	LC_{50} Oil	LC_{50} Oil
C0	0	x	x	x	x	x
C0d	0					
C1	0.001	x				
C1,5	0.002					
C2	0.003		x	x		
C3	0.010	x	x	x	x	
C3,5	0.019					
C4	0.029		x	x	x	x
C4,5	0.067			x	x	x
C4.7	0.081					
C5	0.096	x	x	x	x	x
C5,2	0.125					x
C5,4	0.163					x
C5,5	0.192				x	x
C6	0.288		x	x	x	x
C7	0.962	x	x	x	x	
C8	2.88		x			
C9	9.62	x				

Table 2B. Nominal oil and dispersant concentrations used in the toxicity studies with Arabian light crude oil and the dispersant SLICKGONE NS.

			TW5	TW6	TW7
Tx	Oil (ml/L)	Dispersant (ml/L)	LC_{50} Dispersed Oil	LC_{50} Dispersed Oil	LC_{50} Dispersed Oil
C0	0	0	x	x	x
C0d	0	0.012	x	x	x
C1	0.001	0.00004	x		
C1,5	0.002	0.00008	x		
C2	0.003	0.00012			
C3	0.010	0.00038	x		
C3,5	0.019	0.00077	x		
C4	0.029	0.001		x	x
C4,5	0.067	0.003		x	x
C4.7	0.081	0.003			x
C5	0.096	0.004	x	x	x
C5,2	0.125	0.005		x	x
C5,4	0.163	0.007			
C5,5	0.192	0.008	x	x	x
C6	0.288	0.012	x	x	
C7	0.962	0.038			
C8	2.885	0.115			
C9	9.615	0.385			

After 48 hrs of stirring the WAF of each 5L bottle was gently poured into five 1L glass test bottles at low light, allowing five replicates per concentration. Gammarids (n=8) were added to each 1L glass beaker containing WAFs. Every test contained one set of controls (n=5) to ensure that test species were only adversely affected by the toxic compounds. After addition of the Gammarids, the test bottles were sealed with hexane-rinsed aluminum foil to reduce evaporation and photo degradation. Oxygen levels were measured prior to and at the end of each test using a Hach© HQ-40d multimeter with an LDO probe. At the start of the test, one test bottle of each concentration was used to measure the oxygen concentration representing the oxygen levels for all test bottles of that specific concentration. At the end of the test, oxygen levels were measured in all replicates of the test bottles.

Gammarid survival was scored every 24 hours, for five days. The obtained mortality data was recorded, used to create dose-response curves and to determine the LC50 values. Dose-response curves were obtained by log transforming the acquired dose data.

Testing continued until at least two test weeks were defined as sufficient for each of the tests. A test week defined as ‘sufficient’ met the following requirements: (1) a maximum of 10% mortality in the blanc (C0); (2) at least one concentration with no mortality (C0 excluded); (3) at least one concentration with 100% mortality; and (4) at least two or more concentrations with a mortality higher than 0% and lower than 100%. In total, 12 test weeks were conducted (Table 3). Of these,

TW3 and TW4 were rated 'sufficient' for the oil WAF toxicity tests and TW6 and TW7 for the dispersed oil CEWAF toxicity tests.

Concentrations reported here are nominal, meaning the volume of oil that was added, not the actual chemical concentrations of the oil components in water (WAF/CEWAF). These actual concentration will be analysed at a later stage. For this purpose ~450 ml of each WAF/CEWAF was stored in 500 ml amber coloured bottles containing 50 mL n-Hexane (Biosolve B.V., Netherlands). The bottles were stored in the climate room at 9°C until transport to the University of Essex.

Table 3: Total of all tests that were conducted to assess the toxicity of WAF and CEWAF of Arabian Crude light oil. 'Sufficient' was allocated based on quality criteria of the tests.

Test week #	**Abbreviation**	**Focus**	**Sufficient**
Test week 0 - range finding	TW0	Oil	No
Test week 1	TW1	Oil	No
Test week 2	TW2	Oil	No
Test week 3	TW3	Oil	Yes
Test week 4	TW4	Oil	Yes
Test week 5	TW5	Dispersed Oil	No
Test week 6	TW6	Dispersed Oil	Yes
Test week 7	TW7	Dispersed Oil	Yes
Test week 8	TW8	Dispersant only	No
Test week 9	TW9	Dispersant only	No
Test week 10	TW10	Dispersant only	No
Test week 11	TW11	Field Test	Yes
Test week 12	TW12	Dispersant only	No

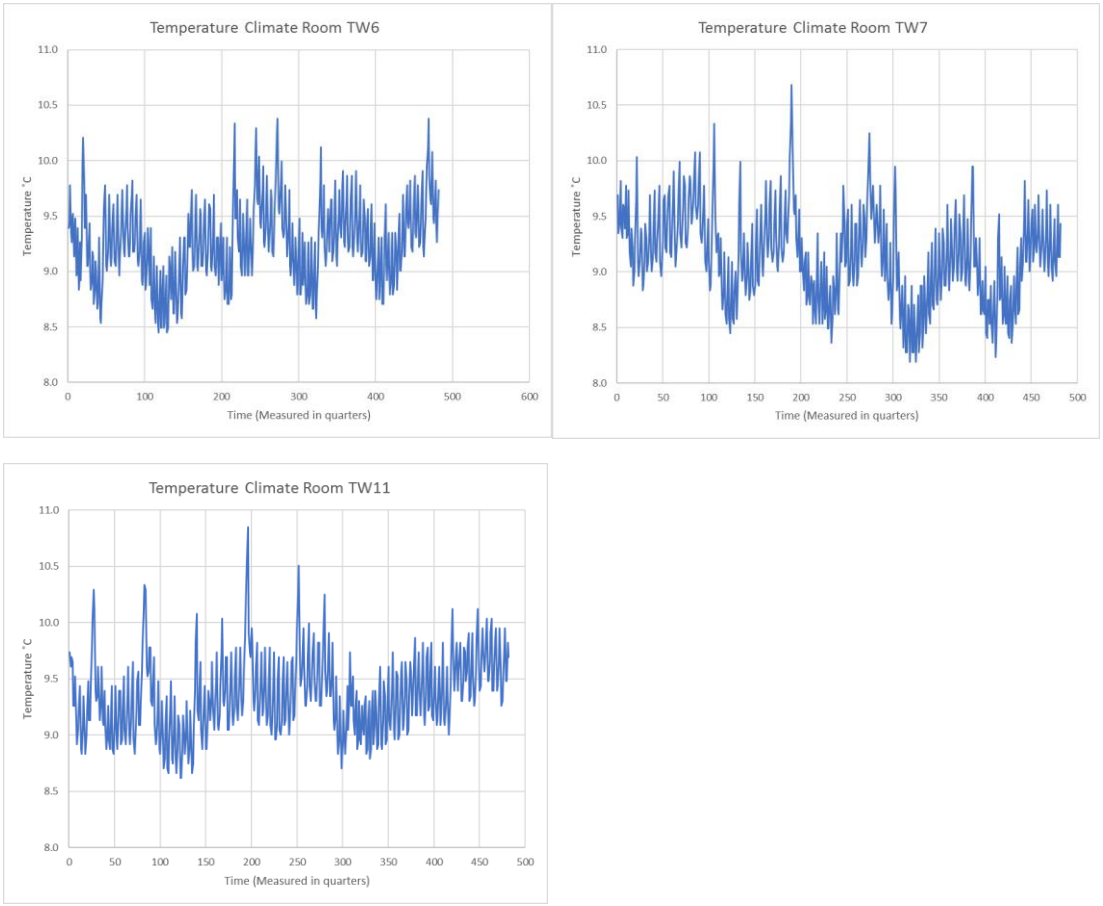

Figure 18. Test temperature of test weeks 6 (Panel A: 9.26˚C ±0.36), 7 (Panel B: 9.14˚C ±0.42) and 11 (Panel C: 9.36˚C ±0.35). No temperature data were available for test weeks 3 and 4. See Table 2 for details on the test weeks. Average test temperature of weeks 6-12 was 9.34˚C ±0.38.

Field test

Field samples were collected during the oil spill field experiment. Each oil slick contained three sample locations; (1) a sample taken in the middle of the slick, at a depth of 1.5 meters, (2) a sample taken in the middle of the slick, at a depth of 5 meters and (3) a sample outside the oil slick, to serve as blanc, at a depth of 1.5 meters. For each sample, three replicates were collected and samples were collected at T1 and T2 for the oil toxicity tests (table 4).

The actual LC50 experiments were conducted at a later time (test week 11). Field samples were stored at -20˚C in the dark until they were tested, to prevent any further weathering of the samples during storage. The samples were slowly melted prior to testing by placing them for 36 hours at test temperature (~9˚C). When the samples reached test temperature, eight individual gammarids were directly placed in each of the sample jars and the test was completed as described above for the 5-day toxicity test.

Data analysis

Dose response curves were created to determine the LC50 of the Arabian light crude oil and the dispersed Arabian light crude oil using Graphpad Prism 8. Data was processed and analysed by executing a non-linear regression.

Table 4. Details on collected water samples from the field experiment, that were provided by the sampling team, to test for oil toxicity using *G. locusta*.

#	Sample code	Date	Time	Coordinate	Coordinate	Slick	Sample position in slick	T1/T2	Depth	Replicate
	on sample jars					*Bravo - Charlie*	*In - out*	*T1 - T2*	*1.5 - 5 m*	*1 - 2 - 3*
1	Bravo T1 1.5C 1	16/apr/19				Control	Out	T1	1.5	1
2	Bravo T1 1.5C 2	16/apr/19				Control	Out	T1	1.5	2
3	Bravo T1 1.5C 3	16/apr/19				Control	Out	T1	1.5	3
4	Bravo T1 1.5 1	16/apr/19	11:35	52°14'52,9"N	3°57'17,5"E	Bravo	In	T1	1.5	1
5	Bravo T1 1.5 2	16/apr/19	11:35	52°14'52,9"N	3°57'17,5"E	Bravo	In	T1	1.5	2
6	Bravo T1 1.5 3	16/apr/19	11:35	52°14'52,9"N	3°57'17,5"E	Bravo	In	T1	1.5	3
7	Bravo T1 5 1	16/apr/19	11:35	52°14'52,9"N	3°57'17,5"E	Bravo	In	T1	5	1
8	Bravo T1 5 2	16/apr/19	11:35	52°14'52,9"N	3°57'17,5"E	Bravo	In	T1	5	2
9	Bravo T1 5 3	16/apr/19	11:35	52°14'52,9"N	3°57'17,5"E	Bravo	In	T1	5	3
10	Charlie T1 1.5 1	16/apr/19	13:46	52°18'56,3"N	3°56'21,3"E	Charlie	In	T1	1.5	1
11	Charlie T1 1.5 2	16/apr/19	13:46	52°18'56,3"N	3°56'21,3"E	Charlie	In	T1	1.5	2
12	Charlie T1 1.5 3	16/apr/19	13:46	52°18'56,3"N	3°56'21,3"E	Charlie	In	T1	1.5	3
13	Charlie T1 5 1	16/apr/19	13:46	52°18'56,3"N	3°56'21,3"E	Charlie	In	T1	5	1
14	Charlie T1 5 2	16/apr/19	13:46	52°18'56,3"N	3°56'21,3"E	Charlie	In	T1	5	2
15	Charlie T1 5 3	16/apr/19	13:46	52°18'56,3"N	3°56'21,3"E	Charlie	In	T1	5	3
16	Bravo T2 1.5C 1	16/apr/19				Control	Out	T2	1.5	1
17	Bravo T2 1.5C 2	16/apr/19				Control	Out	T2	1.5	2
18	Bravo T2 1.5C 3	16/apr/19				Control	Out	T2	1.5	3
19	Bravo T2 1.5 1	16/apr/19	14:42	52°20'09,7"N	3°57'40,3"E	Bravo	In	T2	1.5	1
20	Bravo T2 1.5 2	16/apr/19	14:42	52°20'09,7"N	3°57'40,3"E	Bravo	In	T2	1.5	2
21	Bravo T2 1.5 3	16/apr/19	14:42	52°20'09,7"N	3°57'40,3"E	Bravo	In	T2	1.5	3
22	Bravo T2 5 1	16/apr/19	14:42	52°20'09,7"N	3°57'40,3"E	Bravo	In	T2	5	1
23	Bravo T2 5 2	16/apr/19	14:42	52°20'09,7"N	3°57'40,3"E	Bravo	In	T2	5	2
24	Bravo T2 5 3	16/apr/19	14:42	52°20'09,7"N	3°57'40,3"E	Bravo	In	T2	5	3
25	Charlie T2 1.5 1	16/apr/19	17:01	52°24'41,3"N	4°01'16,1"E	Charlie	In	T2	1.5	1
26	Charlie T2 1.5 2	16/apr/19	17:01	52°24'41,3"N	4°01'16,1"E	Charlie	In	T2	1.5	2
27	Charlie T2 1.5 3	16/apr/19	17:01	52°24'41,3"N	4°01'16,1"E	Charlie	In	T2	1.5	3
31	Charlie T2 5 1	16/apr/19	17:01	52°24'41,3"N	4°01'16,1"E	Charlie	In	T2	5	1
32	Charlie T2 5 2	16/apr/19	17:01	52°24'41,3"N	4°01'16,1"E	Charlie	In	T2	5	2
33	Charlie T2 5 3	16/apr/19	17:01	52°24'41,3"N	4°01'16,1"E	Charlie	In	T2	5	3

Results and discussion

LC50 value – oil

Test weeks 3 and 4 both showed a steep dose response curve indicating a rapid increasing toxicity of the tested oil (Figure 19). The corresponding LC50 values were 0,125 ml oil/L for TW3 and 0,127 ml oil/L for TW4. As both dose response curves (and corresponding LC50 values) were very similar, dose response values were combined, resulting in an averaged LC50 value of 0,126 ml oil/L for Arabian light crude oil (based on test weeks 3 & 4). The dispersant SLICKGONE NS did not show any signs of toxicity in the used concentrations as the highest concentrations were applied in additional blanks and no additional mortality was observed.

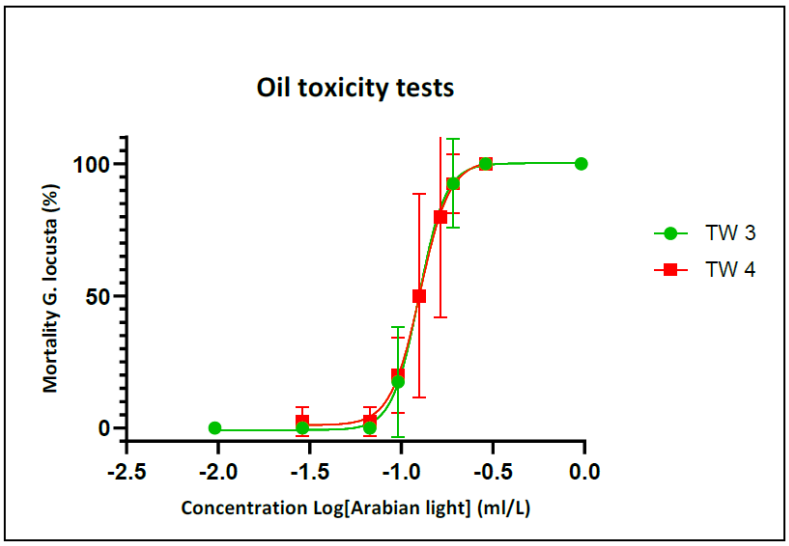

Figure 19. Dose response curves of *Gammarus locusta* exposed to different concentrations of Arabian light crude oil at 9˚C (test weeks 3 and 4). Concentrations are based on nominal values.

LC50 value – dispersed oil

Test week 6 and 7 (TW6 and TW7) produced steep dose response curves (figure 20). The LC50 values for Arabian light crude oil dispersed with SLICKGONE NS were 0.115 ml oil/L for TW6 and 0.100 ml oil/L for TW7. As the two test weeks showed similar values and trends, the two test weeks were combined to an averaged LC50 value for Arabian light crude oil dispersed with SLICKGONE NS of 0.105 ml oil/L (based on TW6 and TW7).

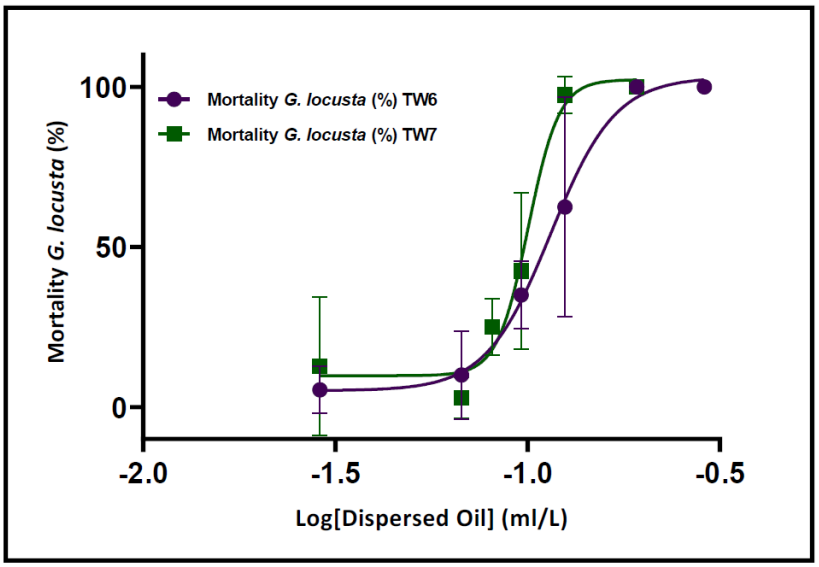

Figure 20. Dose response curves of *Gammarus locusta* exposed to different concentrations of dispersed oil based on Arabian light crude oil and SLICKGONE NS at 9˚C (test weeks 6 and 7). Concentrations are based on nominal values.

Comparison LC50 value – oil and dispersed oil

Averaged dose-response curves of Arabian light crude oil and Arabian light crude oil dispersed with SLICKGONE NS showed that the dispersed oil (0.105 ml oil/L) was slightly more toxic (factor 1.2 times) than non-dispersed oil (0.126 ml oil/L), when based on nominal concentrations (figure 21). Actual chemical concentrations will be determined, though results will be too late for incorporation in this report.

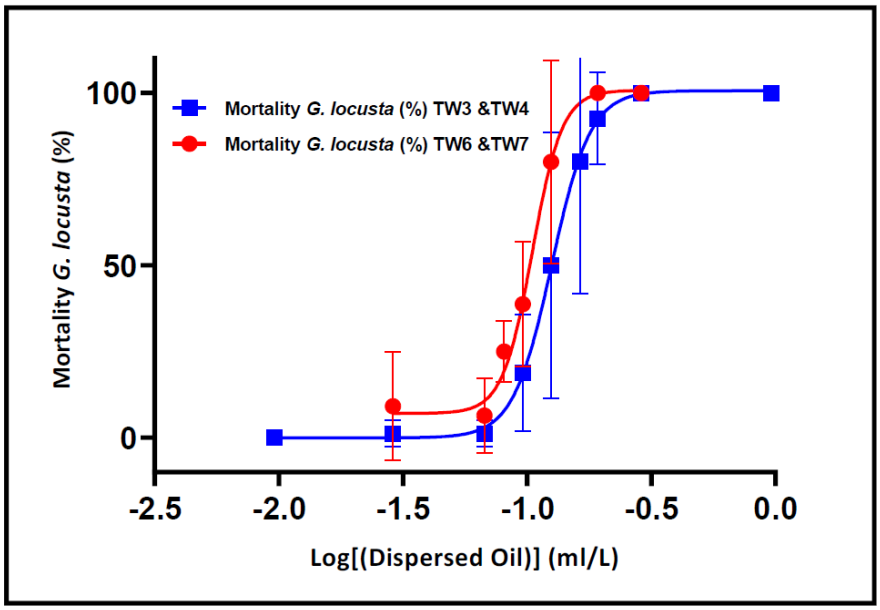

Figure 21. Dose response curves of *Gammarus locusta* exposed to different concentrations of Arabian light crude oil (based on TW3 & TW4) and Arabian light crude oil dispersed with SLICKGONE NS (based on TW6 & TW7) at 9˚C. Concentrations are based on nominal values.

Field test

Although a weak oil odour was noted in the water collected from the field experiment, the gammarids exposed to samples collected in the field showed a survival rate of 100%. Of all test organisms one individual died, in one of the control samples. This indicated that concentrations of oil in the field samples were similar to or lower than the No Observed Effect Concentrations (NOEC) of 0.03 ml oil/L and 0.002 ml oil/L for both oil and dispersed oil respectively. As the chemical analysis of the field samples have not been conducted yet, no further comparison with the laboratory tests can be made.

Laboratory tests were conducted in full darkness and with the prevention of evaporation, while the oil slicks in the field tests were influenced by evaporation, spreading, photo-oxidation and other relevant weathering processes that influence the presence of dissolved oil component in the water phase.

Discussion/Conclusion

Averaged LC50 values for *G. locusta* exposed for 5 days at 9˚C to Arabian light crude oil and Arabian light crude oil dispersed with SLICKGONE NS were 0.126 ml oil/L and 0.105 ml oil/L respectively, indicating that the dispersed oil was slightly more toxic (factor 1.2) than non-dispersed oil when based on nominal concentrations. Samples collected from the field during the field experiment with

Arabian light crude oil and Arabian light crude oil dispersed with SLICKGONE NS did not show mortality indicating that the oil concentrations in the field were at or below the No Observed Effect Concentrations (NOEC) for this oil type and dispersant.

Acknowledgements

Vincent Escaravage is thanked for organising the sampling of water during the field experiment.

References

Costa, F.O., Correia, A.D., Costa, M.H. (1998). Acute Marine Sediment Toxicity: A Potential New Test with the Amphipod *Gammarus locusta*. Ecotoxicology and Environmental Safety, 40(1-2), 81-87.

Costa, F.O., Costa, M.H. (1999). Life history of the amphipod *Gammarus locusta* in the Sado estuary (Portugal). Acta oecologica, 20(4), 305-314.

Hartog den, C. (1963). The amphipods of the deltaic region of the rivers Rhine, Meuse and Scheldt in relation to the hydrography of the area part II. The Talitridae. Netherlands Journal of Sea Research, 2(1), 40-67.

Lincoln R.J., British Marine Amphipoda: Gammaridea, British Museum (Natural History), London, 1979, 658 p.

4 Related laboratory studies

Brussaard, Corina (NIOZ/UvA) and Gianluca Bizzaro (NIOZ)

In collaboration with the WUR lab experiments were performed, whereby WUR focused mostly on floc formation after exposure with dispersant under different growth conditions and NIOZ tested sensitivity of phytoplankton to dispersant exposure as well as the effect of dispersant on virus-host interactions.

***Objective 1**: Test sensitivity of phytoplankton to exposure with dispersant: Corexit (earier used by WUR; Van Eenennaam et al. 2016) and Slickgone (used during the ExpOS'D spills).*

We successfully used 6 different phytoplankton species, representing major phytoplankton taxonomic groups in Dutch coastal waters. We furthermore tested mixed culture of different diatoms (WUR culture collection) but this one failed to grow consistently and was dismissed for further research. For both Corexit and Slickgone, seven concentrations ranging from 0.01 to 0.5 mL/L (final concentration) were tested against control cultures receiving medium instead of dispersant. Considering we also wanted to examine the effect of dispersant on virus-host interactions, we needed to make sure to find a dispersant concentration at which the two algal model species used were still alive as only living cells allow the production of virus progeny after infection. As expected, all control cultures grew well. The treated cultures, however, quickly showed a reduction in growth or even displayed cell death. The sensitivity to the dispersants differed by a factor 10 to 100 between the species tested. Despite a general sensitivity to high dispersant concentration exposure, the more detailed response does not seem to be general or even class-specific. High sensitivity of some species to very low concentrations of dispersant are still ecologically relevant as under natural conditions the dispersant is (rapidly) diluted by mixing.

***Objective 2**: Test at what concentration of dispersant (COREXIT and SLICKGONE) visible flocculation of the algal cultures occurs (extracellular polymer substances, EPS).*

All phytoplankton species tested for objective 1 were also used for objective 2 (exponentially growing, using glass tubes and settling columns). The tubes were only gently mixed the first day to accommodate larger floc formation over time. Cultures where visually monitored for two weeks; every hour for the first 8 h to check for potential immediate flocculation and thereafter once a day. In general, only high concentrations of dispersant were capable of inducing visible EPS flocs in the algal cultures. The two dispersants produced different type of flocs. At these concentrations, most phytoplankton species died. Using Corexit, flocs were often small, but eventually sank to the bottom of the tube. Earlier experiments with Dunaliella indicated floc formation (Van Eenennaam et al. 2016), however in our experiments Dunaliella did not show visual floc production (also not in a second trial with higher algal abundances). The response to dispersant exposure may be strain-specific.

***Objective 3**: To study how environmental relevant concentrations of two types of dispersants affect the host-virus interaction during the infection cycle.*

One-step infection cycle experiments were conducted using two virus-algal host model systems. Samples were taken for flow cytometric enumeration of algal cells and viruses. The non-infected cultures grew well during the experiment, and the non-treated infected cultures displayed a typical infection cycle. Upon addition of dispersant, species-specific responses were observed. There are, to our knowledge, no data published on the effect of dispersant on virus-host

dynamics despite the importance of viruses as mortality factor of phytoplankton (Mojica et al. 2016). We show that the use of dispersants can selectively impact viral lysis of phytoplankton. This will likely favor specific species over others, assuming other loss factors such as grazing, are not affected by dispersant exposure.

We are currently writing a scientific paper about this research, which will contain a more comprehensive description of the experiment and its results.

References

Mojica, K.D.A., Huisman, J., Wilhelm, S.W., Brussaard, C.P.D. (2016). Latitudinal variation in virus-induced mortality of phytoplankton across the North Atlantic Ocean. ISME Journal, 10, 500–513.

Van Eenennaam, J.S., Wei, Y., Grolle, K.C.F., Foekema, E.M., Tinka A.J. (2016). Oil spill dispersants induce formation of marine snow by phytoplankton-associated bacteria. Marine Pollution Bulletin, 104, 294-302.

Appendix 2: Published Paper – Bacterial Community Legacy Effects following the Agia Zoni II Oil-Spill, Greece

Thomas, G.E., Cameron, T.C., Campo, P., Clark, D.R., Coulon, F., Gregson, B.H., et al. (2020) Bacterial Community Legacy Effects Following the Agia Zoni II Oil-Spill, Greece. *Front Microbiol* **11**: 1–15.

frontiers in Microbiology

ORIGINAL RESEARCH
published: 17 July 2020
doi: 10.3389/fmicb.2020.01706

Bacterial Community Legacy Effects Following the Agia Zoni II Oil-Spill, Greece

Gareth E. Thomas[1], Tom C. Cameron[1], Pablo Campo[2], Dave R. Clark[1,3], Frederic Coulon[2], Benjamin H. Gregson[1], Leanne J. Hepburn[1], Terry J. McGenity[1], Anastasia Miliou[4], Corinne Whitby[1] and Boyd A. McKew[1]**

[1] School of Life Sciences, University of Essex, Colchester, United Kingdom, [2] School of Water, Energy and Environment, Cranfield University, Cranfield, United Kingdom, [3] Institute for Analytics and Data Science, University of Essex, Wivenhoe Park, Essex, United Kingdom, [4] Archipelagos Institute of Marine Conservation, Samos, Greece

In September 2017 the Agia Zoni II sank in the Saronic Gulf, Greece, releasing approximately 500 tonnes of heavy fuel oil, contaminating the Salamina and Athens coastlines. Effects of the spill, and remediation efforts, on sediment microbial communities were quantified over the following 7 months. Five days post-spill, the concentration of measured hydrocarbons within surface sediments of contaminated beaches was 1,093–3,773 $\mu g\ g^{-1}$ dry sediment (91% alkanes and 9% polycyclic aromatic hydrocarbons), but measured hydrocarbons decreased rapidly after extensive clean-up operations. Bacterial genera known to contain oil-degrading species increased in abundance, including *Alcanivorax*, *Cycloclasticus*, *Oleibacter*, *Oleiphilus*, and *Thalassolituus*, and the species *Marinobacter hydrocarbonoclasticus* from approximately 0.02 to >32% (collectively) of the total bacterial community. Abundance of genera with known hydrocarbon-degraders then decreased 1 month after clean-up. However, a legacy effect was observed within the bacterial community, whereby *Alcanivorax* and *Cycloclasticus* persisted for several months after the oil spill in formerly contaminated sites. This study is the first to evaluate the effect of the Agia Zoni II oil-spill on microbial communities in an oligotrophic sea, where *in situ* oil-spill studies are rare. The results aid the advancement of post-spill monitoring models, which can predict the capability of environments to naturally attenuate oil.

Keywords: Mediterranean, hydrocarbons, Agia Zoni II, oil spill, *Alcanivorax*, *Cycloclasticus*, *Idiomarina*, Greece

OPEN ACCESS

Edited by:
Tony Gutierrez, Heriot-Watt University, United Kingdom

Reviewed by:
Joaquim Vila, University of Barcelona, Spain
Camilla Lothe Nesbø, University of Alberta, Canada
Casey R. J. Hubert, University of Calgary, Canada

****Correspondence:***
Gareth E. Thomas
gthomab@essex.ac.uk
Boyd A. McKew
boyd.mckew@essex.ac.uk

Specialty section:
This article was submitted to Aquatic Microbiology, a section of the journal Frontiers in Microbiology

Received: *12 March 2020*
Accepted: *29 June 2020*
Published: *17 July 2020*

Citation:
Thomas GE, Cameron TC, Campo P, Clark DR, Coulon F, Gregson BH, Hepburn LJ, McGenity TJ, Miliou A, Whitby C and McKew BA (2020) Bacterial Community Legacy Effects Following the Agia Zoni II Oil-Spill, Greece. Front. Microbiol. 11:1706. doi: 10.3389/fmicb.2020.01706

INTRODUCTION

On the 10th of September 2017, the Agia Zoni II tanker sank in the inner Saronic Gulf, Greece, releasing approximately 500 metric tonnes of heavy fuel oil into the waters and contaminating the surrounding coastlines (IOPC, 2017). The Hellenic Coast Guard deployed ∼600 m of oil boom out to sea within 8 h, which increased to ∼9 km of booms and absorbents in the following weeks. Despite this response, the oil had spread far from the spill site and impacted over 4 km of the Salamina coastline and over 25 km of the Athens Riviera including Glyfada and the port of Piraeus, due to a change in the wind direction (**Figure 1**). An extensive clean-up response was undertaken on all contaminated beaches, including manual removal of tar balls, flushing and trenching, high-powered washing, removal of sediments for either washing/replacement or disposal at landfill,

and the use of absorbents (see **Figure 1** and **Supplementary Table S1** for sample location and specific treatment/action undertaken at each site). On the 30th November, 2017 the shipwreck was removed, and the clean-up operations ceased in February 2018. On the 28th April, 2018 the Greek government lifted maritime restrictions.

Oil spills dramatically alter marine microbial community composition, resulting in a decrease in species richness and diversity, in conjunction with selection for oil-degrading bacteria (Head et al., 2006; McGenity et al., 2012). Certain microbes can degrade a range of hydrocarbons found in crude oil and its derivatives, including obligate hydrocarbonoclastic bacteria (OHCB), which use hydrocarbons as an almost exclusive source of carbon and energy (Yakimov et al., 2007). While OHCB have been demonstrated to degrade other compounds in pure culture (Radwan et al., 2019; Zadjelovic et al., 2020), there is still limited evidence that the OHCB are competitive for non-hydrocarbon substrates in the environment. This is evidenced by the fact OHCB are typically present in extremely low numbers in uncontaminated environments but rapidly increase in abundance following oil-spills (Yakimov et al., 2004a; Atlas and Hazen, 2011; Acosta-González et al., 2015; Nogales and Bosch, 2019). Therefore, while it is evident that OHCB use a few other carbon and energy sources, for clarity we refer to them hereafter as "OHCB" to distinguish between these highly adapted and competitive hydrocarbon degraders and those more metabolically diverse bacteria, which can also degrade hydrocarbons. Since the deepwater horizon well blowout, there has been increased emphasis on understanding oil-spill microbial ecology, with much of the focus on deep sea oil plumes (Hazen et al., 2010; Mason et al., 2012; Redmond and Valentine, 2012), salt marsh sediments (Beazley et al., 2012), or benthic sediments (Mason et al., 2014). Though some studies have focused on coastal sediments (Kostka et al., 2011; Lamendella et al., 2014; Huettel et al., 2018) most were conducted either *ex situ* (Röling et al., 2002; Da Silva et al., 2009; Almeida et al., 2013) or retrospectively (De La Huz et al., 2005; Short et al., 2007; Boufadel et al., 2010), and represented a bias toward a single oil-spill event, deepwater horizon. Therefore, the *in situ* establishment and succession of specialized oil-degrading microbial taxa, in the Mediterranean immediately following an oil spill, are less well understood. This is especially true for coastal sediments in the Mediterranean (see **Supplementary Table S2**). Understanding how such ecosystems, and particularly oil-degrading microbial communities, respond to such events will allow for better post-spill monitoring (Kirby et al., 2018). Exposure of environments to oil can also lead to a long-lasting adaptation within the microbial community. This phenomenon of prior exposure can be important in determining the rate at which any subsequent hydrocarbon inputs may be biodegraded (Leahy and Colwell, 1990). Such knowledge will also assist in designing or improving models such as the Ecological Index of Hydrocarbon Exposure (EIHE) (Lozada et al., 2014) and inform future oil-spill response, such as indicating the thoroughness of clean-up efforts and identifying when tourist/fishing activities can recommence.

The Mediterranean is an oligotrophic sea with extremely low levels of phosphorus (Thingstad et al., 2005) and is virtually an enclosed basin with limited oceanic exchange. Phosphorous is a macronutrient that is vital for microbial growth and especially for hydrocarbon degradation (Seah and McFerran, 2016); and therefore, the availability of these nutrients in the presence of hydrocarbons is vital (Ron and Rosenberg, 2014). From 1977 to 2018 the Mediterranean has been subject to 989 recorded oil-pollution incidents (REMPEC, 2018). Additionally, the Mediterranean has been the location of three of the world's top 20 largest tanker oil spills; including the tankers Haven (1991, 144,000 tonnes, Italy), Irenes Serenade (1980, 100,000 tonnes, Greece), and Independenta (1979, 95,000 tonnes, Turkey) (ITOPF, 2019). The majority of accidents resulting in oil-pollution occur in the Eastern Mediterranean, especially around Greece (Girin and Carpenter, 2019). The Mediterranean currently contains two refineries, two oil terminals, and three oil ports (REMPEC, 2018), with an additional 480 active shipping ports, 50% of which are in located around Greece and Italy (Xue et al., 2004). The Mediterranean is highly socio-politically complex with 21 countries bordering the sea, and future predictions indicate increased levels of oil and gas drilling in the region (Union et al., 2016). Oil pollution in the Mediterranean therefore represents a significant threat to the environment. Despite this, there remains a paucity of information on how oil pollution affects Mediterranean sediment microbial communities.

Our early sampling (5 days post spill) of the Agia Zoni II incident allowed a very rare opportunity to investigate the immediate impact on the microbial community and identify the earliest key colonizing oil-degrading bacteria from an oil spill that covered a large area of coastal sediment, in a region where fishing and tourism play a pivotal socio-economic role. We quantified hydrocarbon concentrations across seven contaminated and two uncontaminated sites 5 days post-spill and after remediation. Additionally, we determined oil-spill-induced changes in gene abundance, diversity, and composition of the sediment microbial communities using qPCR and high throughput sequencing of the 16S rRNA gene.

RESULTS

Sediment Hydrocarbon Concentrations

Five days after the oil spill, the surface sediments at three sample sites on the Athens Riviera were visibly contaminated by hydrocarbons (**Figure 2**). The concentrations of the aliphatic hydrocarbons fraction including *n*-alkanes from undecane (C_{11}) to dotriacontane (C_{32}) and the branched alkanes (pristane and phytane) ranged from 1,536 ± 557 to 2,803 ± 549 $\mu g\ g^{-1}$ dry sediment (**Figure 2**). The concentrations of the aromatic fraction, containing the 2–5 fused-ring polycyclic aromatic hydrocarbons (PAHs), including methylnaphthalenes, dimethylnapthalenes, methylphenanthrenes, and methylanthracenes ranged from 88.20 ± 13.50 to 332 ± 99 $\mu g\ g^{-1}$ dry sediment. One-month post-spill, the concentration of total *n*-alkanes, branched alkanes, and PAHs reduced to almost undetectable levels at both the

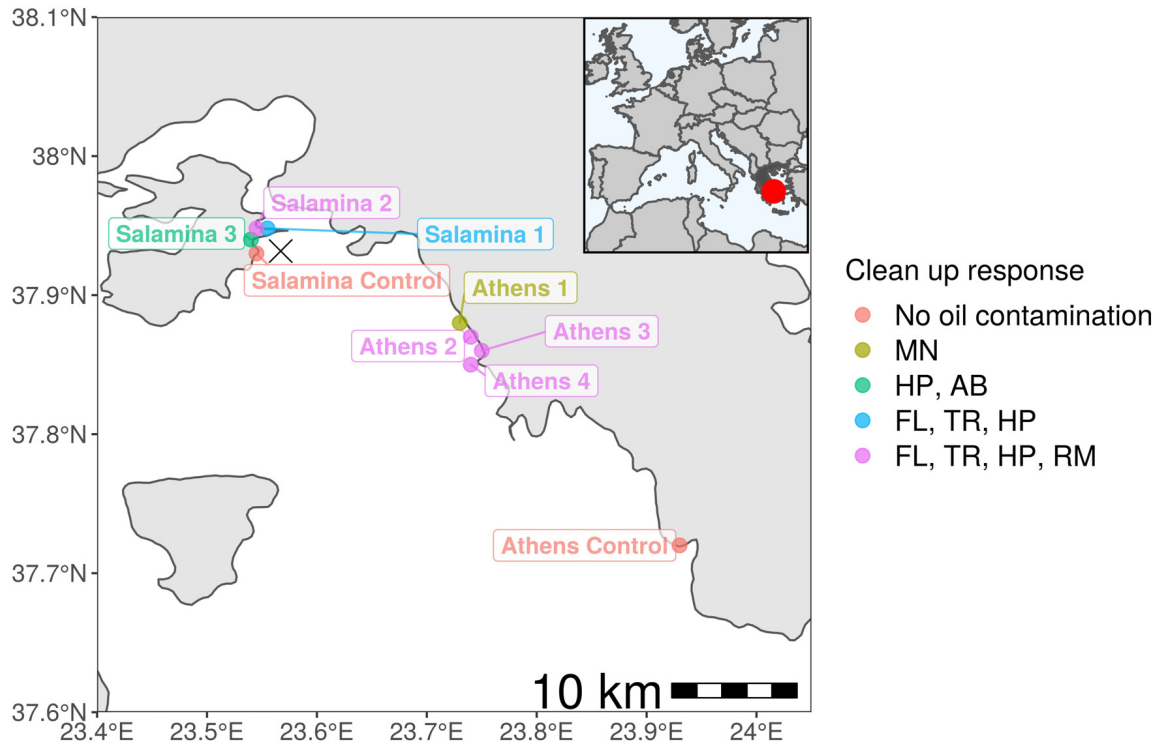

FIGURE 1 | Sampling sites from the Agia Zoni II oil-spill (marked as an X where tanker sank) in Greece (inlet; dark gray; red dot highlights spill-site) and affected Athens Riviera and Salamina coastline. Abbreviations for clean-up response applied at oil-contaminated sample sites (Athens 1–4 and Salamina 1–3): MN (manual removal of tar balls), HP (high-powered washing, to remove oil from hard surfaces), AB (use of absorbents to collect floating oil from the water surface), FL (flushing of sediment with medium pressure water), TR (trenching, used in conjunction with flushing to collect oil), and RM (removal of coastal sediment, either washed and replaced or disposed in landfill).

Athens Riviera and Salamina sites (**Figure 3**). Additionally, we found no significant differences in phosphate, nitrate, and ammonium concentrations between contaminated sites and uncontaminated control sites when compared to coastal water samples (**Supplementary Figure S1**).

Effects of the Oil-Spill on Sediment Microbial Community Composition and Abundance

In order to evaluate any effect that the oil-spill had on microbial community composition or abundance, 16S rRNA bacterial and archaeal genes were analyzed by qPCR and amplicon library sequencing [see operational taxonomic units (OTU) tables in **Supplementary Tables S3, S4**]. High-throughput 16S rRNA gene sequencing resulted in an average of 55,591 (range 8,093–209,105) and 49,983 (range 3,822–196,697) sequence reads for bacteria and archaea, respectively. Five days post-spill, the mean bacterial 16S rRNA gene abundance (1.6×10^8 copies g^{-1} dry sediment) in Athens contaminated sediments was ∼2.5 fold greater, but not statistically significant, than in the uncontaminated control sediments (**Supplementary Figure S2A**). Archaeal 16S rRNA gene abundance was typically two orders of magnitude lower than the Bacteria (**Supplementary Figure S2B**) and no significant changes were observed in archaeal 16S rRNA gene abundance in response to the oil spill. Simpson Diversity Index analysis of archaeal and bacterial 16S rRNA gene amplicon libraries revealed no significant difference between contaminated (average across all samples, archaea 0.35 and bacteria 0.99) and uncontaminated (archaea 0.26 and bacteria 0.99) sites, at any month. Archaeal community analysis revealed a high relative abundance of *Candidatus* Giganthauma and *Nitrosopumilus*, though no significant differences were observed between contaminated and uncontaminated sediment samples. This suggests archaea did not play a significant role in biodegradation of, and were unaffected by, the oil (**Supplementary Figure S3**).

Operational taxonomic units affiliated to numerous OHCB in contaminated sites 5 days post-spill were significantly more relatively abundant in comparison to uncontaminated control sites. These changes included higher relative abundance of members of *Marinobacter*, closely related to *M. hydrocarbonoclasticus*, *Alcanivorax* spp., *Oleibacter* spp., *Oleiphilus* spp., and *Thalassolituus* spp. (**Figure 4**) in comparison to uncontaminated sites. In October and December higher relative abundance of *Cycloclasticus*, a known PAH-degrading genus (Dyksterhouse et al., 1995) was also observed in the contaminated site "Salamina Oil 1." There was also significantly higher relative abundance of sequences affiliated to more catabolically versatile genera or species (i.e., those that use a

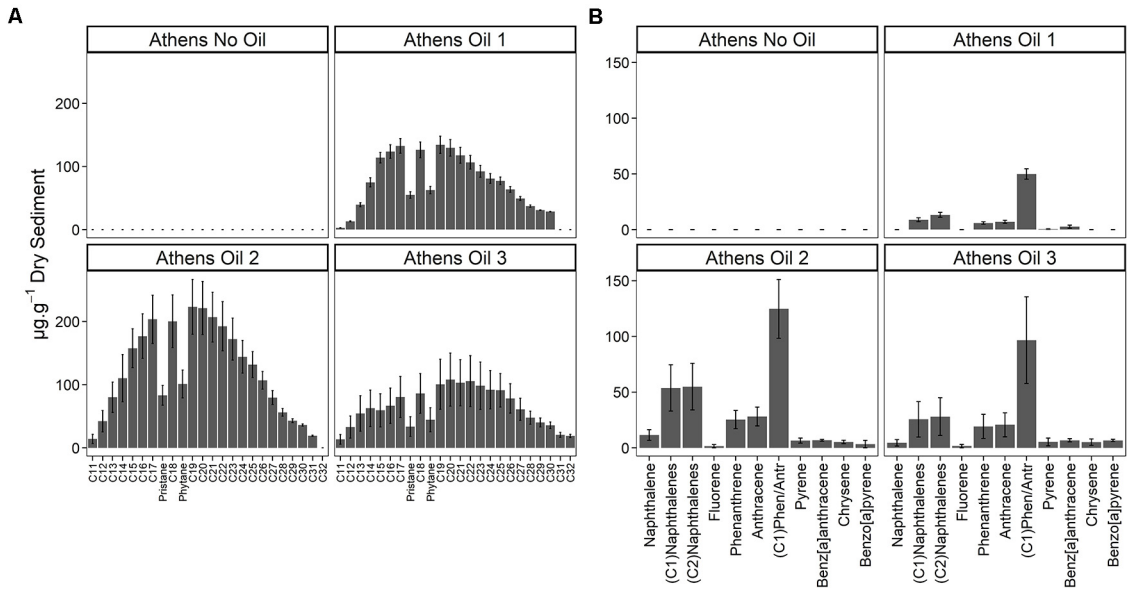

FIGURE 2 | Hydrocarbon concentrations (mean ± SE, *n* = 3) of the three contaminated sites (Athens Oil 1-3) and the uncontaminated control site (Athens No Oil), September 2017. **(A)** *n*-alkanes from C11 to C32 and the branched alkanes pristane and phytane. **(B)** PAHs from 2-ring naphthalene to 5-ring benzo[*a*]pyrene. No samples were taken for Salamina in September 2017.

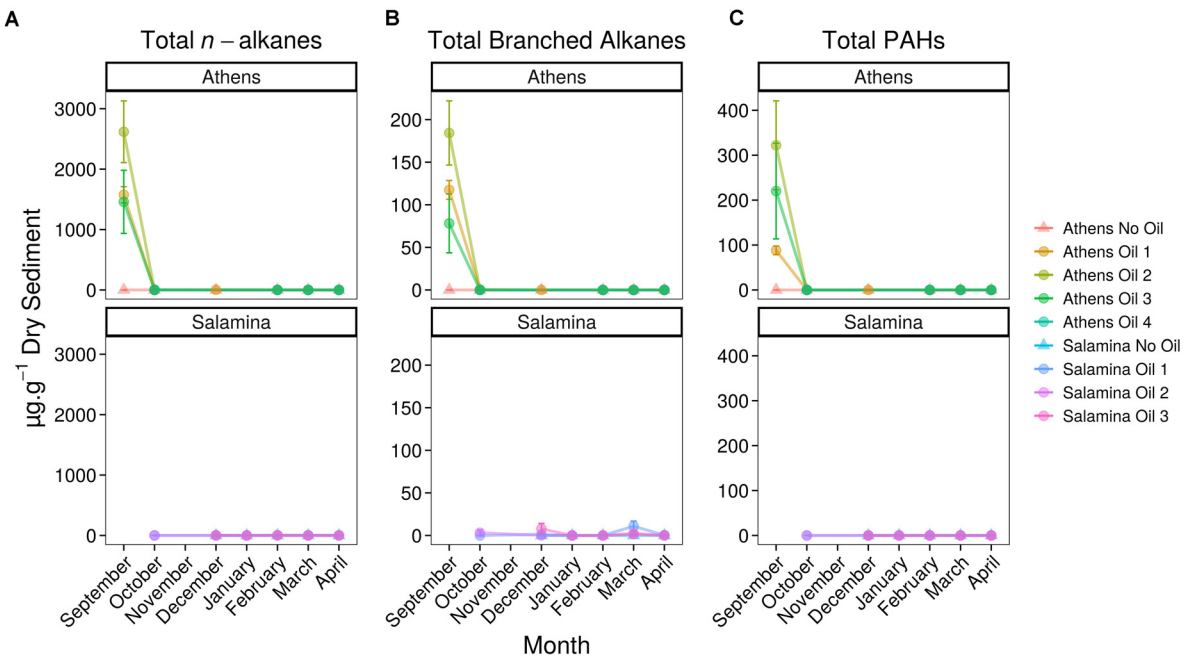

FIGURE 3 | Concentrations (mean ± SE, *n* = 3) of hydrocarbons in control (Suffix "No Oil") and contaminated (Suffix "Oil") sediments along the Athens Riviera and Salamina coastline, sampled from September 2017 to April 2018. **(A)** Total *n*-alkanes, **(B)** total branched alkanes (pristane and phytane), and **(C)** total PAHs. No samples were collected for all Salamina sites in September 2017, "Salamina No Oil" in October 2017, or all Salamina and Athens sites in November 2017.

wider range of substrates than the OHCB whose substrate range in the environment is typically restricted to hydrocarbons) in comparison to uncontaminated sites. These genera have been shown to contain representatives that can degrade hydrocarbons; including *Marinobacter* spp., *Idiomarina* spp., *Alteromonas* spp., *Vibrio* spp., *Erythrobacter* spp., and *Roseovarius* spp. (**Figure 5**; see **Supplementary Table S2**). Dissimilarities in bacterial community composition were evident between uncontaminated

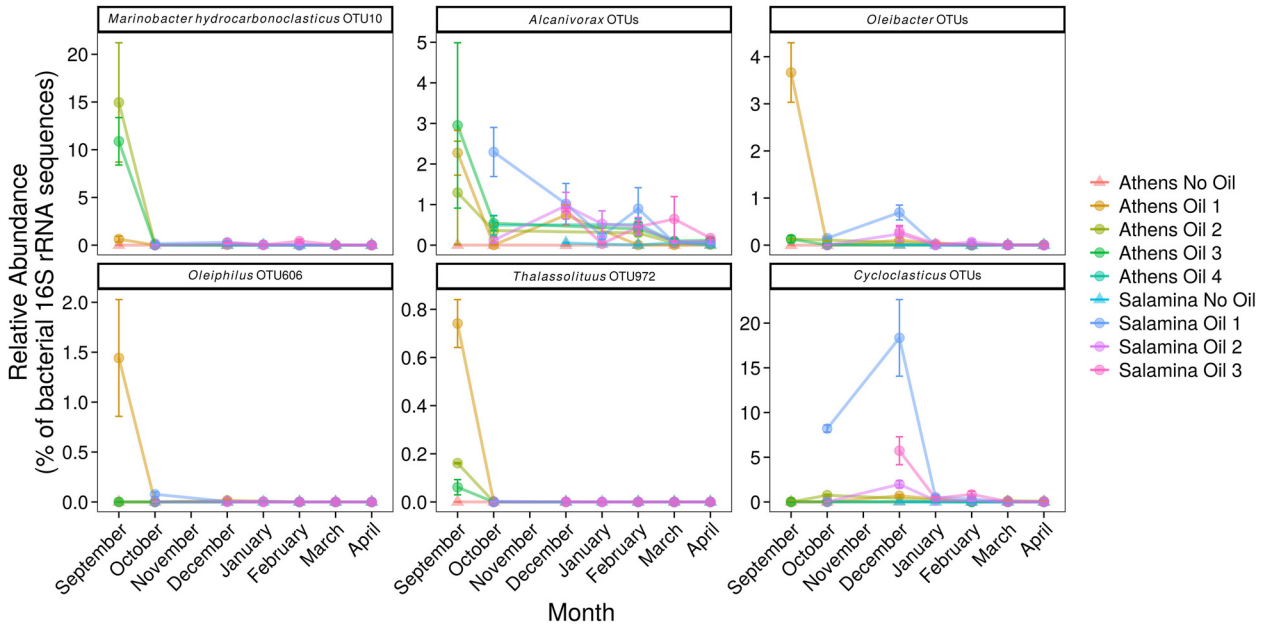

FIGURE 4 | Relative abundance (% of the bacterial community; mean ± SE, $n = 3$) of 16S rRNA gene OTUs assigned to putative obligate hydrocarbonoclastic bacteria (including OTU-10 which has a 100% identity match to *M. hydrocarbonoclasticus*) in sediments from control (Suffix "No Oil") and contaminated (Suffix "Oil") sites along the Athens Riviera and Salamina coastline, from September 2017 to April 2018. No samples were collected for all Salamina sites in September 2017, "Salamina No Oil" in October 2017, or all Salamina and Athens sites in November 2017. Bacteria and Archaea OTU tables are available in **Supplementary Tables S3**, **S4**.

and contaminated sites in September 2017 immediately after the oil-spill. However, from October 2017 onward the bacterial community composition at the oiled sites become increasingly similar to as those found at the uncontaminated sites (**Supplementary Figure S4**).

Several of the OTUs that were significantly more relatively abundant at contaminated versus uncontaminated sites were affiliated to OHCB and specifically to known alkane degraders. For example, OTU-10 (100% 16S rRNA sequence identity to *Marinobacter hydrocarbonoclasticus*; **Figures 4**, **6**), had significantly higher relative abundance at some contaminated sites (coef. = 10.88, $z = 18.13$, $p < 0.001$) compared to uncontaminated sites. Five days post-spill, OTU-10, represented 15 and 11% at "Athens Oil 2 and 3," respectively, but sharply decreased in relative abundance to virtually undetectable levels from October onward. The increase in the relative abundance of *M. hydrocarbonoclasticus* represented an increase of 2.14×10^7 16S rRNA gene copies assigned to *M. hydrocarbonoclasticus* compared to uncontaminated Athens sediments. Five OTUs assigned to the OHCB genus *Alcanivorax* (**Figures 4**, **6**) were significantly more relatively abundant in all contaminated sites (September 2.19% ± 1.52%; coef. = 2.28, $z = 6.40$, $p < 0.001$) compared to uncontaminated sites where it was generally undetectable. From October the relative abundance of *Alcanivorax* OTUs steadily decreased in the contaminated sites, though always remained at least 5- to 297-fold greater than the uncontaminated control sites, where they were often undetectable. Similarly, OTUs from the genus *Oleibacter* (OTU-200 and OTU-265) and OTU-606 from *Oleiphilus* (**Figures 4**, **6**) were significantly more abundant in "Athens Oil 1" immediately after the oil-spill in September (coef. = 1.44, $z = 13.35$, $p < 0.001$) from uncontaminated control levels (3.67 ± 0.89% and 1.44 ± 0.83%, respectively). However, in April the relative abundance of both genera decreased to levels below 0.01%. Finally, OTU-972 assigned to *Thalassolituus* (**Figures 4**, **6**), a genus containing species that can degrade a wide range of alkanes (Yakimov et al., 2004b; Gregson et al., 2018), was significantly more relatively abundant in sediments from contaminated sites in September (0.74%; coef. = 0.16, $z = 7.52$, $p < 0.001$) compared to uncontaminated control sediments. The relative abundance of *Thalassolituus* decreased in the months thereafter to undetectable levels. The increase in the relative abundance of *Thalassolituus* represented an increase of 1.22×10^6 16S rRNA gene copies compared to uncontaminated Athens sediments, even though *Thalassolituus* was the least abundant OCHB genus.

No known PAH-degrading OHCB were detected five days post-spill when high PAH concentrations were measured. However, OTUs from more metabolically diverse genera (which have been demonstrated to degrade PAHs; see **Supplementary Table S2**) were observed in significantly higher relative abundance (coef. = 1.75, $z = 6.06$, $p < 0.001$) compared to uncontaminated levels, including *Alteromonas* spp. (10.46 ± 2.91% at "Athens Oil 1"), *Idiomarina* spp. (13.96 ± 11.75% at "Athens Oil 2 and 3"), and *Vibrio* spp. (2.09 ± 2.03% across "Athens Oil 1, 2, and 3"). OTU-31 and

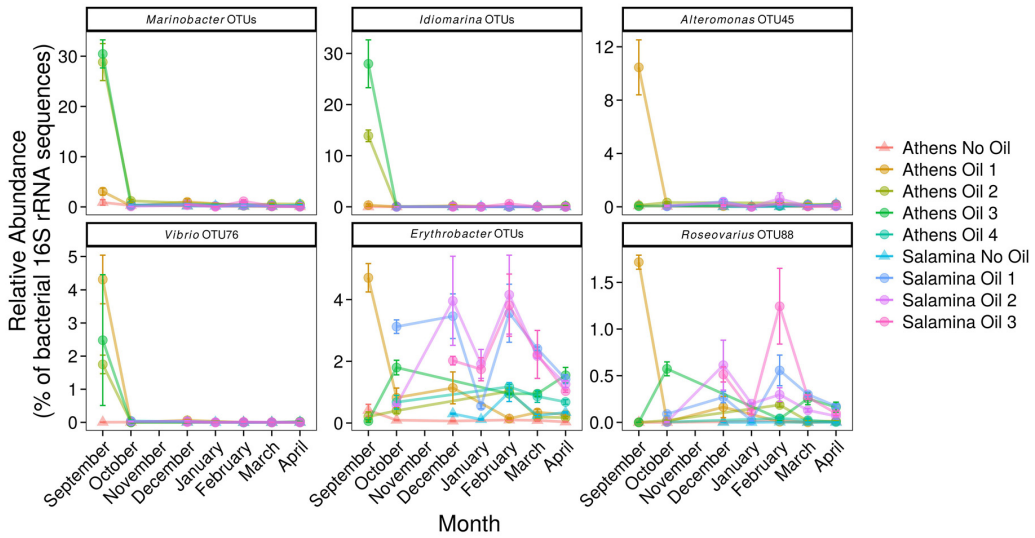

FIGURE 5 | Relative abundance (% of the bacterial community; mean ± SE, $n = 3$) of 16S rRNA gene OTUs assigned to Bacteria associated with oil-degradation, in sediments from control (Suffix "No Oil") and contaminated (Suffix "Oil") sites along the Athens Riviera and Salamina coastline, from September 2017 to April 2018. No samples were collected for all Salamina sites in September 2017, "Salamina No Oil" in October 2017, or all Salamina and Athens sites in November 2017. Bacteria and archaea OTU tables are available in **Supplementary Tables S3**, **S4**.

OTU-32, assigned to the PAH-degrading genus *Cycloclasticus* (**Figures 4**, **6**), had significantly greater relative abundance in some contaminated locations compared with uncontaminated control sites. For example, in October and December they contributed up to 19% of relative abundance at "Salamina Oil 1" (coef. = 18.31, $z = 19.21$, $p < 0.001$), sharply reducing thereafter.

Ten OTUs belonging to the genus *Marinobacter* (excluding sequences assigned to the OHCB species *M. hydrocarbonoclasticus*) (**Figures 5**, **6**), were significantly more relatively abundant in sediments taken in September from "Athens Oil 2 and 3" (30%; coef. = 27.94, $z = 43.21$, $p < 0.001$) relative to the uncontaminated sites, decreasing sharply from October. Similarly, five OTUs assigned to the genus *Idiomarina* (**Figures 5**, **6**) were also significantly greater in relative abundance (coef. = 13.88, $z = 23.40$, $p < 0.001$), at 14 and 28% from sediments in "Athens Oil 2 and 3," respectively, decreasing from October onward. OTU-45 assigned to the genus *Alteromonas* and OTU-76 assigned to the genus *Vibrio* (**Figures 5**, **6**) significantly increased in relative abundance (coef. = 10.37, $z = 26.11$, $p < 0.001$), from uncontaminated control levels, particularly at contaminated "Athens Oil 1" to approximately 10 and 3% respectively, before sharply decreasing from October onward.

Two genera from the class Alphaproteobacteria also increased following oil contamination, which included five OTUs assigned the genus *Erythrobacter* and OTU-88 assigned to the species *Roseovarius* spp. (**Figures 5**, **6**), which were significantly higher in relative abundance at contaminated sites from September to April, relative to levels at the uncontaminated sites.

Five days after the oil spill in September there was a strong positive correlation ($R^2 = 0.80$, $p < 0.01$) between the relative abundance of 16S rRNA sequences assigned to hydrocarbon-degrading bacteria (all OTUs displayed in **Figure 6**) and the concentration of measured hydrocarbons. In addition, the EIHE, which quantifies the proportion of the bacterial community with hydrocarbon bioremediation potential on a scale of 0–1, whereby 1 represents 100% (Lozada et al., 2014), was calculated at 0.52 ± 0.14 in September. This EIHE result was significantly ($p < 0.05$) higher than the control site at 0.30 ± 0.11. At the genus level, some correlative relationships between bacterial genera containing hydrocarbon-degraders were observed. OTUs from the genera *Marinobacter* and *Idiomarina* typically co-occurred and were significantly correlated ($R^2 = 0.80$, $p < 0.05$). A difference in the bacterial community composition occurred at different contaminated sites, despite the presence of similar hydrocarbons. For example, at "Athens Oil 2 and 3," when *Marinobacter* and *Idiomarina* were in high relative abundance (collectively 46%) *Alteromonas*, *Oleibacter*, *Oleiphilus*, and *Thalassolituus* had low relative abundance of approximately 0.64%, collectively. In contrast, when *Marinobacter* and *Idiomarina* were in low relative abundance (collectively 4% at "Athens Oil 1" in September) *Alteromonas*, *Oleibacter*, *Oleiphilus*, and *Thalassolituus* had a relative abundance of approximately 16%, collectively, at the same site in September. The full correlation analysis showing the co-occurrence of taxa is provided in **Supplementary Figure S5**.

DISCUSSION

Sediment Hydrocarbon Concentrations and Clean-Up Operations

Five days after the oil spill, GC-MS analysis revealed extensive oil contamination in the surface sediments at multiple beaches

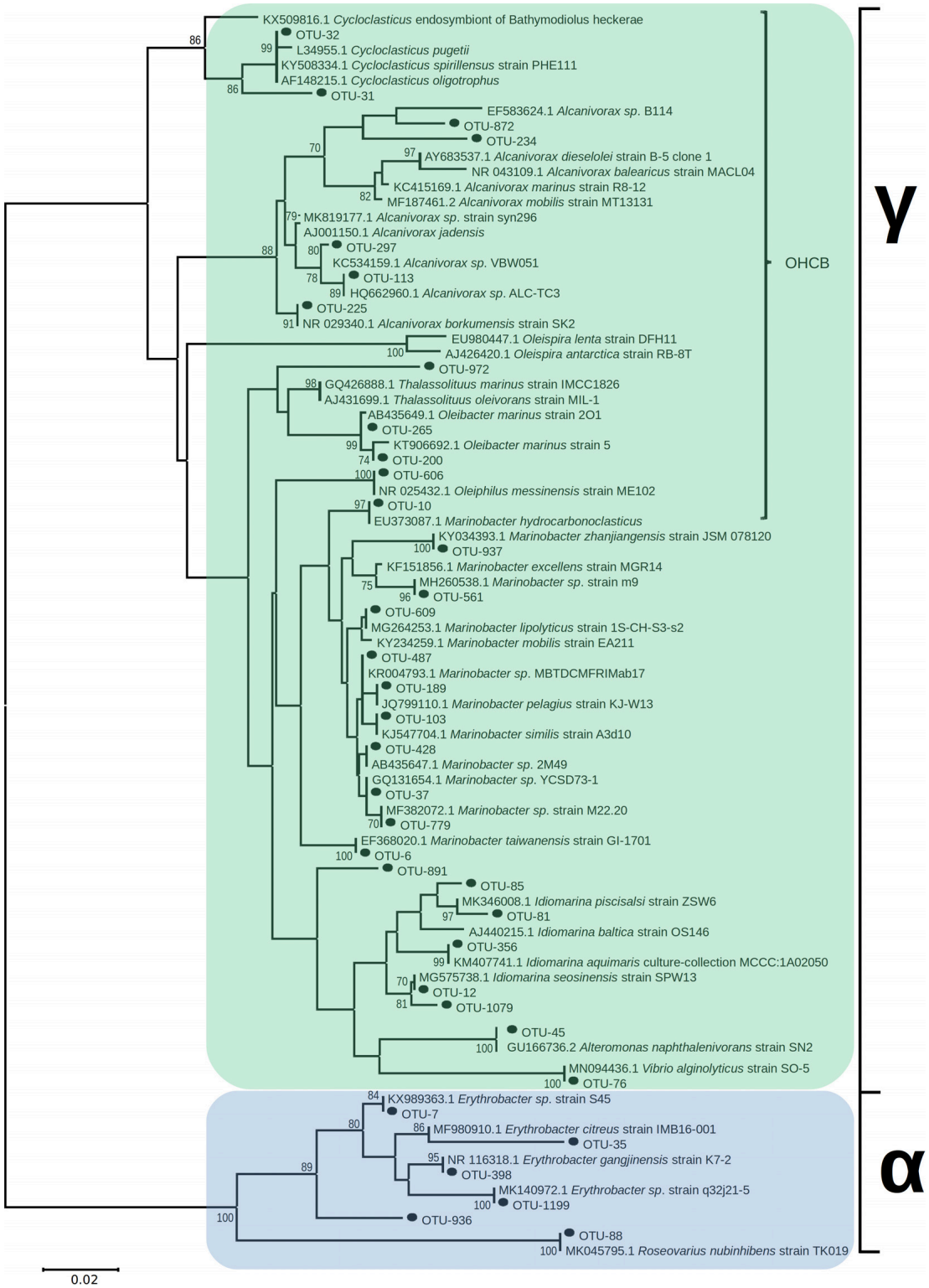

FIGURE 6 | Unrooted neighbor-joining phylogeny of 16S rRNA bacterial OTUs, in sediments from contaminated sites along the Athens Riviera and Salamina coastline, from September 2017 to April 2018, aligned with known hydrocarbon-degrading bacteria and closest relatives; bootstrap values >70 displayed (1,000 iterations). Evolutionary distances computed by Maximum Composite Likelihood protocol (using the Tamura-Nei model, Tamura and Nei, 1993), sum of branch length = 1.15. Analysis involved 82 nucleotide sequences (36 OTUs) with a total of 258 positions in the final dataset. Evolutionary analyses were conducted in MEGA7. Bacteria and archaea OTU tables are available in **Supplementary Tables S3**, **S4**.

along the Athens Riviera. This contamination occurred due to rapid transfer of the oil from the water onto the coastal sediments within the first few days of the spill, due to sustained prevailing winds (Parinos et al., 2019). The level of total measured hydrocarbons, 2,158 ± 800 $\mu g\ g^{-1}$ dry sediment, was similar to that observed from surface sediments in the Exxon Valdez oil-spill, 4,636 ± 1,628 $\mu g\ g^{-1}$ sediment (Bragg et al., 1994). However, Agia Zoni II hydrocarbon sediment concentrations were much lower than that observed in buried sediments in Pensacola Beach, Florida (11,000 $\mu g\ g^{-1}$ sediment total petroleum hydrocarbons) which was impacted by the Macondo oil spill (Huettel et al., 2018). Unbranched alkanes and PAHs from sediments after the Agia Zoni II oil spill were undetected from October 2017 onward; though some branched alkanes persisted at low concentrations (primarily at contaminated Salamina sites, Oct–Apr 7.31 ± 7.04 $\mu g\ g^{-1}$ sediment).

The near complete reduction of hydrocarbons to undetectable levels, from October 2017 onward, is in line with measurements taken by the Hellenic Centre for Marine Research (HCMR) (Parinos et al., 2019) and is indicative of efficient physical removal and other clean-up operations, which occurred immediately after the oil-spill incident and continued through to February 2018. The preferential removal of the more readily degradable linear *n*-alkanes, as indicated by the presence of branched alkanes and no measurable *n*-alkanes or PAHs from October 2017 onward, would suggest biodegradation was occurring. The extent to which the removal of hydrocarbons can be attributed to either biodegradation, natural processes, or remediation efforts cannot be determined from our data. However, hydrocarbon data from Parinos et al. (2019) suggested the early onset of biodegradation, which was sustained for 85 days post-oil-spill, especially amongst phenanthrenes.

While absorbents, flushing, and sediment washing were used, a large proportion of the clean-up operations at the study sites consisted of direct sediment removal (whether contaminated or not) (International Oil Pollution Compensation Funds, 2018). Though effective in the removal of oil (Dave and Ghaly, 2011), the bulk removal of coastal sediment can be environmentally damaging (Owens, 1972; Gundlach and Hayes, 1978; Petersen et al., 2002), and, has economic and environmental costs associated with disposal, often to landfill sites. In the case of Agia Zoni II, some sediment washing and replacement occurred, but these responses were not adopted to the same degree as removal, likely due to the need for a rapid clean up to minimize the economic impact from loss of tourism.

Ecology of Obligate Hydrocarbonoclastic Bacteria

An oil-spill perturbation is indicative of a discrete short term disturbance event (Shade et al., 2012), whereby changes in microbial community are largely trait driven, by the ability of individual species to occupy available niches due to hydrocarbon-degradation processes and pressures. This often manifests as a large increase in the absolute abundance of Bacteria, due to selection for hydrocarbon-degrading bacteria (Head et al., 2006), which was observed here with a ∼2.5-fold increase, but not significant, in the absolute abundance of the bacterial 16S rRNA gene immediately following the oil-spill. In particular, there was significantly greater relative abundance of genera with known hydrocarbon-degrading bacteria at contaminated sites in comparison to uncontaminated sites. These notable increases, along with a history of hydrocarbon pollution in the Saronic Gulf, indicates an indigenous community of hydrocarbon-degrading bacteria, albeit at mostly very low or undetectable levels, allowing for rapid colonization of oiled sediments and growth. Hydrocarbons within sediments five days after the oil spill supported the growth of OHCB, which rapidly became dominant, and were almost undetectable in uncontaminated sediments.

Alcanivorax is an obligate degrader of branched- and *n*-alkanes (Yakimov et al., 1998), although it has been shown to enhance degradation of PAHs (McKew et al., 2007). *Alcanivorax* is ubiquitous in the marine environment and is observed in a variety of hydrocarbon polluted environments (see **Supplementary Table S2**). In agreement with the results presented here, *Alcanivorax* is often observed to become abundant early on in coastal beach sediments and decrease in abundance as *n*-alkanes are removed from the environment (Head et al., 2006; Kostka et al., 2011; Rodriguez-R et al., 2015). *Alcanivorax* persisted for many months after hydrocarbons (unbranched alkanes and PAHs) were undetected within the environment. This legacy effect could be caused by several processes, including the use of wax esters (Rontani, 2010) or polyhydroxyalkanoates (Możejko-Ciesielska and Kiewisz, 2016) as a carbon and energy store for use when nutrient availability (e.g., N & P) is more favorable for cellular growth. Alternatively, this persistence could be due to the low levels of branched alkanes, such as pristane and phytane, observed within the sediments in the months following September. Unlike most OHCB, certain species of *Alcanivorax* can use branched alkanes, for example, *A. borkumensis* SK2T (Yakimov et al., 1998; Gregson et al., 2019), *A. dieselolei* B-5 (Liu et al., 2011), and *A. hongdengensis* A-11-3 (Wang and Shao, 2012).

Other alkane-degrading OHCB genera detected included *Oleibacter* (Teramoto et al., 2011), *Oleiphilus* (Golyshin et al., 2002), and *Thalassolituus* (Yakimov et al., 2004b; Gregson et al., 2018); though their abundance was primarily restricted to "Athens Oil 1" sediments. *Oleibacter*, *Oleiphilus*, and *Thalassolituus* have all been observed to increase in abundance in oil-contaminated marine environments, though until now evidence is lacking for detection in coastal sandy sediments (see **Supplementary Table S2**). Previous studies of oil-contaminated sediment (Coulon et al., 2012) and seawater (Teramoto et al., 2013) observed *Oleibacter* and *Alcanivorax* in similar abundances, in line with our observations. However, in seawater-based laboratory experiments *Thalassolituus* has been observed to outcompete other alkane-degraders such as *Alcanivorax* (McKew et al., 2007), through its use of medium- and long-chained alkanes (Gregson et al., 2019); this was not observed in the sediment samples collected from the Agia Zoni II oil-spill, whereby *Alcanivorax* was in greater abundance.

Cycloclasticus is a PAH-degrading genus (Dyksterhouse et al., 1995), apart from one lineage that degrades very short-chained

alkanes (symbiont of *Bathymodiolus*, undetected in this study; Rubin-Blum et al., 2017). *Cycloclasticus*, which has been observed to grow in many marine environments including sandy coastal sediments (see **Supplementary Table S2**), was mostly undetected in sediments from Athens, but was observed in high abundance from October through December in Salamina sediments (note that no Salamina samples were taken in September). As found with *Alcanivorax*, *Cycloclasticus* demonstrated an oil-legacy effect, persisting in the sediments for several months after PAH contamination was undetectable. Once again this could be due to carbon and energy storage, or the persistence of trace amounts of high molecular weight PAHs. Alternatively, hydrocarbons can be undetected through analytical methods such as GC-MS (McKenna et al., 2013) when weathered hydrocarbons from an oil spill undergo transformation into oxygenated hydrocarbons (though currently there is no evidence that *Cycloclasticus* is able to degrade oxygenated hydrocarbons) (Kiruri et al., 2013), which can persist for years within oil/sand aggregates (Aeppli et al., 2018).

Ecology of Metabolically Versatile Oil-Degrading Bacteria and Microbial Interactions

The specialist PAH degrader, *Cycloclasticus*, was mostly undetected in sediments collected in September from Athens, possibly because it was outcompeted by more metabolically versatile bacteria that can also degrade PAHs. Potential candidates for this PAH degradation are the genera *Idiomarina* [including OTUs most closely matched to PAH degraders *I. seosinensis* (Yuan et al., 2015; Gomes et al., 2018) (100% similarity) and *I. piscisalsi* (Nzila et al., 2018) (98.83% similarity)] and *Alteromonas* [including an OTU most closely matched to PAH degrading *A. naphthalenivorans* (Jin et al., 2011) (100% similarity)]. *Idiomarina* and *Alteromonas* can use a range of substrates for growth, including PAHs, and in this region (Athens) may have outcompeted *Cycloclasticus*, in contrast to the latter months in Salamina where *Cycloclasticus* dominated. Given the dominance of *Cycloclasticus* in October/December in Salamina, it could be speculated that this genus was also dominant in September, in contrast to Athens where more metabolically versatile bacteria became established. Alternatively, differences in the clean-up response may partly account for the observed differences in *Cycloclasticus* relative abundance, as, for example, the remediation process of sediment removal did not occur at "Salamina Oil 1 and 3" (see **Figure 1** and **Supplementary Table S1**), where an increased relative abundance of *Cycloclasticus* occurred. This is also the case for sediments from "Athens Oil 1" where the presence of *Cycloclasticus* was observed, but not in "Athens Oil 2 and 3" sediments.

Idiomarina and *Alteromonas* have been found in a range of oil-contaminated environments, including sandy coastal sediments (see **Supplementary Table S2**). In this study it was observed that while both these genera increased in abundance in contaminated sites compared to uncontaminated sites, they did not co-occur. *Idiomarina* did, however, positively correlate with the genus *Marinobacter*; including OTU-10 most closely related to *M. hydrocarbonoclasticus*, which has been shown to degrade a range of alkanes (Gauthier et al., 1992). The co-occurrence of *Idiomarina* and *Marinobacter* was most notable between sediments from "Athens Oil 1" and "Athens Oil 2 and 3" and was to the competitive exclusion of other genera with known oil-degrading bacteria, including: *Alteromonas*, *Erythrobacter*, *Oleibacter*, *Oleiphilus*, and *Roseovarius*, which co-occurred. *Alteromonas* and *Oleibacter* have been recorded previously to co-occur (Neethu et al., 2019). The dominance of *Idiomarina* and *Marinobacter*, at "Athens Oil 2 and 3," could potentially be due to indigenous species having a priority effect, providing a competitive advantage, or potentially due to source point pollution events. Alternatively, the absence of *M. hydrocarbonoclasticus* and *Idiomarina* from "Athens Oil 1" sediments could be due to the different remediation efforts at this site, where visible oil contamination was not as evident and thus only manual removal of tar balls occurred (see **Figure 1** and **Supplementary Table S1**). The positive relationship between *Marinobacter* and *Idiomarina* has been observed before, including in oil-sludge samples (Albokari et al., 2015) and in sandy coastal sediments from the Macondo oil-spill where these two genera dominated (Joye et al., 2014). Additionally, Joye et al. (2014) observed that *Alcanivorax* was able to co-occur with *Marinobacter* and *Idiomarina*, as also observed in sediments from this study.

This study also demonstrates the ability of *Vibrio* (which is a genus that contains species that can degrade alkanes (Al-Awadhi et al., 2012; Imron and Titah, 2018) and PAHs (Melcher et al., 2002) to grow in several oil-contaminated environments; see **Supplementary Table S2**) to also avoid competitive-exclusion by *Marinobacter* and *Idiomarina*. This finding could indicate the ability of certain *Vibrio* to degrade a wide range of hydrocarbons, potentially including branched alkanes, like *Alcanivorax*, which may indicate why these genera are unaffected by the prevailing dominance of *Marinobacter* and *Idiomarina*. Indeed, certain species of *Vibrio* are known to attach to algal cells (Kumazawa et al., 1991; Hood and Winter, 1997) and many algae are known to produce branched alkanes (Binark et al., 2000) so perhaps there is a phototrophic–heterotroph interaction (McGenity et al., 2012) through the utilization of branched alkanes by *Vibrio*. However, increased relative abundance in *Vibrio* spp. was not matched with increased branched alkane concentration in Salamina, and therefore this remains unverified. This co-occurrence could also occur due to *Vibrio* using PAHs.

Lastly, species within the genera *Erythrobacter* and *Roseovarius* can degrade a range of hydrocarbons and grow in oil-contaminated marine environments, including sandy coastal sediments (see **Supplementary Table S2**). *Erythrobacter* and *Roseovarius* maintained consistently higher abundances at the previously oiled sites in comparison to uncontaminated sites. Suggesting that once the genera have established a presence within the community, through the utilization of hydrocarbons, they are able to maintain this even in the absence of such carbon and energy sources.

Are Archaea Affected by Oil-Contamination Within Coastal Sediments?

In agreement with many studies, archaeal abundance and diversity was mostly unaffected in the sediment samples taken from after the Agia Zoni II oil-spill (Redmond and Valentine, 2012; Urakawa et al., 2012; King et al., 2015; Sanni et al., 2015). Archaea are not commonly considered as hydrocarbon-degraders, apart from certain *Halobacteria* (McGenity, 2010; Oren, 2017) which typically do not prevail in coastal seawater (exception herein being the genera *Haladaptatus* and *Halogranum*). There is growing evidence that growth of nitrifying-archaea, especially from the genus *Nitrosopumilus*, is inhibited by crude oil (Urakawa et al., 2012, 2019), though some studies do not show any significant inhibition by oil on archaeal populations (Newell et al., 2014; Bernhard et al., 2016). In this study, while there were some between-site differences in the relative abundance of OTUs assigned to *Nitrosopumilus* these were not significantly different. By quantifying archaeal species which are sensitive to oil-spill disturbances, post-oil-spill monitoring models can be made more efficient by including them as sentinel species (Kirby et al., 2018).

Post-Oil-Spill Monitoring of Microbial Communities

The ability of those responding to an oil-spill (oil-spill responders, Government bodies, local authorities, oil-industries, NGOs) to evaluate the efficiency of clean-up operations, and thus provide guidance on future risk-based scenarios, is a vital endeavor to protect the environment and reduce socioeconomic impact. This has been recognized across the globe, and in the United Kingdom the cross-government initiative "PREMIAM" was published to this accord (Kirby et al., 2018). Understanding how microbes respond to such perturbations can assist to this regard and has the potential to be incorporated into tools such as the Spill Impact Mitigation Assessment (IPIECA and IOGP, 2017). Combining the data from both hydrocarbon analysis, microbial ecology, and other environmental sources, a more detailed and holistic understanding can be revealed. Microbial community analysis can highlight whether biodegradation may be taking place and the likelihood of the environment to naturally attenuate the oil-spill. Nutrient concentration analysis would reveal whether the environment is nutrient limited and should therefore be supplemented with fertilizer. Hydrocarbon analysis can detect the proportion of light and heavy molecules that could indicate the need for additional remediation operations.

Using microbial ecology as a post-oil-spill monitoring tool is still in its infancy, however, models and indices to assist in this effort are available. Lozada et al. (2014) published an "EIHE," whereby hydrocarbon contamination was assumed based on the relative abundance of genera known to contain hydrocarbon-degrading bacteria. The simplicity of this model is both a strength and a weakness. It is simple enough that it can easily be adapted as oil-spill microbial knowledge progresses, but it is too simple to fully establish hydrocarbon exposure. For example, in this study our uncontaminated control sites had an EIHE index of 0.30 ± 0.11 (on a scale of 0–1), despite no hydrocarbons being detected. This is due to the model including all species within functionally diverse bacterial genera such as *Pseudomonas* which includes >200 different species, of which only a small minority are known to degrade hydrocarbons. The EIHE could be improved further by analyzing microbial community composition at a finer detail, perhaps at a species level, though this would require a tool to phylogenetically match OTUs to known oil-degrading species. Additionally, the inclusion of sentinel microbes, those that are adversely affected by oil-contamination (i.e., ammonia-oxidizing archaea; Urakawa et al., 2012, 2019), would also add comprehension to the index. By advancing the knowledge of oil-spill microbial ecology, understanding the genetics and metabolic capabilities of all hydrocarbon-degrading bacteria and their microbial community interactions, and then combining this with hydrocarbon and environmental data, models such as the EIHE can be improved.

Experimental Procedures

Sampling Locations and Schedule

Sediments were surveyed at both the surface (0–5 cm) and deeper depths (down to approximately 60 cm) on initial and subsequent site visits. However, only surface sediments were observed to be oil contaminated, so all analyses were focused on this upper layer. Samples were collected, in triplicate, in sterile 50 ml sterile polypropylene containers from control (uncontaminated) and contaminated (oil contaminated) sites along the Athens Riviera and Salamina Island coast, Greece (see **Figure 1** and **Supplementary Table S1**). Sediments were randomly sampled (n = 3) across the distance of each beach. Additionally, coastal seawater samples were collected (we were unable to obtain seawater samples from Athens or Salamina for September 2017) for nutrient analysis [ammonium (NH_4^+), phosphate (PO_4^{3-}), silicate (SiO_2^-), nitrate (NO_3^-), and nitrite (NO_2^-)] using a SEAL Analytical AA3 HR AutoAnalyzer tandem JASCO FP-2020 Plus fluorescence detector. Samples were collected in September 2017 5 days after the oil-spill, when oiling of sediment was visible, at the Athens sites. However, we were unable to obtain sediment samples from all Salamina site for September 2017. Thereafter, samples were collected over a 7-month period (except for October when no samples for "Salamina No Oil" were collected and November when no samples for all site were collected). Samples were immediately frozen on collection and stored at −20°C.

Hydrocarbon Degradation (GC-MS)

Hydrocarbons were extracted from thawed sediments. Samples (2 g) were dried with 2 g of anhydrous sodium (Na_2SO_4). Dried samples were extracted with 12 ml of hexane:dichloromethane (50:50) in 20 ml vials with Teflon-lined screw caps by horizontal shaking at 150 oscillations per min over 16 h and finally sonicated for 30 min at 20°C. After centrifugation 12,000 × g for 5 min, extracts were cleaned on Florisil[§] columns by elution with hexane. Extracts were transferred in conical tubes and evaporated to 0.7 ml over an ice bath to minimize loss of light PAHs. Deuterated alkanes (nonadecane $C_{19}d_{40}$ and triacontane $C_{30}d_{62}$ at 10 μg ml^{-1}) and PAH (naphthalene-d_8

and anthrancene-d_{10} at 10 $\mu g\ ml^{-1}$) internal standards were added to each sample and quantification was performed on an Agilent 7890A Gas Chromatography system coupled with a Turbomass Gold Mass Spectrometer with Triple-Axis detector, operating at 70 eV in positive ion mode, using conditions as previously described by Coulon et al. (2007). External multilevel calibrations were carried out using alkanes [Standard Solution (C_8–C_{40}); Sigma], methylated-PAHs (1-methylnapthalene, 2-methylanthracene, and 9,10-dimethylanthracene; Sigma), and PAH (QTM PAH Mix; Sigma) standards, the concentrations of which ranged from 1.125 to 18 $\mu g\ ml^{-1}$. For quality control, a calibration standard (10 $\mu g\ ml^{-1}$) and a blank were analyed every 10 samples. We quantified alkanes between C_{10} and C_{36} including pristane and phytane and the following PAHs: naphthalene; all isomers of methyl-, dimethyl- and trimethyl-naphthalenes; acenaphthylene; acenaphthene; fluorene; phenanthrene; all isomers of methyl- and dimethyl-phenanthrenes/anthracenes; fluoranthene; pyrene; all isomers of methyl- and dimethyl-pyrene; chrysene; all isomers of methyl- and dimethyl-chrysene. Only those hydrocarbons detected are shown in **Figure 3**.

qPCR Analysis of Bacterial and Archaeal 16S rRNA Genes

DNA was extracted from 0.25 g of thawed sediment samples with a DNeasy PowerSoil Kit (Qiagen), according to the manufacturer's instructions. The primers used for quantification of archaeal 16S rRNA gene were 344f – ACGGGGYGCAGCAGGCGCGA (Raskin et al., 1994) and 915r – GTGCTCCCCCGCCAATTCCT (Stahl and Amann, 1991), and for bacterial 16S rRNA gene, 341f – CCTACGGGNGGCWGCAG, and 785r – GACTACHVGGGTATCTAATCC (Klindworth et al., 2013) were used. These primers have been successfully used to quantify archaeal (Huby et al., 2020) and bacterial (Clark et al., 2020) 16S rRNA gene abundances in environmental samples previously. Furthermore, inspection of standard curves showed that all assays produced satisfactory efficiency (85%) and R^2 values (>0.99). All qPCR reactions were performed using a CFX384^{TM} Real-Time PCR Detection System (BioRad) using reagents, cycle conditions, and standards as previously described (McKew and Smith, 2015; Tatti et al., 2016).

Amplicon Sequencing and Bioinformatics

Amplicon libraries were prepared, as per Illumina instructions, by a 25-cycle (bacteria) and 31-cycle (archaea) PCR. PCR primers were the same as those used for qPCR but flanked with Illumina Nextera overhang sequences. A unique combination of Nextera XT Indices (Illumina) were added to PCR products from each sample, via an eight-cycle PCR. PCR products were quantified using PicoGreen and pooled in equimolar concentrations. Quantification of the amplicon libraries was determined via NEBNext® Library Quant Kit for Illumina (New England BioLabs Inc.), prior to sequencing on the Illumina MiSeq® platform, using a MiSeq® 600 cycle v3 reagent kit and 20% PhiX sequencing control standard. Raw sequence data have been submitted to the European Nucleotide Archive database under accession number PRJEB33987. Sequence output from the Illumina MiSeq platform were analyzed within BioLinux (Field et al., 2006), using a bioinformatics pipeline as described by Dumbrell et al. (2016). Forward sequence reads were quality trimmed using Sickle (Joshi and Fass, 2011) prior to error correction within Spades (Nurk et al., 2013) using the BayesHammer algorithm (Nikolenko et al., 2013). The quality filter and error corrected sequence reads were dereplicated, sorted by abundance, and clustered into OTUs at the 97% sequence identity level via VSEARCH (Rognes et al., 2016). Singleton OTUs were discarded, as well as chimeras using reference based chimera checking with UCHIME (Edgar et al., 2011). Lastly, taxonomic assignment was conducted with the Ribosomal Database Project (RDP) classifier (Wang et al., 2007). Non-locus-specific, or artifactual, OTUs were discarded prior to statistical analyses, along with any OTUs that had <70% identity with any sequence in the RDP database.

Phylogenetic Analysis

The neighbor-joining protocol (Nei and Saitou, 1987) was used to infer the evolutionary history of partial 16S rRNA gene sequence Bacterial OTUs, aligned with known hydrocarbon-degrading bacteria and closest neighboring accessions using MUSCLE (Edgar, 2004). Bootstrapping analysis (1,000 iterations) was conducted to determine the percentage of time associated taxa clustered together in replicate trees (Felsenstein, 1985); only bootstrap values >70% are shown. Evolutionary distances, units in the number of base substitutions per site, were calculated with the use of Maximum Composite Likelihood protocol (Hanson and McElroy, 2015). Phylogenetic analyses were conducted in MEGA7.

Statistical Analysis

Prior to community analysis, sequence data were rarefied to the lowest library sequence value (8,093). Data were first tested for normality (Shapiro–Wilks test), those data which were normally distributed were tested for significance with ANOVAs or appropriate linear models. Non-normally distributed data were analyzed using appropriate GLMs (Generalized Linear Models) as follows. The relative abundance of OTUs or genera in relation to oil exposure, site, and sample month were modeled using multivariate negative binomial GLMs (Wang et al., 2010). Here, the number of sequences in each library was accounted for using an offset term, as described previously (Alzarhani et al., 2019). The abundance of archaeal and bacterial 16S rRNA gene copies was also modeled using negative binomial GLMs (Venables and Ripley, 2002). The significance of model terms was assessed via likelihood ratio tests. The EIHE (Lozada et al., 2014) was calculated using the script available at the ecolFudge GitHub page[1] (Clark, 2019) and EIHE values modeled using Poisson GLMs. Correlations were performed using the Pearson's correlation with an alpha of 0.05. All statistical analyses were carried out in R3.6.1

[1]https://github.com/Dave-Clark/ecolFudge

(R Development Core Team, 2011) using a variety of packages available through the references (Venables and Ripley, 2002; Becker et al., 2016; Auguie, 2017; Lenth, 2020). All plots were constructed using the (Wickham, 2010) and "patchwork" (Pedersen, 2019) R packages.

DATA AVAILABILITY STATEMENT

The datasets generated for this study can be found in the European Nucleotide Archive under accession number PRJEB33987.

AUTHOR CONTRIBUTIONS

GT, CW, TC, and BM carried out the sampling campaign. AM provided the country logistics and sampling support. GT and BG performed the molecular work. GT, PC, and FC performed the analytical chemistry. GT, BM, and DC performed the data and statistical analysis. GT wrote the manuscript, supplementary information, and produced all figures and tables. All authors reviewed the manuscript, supplementary information, figures, and tables. BM, TM, CW, TC, LH, and AM secured the funding. All authors contributed to the article and approved the submitted version.

FUNDING

We would like to acknowledge and thank the National Environmental Research Council (NERC) for primary funding of this work (NE/R016569/1). Additionally, we thank NERC EnvEast (NE/L002582/1) for funding of this work. DC was supported by NERC funding while contributing to this work (NE/P011624/1). BM also acknowledges funding from the Eastern Academic Research Consortium.

ACKNOWLEDGMENTS

We acknowledge Thodoris Tsimpidis and volunteers at Archipelagos Institute of Marine Conservation (Samos, Greece), for their support during sample collection. We acknowledge ITOPF for providing technical information regarding clean-up operations. Additionally, we acknowledge John Green, Tania Cresswell-Maynard, and Ben Archer from the University of Essex for providing technical and sampling support.

SUPPLEMENTARY MATERIAL

The Supplementary Material for this article can be found online at: https://www.frontiersin.org/articles/10.3389/fmicb.2020.01706/full#supplementary-material

REFERENCES

Acosta-González, A., Martirani-von Abercron, S. M., Rosselló-Móra, R., Wittich, R. M., and Marqués, S. (2015). The effect of oil spills on the bacterial diversity and catabolic function in coastal sediments: a case study on the Prestige oil spill. *Environ. Sci. Pollut. Res.* 22, 15200–15214. doi: 10.1007/s11356-015-4458-y

Aeppli, C., Swarthout, R. F., O'Neil, G. W., Katz, S. D., Nabi, D., Ward, C. P., et al. (2018). How persistent and bioavailable are oxygenated deepwater horizon oil transformation products? *Environ. Sci. Technol.* 52, 7250–7258. doi: 10.1021/acs.est.8b01001

Al-Awadhi, H., Dashti, N., Kansour, M., Sorkhoh, N., and Radwan, S. (2012). Hydrocarbon-utilizing bacteria associated with biofouling materials from offshore waters of the Arabian Gulf. *Int. Biodeterior. Biodegrad.* 69, 10–16. doi: 10.1016/j.ibiod.2011.12.008

Albokari, M., Mashhour, I., Alshehri, M., Boothman, C., and Al-Enezi, M. (2015). Characterization of microbial communities in heavy crude oil from Saudi Arabia. *Ann. Microbiol.* 65, 95–104. doi: 10.1007/s13213-014-0840-0

Almeida, C. M. R., Reis, I., Couto, M. N., Bordalo, A. A., and Mucha, A. P. (2013). Potential of the microbial community present in an unimpacted beach sediment to remediate petroleum hydrocarbons. *Environ. Sci. Pollut. Res.* 20, 3176–3184. doi: 10.1007/s11356-012-1240-2

Alzarhani, A. K., Clark, D. R., Underwood, G. J. C., Ford, H., Cotton, T. E. A., and Dumbrell, A. J. (2019). Are drivers of root-associated fungal community structure context specific? *ISME J.* 13, 1330–1344. doi: 10.1038/s41396-019-0350-y

Atlas, R. M., and Hazen, T. C. (2011). Oil biodegradation and bioremediation: a tale of the two worst spills in U.S. history. *Environ. Sci. Technol.* 45, 6709–6715. doi: 10.1021/es2013227

Auguie, B. (2017). *gridExtra: Functions in Grid Graphics. R Package Version 2.3*. Available online at: https://cran.r-project.org/web/packages/gridExtra/index.html (accessed September 9, 2017).

Beazley, M. J., Martinez, R. J., Rajan, S., Powell, J., Piceno, Y. M., Tom, L. M., et al. (2012). Microbial community analysis of a coastal salt marsh affected by the Deepwater Horizon oil spill. *PLoS One* 7:e41305. doi: 10.1371/journal.pone.0041305

Becker, R. A., Wilks, A. R., Brownrigg, R., Minka, T. P., and Deckmyn, A. (2016). *Package "maps": Draw Geographical Maps. R Packag. version 2.3-6*. Available online at: https://cran.r-project.org/web/packages/maps/maps.pdf (accessed April 3, 2018).

Bernhard, A. E., Sheffer, R., Giblin, A. E., Marton, J. M., and Roberts, B. J. (2016). Population dynamics and community composition of ammonia oxidizers in salt marshes after the Deepwater Horizon oil spill. *Front. Microbiol.* 7:854. doi: 10.3389/fmicb.2016.00854

Binark, N., Güven, K. C., Gezgin, T., and Ünlü, S. (2000). Oil pollution of marine algae. *Bull. Environ. Contam. Toxicol.* 64, 866–872. doi: 10.1007/s0012800083

Boufadel, M. C., Sharifi, Y., Van Aken, B., Wrenn, B. A., and Lee, K. (2010). Nutrient and oxygen concentrations within the sediments of an Alaskan beach polluted with the Exxon Valdez oil spill. *Environ. Sci. Technol.* 44, 7418–7424. doi: 10.1021/es102046n

Bragg, J. R., Prince, R. C., Harner, E. J., and Atlas, R. M. (1994). Effectiveness of bioremediation for the Exxon Valdez oil spill. *Nature* 368, 413–418. doi: 10.1038/368413a0

Clark, D. R. (2019). *ecolFudge*. Available online at: https://github.com/Dave-Clark/ecolFudge (accessed October 1, 2019).

Clark, D. R., McKew, B. A., Dong, L. F., Leung, G., Dumbrell, A. J., Stott, A., et al. (2020). Mineralization and nitrification: archaea dominate ammonia-oxidising communities in grassland soils. *Soil Biol. Biochem.* 143, 107725. doi: 10.1016/j.soilbio.2020.107725

Coulon, F., Chronopoulou, P. M., Fahy, A., Païssé, S., Goñi-Urriza, M., Peperzak, L., et al. (2012). Central role of dynamic tidal biofilms dominated by aerobic hydrocarbonoclastic bacteria and diatoms in the biodegradation of hydrocarbons in coastal mudflats. *Appl. Environ. Microbiol.* 78, 3638–3648. doi: 10.1128/AEM.00072-12

Coulon, F., McKew, B. A., Osborn, A. M., McGenity, T. J., and Timmis, K. N. (2007). Effects of temperature and biostimulation on oil-degrading microbial communities in temperate estuarine waters. *Environ. Microbiol.* 9, 177–186. doi: 10.1111/j.1462-2920.2006.01126.x

Da Silva, A. C., De Oliveira, F. J. S., Bernardes, D. S., and De França, F. P. (2009). Bioremediation of marine sediments impacted by petroleum. *Appl. Biochem. Biotechnol.* 153, 58–66. doi: 10.1007/s12010-008-8457-z

Dave, D., and Ghaly, A. E. (2011). Remediation technologies for marine oil spills: a critical review and comparative analysis. *Am. J. Environ. Sci.* 7, 424–440. doi: 10.3844/ajessp.2011.424.440

De La Huz, R., Lastra, M., Junoy, J., Castellanos, C., and Viéitez, J. M. (2005). Biological impacts of oil pollution and cleaning in the intertidal zone of exposed sandy beaches: preliminary study of the "prestige" oil spill. *Estuar. Coast. Shelf Sci.* 65, 19–29. doi: 10.1016/j.ecss.2005.03.024

Dumbrell, A. J., Ferguson, R. M. W., and Clark, D. R. (2016). "Microbial community analysis by single-amplicon high-throughput next generation sequencing: data analysis – from raw output to ecology," in *Hydrocarbon and Lipid Microbiology Protocols*, eds T. J. McGenity, K. N. Timmis, and B. Nogales, (Berlin: Springer Protocols Handbooks), 155–206. doi: 10.1007/8623_2016_228

Dyksterhouse, S. E., Gray, J. P., Herwig, R. P., Lara, J. C., and Staley, J. T. (1995). *Cycloclasticus pugetti* gen. nov., sp. nov., an aromatic hydrocarbon-degrading bacterium from marine sediments. *Int. J. Syst. Bacteriol.* 45, 116–123. doi: 10.1099/00207713-45-1-116

Edgar, R. C. (2004). MUSCLE: multiple sequence alignment with high accuracy and high throughput. *Nucleic Acids Res.* 32, 1792–1797. doi: 10.1093/nar/gkh340

Edgar, R. C., Haas, B. J., Clemente, J. C., Quince, C., and Knight, R. (2011). UCHIME improves sensitivity and speed of chimera detection. *Bioinformatics* 27, 2194–2200. doi: 10.1093/bioinformatics/btr381

Felsenstein, J. (1985). Confidence limits on phylogenies: an approach using the bootstrap. *Evolution* 39, 783–791. doi: 10.2307/2408678

Field, D., Houten, S., Thurston, M., Swan, D., Tiwari, B., Booth, T., et al. (2006). Open software for biologists: from famine to feast. *Nat. Biotechnol.* 24, 801–803. doi: 10.1038/nbt0706-801

Gauthier, M. J., Lafay, B., Christen, R., Fernandez, L., Acquaviva, M., Bonin, P., et al. (1992). *Marinobacter hydrocarbonoclasticus* gen. nov., sp. nov., a New, Extremely halotolerant, hydrocarbon-degrading marine bacterium. *Int. J. Syst. Bacteriol.* 42, 568–576. doi: 10.1099/00207713-42-4-568

Girin, M., and Carpenter, A. (2019). "Shipping and oil transportation in the mediterranean sea," in *Pollution in the Mediterranean Sea: Part I - The International Context*, eds A. Carpenter, and A. G. Kostianoy, (Berlin: Springer International Publishing). doi: 10.1007/698_2017_6

Golyshin, P. N., Chernikova, T. N., Abraham, W. R., Lünsdorf, H., Timmis, K. N., and Yakimov, M. M. (2002). Oleiphilaceae fam. nov., to include *Oleiphilus messinensis* gen. nov., sp. nov., a novel marine bacterium that obligately utilizes hydrocarbons. *Int. J. Syst. Evol. Microbiol.* 52, 901–911. doi: 10.1099/ijs.0.01890-0

Gomes, M. B., Gonzales-Limache, E. E., Sousa, S. T. P., Dellagnezze, B. M., Sartoratto, A., Silva, L. C. F., et al. (2018). Exploring the potential of halophilic bacteria from oil terminal environments for biosurfactant production and hydrocarbon degradation under high-salinity conditions. *Int. Biodeterior. Biodegrad.* 126, 231–242. doi: 10.1016/j.ibiod.2016.08.014

Gregson, B. H., Metodieva, G., Metodiev, M. V., Golyshin, P. N., and McKew, B. A. (2018). Differential protein expression during growth on medium versus long-chain alkanes in the obligate marine hydrocarbon-degrading bacterium *Thalassolituus oleivorans* MIL-1. *Front. Microbiol.* 9:3130. doi: 10.3389/fmicb.2018.03130

Gregson, B. H., Metodieva, G., Metodiev, M. V., and McKew, B. A. (2019). Differential protein expression during growth on linear versus branched alkanes in the obligate marine hydrocarbon-degrading bacterium *Alcanivorax borkumensis* SK2T. *Environ. Microbiol.* 21, 2347–2359. doi: 10.1111/1462-2920.14620

Gundlach, E. R., and Hayes, M. O. (1978). Vulnerability of coastal environments to oil spill impacts. *Mar. Technol. Soc. J.* 12, 18–27.

Hanson, K. M., and McElroy, E. J. (2015). Anthropogenic impacts and long-term changes in herpetofaunal diversity and community composition on a barrier island in the Southeastern United States. *Herpetol. Conserv. Biol.* 10, 765–780. doi: 10.1073/pnas.0404206101

Hazen, T. C., Dubinsky, E. A., DeSantis, T. Z., Andersen, G. L., Piceno, Y. M., Singh, N., et al. (2010). Deep-sea oil plume enriches indigenous oil-degrading bacteria. *Science* 330, 204–208. doi: 10.1126/science.1195979

Head, I. M., Jones, D. M., and Röling, W. F. M. (2006). Marine microorganisms make a meal of oil. *Nat. Rev. Microbiol.* 4, 173–182. doi: 10.1038/nrmicro1348

Hood, M. A., and Winter, P. A. (1997). Attachment of *Vibrio cholerae* under various environmental conditions and to selected substrates. *FEMS Microbiol. Ecol.* 22, 215–223. doi: 10.1016/S0168-6496(96)00092-X

Huby, T. J. C., Clark, D. R., McKew, B. A., and McGenity, T. J. (2020). Extremely halophilic archaeal communities are resilient to short-term entombment in halite. *Environ. Microbiol.* doi: 10.1111/1462-2920.14913

Huettel, M., Overholt, W. A., Kostka, J. E., Hagan, C., Kaba, J., Wells, W. B., et al. (2018). Degradation of Deepwater Horizon oil buried in a Florida beach influenced by tidal pumping. *Mar. Pollut. Bull.* 126, 488–500. doi: 10.1016/j.marpolbul.2017.10.061

Imron, M. F., and Titah, H. S. (2018). Optimization of diesel biodegradation by vibrio alginolyticus using Box-Behnken design. *Environ. Eng. Res.* 23, 374–382. doi: 10.4491/eer.2018.015

International Oil Pollution Compensation Funds, (2018). *Agia Zoni II*. Available online at: https://www.iopcfunds.org/incidents/incident-map#1740-09-September-2017 (accessed September 9, 2017).

IOPC, (2017). *Incident Report: Agia Zoni II. 1–5*. Available online at: https://documentservices.iopcfunds.org/wp-content/uploads/sites/2/2019/10/IOPC-OCT19-3-11_e.pdf (accessed September 17, 2018).

IPIECA, and IOGP, (2017). *Guidelines on Implementing Spill Impact Mitigation Assessment, SIMA. IPIECA/IOGP Oil Spill Response JIP*. Available online at: http://www.ipieca.org/resources/ (accessed May 28, 2020).

ITOPF, (2019). *Oil Tanker Spill Statistics 2018*. London: ITOPF.

Jin, H. M., Jeong, H., Moon, E. J., Math, R. K., Lee, K., Kim, H. J., et al. (2011). Complete genome sequence of the polycyclic aromatic hydrocarbon-degrading bacterium *Alteromonas* sp. strain SN2. *J. Bacteriol.* 193, 4292–4293. doi: 10.1128/JB.05252-11

Joshi, N. A., and Fass, J. N. (2011). *Sickle: A Sliding-Window, Adaptive, Quality-Based Trimming Tool for FastQ files (Version 1.33)*. Available online at: https://github.com/najoshi/sickle.

Joye, S. B., Teske, A. P., and Kostka, J. E. (2014). Microbial dynamics following the macondo oil well blowout across gulf of Mexico environments. *Bioscience* 64, 766–777. doi: 10.1093/biosci/biu121

King, G. M., Kostka, J. E., Hazen, T. C., and Sobecky, P. A. (2015). Microbial responses to the deepwater horizon oil spill: from coastal wetlands to the deep sea. *Ann. Rev. Mar. Sci.* 7, 377–401. doi: 10.1146/annurev-marine-010814-015543

Kirby, M. F., Brant, J., Moore, J., and Lincoln, S. (2018). *PREMIAM – Pollution Response in Emergencies – Marine Impact Assessment and Monitoring: Post-incident monitoring guidelines. Secone Edition. Science Series Technical Report. Lowestoft*. Available online at: https://www.cefas.co.uk/premiam/guidelines/ (accessed May 28, 2020).

Kiruri, L. W., Dellinger, B., and Lomnicki, S. (2013). Tar balls from deep water horizon oil spill: environmentally persistent free radicals (EPFR) formation during crude weathering. *Environ. Sci. Technol.* 47, 4220–4226. doi: 10.1021/es305157w

Klindworth, A., Pruesse, E., Schweer, T., Peplies, J., Quast, C., Horn, M., et al. (2013). Evaluation of general 16S ribosomal RNA gene PCR primers for classical and next-generation sequencing-based diversity studies. *Nucleic Acids Res.* 41, 1–11. doi: 10.1093/nar/gks808

Kostka, J. E., Prakash, O., Overholt, W. A., Green, S. J., Freyer, G., Canion, A., et al. (2011). Hydrocarbon-degrading bacteria and the bacterial community response in Gulf of Mexico beach sands impacted by the deepwater horizon oil spill. *Appl. Environ. Microbiol.* 77, 7962–7974. doi: 10.1128/AEM.05402-11

Kumazawa, N. H., Fukuma, N., and Komoda, Y. (1991). Attachment of *Vibrio parahaemolyticus* strains to Estuarine Algae. *J. Vet. Med. Sci.* 53, 201–205. doi: 10.1292/jvms.53.201

Lamendella, R., Strutt, S., Borglin, S., Chakraborty, R., Tas, N., Mason, O. U., et al. (2014). Assessment of the deepwater horizon oil spill impact on gulf coast microbial communities. *Front. Microbiol.* 5:130. doi: 10.3389/fmicb.2014.00130

Leahy, J. G., and Colwell, R. R. (1990). Microbial degradation of hydrocarbons in the environment. *Microbiol. Rev.* 54, 305–315. doi: 10.1128/mmbr.54.3.305-315.1990

Lenth, R. (2020) *emmeans: Estimated Marginal Means, aka Least-Squares Means. R package version 1.4.7*. Available online at: https://CRANR-project.org/package=emmeans

Liu, C., Wang, W., Wu, Y., Zhou, Z., Lai, Q., and Shao, Z. (2011). Multiple alkane hydroxylase systems in a marine alkane degrader, *Alcanivorax dieselolei* B-5. *Environ. Microbiol.* 13, 1168–1178. doi: 10.1111/j.1462-2920.2010.02416.x

Lozada, M., Marcos, M. S., Commendatore, M. G., Gil, M. N., and Dionisi, H. M. (2014). The bacterial community structure of hydrocarbon-polluted marine environments as the basis for the definition of an ecological index of hydrocarbon exposure. *Microbes Environ.* 29, 269–276. doi: 10.1264/jsme2.me14028

Mason, O. U., Hazen, T. C., Borglin, S., Chain, P. S. G., Dubinsky, E. A., Fortney, J. L., et al. (2012). Metagenome, metatranscriptome and single-cell sequencing reveal microbial response to Deepwater Horizon oil spill. *ISME J.* 6, 1715–1727. doi: 10.1038/ismej.2012.59

Mason, O. U., Scott, N. M., Gonzalez, A., Robbins-Pianka, A., Bælum, J., Kimbrel, J., et al. (2014). Metagenomics reveals sediment microbial community response to Deepwater Horizon oil spill. *ISME J.* 8, 1464–1475. doi: 10.1038/ismej.2013.254

McGenity, T. J. (2010). "Halophilic hydrocarbon degraders," in *Handbook of Hydrocarbon and Lipid Microbiology*, ed. K. N. Timmis, (Berlin: Springer). doi: 10.1007/978-3-540-77587-4_142

McGenity, T. J., Folwell, B. D., McKew, B. A., and Sanni, G. O. (2012). Marine crude-oil biodegradation: a central role for interspecies interactions. *Aquat. Biosyst.* 8, 1–19. doi: 10.1186/2046-9063-8-10

McKenna, A. M., Nelson, R. K., Reddy, C. M., Savory, J. J., Kaiser, N. K., Fitzsimmons, J. E., et al. (2013). Expansion of the analytical window for oil spill characterization by ultrahigh resolution mass spectrometry: beyond gas chromatography. *Environ. Sci. Technol.* 47, 7530–7539. doi: 10.1021/es305284t

McKew, B. A., Coulon, F., Yakimov, M. M., Denaro, R., Genovese, M., Smith, C. J., et al. (2007). Efficacy of intervention strategies for bioremediation of crude oil in marine systems and effects on indigenous hydrocarbonoclastic bacteria. *Environ. Microbiol.* 9, 1562–1571. doi: 10.1111/j.1462-2920.2007.01277.x

McKew, B. A., and Smith, C. J. (2015). "Real-time PCR approaches for analysis of hydrocarbon-degrading bacterial communities," in *Hydrocarbon and Lipid Microbiology Protocols*, eds T. J. McGenity, K. N. Timmis, and B. N. Fernandez, (Berlin: Springer Protocols Handbooks). doi: 10.1007/8623_2015_64

Melcher, R. J., Apitz, S. E., and Hemmingsen, B. B. (2002). Impact of irradiation and polycyclic aromatic hydrocarbon spiking on microbial populations in marine sediment for future aging and biodegradability studies. *Appl. Environ. Microbiol.* 68, 2858–2868. doi: 10.1128/AEM.68.6.2858-2868.2002

Możejko-Ciesielska, J., and Kiewisz, R. (2016). Bacterial polyhydroxyalkanoates: still fabulous? *Microbiol. Res.* 192, 271–282. doi: 10.1016/j.micres.2016.07.010

Neethu, C. S., Saravanakumar, C., Purvaja, R., Robin, R. S., and Ramesh, R. (2019). Oil-spill triggered shift in indigenous microbial structure and functional dynamics in different marine environmental matrices. *Sci. Rep.* 9:1354. doi: 10.1038/s41598-018-37903-x

Nei, M., and Saitou, N. (1987). The neighbor-joining method: a new method for reconstructing phylogenetic trees. *Mol. Biol. Evol.* 4, 406–425.

Newell, S. E., Eveillard, D., Mccarthy, M. J., Gardner, W. S., Liu, Z., and Ward, B. B. (2014). A shift in the archaeal nitrifier community in response to natural and anthropogenic disturbances in the northern Gulf of Mexico. *Environ. Microbiol. Rep.* 6, 106–112. doi: 10.1111/1758-2229.12114

Nikolenko, S. I., Korobeynikov, A. I., and Alekseyev, M. A. (2013). BayesHammer: bayesian clustering for error correction in single-cell sequencing. *BMC Genomics* 14:S7. doi: 10.1186/1471-2164-14-S1-S7

Nogales, B., and Bosch, R. (2019). "Microbial communities in hydrocarbon-polluted harbors and marinas," in *Microbial Communities Utilizing Hydrocarbons and Lipids: Members, Metagenomics and Ecophysiology*, ed. T. McGenity, (Cham: Springer). doi: 10.1007/978-3-319-60063-5_18-1

Nurk, S., Bankevich, A., Antipov, D., Gurevich, A., Korobeynikov, A., Lapidus, A., et al. (2013). "Assembling genomes and mini-metagenomes from highly chimeric reads," in *Lecture Notes in Computer Science (Including Subseries Lecture Notes in Artificial Intelligence and Lecture Notes in Bioinformatics)*, eds M. Deng, R. Jiang, F. Sun, and X. Zhang, (Berlin: Springer), 158–170. doi: 10.1007/978-3-642-37195-0_13

Nzila, A., Jung, B. K., Kim, M. C., Ibal, J. C., Budiyanto, F., Musa, M. M., et al. (2018). Complete genome sequence of the polycyclic aromatic hydrocarbons biodegrading bacterium Idiomarina piscisalsi strain 10PY1A isolated from oil-contaminated soil. *Korean J. Microbiol.* 54, 289–292. doi: 10.7845/kjm.2018.8034

Oren, A. (2017). "Aerobic hydrocarbon-degrading Archaea," in *Taxonomy, Genomics and Ecophysiology of Hydrocarbon-Degrading Microbes. Handbook of Hydrocarbon and Lipid Microbiology*, ed. T. J. McGenity, (Cham: Springer), 1–12. doi: 10.1007/978-3-319-60053-6_5-1

Owens, E. H. (1972). "The cleaning of gravel beaches polluted by oil," in *Proceedings of the 13th International Conference on Coastal Engineering*, Vancouver. doi: 10.9753/icce.v13.143

Parinos, C., Hatzianestis, I., Chourdaki, S., Plakidi, E., and Gogou, A. (2019). Imprint and short-term fate of the Agia Zoni II tanker oil spill on the marine ecosystem of Saronikos Gulf. *Sci. Total Environ.* 693, 133568. doi: 10.1016/j.scitotenv.2019.07.374

Pedersen, T. L. (2019). *patchwork: The Composer of Plots. Cran*. Available online at: https://cran.r-project.org/package=patchwork (accessed June 22, 2020).

Petersen, J., Michel, J., Zengel, S., White, M., Lord, C., and Plank, C. (2002). *Environmental Sensitivity Index Guidelines. Version 3.0. NOAA Technical Memorandum NOS OR&R 11*. Seattle, WA: NOAA.

R Development Core Team, (2011). *R: A Language and Environment for Statistical Computing*. Vienna: R Core Team.

Radwan, S. S., Khanafer, M. M., and Al-Awadhi, H. A. (2019). Ability of the so-called obligate hydrocarbonoclastic bacteria to utilize nonhydrocarbon substrates thus enhancing their activities despite their misleading name. *BMC Microbiol.* 19:41. doi: 10.1186/s12866-019-1406-x

Raskin, L., Stromley, J. M., Rittmann, B. E., and Stahl, D. A. (1994). Group-specific 16S rRNA hybridization probes to describe natural communities of methanogens. *Appl. Environ. Microbiol.* 60, 1232–1240. doi: 10.1128/aem.60.4.1232-1240.1994

Redmond, M. C., and Valentine, D. L. (2012). Natural gas and temperature structured a microbial community response to the Deepwater Horizon oil spill. *Proc. Natl. Acad. Sci. U.S.A.* 109, 20292–20297. doi: 10.1073/pnas.1108756108

REMPEC, (2018). *Mediterranean Integrated GIS on Marine Pollution Risk Assessment and Response*. Valletta: REMPEC.

Rodriguez-R, L. M., Overholt, W. A., Hagan, C., Huettel, M., Kostka, J. E., and Konstantinidis, K. T. (2015). Microbial community successional patterns in beach sands impacted by the Deepwater Horizon oil spill. *ISME J.* 9, 1928–1940. doi: 10.1038/ismej.2015.5

Rognes, T., Flouri, T., Nichols, B., Quince, C., and Mahé, F. (2016). VSEARCH: a versatile open source tool for metagenomics. *PeerJ* 4:e2584. doi: 10.7717/peerj.2584

Röling, W. F. M., Milner, M. G., Jones, D. M., Lee, K., Daniel, F., Swannell, R. J. P., et al. (2002). Robust hydrocarbon degradation and dynamics of bacterial communities during nutrient-enhanced oil spill bioremediation. *Appl. Environ. Microbiol.* 68, 5537–5548. doi: 10.1128/AEM.68.11.5537-5548.2002

Ron, E. Z., and Rosenberg, E. (2014). Enhanced bioremediation of oil spills in the sea. *Curr. Opin. Biotechnol.* 27, 191–194. doi: 10.1016/j.copbio.2014.02.004

Rontani, J.-F. (2010). "Production of wax esters by bacteria," in *Handbook of Hydrocarbon and Lipid Microbiology*, ed. K. Timmis, (Berlin: Springer), 459–470. doi: 10.1007/978-3-540-77587-4_34

Rubin-Blum, M., Antony, C. P., Borowski, C., Sayavedra, L., Pape, T., Sahling, H., et al. (2017). Short-chain alkanes fuel mussel and sponge *Cycloclasticus* symbionts from deep-sea gas and oil seeps. *Nat. Microbiol.* 2:17093. doi: 10.1038/nmicrobiol.2017.93

Sanni, G. O., Coulon, F., and McGenity, T. J. (2015). Dynamics and distribution of bacterial and archaeal communities in oil-contaminated temperate coastal mudflat mesocosms. *Environ. Sci. Pollut. Res.* 22, 15230–15247. doi: 10.1007/s11356-015-4313-1

Seah, C. H., and McFerran, K. S. (2016). The transition to practice experience of five music therapy graduates. *Nord. J. Music Ther.* 25, 352–371. doi: 10.1080/08098131.2015.1080288

Searle, S. R., Speed, F. M., and Milliken, G. A. (1980). Population marginal means in the linear model: an alternative to least squares means. *Am. Stat.* 34, 216–221. doi: 10.1080/00031305.1980.10483031

Shade, A., Peter, H., Allison, S. D., Baho, D. L., Berga, M., Bürgmann, H., et al. (2012). Fundamentals of microbial community resistance and resilience. *Front. Microbiol.* 3:417. doi: 10.3389/fmicb.2012.00417

Short, J. W., Irvine, G. V., Mann, D. H., Maselko, J. M., Pella, J. J., Lindeberg, M. R., et al. (2007). Slightly weathered Exxon Valdez oil persists in Gulf of Alaska beach sediments after 16 years. *Environ. Sci. Technol.* 41, 1245–1250. doi: 10.1021/es0620033

Stahl, D. A., and Amann, R. (1991). "Development and application of nucleic acid probes in bacterial systematics," in *Nucleic Acid Techniques in Bacterial Systematics*, eds E. Stackebrandt, and M. Goodfellow, (Chichester: John Wiley & Sons Ltd), 205–248.

Tamura, K., and Nei, M. (1993). Estimation of the number of nucleotide substitutions in the control region of mitochondrial DNA in humans and chimpanzees. *Mol. Biol. Evol.* 10, 512–526. doi: 10.1093/oxfordjournals.molbev.a040023

Tatti, E., McKew, B. A., Whitby, C., and Smith, C. J. (2016). Simultaneous dna-rna extraction from coastal sediments and quantification of 16S rRNA genes and transcripts by real-time PCR. *J. Vis. Exp.* 2016:e54067. doi: 10.3791/54067

Teramoto, M., Ohuchi, M., Hatmanti, A., Darmayati, Y., Widyastuti, Y., Harayama, S., et al. (2011). *Oleibacter marinus* gen. nov., sp. nov., a bacterium that degrades petroleum aliphatic hydrocarbons in a tropical marine environment. *Int. J. Syst. Evol. Microbiol.* 61, 375–380. doi: 10.1099/ijs.0.018671-0

Teramoto, M., Queck, S. Y., and Ohnishi, K. (2013). Specialized Hydrocarbonoclastic bacteria prevailing in seawater around a port in the strait of malacca. *PLoS One* 8:e66594. doi: 10.1371/journal.pone.0066594

Thingstad, T. F., Krom, M. D., Mantoura, R. F. C., Flaten, C. A. F., Groom, S., Herut, B., et al. (2005). Nature of phosphorus limitation in the ultraoligotrophic eastern Mediterranean. *Science* 309, 1068–1071. doi: 10.1126/science.1112632

Union, E. U. E., Ttf, D., and International Association of Oil & Gas, (2016). *Europe Exploration and Production Trends 2016*. London: International Association of Oil & Gas.

Urakawa, H., Garcia, J. C., Barreto, P. D., Molina, G. A., and Barreto, J. C. (2012). A sensitive crude oil bioassay indicates that oil spills potentially induce a change of major nitrifying prokaryotes from the Archaea to the Bacteria. *Environ. Pollut.* 164, 42–45. doi: 10.1016/j.envpol.2012.01.009

Urakawa, H., Rajan, S., Feeney, M. E., Sobecky, P. A., and Mortazavi, B. (2019). Ecological response of nitrification to oil spills and its impact on the nitrogen cycle. *Environ. Microbiol.* 21, 18–33. doi: 10.1111/1462-2920.14391

Venables, W. N., and Ripley, B. D. (2002). *Modern Applied Statistics with S (Fourth Edition)*. New York, NY: Springer-Verlag.

Wang, Q., Garrity, G. M., Tiedje, J. M., and Cole, J. R. (2007). Naïve Bayesian classifier for rapid assignment of rRNA sequences into the new bacterial taxonomy. *Appl. Environ. Microbiol.* 73, 5261–5267. doi: 10.1128/AEM.00062-07

Wang, W., and Shao, Z. (2012). Genes involved in alkane degradation in the alcanivorax hongdengensis strain A-11-3. *Appl. Microbiol. Biotechnol.* 94, 437–448. doi: 10.1007/s00253-011-3818-x

Wang, W., Wang, L., and Shao, Z. (2010). Diversity and abundance of oil-degrading bacteria and alkane hydroxylase (alkB) genes in the subtropical seawater of Xiamen island. *Microb. Ecol.* 60, 429–439. doi: 10.1007/s00248-010-9724-4

Wickham, H. (2010). A layered grammar of graphics. *J. Comput. Graph. Stat.* 19, 3–28.

Wilke, C. O. (2015). *Cowplot: Streamlined Plot Theme and Plot Annotations for ggplot2. R Packag. Version 0.5.0*. Available online at: https://cran.r-project.org/web/packages/cowplot/index.html (accessed July 11, 2019).

Xue, X., Hong, H., and Charles, A. T. (2004). Cumulative environmental impacts and integrated coastal management: the case of Xiamen. *China. J. Environ. Manage.* 71, 271–283. doi: 10.1016/j.jenvman.2004.03.006

Yakimov, M. M., Gentile, G., Bruni, V., Cappello, S., D'Auria, G., Golyshin, P. N., et al. (2004a). Crude oil-induced structural shift of coastal bacterial communities of rod bay (Terra Nova Bay, Ross Sea, Antarctica) and characterization of cultured cold-adapted hydrocarbonoclastic bacteria. *FEMS Microbiol. Ecol.* 49, 419–432. doi: 10.1016/j.femsec.2004.04.018

Yakimov, M. M., Giuliano, L., Denaro, R., Crisafi, E., Chernikova, T. N., Abraham, W. R., et al. (2004b). *Thalassolituus oleivorans* gen. nov., sp. nov., a novel marine bacterium that obligately utilizes hydrocarbons. *Int. J. Syst. Evol. Microbiol.* 54, 141–148. doi: 10.1099/ijs.0.02424-0

Yakimov, M. M., Golyshin, P. N., Lang, S., Moore, E. R. B., Abraham, W. R., Lünsdorf, H., et al. (1998). *Alcanivorax borkumensis* gen. nov., sp. nov., a new, hydrocarbon- degrading and surfactant-producing marine bacterium. *Int. J. Syst. Bacteriol.* 48, 339–348. doi: 10.1099/00207713-48-2-339

Yakimov, M. M., Timmis, K. N., and Golyshin, P. N. (2007). Obligate oil-degrading marine bacteria. *Curr. Opin. Biotechnol.* 18, 257–266. doi: 10.1016/j.copbio.2007.04.006

Yuan, J., Lai, Q., Sun, F., Zheng, T., and Shao, Z. (2015). The diversity of PAH-degrading bacteria in a deep-sea water column above the southwest Indian ridge. *Front. Microbiol.* 6:853. doi: 10.3389/fmicb.2015.00853

Zadjelovic, V., Chhun, A., Quareshy, M., Silvano, E., Hernandez-Fernaud, J. R., Aguilo-Ferretjans, M. M., et al. (2020). Beyond oil degradation: enzymatic potential of Alcanivorax to degrade natural and synthetic polyesters. *Environ. Microbiol.* 22, 1356–1369. doi: 10.1111/1462-2920.14947

Conflict of Interest: The authors declare that the research was conducted in the absence of any commercial or financial relationships that could be construed as a potential conflict of interest.